Dissertation

Molecular pathology of infectious and neoplastic diseases of the respiratory tract

submitted by

Dr. med. univ. Martin Zacharias

for the Academic Degree of

Doctor of Medical Science
(Dr. scient. med.)

at the
Medical University of Graz

Diagnostic and Research Institute of Pathology

under the supervision of

Assoz. Prof. Dr. med. univ. Gregor Gorkiewicz

2026

Declaration

I hereby confirm that the present dissertation is the result of my own independent scholarly work. I also confirm that in all cases, where material from the work of others (in books, articles, essays, dissertations, and on the internet) is acknowledged, quotations and paraphrases are clearly indicated. No material other than that cited in the reference list has been used. I have read and understood the Medical University's regulations and procedures concerning plagiarism. Furthermore, I hereby declare that if artificial intelligence (AI) tools were used for the generation and/or correction of certain text passages in the creation of this work, such employment was conducted in compliance with ethical principles, academic integrity, and the regulations of my university. Additionally, it was ensured that this usage was transparently disclosed and appropriately attributed.

Graz, February 2026 Martin Zacharias eh.

Disclosures

This cumulative thesis is based on the following 5 peer-reviewed journal articles:

Publication I:
Zacharias, M*; Kashofer, K*; Wurm, P*; Regitnig, P; Schütte, M; Neger, M; Ehmann, S; Marsh, LM; Kwapiszewska, G; Loibner, M; Birnhuber, A; Leitner, E; Thüringer, A; Winter, E; Sauer, S; Pollheimer, MJ; Vagena, FR; Lackner, C; Jelusic, B; Ogilvie, L; Durdevic, M; Timmermann, B; Lehrach, H; Zatloukal, K; Gorkiewicz, G.
Host and microbiome features of secondary infections in lethal covid-19.
iScience. 2022. https://doi.org/10.1016/j.isci.2022.104926

Publication II:
Zacharias, M; Stangl, V; Thüringer, A; Loibner, M; Wurm, P; Wolfgruber, S; Zatloukal, K; Kashofer, K; Gorkiewicz, G.
Rapid antigen test for postmortem evaluation of SARS-CoV-2 carriage.
Emerg Infect Dis. 2021. https://doi.org/10.3201/eid2706.210226

Publication III:
Zacharias, M; Thüringer, A; Krause, R; Kashofer, K; Gorkiewicz, G.
The mutual value of histopathology and ITS sequencing in the diagnosis of mucormycosis.
Histopathology. 2024. https://doi.org/10.1111/his.15131

Publication IV:
Zacharias, M*; Absenger, G*; Kashofer, K; Wurm, R; Lindenmann, J; Terbuch, A; Konjic, S; Sauer, S; Gollowitsch, F; Gorkiewicz, G; Brcic, L.
Reflex testing in non-small cell lung carcinoma using DNA- and RNA-based next-generation sequencing - a single-center experience.
Transl Lung Cancer Res. 2021. https://doi.org/10.21037/tlcr-21-570

Publication V:
Zacharias, M; Konjic, S; Kratochwill, N; Absenger, G; Terbuch, A; Jost, PJ; Wurm, R; Lindenmann, J; Kashofer, K; Gollowitsch, F; Gorkiewicz, G; Brcic, L.
Expanding broad molecular reflex testing in non-small cell lung cancer to squamous histology.
Cancers. 2024. https://doi.org/10.3390/cancers16050903

*contributed equally

For all included publications, the dissertation candidate contributed substantially to study design, data analysis, and manuscript preparation as first author or shared first author. Details about individual contributions of co-authors are given in the attached full text original publications (Appendix section).

The dissertation candidate has been affiliated with the Doctoral School Molecular Medicine and Inflammation. No specific funding was received in this context.

Abstract

This cumulative dissertation investigates the role of molecular pathology in the study of infectious and neoplastic diseases of the respiratory tract. The conceptual and methodological foundation is an integrative morpho-molecular approach that combines traditional histopathology with innovative high-throughput technologies. The aim was to apply this approach to both pathogenetic and diagnostic questions in pulmonary pathology.

Our multi-omics autopsy study on the immunopathology of lethal Covid-19 with particular emphasis on host and microbial alterations in the context of secondary infections is paradigmatic for this integrative research approach. By combining systematic histopathology, transcriptomics, protein-based assays, and microbiome analyses, we were able to define pathogenetically relevant subtypes. The molecular and microbial signatures reflected but also substantially refined the histomorphological patterns. For example, we identified pronounced alterations of the local immune microenvironment that probably predispose to the development of secondary infections. Our prospective study evaluating the performance of a SARS-CoV-2 antigen test in the postmortem setting demonstrated a strong correlation with viral cultivability and thus infectivity, indicating its potential use as a screening tool in this context. In mucormycosis, we showed that the combination of histopathology and ITS sequencing enables sensitive tissue-based fungal diagnostics that can be seamlessly integrated into routine histopathological workflows due to its FFPE compatibility. In the area of neoplastic diseases of the respiratory tract, we analyzed the implementation and further development of comprehensive DNA- and RNA-based NGS approaches for molecular tumor profiling. We demonstrated that broad molecular testing at the time of diagnosis (“reflex testing”) is technically robust and increases both the detection rate of therapeutically relevant genetic alterations and the proportion of patients receiving targeted therapy. In a subsequent study, we expanded this approach to pulmonary squamous cell carcinoma and showed that clinically relevant genetic alterations are also present in a subset of cases that would have been missed by more restrictive testing strategies.

In summary, the studies presented in this thesis demonstrate that the integration of histopathology and molecular analyses is indispensable for the investigation of respiratory diseases. Such an integrative approach also positions academic pathology as a key discipline within molecular medicine.

Zusammenfassung

Die vorliegende kumulative Dissertation untersucht die Bedeutung der Molekularpathologie in der Erforschung infektiöser und neoplastischer Erkrankungen des Respirationstrakts. Die konzeptionelle und methodische Grundlage dafür ist ein integrativer morpho-molekularer Ansatz, der traditionelle Histopathologie mit innovativen Hochdurchsatztechnologien verbindet. Ziel war es, diesen Ansatz sowohl für pathogenetische als auch für diagnostische Fragestellungen in der Lungenpathologie zu verfolgen.

Paradigmatisch für diesen integrativen Forschungsansatz ist unsere Multiomics-basierte Autopsiestudie zur Immunpathologie von letalem Covid-19 mit besonderem Augenmerk auf gewebliche und mikrobielle Veränderungen im Rahmen von Sekundärinfektionen. Durch eine Kombination von systematischer Histopathologie, Transkriptomik, proteinbasierter Assays und Mikrobiomanalysen konnten wir pathogenetisch relevante Subtypen definieren. Die molekularen und mikrobiellen Signaturen spiegelten einerseits die histomorphologischen Muster wider, verfeinerten diese aber auch substanziell. So konnten wir beispielsweise ausgeprägte Veränderungen des lokalen Immunmilieus feststellen, die vermutlich die Entstehung von Sekundärinfektionen begünstigen. Unsere prospektive Untersuchung zur Performance eines SARS-CoV-2 Antigentests im postmortalen Setting zeigte eine starke Korrelation mit viraler Kultivierbarkeit bzw. Infektiosität, was auf eine mögliche Einsetzbarkeit als Screening Tool in diesem Kontext hindeutet. Am Beispiel der Mukormykose konnten wir zeigen, dass die Kombination aus Histopathologie und ITS-Sequenzierung eine sensitive Gewebe-basierte Pilzdiagnostik ermöglicht, die durch ihre FFPE-Kompatibilität nahtlos in histopathologische Routineabläufe integriert werden kann. Im Bereich neoplastischer Erkrankungen des Respirationstrakts haben wir die Etablierung und Weiterentwicklung umfassender DNA- und RNA-basierter NGS-Ansätze zur molekularen Tumorprofilierung analysiert. Dabei konnten wir zeigen, dass eine umfassende molekulare Testung zum Zeitpunkt der Diagnose („Reflextestung“) technisch robust ist und sowohl den Anteil therapierelevanter genetischer Veränderungen als auch von Patient:innen mit zielgerichteter Therapie erhöht. In einer Folgestudie haben wir zudem durch eine Ausweitung dieses Ansatzes auf Plattenepithelkarzinome der Lunge gezeigt, dass auch in dieser Entität klinisch relevante genetische Veränderungen in einer kleineren Subgruppe vorhanden sind, welche durch restriktivere Teststrategien nicht erfasst worden wären.

Zusammenfassend zeigen die in dieser Arbeit dargelegten Studien, dass die Integration von Histopathologie und molekularen Analysen für die Erforschung respiratorischer Erkrankungen unabdingbar ist. Ein solcher integrativer Ansatz positioniert auch die akademische Pathologie als Schlüsseldisziplin innerhalb der molekularen Medizin.

Table of contents

List of abbreviations

AFIP	Armed Forces Institute of Pathology
AIDS	acquired immunodeficiency syndrome
ALK	anaplastic lymphoma kinase
AMP	Association for Molecular Pathology
ARDS	acute respiratory distress syndrome
BCR-ABL1	breakpoint cluster region-Abelson 1 fusion
BRAF	B-raf proto-oncogene, serine/threonine kinase
BTK	Bruton tyrosine kinase
CAP	College of American Pathologists
CAR T-cell	chimeric antigen receptor T cell
CMV	cytomegalovirus
CML	chronic myeloid leukemia
CNV	copy number variation
Covid-19	coronavirus disease 2019
CUP	cancer of unknown primary
DAD	diffuse alveolar damage
ddPCR	droplet digital polymerase chain reaction
DNA	deoxyribonucleic acid
EBER	EBV-encoded small RNA
EBV	Epstein-Barr virus
EGFR	epidermal growth factor receptor
ERBB2	erb-b2 receptor tyrosine kinase 2 (HER2 gene)
ESMO	European Society for Medical Oncology
FFPE	formalin-fixed paraffin-embedded
FMT	fecal microbiota transplantation
HBV	hepatitis B virus
HHV8	human herpesvirus 8
HGP	Human Genome Project
HER2	human epidermal growth factor receptor 2
HIV	human immunodeficiency virus
HPV	human papillomavirus
HSV	herpes simplex virus
IHC	immunohistochemistry
iBALT	inducible bronchus-associated lymphoid tissue
ISH	in situ hybridization
ITS	internal transcribed spacer
KRAS	KRAS proto-oncogene, GTPase
LAIR-1	leukocyte-associated immunoglobulin-like receptor 1
MALDI-TOF MS	matrix-assisted laser desorption/ionization time-of-flight mass spectrometry
MET	MET proto-oncogene, receptor tyrosine kinase
MicroCart	Microbiome Cartography
mRNA	messenger ribonucleic acid
NF-κB	nuclear factor kappa B
NGS	next-generation sequencing

NCCN	National Comprehensive Cancer Network
NSCLC	non-small cell lung cancer
NSCLC-NOS	non-small cell lung cancer, not otherwise specified
NTRK	neurotrophic tyrosine receptor kinase
PCR	polymerase chain reaction
PD-L1	programmed death-ligand 1
qPCR	quantitative polymerase chain reaction
RAT	rapid antigen test
RET	rearranged during transfection
RNA	ribonucleic acid
rRNA	ribosomal ribonucleic acid
ROS1	ROS proto-oncogene 1, receptor tyrosine kinase
RT-PCR	reverse transcription polymerase chain reaction
SARS-CoV-1	severe acute respiratory syndrome coronavirus 1
SARS-CoV-2	severe acute respiratory syndrome coronavirus 2
SCC	squamous cell carcinoma
SETDB2	SET domain bifurcated histone lysine methyltransferase 2
SHE	spatiotemporal hallmark ecosystems
SHM-seq	spatial host-microbiome sequencing
SmT	spatial metatranscriptomics
SNV	single-nucleotide variant
TTF-1	thyroid transcription factor 1
TMB	tumor mutational burden
TME	tumor microenvironment
TKI	tyrosine kinase inhibitor
WHO	World Health Organization

1 Introduction

1.1 Molecular pathology - General considerations

The scientific field of pathology is mainly concerned with the study of pathogenesis and the optimization of diagnostics. Its progress has always been driven by technological advancements. Scientific milestones in molecular biology that created the foundation for molecular pathology included, among others, the discovery of DNA's double-helix structure by Watson and Crick [1] and the development of polymerase chain reaction (PCR) by Mullis [2]. In 2003, the Human Genome Project (HGP) was completed, mapping nearly the entire human genome and providing reference sequences for research and clinical practice [3]. From a methodological standpoint, high-throughput sequencing technologies such as next-generation sequencing (NGS) have revolutionized the field by providing unprecedented speed and resolution [4,5]. Decreasing costs of NGS also allowed for the widespread implementation of comprehensive molecular pathology assays both in research laboratories and routine diagnostic practice [6]. Today, molecular pathology is a cornerstone of tissue-based analyses by integrating molecular techniques to investigate disease mechanisms and support clinical decision-making. These developments had particularly profound implications for infectious disease pathology and tumor pathology.

1.2 Molecular pathology of infectious disease

1.2.1 Principles of infectious disease pathology

Historically, pathologists were at the forefront of studying the pathophysiology and diagnosis of infectious diseases [7,8]. Although the field of medical microbiology grew separately and is now also primarily dealing with infectious diseases, the view and methodology of pathology have several complementary advantages. One of the most important ones is that histopathology allows for the assessment of the tissue reaction induced by the pathogen. Especially considering the increasingly available molecular detection methods with high sensitivity, a correlation of the molecular results with histomorphology or cytomorphology is essential to avoid overdiagnosis, e.g. due to microbial contamination of the sample [7,9]. Furthermore, with a thorough histomorphological or cytomorphological evaluation the inflammatory host response can be classified, potentially adding additional clinically relevant information. A prime example

of this are viral infections complicated by secondary bacterial or fungal infections, a phenomenon often regarded underdiagnosed [10–14]. Indeed, in the 1918 Influenza pandemic the majority of the approximately 50 million deaths worldwide were caused by bacterial pneumonia secondary to viral infection. Evidence for this finding came not only from epidemiology but also from reviews of pathological data often documenting an immune infiltrate rich in neutrophils (typical for bacterial infections) rather than lymphocytes (typical for pure viral infections) [12–14]. Hence, also in today's diagnostic practice histomorphological or cytomorphological findings might at least suggest a secondary bacterial or fungal infection, underlining the clinical relevance of a thorough characterization of the host response. Furthermore, there are a plethora of ancillary methods that enable the detection of a putative pathogen directly on formalin fixed paraffin embedded (FFPE) tissue if there is a clinical or histopathological suspicion for an infectious process.

1.2.2 In-situ visualization of specific microbes

Ancillary methods visualizing microbes within their human tissue context have further refined our understanding of spatial host-microbe interactions. Furthermore, they enable a rather cost- and time-efficient detection of a putative pathogen and integrate seamlessly with the histopathological workflow. Most pathology departments are equipped with an ever-increasing armamentarium of histological stains, immunohistochemistry (IHC) antibodies, and in situ hybridization (ISH) probes. Electron microscopy, although a valuable tool in some research settings, has proven less valuable in the routine infectious disease diagnostics setting, mostly because of technical but also interpretative difficulties as shown for example in SARS-CoV-2 [15,16]. According to a recent review by Hofman and colleagues, pathology laboratories should be equipped with at least the following IHC and ISH reagents for detection of infectious agents: IHC antibodies against herpes simplex virus (HSV), human herpes virus 8 (HHV8), cytomegalovirus (CMV), adenovirus, human immune deficiency virus (HIV, e.g. HIVp24), JC virus, BK virus, hepatitis B virus (HBV) core and surface Antigen, p16, Treponema pallidum, Toxoplasma gondii, as well as ISH probes against Epstein-Barr virus (EBV)-encoded small RNA (EBER) and human papillomavirus (HPV) types 16/18 [7]. However, this list might not be exhaustive and should probably be adapted according to current epidemiological data in respective countries. Notably, some of these antibodies and probes are also of value in neoplastic disease, primarily in virus-associated malignancies such as HPV-associated squamous cell carcinoma and EBV-associated lymphomas. In EBV-associated lymphomas, an

in-situ approach is particularly relevant because subcategorization of specific lymphoma entities requires determining whether EBV positivity resides in the neoplastic cells or in the surrounding microenvironment [17,18]. Thus, in situ techniques clearly continue to play an important role in infectious disease pathology in selected scenarios, even though modern molecular assays often offer superior analytical performance.

1.2.3 Molecular detection of microbes

Targeted molecular detection methods excel in specificity, sensitivity, and high-throughput capability. Moreover, quantitative PCR (qPCR) and droplet digital PCR (ddPCR) enable accurate quantification of microbial load, which is particularly valuable for comparative analyses between patients or across timepoints (e.g., pre- and post-therapy). In contrast, non-targeted NGS-based approaches allow the simultaneous identification of a broad spectrum of microbial species within a single assay [19]. A commonly used approach for bacteria is based on the sequence of the 16S ribosomal (rRNA) gene which is present in all bacteria (pan-bacterial approach). The 16S rRNA gene encodes a component of the small subunit of the prokaryotic ribosome and contains both conserved and hypervariable regions. While the former is used for PCR primer design, sequencing of the latter allows for discrimination between bacterial taxa across different phylogenetic levels by comparing the resulting sequences against reference databases [20–24]. Intriguingly, several bacterial pathogens have been newly characterized using such a broad-range PCR approach, including *Bartonella henselae* (causing bacillary angiomatosis and cat scratch disease), *Ehrlichia chaffeensis* (causing human monocyte ehrlichiosis), and *Tropheryma whipplei* (causing whipple´s disease) [25–28]. Analogous to 16S rRNA gene sequencing for bacterial taxa, sequencing of the nuclear ribosomal internal transcribed spacer (ITS) region can be used to discriminate fungal taxa [24,29–31] and is an increasingly relevant approach in light of the high global incidence and mortality of severe fungal disease [32].

1.2.4 Shotgun metagenomics

In contrast to the above-discussed pan-bacterial and pan-fungal methods, commonly referred to as broad-spectrum approaches, metagenomic sequencing enables the simultaneous detection of microbial DNA across multiple biological kingdoms and is therefore often considered a universal approach. Beyond taxonomic identification, metagenomics can provide functional insights, including information on antimicrobial resistance determinants and metabolic

potential, thereby substantially advancing our understanding of microbial ecology in both health and disease [33,34]. It is important to note, however, that no metagenomic assay is truly universal or free of bias. Rather, systematic biases may be introduced at multiple stages of the analytical workflow, including preanalytical steps such as sample collection and processing, laboratory procedures such as DNA extraction and library preparation, as well as postanalytical steps involving bioinformatic pipelines and the selection of reference databases for data interpretation [33]. Several metagenomic pipelines have been developed that can potentially be used for unbiased infectious disease diagnostics. *PathSeq*, for example, was one of the first software tools that has been developed to identify microbial sequences from transcriptome or whole-genome sequencing data by subtracting eukaryotic (e.g. human) reads [35,36]. Interestingly, it has also been demonstrated that applying metagenomics on body fluid or tissue samples allows for the concomitant detection of pathogens and cancer on the molecular level [37,38]. Such a dual assay might have important clinical applications since cancer patients are more susceptible to infections because of immunosuppression from the malignancy itself and from treatments such as chemotherapy [39,40]. This predilection to infections can be observed both in solid tumors and, even more so, in hematologic malignancies [41,42]. Broad-spectrum sequencing approaches and shotgun metagenomics have not only revolutionized infectious disease diagnostics but also our understanding of the human microbiome by enabling comprehensive, culture-independent profiling of microbial communities across various body sites [43,44].

1.2.5 Studying the human microbiome

The human microbiome is defined as the sum of all microorganisms, including bacteria, fungi, archaea, viruses and protozoa, colonizing our environmentally exposed body surfaces, including the skin, the gastrointestinal tract, the urogenital tract, and the respiratory tract [45,46]. The biomass and composition of the microbiome differ across different habitats, with the majority of microbial cells being bacteria and residing in the colon (up to 10^{13} bacteria) [43,47]. Comparable to macroscale ecosystems such as a forest, ecosystems within the human body (e.g. the gut) are not homogenous mixtures of microbial species and environments but rather spatially highly organized. This organization is shaped by marked spatial heterogeneity across host environments such as exact anatomical location. Along the longitudinal axis of the human gut, for example, there is systematic variation in physiological parameters (e.g., luminal pH, oxygen tension, mechanical forces generated by intestinal motility, antimicrobial effector

molecules, mucus composition and thickness, and nutrient availability), generating selective pressures that favor specific microbial compositions [48].

From a methodological standpoint, the rise of human microbiome research in recent years was sparked by technological progress in high-throughput sequencing approaches and reduction in associated costs. These enabled large-scale studies linking microbiome profiles to an expanding spectrum of physiological and pathological conditions. However, the analysis of homogenized samples necessarily entails a loss of spatial information and fails to capture the pronounced heterogeneity of microbial organization within the host. In recent years, increasing awareness of these limitations and technological advances in spatial biology have led to a conceptual shift toward spatially resolved investigations of the (gut) microbiome. Similar to developments observed in other areas of molecular pathology, where integration of morphological context with molecular data has proven essential for accurate interpretation, there is growing recognition that microbial community structure and function must be interpreted within their native tissue environment [48]. To do so in a comprehensive way, several spatially resolved approaches for simultaneous host transcriptome- and microbiome-wide characterization of tissues have recently been developed, such as SmT ("spatial metatranscriptomics") [49], SHM-seq ("spatial host-microbiome sequencing") [50], or MicroCart ("Microbiome Cartography") [51]. Approaches like these will potentially fuel our understanding of host-microbiome interactions but could also be used in the context of infectious disease.

1.2.6 The microbiome and infectious disease

The human microbiome plays a central role in both the pathophysiology and therapy of infectious diseases. Importantly, a substantial proportion of clinically relevant infections are caused by microorganisms that, under physiological conditions, coexist with the host in a state of homeostasis. However, disruption of tissue integrity, such as visceral perforation as a complication of appendicitis or diverticulitis, can facilitate translocation of bacteria into non-adapted, often sterile compartments, thereby giving rise to severe infections [52]. Additional examples include bacterial endocarditis, which is commonly caused by oral commensals entering the bloodstream and colonizing damaged or calcified heart valves in predisposed individuals, or urinary tract infections, which are also mainly caused by bacterial species that otherwise constitute part of the normal microbiota [52–54]. This principle is not restricted to

bacteria, as certain viruses, such as JC polyomavirus, may persist as commensals during early life but emerge as pathogens later in life or in the setting of immunosuppression [52,55].

The involvement of the microbiome in infectious disease therapy is bidirectional. On the one hand, the widespread use of antibiotics has not only contributed to the emergence and global spread of antimicrobial resistance[56], but also exerts profound ecological effects within the host by disrupting the composition and function of the microbiome. Such perturbations may have downstream consequences for immune regulation, metabolic homeostasis, the gut-brain axis, as well as for the effectiveness of cancer immunotherapies [52,57–60]. On the other hand, deliberate modulation of the microbiome offers therapeutic opportunities to improve outcomes in infectious diseases [52]. A prominent example is fecal microbiota transplantation (FMT), which has become an established treatment strategy for recurrent *Clostridioides difficile* colitis [61]. Conceptually, FMT aims to restore a balanced gut microbial ecosystem, thereby re-establishing colonization resistance against the pathogen. In line with principles of targeted pharmacological intervention, the administration of defined bacterial products has likewise been shown to reduce the risk of recurrent infection [62].

1.3 Molecular pathology of neoplastic disease

1.3.1 Principles of tumor pathology

Cancer is a heterogeneous group of diseases defined by a set of fundamental biological characteristics, including uncontrolled cell proliferation, evasion of programmed cell death, and the capacity for tissue invasion and metastatic dissemination [63]. Despite progress in clinical evaluation and imaging, the definitive diagnosis of solid tumors continues to rely on the histopathological evaluation of tissue obtained by biopsy or surgical resection. The diagnostic process is anchored in the systematic assessment of tumor histomorphology, including architectural growth patterns and cytological features. Remarkably, the core principles of histopathological tumor assessment have remained conceptually consistent for more than a century and a half, tracing back to the foundational work of early pioneers in cell biology and pathology, most notably Rudolf Virchow. His meticulous observations established the cellular basis of disease and laid the groundwork for modern tumor pathology [64]. While the fundamental reliance on morphology has persisted, the biological understanding of tumors and their nosology have evolved substantially. Contemporary classification systems, most

importantly those from the World Health Organization (WHO), increasingly integrate morphological criteria with concepts of histogenesis, reflecting the presumed cell of origin and differentiation lineage of individual tumor entities. This refinement of tumor classification has been enabled by methodological advances in histopathology, particularly through the characterization of gene and protein expression patterns within tumors. As a result, many tumor entities are now defined not only by their morphological features but also by specific immunophenotypic profiles. In routine diagnostic practice, immunohistochemistry has therefore become an indispensable adjunct to morphological assessment [65].

1.3.2 Genetic alterations in cancer

At its core, cancer can be regarded as a genetic disease driven by the accumulation of alterations affecting oncogenes and tumor suppressor genes, ultimately resulting in malignant transformation of cells [63,66–68]. In the vast majority of cases, these alterations are acquired somatically during a patient´s lifetime. However, germline mutations in cancer susceptibility genes may confer a markedly increased lifetime risk of developing malignancy and underlie hereditary cancer predisposition syndromes [69]. Functionally, gain-of-function mutations in oncogenes such as *KRAS* or *BRAF* promote constitutive signaling through pathways regulating cellular proliferation and survival. Conversely, loss-of-function alterations in tumor suppressor genes, including *TP53* and *RB1*, impair critical protective mechanisms such as cell-cycle control or DNA damage repair [63,66–68]. Importantly, not all detected variants are biologically meaningful. The functional consequence (pathogenicity) of an alteration must therefore be carefully evaluated before clinical relevance can be assumed. To standardize this process, consensus frameworks for variant interpretation have been established, classifying alterations as pathogenic, likely pathogenic, variants of uncertain significance, likely benign, or benign [70–73]. The implementation of such classification systems in molecular reporting is essential for ensuring consistent interpretation and supporting evidence-based precision oncology.

There are multiple mechanisms through which the cancer genome may be altered, including single-nucleotide variants (SNVs), copy number variations (CNVs), and structural alterations such as gene rearrangements or fusions [74,75]. The progressive accumulation of such alterations reflects underlying genomic instability, a hallmark of cancer that promotes clonal evolution and tumor progression. A historical paradigm illustrating the clinical relevance of

structural alterations is the *BCR-ABL1* fusion resulting from the reciprocal translocation t(9;22)(q34;q11). This rearrangement constitutes both the defining molecular event and a therapeutic target in chronic myeloid leukemia (CML) and is widely regarded as an early model of precision oncology [76]. The success of targeted therapy in this disease exemplifies the diagnostic and therapeutic value of molecular tumor pathology.

1.3.3 Diagnostic value of molecular tumor pathology

Cancer classification has traditionally been based on histomorphological and immunohistochemical characteristics within an organ-based framework. Advances in cancer genomics have prompted proposals for alternative, purely molecular classification systems, including a recent provocative commentary by André and colleagues in *Nature* [77]. However, current tumor classifications increasingly integrate molecular diagnostic criteria rather than replacing morphological assessment, thereby reinforcing the concept of an integrative morpho-molecular approach. In diagnostic practice, molecular testing plays a critical role in resolving diagnostically challenging cases, particularly when histomorphology and immunophenotype are ambiguous or overlapping. Recurring, entity-defining genetic alterations may establish a definitive diagnosis, whereas additional molecular findings may further refine tumor classification or enable the recognition of biologically distinct subgroups within morphologically similar entities. Such approaches are especially relevant for tumors of the central nervous system, haematolymphoid neoplasms, and soft tissue tumors, in which molecular alterations are routinely assessed and incorporated into diagnostic criteria [78–80], with increasing applicability across a broad range of additional tumor entities. Beyond mutation detection, DNA methylation analysis has been demonstrated to refine tumor classification systems and enhance diagnostic precision [81–84]. In addition, methylation profiling can assist in distinguishing primary tumors from metastatic lesions, particularly relevant in organs sites such as the lung, where both occur frequently. For instance, this approach has been successfully applied to differentiate primary pulmonary squamous cell carcinomas from metastases originating in the head and neck region [85], as well as pulmonary enteric adenocarcinomas from colorectal metastases [86]. Moreover, DNA methylation analysis may facilitate the identification of the primary site in cancers of unknown primary (CUP) [87–90]. While these approaches may be appropriate in selected cases, such as within an interdisciplinary molecular tumor board, their broader adoption into routine clinical practice requires further validation.

1.3.4 Prognostic and predictive value of molecular tumor pathology

Apart from diagnostic applications, molecular testing in oncology has acquired important prognostic and, increasingly, predictive relevance. Prognostic biomarkers provide information about the expected natural course of a disease independent of therapeutic intervention and are therefore primarily used for estimation of clinical outcomes such as recurrence or survival [91] . Such assessments may guide therapeutic decision-making, for example when evaluating the potential benefit of adjuvant chemotherapy. The most established prognostic biomarkers are histopathological parameters (e.g., tumor stage, grade, proliferation rate, or vascular invasion), which constitute integral components of pathology reports across tumor entities [92] . Molecular prognostic biomarkers include gene alterations associated with defined clinical outcomes. Mutations in *TP53*, for instance, are linked to an adverse prognosis across multiple tumor types [93], most notably in acute myeloid leukemia where *TP53* mutation status has also been incorporated into disease subclassification [94]. Additionally, transcript-based assays can estimate the risk of recurrence following surgical resection and are routinely applied in selected breast cancer subtypes [95,96].

In contrast, predictive biomarkers indicate the likelihood of response or resistance to a specific therapy and thereby directly inform treatment selection [96]. The development of many targeted therapies has been enabled by the identification of pharmacologically actionable alterations, particularly activating mutations and gene fusions affecting key oncogenic drivers such as *EGFR*, *HER2*, *BRAF*, and *ALK* [96]. However, predictive biomarkers are not limited to targeted therapies but also play a critical role in refining patient selection for immunotherapeutic approaches. Established biomarkers include programmed death-ligand 1 (PD-L1) expression, typically assessed by immunohistochemistry on tumor cells and/or tumor-associated immune cells [97]. In addition, genomic parameters such as tumor mutational burden (TMB) have been associated with improved response to immune checkpoint inhibition [98,99]. Emerging evidence further suggests that the composition of the gut microbiome may influence immunotherapy outcomes, although its clinical utility has not yet been fully established [60,100,101].

1.3.5 Beyond the cancer genome: tumors as ecosystems

Although cancer is fundamentally a genetic disease, attributing tumor pathogenesis exclusively to genomic alterations is insufficient to capture its biological complexity. Tumors are now

understood as dynamic ecosystems composed not only of neoplastic cells but also of diverse non-neoplastic cell populations such as immune cells and fibroblasts, as well as acellular components such as the extracellular matrix and soluble signaling factors, together forming the tumor microenvironment (TME) [102]. The spatial organization of the TME and its bidirectional interactions with neoplastic cells are highly structured, a concept reinforced by recent advances in spatially resolved technologies. Importantly, this ecosystem evolves over time as tumor progression is accompanied by clonal selection and microenvironmental remodeling [102].

In response to this expanding view of tumor biology, integrative conceptual models have been proposed to better capture the multidimensional nature of cancer [103]. Building upon the traditional hallmarks of cancer framework [63], we recently introduced the concept of spatiotemporal hallmark ecosystems (SHEs), which aims to integrate spatial organization, temporal dynamics, and key biological hallmark capabilities into a unified framework of cancer evolution (schematically visualized in Figure 1). Within this perspective, hallmark capabilities are interpreted as context-dependent programs emerging from interactions between genetic drivers, tissue architecture, and systemic influences, rather than as fixed consequences of individual mutations [104].

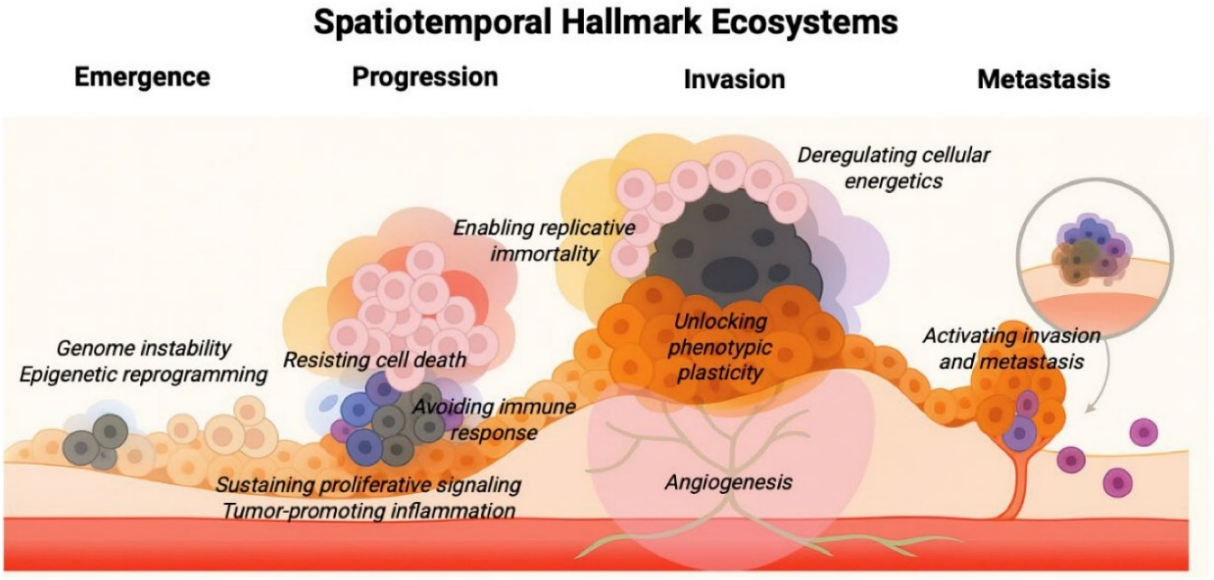

Figure 1. Spatiotemporal Hallmark Ecosystems. Illustrative representation of how different cancer hallmarks (e.g., genome instability, avoiding immune response) dominate at distinct spatial and temporal stages of tumor evolution. Reproduced from Sibai M, Zacharias M, McGranahan N, Jamal-Hanjani M, Porta-Pardo E (2025) Cancer in 4D: Towards Spatiotemporal Hallmark Ecosystems. Preprints. 2025. DOI: 10.20944/preprints202509.1469.v1. [104]. Licensed under CC BY 4.0.

Notably, the hallmarks of cancer framework itself has undergone successive refinements since its original publication, reflecting the growing appreciation of tumor complexity [63,66,67]. The most recent update highlights phenotypic plasticity and disrupted differentiation as an emerging hallmark capability and identifies nonmutational epigenetic reprogramming and polymorphic microbiomes as enabling characteristics that facilitate the acquisition of hallmark traits [66]. The recognition of polymorphic microbiomes underscores the growing understanding that microbial communities are integral to tumor biology.

1.3.6 The tumor microbiome

Microbial communities influence tumor biology through both indirect mechanisms, including systemic effects mediated by the gut microbiota, and direct interactions involving bacteria localized within tumor tissue [105]. Indirect effects are thought to be largely mediated through modulation of host immunity, an interpretation supported by numerous studies demonstrating associations between gut microbiome composition and response to immune checkpoint blockade across multiple cancer types [100,101,106–109]. Although the precise mechanisms underlying this relationship remain incompletely understood, recent experimental evidence suggests that gut microbial components can enhance antitumor immunity by promoting dendritic cell maturation and migration from the gut, thereby expanding the pool of $CD8^+$ T cells capable of recognizing tumor antigens [110]. These observations have prompted translational efforts aimed at modulating the gut microbiome. In this context, fecal microbiota transplantation has shown promising results when combined with anti-PD-1 immunotherapy in early clinical studies, highlighting the therapeutic potential of microbiome modulation to augment anticancer immunity [111–115].

Direct tumor-microbe interactions have been most extensively studied in gastrointestinal malignancies, particularly colorectal carcinoma. Among the microorganisms implicated, *Fusobacterium nucleatum*, a Gram-negative anaerobe commonly residing in the oral cavity, has consistently been identified as a tumor-associated bacterium. Accumulating evidence suggests that *F. nucleatum* may contribute to colorectal carcinogenesis through multiple mechanisms, including modulation of antitumor immunity, promotion of a protumorigenic inflammatory milieu, and activation of oncogenic signaling pathways. Collectively, these observations support the concept that tumor-associated bacteria can actively shape colorectal carcinoma development rather than merely reflecting secondary colonization [116–121]. Beyond

gastrointestinal malignancies, tumor-associated microbial signatures have been described across a broad spectrum of cancers, including pancreatic, breast, head and neck, lung, and brain tumors, although their functional significance remains under investigation [122–128]. Compared with the relatively high microbial biomass of the gastrointestinal tract and associated tumors, non-gastrointestinal tissues and tumors are generally characterized by considerably lower microbial abundance [105,126]. Such low-biomass environments pose significant methodological challenges for DNA-based sequencing approaches, rendering them more susceptible to low-level environmental and reagent-derived contamination. Importantly, recent well-controlled studies have demonstrated that biologically meaningful signals can be detected despite technical constraints [127,128]. A recent consensus statement therefore provides methodological recommendations for minimizing and transparently reporting contamination in low-biomass microbiome studies [129]. Accordingly, findings derived from intratumoral microbiome analyses in these settings should be interpreted with appropriate caution before attributing biological relevance. At the same time, further rigorously controlled investigations of non-gastrointestinal malignancies are needed to establish if tumor-associated microbes represent a general component of tumors across different entities or not [130].

1.4 Autopsy pathology and its role in biomedical research

1.4.1 Autopsies as a tool to understand disease

Beyond their clinical role in quality management and precise determination of the cause of death, autopsies constitute an indispensable resource for biomedical research by providing unique insights into disease pathogenesis, particularly in the context of advanced and multiorgan disease manifestations. During the second half of the 20th century, autopsies led to the discovery or critical clarification of more than 80 medical disorders, a contribution that continues to shape contemporary biomedical research [131,132]. Furthermore, autopsies may be performed specifically to procure human tissue for basic and translational research. Such efforts initially centered on the collection of brain tissue for the study of neurological disorders and subsequently led to the establishment of formal brain banking programs in the United States, enabling the systematic procurement and processing of tissue from consenting individuals [133,134]. Building upon these early initiatives, research autopsies have proven particularly valuable for advancing the understanding of infectious and neoplastic diseases.

1.4.2 Infectious disease autopsy pathology

Autopsies have long been a cornerstone for the detection and investigation of infectious diseases, with estimates indicating that 20-30% of infections in hospitalized patients remain unrecognized until postmortem examination [131,135–137]. Beyond improving diagnostic accuracy, autopsy pathology enables precise characterization of tissue manifestations and provides critical insights into disease pathogenesis, thereby contributing substantially to the understanding of both established and emerging infections [138]. A paradigmatic example is tuberculosis, which remains among the leading causes of death worldwide. The disease is inherently difficult to investigate, as it is rarely accessible to biopsy or surgical resection, and existing animal models often fail to fully recapitulate the complexity of human tuberculosis, particularly the distinct manifestations of primary and post-primary disease [131,139,140]. Furthermore, the pathogenesis of a plethora of viral infections has been elucidated through autopsies and subsequent tissue-based analyses, including HIV [141,142], hantavirus [143,144], SARS-CoV-1 [145,146], SARS-CoV-2 [147–149], and influenza [150,151]. Particularly influential are studies based on historical autopsy material curated by the National Tissue Repository of the Armed Forces Institute of Pathology (AFIP) from the 1918 influenza pandemic, which resulted in approximately 50 million deaths worldwide. Histopathological analysis of these specimens revealed histological features of bacterial pneumonia in all 68 examined cases, underscoring the critical role of secondary infections in pandemic influenza mortality [152]. The integration of modern tissue-based omics technologies with traditional autopsy approaches has emerged as a powerful strategy for advancing our understanding of infectious disease pathogenesis, as exemplified by recent investigations in Covid-19 [24,153–155], see also Figure 2 for our approach to this. By enabling whole-body assessment of pathogen distribution and host response, autopsies provide an integrative, organism-level view that cannot be achieved through conventional sampling approaches. Despite this potential, dedicated research autopsy programs focusing on infectious diseases, such as the “Last Gift” HIV study, remain comparatively scarce relative to those for neoplastic diseases [156].

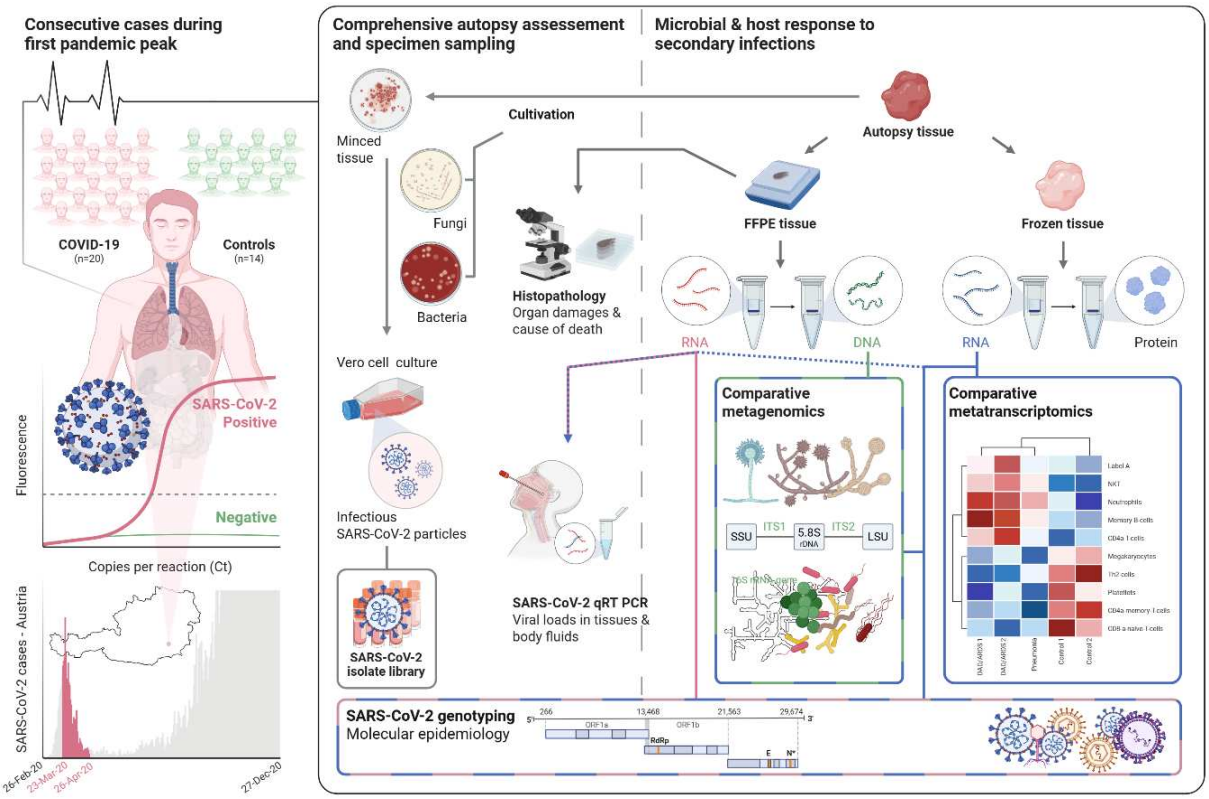

Figure 2. Integrative multi-omics research autopsy approach. Schematic illustration of how comprehensive postmortem tissue sampling can be combined with high-dimensional molecular profiling to enable systematic investigations of infectious disease pathogenesis. Adapted from Zacharias et al., iScience 2022 [24]. Licensed under CC BY 4.0.

1.4.3 Tumor autopsy pathology

Modern concepts of cancer biology have been profoundly shaped by autopsy-based investigations. One of the earliest and most influential examples is the work of Stephen Paget, who in 1889 proposed that metastatic dissemination is not a random process but reflects a biological affinity between tumor cells and specific organ environments. Through systematic analysis of autopsy records from 735 patients with breast cancer, Paget identified distinct patterns of metastatic spread, leading to the formulation of the seminal “seed and soil” hypothesis [133,157]. More than a century later, dedicated research autopsies emerged as a powerful tool in translational oncology, particularly in the study of advanced metastatic disease. Early contemporary programs focused on metastatic prostate cancer, allowing systematic characterization of metastatic disease and advancing the understanding of tumor progression [133,158]. Since then, numerous cancer research autopsy programs have been established worldwide, generating fundamental insights into key aspects of tumor biology, including mechanisms of progression and metastatic dissemination, interactions with the tumor

microenvironment, tumor cell dormancy, and the development of therapeutic resistance [159]. Moreover, these programs have enabled integrative approaches that combine circulating biomarkers such as liquid biopsy with multisite tissue analysis, providing a more holistic view of systemic cancer biology [159–161]. Unlike conventional biopsies, research autopsies enable simultaneous sampling across all metastatic sites, thereby providing an unparalleled opportunity to study spatial tumor heterogeneity and evolutionary trajectories. The importance of including non-neoplastic tissue in cancer research autopsies is underscored by a recent genomic study employing high-depth duplex sequencing across 168 cancer-free samples from 16 organs in 22 patients with metastatic disease. Somatic mutations were detected in all samples at low variant allele frequencies and displayed non-random mutational signatures consistent with cumulative lifetime exposures, including tobacco and alcohol use as well as prior cancer therapy [162]. Taken together, the comprehensive sampling enabled by cancer research autopsies, especially when combined with advanced molecular analyses, offers a powerful strategy for investigations of tumor heterogeneity and evolutionary dynamics in human disease.

1.5 The respiratory tract as landscape of infectious and neoplastic disease

1.5.1 Biogeography of the respiratory ecosystem

Beyond its essential function in gas exchange, the respiratory tract represents a dynamic interface between the host and the external environment. Continuous exposure to inhaled particles and microbes is mirrored by a pronounced structural, immunological, and microbial compartmentalization along its anatomical axis (Figure 3).

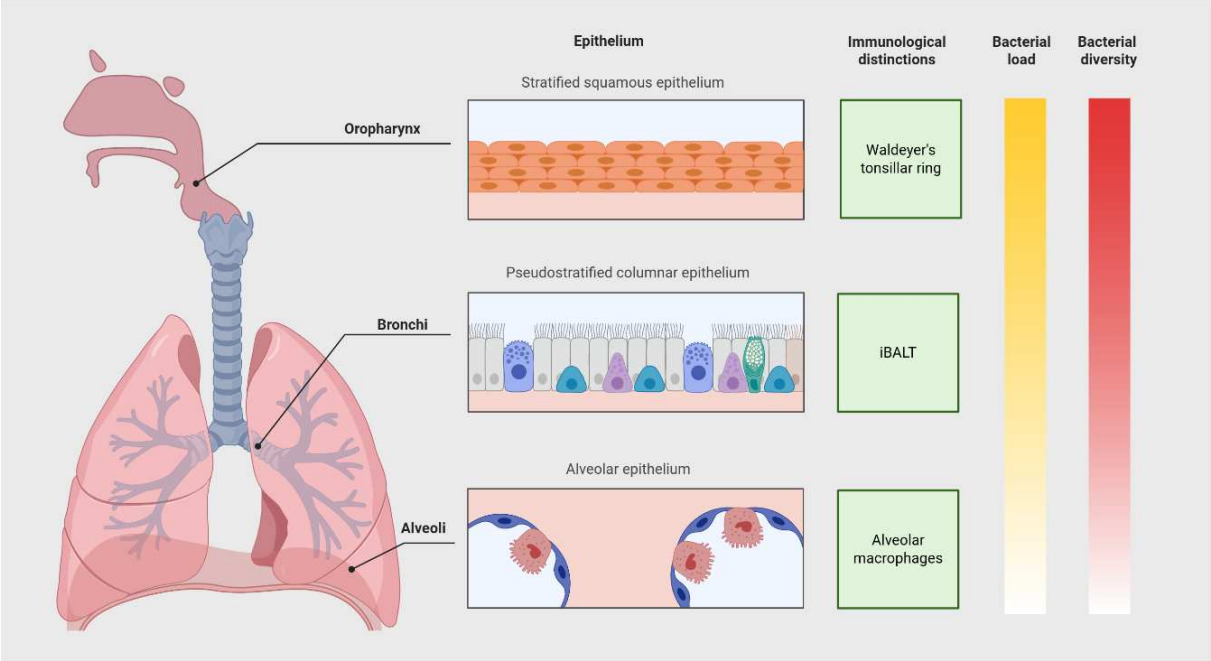

Figure 3. Biological properties of respiratory habitats. Created with BioRender.com.

Regions of the upper respiratory tract most directly exposed to mechanical stress and environmental insults are lined by stratified squamous epithelium that provides enhanced mechanical barrier protection. Compartments such as the paranasal sinuses, the larynx, the trachea and the bronchial tree are lined by a ciliated columnar epithelium contributing to coordinated mucociliary clearance. In contrast, the lower respiratory tract is optimized for efficient gas exchange and therefore characterized by thinner epithelial layers and an extensive alveolar surface area. Furthermore, tissue structures responsible for producing and secreting serous and mucinous secretions differ along the respiratory tract. For example, submucosal glands are abundant in the trachea and larger bronchi, progressively decrease in smaller airways, and are absent in alveoli [163,164]. Parallel to these structural differences, distinct immune niches are distributed along the respiratory tract, including organized mucosa-associated lymphoid tissues such as tonsils, adenoids, and inducible bronchus-associated lymphoid tissue (iBALT), as well as specialized innate and adaptive immune cell populations that coordinate local immune surveillance. Particularly in the distal lung, immune responses must be balanced between effective antimicrobial defense and minimization of collateral tissue injury in order to preserve the delicate architecture required for gas exchange. Disruption of this equilibrium is central to the immunopathogenesis of a wide spectrum of respiratory diseases, including infectious pneumonias and lung tumors [165–167].

Microbial communities also follow an anatomical gradient along the respiratory tract. The upper respiratory tract harbors a relatively high microbial biomass with considerable diversity and temporal stability, whereas the lower respiratory tract is characterized by a markedly lower microbial biomass, generally lower diversity, and more transient microbial communities [166,168–170] (Figure 3). Although the healthy lung was long considered sterile, culture-independent molecular approaches have demonstrated that microbes and microbial products are detectable even in peripheral lung compartments [164,171]. In contrast to the gut microbiome, the lung microbiome is not regarded as a fixed, site-specific community but rather a dynamic system dominated by continuous fluxes of microbial immigration and elimination. Microbial immigration occurs predominantly through microaspiration of oropharyngeal contents and is counterbalanced by elimination mechanisms such as mucociliary clearance and innate and adaptive immune responses [172]. Accordingly, “eubiosis” in the lower airways is more accurately understood as a dynamic equilibrium maintained by these opposing forces rather than a stable compositional state [170]. While bacteria represent the dominant detected kingdom, metagenomic analyses have further revealed the presence of fungi, viruses, and archaea, which may be especially relevant in settings of immune dysregulation or structural lung disease [173–175]. However, the inherently low microbial biomass of the distal lung necessitates careful study design and rigorous contamination control when interpreting sequencing-based microbiome data [129].

The structural and microbial compartmentalization of the respiratory tract is accompanied by physicochemical gradients, including non-random variations in temperature, humidity, pH, gas tensions, and particle deposition patterns (Figure 4). These gradients shape local airway ecosystems and contribute to specific patterns of disease localization. A classical example is the predilection of pulmonary tuberculosis for the apical lung regions, a pattern long recognized but poorly understood in clinical practice [176]. It has been subsequently shown that the higher oxygen tension in the upper lung regions contributes to a favorable niche for the obligate aerobe *Mycobacterium tuberculosis*, thereby illustrating how physiological gradients directly influence spatial host-microbe interactions [177].

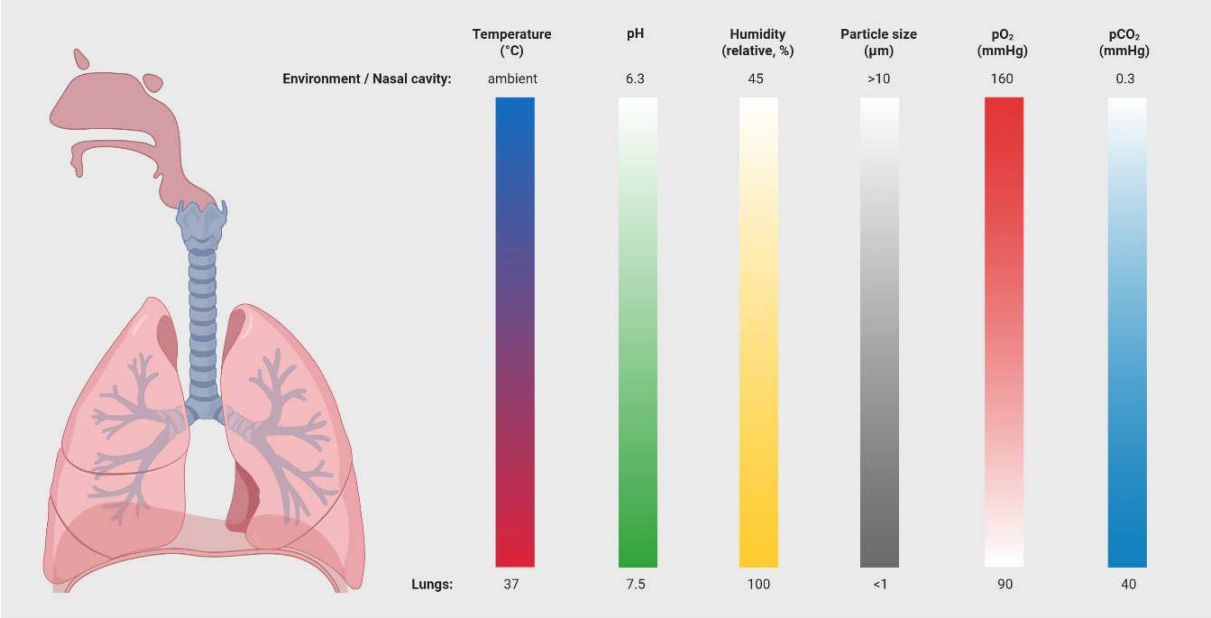

Figure 4. Physicochemical properties of respiratory habitats. Created with BioRender.com.

Collectively, these structural, immunological, microbial, and physicochemical gradients define the respiratory tract as a spatially heterogeneous ecosystem that shapes the emergence and pathogenesis of both infectious and neoplastic diseases.

1.5.2 Covid-19

Coronavirus disease 2019 (Covid-19), caused by severe acute respiratory syndrome coronavirus 2 (SARS-CoV-2), emerged in late 2019 and rapidly evolved into a global pandemic in early 2020. Sensitive detection of SARS-CoV-2 RNA is achieved by reverse transcription polymerase chain reaction (RT-PCR) performed on upper respiratory tract specimens, most commonly nasopharyngeal swabs [178–180]. Rapid antigen-based tests provide a complementary diagnostic approach, as their limits of detection generally correspond to viral concentrations associated with a higher likelihood of transmissibility. Due to their short turnaround time and ease of use, they represent a practical alternative in certain clinical and public health settings [181–184]. Clinical manifestations of Covid-19 range from asymptomatic infection to critical illness and death, most commonly resulting from respiratory failure due to acute respiratory distress syndrome (ARDS) [185,186].

The pathogenesis of severe disease is commonly conceptualized as a biphasic process. In the initial phase, viral entry and replication occur within susceptible epithelial cells of the respiratory tract, leading to direct virus-induced cell and tissue injury. The magnitude and

anatomical distribution of this early damage influence subsequent disease manifestations, which are increasingly dominated by host immune responses. During this later phase, recruitment and activation of effector immune cells drive local and systemic inflammation that may persist despite declining viral loads, indicating that host-mediated mechanisms substantially contribute to pulmonary pathology [186–188]. Postmortem analyses of patients who died from Covid-19 have been instrumental in characterizing the pathological hallmarks of severe disease, revealing that respiratory failure is less attributable to extensive virus-induced injury than to dysregulated host immune responses resulting in inflammatory lung tissue damage [24,186–188]. In addition, secondary infections have been reported to complicate the clinical course in up to 42% of critically ill patients [11]. Beyond bacterial superinfections, an increased incidence of invasive fungal infections has been observed, including Covid-19-associated mucormycosis [189]. The pathophysiological mechanisms that predispose to these secondary infections, however, remain poorly defined.

The Covid-19 pandemic has underscored the continued value of autopsy studies in elucidating the pathogenesis of emerging infectious diseases. However, their broader implementation and application to other infectious conditions remain limited, most notably due to the restricted availability of adequately equipped autopsy facilities and the infrastructure required for the safe handling of deceased individuals and associated postmortem specimens [190–192]. To mitigate the biosafety risks associated with conventional autopsy procedures, minimally invasive tissue sampling using ultrasound-guided postmortem biopsies has emerged as a feasible alternative for Covid-19 and other infectious diseases [193–196].

1.5.3 Mucormycosis

Mucormycosis is a rapidly progressive angioinvasive fungal infection characterized by high mortality and frequent pulmonary involvement in immunocompromised hosts. Well-established risk factors include hematologic malignancies, solid organ or hematopoietic stem cell transplantation, and diabetes mellitus [197,198]. More recently, severe Covid-19, treatment with Bruton tyrosine kinase inhibitors such as ibrutinib, and chimeric antigen receptor T-cell therapy have been recognized as additional predisposing factors [189,199–201]. Mucormycosis presents in several well-recognized clinical forms, including rhino-orbital-cerebral, pulmonary, gastrointestinal, cutaneous, musculoskeletal, and disseminated disease [197,198]. It is caused by filamentous fungi of the order *Mucorales*, most commonly by species of the genera

Rhizopus, *Mucor*, *Rhizomucor*, *Actinomucor*, *Lichtheimia*, and *Cunninghamella*. Certain taxa, most notably *Cunninghamella bertholletiae*, have been associated with increased virulence and higher mortality [197,202–205]. Species of the order *Mucorales* are ubiquitous in the environment, particularly in soil, where they grow as mycelia that produce sporangiospores. Following inhalation into the respiratory tract, these spores are usually eliminated via mucociliary clearance mediated by the ciliated respiratory epithelium or via phagocytosis by pulmonary alveolar macrophages. Invasive disease typically develops in the presence of quantitative or qualitative defects of the innate immune system, particularly neutropenia or impaired phagocyte function. Because of the marked endothelial tropism of *Mucorales*, mediated by specific host-pathogen receptor interactions, mucormycosis is characterized by angioinvasion, vascular thrombosis, and subsequent tissue infarction [197].

Early diagnosis and prompt initiation of antifungal therapy are critical determinants of survival in mucormycosis. Among patients with underlying hematologic malignancies, delayed treatment has been associated with a marked increase in mortality from 48.6% to 82.9% [206], underscoring the need for rapid and reliable diagnostic workflows. Although mucormycosis may be suspected based on clinical and radiological evidence, definitive diagnosis relies on analyses of patient-derived specimens. Conventional fungal culture and histopathological examination remain the most established and widely available diagnostic methods due to their technical simplicity and cost-effectiveness [207–210]. In parallel, matrix-assisted laser desorption/ionization time-of-flight mass spectrometry (MALDI-TOF MS) and molecular detection methods are increasingly being used in routine practice, substantially expanding diagnostic capabilities [31,211–214]. Of particular interest are strategies aimed at earlier detection, including the screening for circulating *Mucorales* DNA in high-risk patient populations and metagenomic sequencing approaches [215,216]. However, integrative studies systematically comparing conventional culture and histopathology with molecular diagnostic approaches are still limited, highlighting a critical need for multimodal workflows that combine morphological and molecular information. More broadly, this underscores the importance of evaluating and adapting molecular diagnostic workflows not only for infectious diseases but also for neoplastic diseases of the respiratory tract.

1.5.4 Non-small cell lung cancer

Lung cancer is the most commonly diagnosed cancer worldwide and the leading cause of cancer-related mortality [217]. Non-small cell lung cancer (NSCLC) accounts for approximately 80-85% of all lung cancers, with adenocarcinoma representing the most common histological subtype, followed by squamous cell carcinoma [218]. By definition, lung adenocarcinomas are characterized by glandular differentiation, mucin production, and/or pneumocytic marker expression (e.g., TTF-1), whereas squamous cell carcinomas are diagnosed based on morphological and/or immunohistochemical evidence of squamous differentiation (e.g., p40) [92]. Treatment options for NSCLC have expanded substantially in recent years, largely driven by the introduction of immunotherapies and targeted therapies. This therapeutic paradigm shift has been enabled by an improved understanding of lung cancer biology, particularly through advances in cancer genomics and tumor immunology [219].

The efficacy of both immunotherapy and targeted therapy in NSCLC depends on predictive biomarkers. Immunotherapy-related biomarkers reflect distinct phases of the antitumor immune response. Markers that are associated with its initial phase (e.g., tumor mutational burden) may indicate a general likelihood of response to immunotherapy, whereas markers that are associated with the effector phase (e.g., PD-L1 expression) are more closely associated with the activity of specific immune checkpoint inhibitors [220]. The clinical efficacy of targeted therapies relies on the presence of specific oncogenic driver alterations that activate defined signaling pathways, thus making comprehensive molecular profiling indispensable for therapeutic planning [221]. Accordingly, molecular diagnostic approaches for NSCLC have evolved rapidly in recent years. Next-generation sequencing is now widely regarded as the method of choice for clinically relevant molecular testing in NSCLC, particularly in view of the continuously expanding spectrum of targetable genomic alterations [222–224]. International guidelines recommend reflex broad molecular profiling in all newly diagnosed advanced adenocarcinomas using gene panels that include *ALK*, *BRAF*, *EGFR*, *ERBB2 (HER2)*, *KRAS*, *MET* exon 14 skipping alterations, *NTRK1-3*, *RET*, and *ROS1* [225–227]. Importantly, the availability of molecular test results before initiation of first-line therapy is associated with significantly improved overall survival [228], underscoring the clinical value of implementing and further developing rapid molecular diagnostic workflows in NSCLC.

2 Integrative rationale of this cumulative thesis

2.1 General challenges in respiratory molecular pathology

Despite major advances in molecular and morphological techniques, the integrated tissue-based characterization of respiratory diseases remains a central challenge in both infectious and neoplastic pathology. A major limiting factor is sample availability. In lung cancer, most routine diagnostic specimens are small biopsies that must suffice for an expanding spectrum of immunohistochemical and next-generation sequencing-based biomarker analyses, frequently exhausting the available material. In infectious diseases, tissue sampling of the lung is uncommon and largely restricted to diagnostically unresolved cases because invasive biopsy procedures carry substantial risk. Research autopsies represent a potential approach to overcome these limitations by providing comprehensive access to well-annotated tissue. However, their broader implementation is constrained by substantial infrastructural and regulatory requirements. In translational lung research, multi-omics studies frequently rely on easily accessible biospecimens such as blood or respiratory fluids and therefore lack the spatial and microenvironmental context provided by tissue. This constitutes an important limitation, especially in the era of widely available spatially resolved omics technologies that can comprehensively characterize tissue environments. In addition, many molecular assays remain insufficiently integrated into established morphology-driven diagnostic workflows, restricting their timely clinical implementation and overall diagnostic impact.

2.2 Gaps in understanding respiratory immunopathology of severe viral disease and superinfection

Severe viral respiratory disease may present with broadly similar clinical and radiological features of acute lung injury, however, the clinical course and response to therapy vary substantially between patients. Clinical and imaging-based studies are often limited in resolving the tissue-level mechanisms that drive these divergent disease trajectories. Because human investigations frequently rely on readily accessible biospecimens such as blood and respiratory fluids, they lack direct correlation with pulmonary histopathology and are therefore unable to interrogate spatial patterns of tissue injury and local immune responses in situ. Even in autopsy-based studies using multi-omics analyses of lung tissue, systematic integration with detailed

histomorphological assessment is often lacking, thereby losing the architectural and compartment-specific context required for a comprehensive interpretation of tissue manifestations. A clinically important contributor to this heterogeneity, classically described in influenza [151], is secondary pneumonia. However, the underlying pathophysiology predisposing to secondary infection and its relevance across different viral respiratory diseases remain incompletely understood. In Covid-19, bacterial superinfections are considered to contribute to adverse outcomes, but reported incidences vary widely, possibly reflecting the clinical and radiological overlap with primary viral disease, which complicates diagnosis [11].

These gaps motivated integrative autopsy-based investigations that combine morphological assessment with multi-omics profiling to link local host response patterns with microbial signals in lethal Covid-19 (Publication I).

2.3 Gaps in integrating molecular diagnostics in infectious respiratory disease

With ongoing technical advances, the diagnostic pathology of respiratory infectious diseases increasingly depends on molecular assays. However, their integration into practical diagnostic workflows lags behind, in part because systematic studies directly comparing molecular readouts with established diagnostic methods and the development of structured diagnostic algorithms for their optimal use remain scarce.

SARS-CoV-2 rapid antigen tests have been primarily evaluated in clinical and public health settings, whereas data in the postmortem setting were initially lacking when Covid-19 emerged. Postmortem virus detection has an important diagnostic role in determining infection status, with direct implications for occupational biosafety during autopsy and tissue handling. A central unresolved question is to what extent antigen test positivity reflects viral viability and thus infectiousness, and how these readouts can be incorporated into postmortem workflows.

Histopathology is often the first modality to raise suspicion for mucormycosis but is unreliable for distinguishing *Mucorales* from other molds such as *Aspergillus*. However, this distinction is clinically highly relevant because antifungal treatment strategies differ substantially. In addition, conventional fungal culture has limited sensitivity for *Mucorales* and is not applicable to FFPE tissue. Molecular approaches such as ITS sequencing are promising but remain variably implemented, with uncertainties regarding their diagnostic performance in relation to

traditional methods (e.g., culture) and their optimal practical use during the histopathological workup.

These gaps motivated systematic evaluations of molecular assays and their integration with complementary diagnostic modalities in respiratory infectious disease pathology (Publications II and III).

2.4 Gaps in implementing comprehensive molecular reflex testing in neoplastic respiratory disease

The rapidly expanding spectrum of approved targeted therapies for NSCLC necessitates continuous adaptation of molecular testing strategies and the inclusion of an increasing number of predictive biomarkers. In routine diagnostics, this frequently results in incomplete molecular profiling, particularly in the context of very small biopsy specimens. This limitation is largely attributable to sequential testing workflows based on low-throughput molecular methods, thereby contributing to suboptimal tissue management. Furthermore, the availability of complete molecular results before initiation of first-line therapy is a critical determinant of optimal treatment selection. Although reflex testing strategies offer the potential to make workflows more efficient and possibly foster timely molecular profiling, real-world data on their practical feasibility and clinical impact have remained limited for DNA-based NGS and even more so for RNA-based NGS.

Furthermore, molecular testing algorithms have traditionally focused on lung adenocarcinoma, whereas recommendations for squamous cell carcinoma are more controversial across international guidelines. This uncertainty largely reflects the scarcity of real-world studies that include cases with squamous histology and systematically evaluate the feasibility and value of comprehensive profiling in this subgroup.

These gaps motivated systematic evaluations of comprehensive DNA- and RNA-based reflex molecular testing strategies within routine diagnostic workflows for NSCLC of different histology (Publications IV and V).

2.5 Conceptual framework and thesis contribution

Collectively, the studies included in this cumulative thesis are unified by an integrative morpho-molecular approach to respiratory disease. They link mechanistic investigation to the implementation of innovative molecular diagnostic workflows in both infectious and neoplastic settings. In the context of severe respiratory viral disease and opportunistic fungal infection, this approach enabled the tissue-based characterization of host-pathogen interactions and the systematic combination of morphological and molecular methods to improve pathogen detection and disease stratification, as addressed in publications I-III. The same conceptual principle was applied to neoplastic diseases of the respiratory tract, where publications IV and V focus on the implementation and evaluation of rapid and comprehensive tissue-based molecular testing workflows for biomarker-driven therapy in NSCLC. Together, these studies demonstrate how this integrative strategy advances both the mechanistic understanding of respiratory disease and the clinical implementation of precision diagnostics. Building on this unified methodological concept, this cumulative thesis pursued specific aims that address key challenges across infectious and neoplastic diseases of the respiratory tract.

3 Aims of this cumulative thesis

The overarching aim of this cumulative thesis is to develop and apply integrative tissue-based morpho-molecular strategies to (i) elucidate the immunopathology of severe viral respiratory disease and associated secondary infections and (ii) implement and evaluate clinically applicable molecular diagnostic workflows for infectious and neoplastic diseases of the lung.

Aim 1: To characterize the tissue-based immunopathology and host-pathogen interactions that underlie secondary infections in lethal Covid-19 by integrating histopathological analyses with comprehensive microbiome and transcriptome profiling. *(Addressed in publication I)*

Aim 2: To develop and evaluate multimodal molecular diagnostic approaches for the detection and characterization of respiratory pathogens in routine and postmortem tissue, and to assess their complementary value within infectious disease pathology. *(Addressed in publications II and III)*

Aim 3: To implement and expand comprehensive DNA- and RNA-based reflex molecular testing strategies for biomarker-driven therapy in non-small cell lung cancer within routine diagnostic workflows. *(Addressed in publications IV and V)*

By addressing these aims, this cumulative thesis contributes to establishing a unified framework for integrative molecular pathology of respiratory disease that links mechanistic insight with clinically applicable diagnostics.

4 Summary of individual publications

4.1 Publication I: Host and microbiome features of secondary infections in lethal Covid-19

Severe Covid-19 is frequently complicated by secondary infections, however, their contribution to mortality and the underlying tissue-level mechanisms remain incompletely understood. To address this gap, we conducted an integrative autopsy-based multi-omics study comprising 20 consecutive Covid-19 patients during the first pandemic wave and 14 control cases without primary respiratory disease. Systematic histopathology was used as the central reference and was complemented with tissue-based RNA sequencing, quantitative SARS-CoV-2 RT-PCR, microbiological culture, and 16S/ITS sequencing in order to relate patterns of lung injury to local microbial communities and host responses. At the morphological level, lethal Covid-19 segregated into two major terminal phenotypes characterized by either diffuse alveolar damage or secondary pneumonia as the dominant cause of death. Microbiome analyses demonstrated a reduced pulmonary microbial diversity in Covid-19 compared with controls and an enrichment of prototypical bacterial and fungal pathogens in cases with secondary pneumonia. Lung transcriptome profiling closely mirrored the histopathological stratification and further resolved diffuse alveolar damage into two distinct subgroups with different cellular compositions. In particular, myeloid- and macrophage-associated signatures, as well as complement C1q emerged as major discriminators, indicating divergent host response patterns. In parallel, a prominent upregulation of inhibitory immune checkpoint molecules was observed. Taken together, these findings suggest that lethal Covid-19 is not a uniform disease entity but comprises distinct subtypes that differ in their immune and stromal composition. It supports a model in which profound immune dysregulation with impaired antimicrobial defense facilitates the development of superimposed bacterial and fungal pneumonia.

4.2 Publication II: Rapid antigen test for postmortem evaluation of SARS-CoV-2 carriage

Rapid and reliable evaluation of infectious risk is essential for the safe performance of autopsies in Covid-19 patients. While rapid antigen tests (RATs) were extensively assessed in clinical settings, their role in the postmortem setting had not been systematically investigated. This

study therefore examined whether RAT could contribute to postmortem SARS-CoV-2 detection and support risk-adapted autopsy practice. In a prospective cohort of 30 consecutive deceased Covid-19 patients, RAT results obtained from nasopharyngeal swabs were compared with quantitative RT-PCR as the reference method. In addition, virus isolation from lung tissue was performed to relate molecular and antigen-based detection to viral cultivability as a surrogate of infectivity during autopsy. Although RAT showed a lower overall sensitivity than RT-PCR, false-negative RAT results were consistently associated with low viral loads that were below the range at which virus cultivation was successful. Reduced viral load and negative RAT results correlated with longer disease duration but not with the postmortem interval. These findings indicate that postmortem RAT primarily identifies corpses with potentially transmissible virus and can therefore assist in selecting cases that require enhanced biosafety conditions when immediate PCR testing is not available.

4.3 Publication III: The mutual value of histopathology and ITS sequencing in the diagnosis of mucormycosis

Mucormycosis is an aggressive invasive fungal infection in which patient survival critically depends on rapid and reliable diagnosis. In routine pathology, the initial suspicion of an invasive mould infection is frequently raised by histopathological evaluation. However, morphological assessment alone is often insufficient, particularly for differentiation from *Aspergillus* species. This is clinically highly relevant because antifungal treatment strategies differ substantially. Although broad-range molecular methods such as ITS sequencing enable species-level identification of fungal DNA directly from tissue, their integration into established histopathology-driven diagnostic workflows has not been systematically evaluated. To address this gap, we performed a retrospective single-centre study assessing the utility of combining histomorphological examination with ITS sequencing in 14 consecutive mucormycosis cases diagnosed with this approach in routine practice. Fungal hyphae were readily detectable by histopathology in all cases and subsequent ITS sequencing enabled identification of a broad spectrum of *Mucorales* species with considerable phylogenetic diversity. In addition, ITS sequencing detected a clinically relevant co-infection with *Pneumocystis jirovecii* in one case. Conventional fungal culture, performed in a subset of cases, showed a markedly lower detection rate than molecular analysis, underscoring its limited sensitivity in mucormycosis. These findings demonstrate that the combination of histopathology and ITS sequencing is feasible and

diagnostically more sensitive than culture for detecting and subtyping *Mucorales* in FFPE tissue. Rather than replacing morphology, molecular testing complements the initial histopathological assessment and enables species-level resolution that cannot be achieved by conventional methods. The study therefore supports an integrated, stepwise diagnostic workflow in which molecular testing is initiated when mucormycosis is suspected histologically.

4.4 Publication IV: Reflex testing in non-small cell lung carcinoma using DNA- and RNA-based next-generation sequencing - a single-center experience

The increasing number of predictive biomarkers in NSCLC requires molecular testing strategies that deliver comprehensive results within clinically relevant timeframes. Although NGS-based reflex testing has the potential to overcome the limitations of sequential low-throughput approaches, real-world evidence on its feasibility and clinical impact has been limited. Therefore, we performed a retrospective single-centre study of 432 consecutive NSCLC cases, comparing two diagnostic periods with different molecular workflows. In the earlier period, routine testing relied primarily on DNA-based NGS for mutation analysis combined with immunohistochemistry for selected gene fusions, whereas in the later period a comprehensive reflex strategy with parallel DNA- and RNA-based NGS was implemented. This change in diagnostic practice enabled an evaluation of reflex broad molecular profiling under routine conditions. Both DNA- and RNA-based assays proved highly robust and yielded evaluable results in the vast majority of cases. The addition of RNA-based NGS led to a marked increase in fusion detection and consequently to a higher proportion of patients receiving biomarker-guided targeted therapy. Moreover, this approach facilitated the identification of rare alterations (e.g. of the so far undescribed *EGFR-NUP160* fusion), highlighting its relevance in detecting emerging therapeutic targets. Together, these findings demonstrate that parallel DNA- and RNA-based reflex NGS is technically feasible in routine diagnostics and provides substantial clinical benefit by improving the detection of actionable alterations. The study therefore supports the implementation of comprehensive molecular reflex testing workflows as a central component of precision diagnostics in NSCLC.

4.5 Publication V: Expanding broad molecular reflex testing in non-small cell lung cancer to squamous histology

Building on the implementation of parallel DNA- and RNA-based reflex testing in NSCLC, this study addressed whether such a comprehensive strategy is also justified in squamous cell carcinoma (SCC), for which current guideline recommendations remain less consistent than for adenocarcinoma. In routine practice, molecular testing in SCC is therefore often restricted to selected clinical subgroups defined by age or smoking history. However, evidence supporting these exclusion criteria is limited, largely because real-world data on the prevalence and clinical relevance of actionable genomic alterations in NSCLC cohorts that include squamous histology remain scarce. To address this gap, we performed a retrospective single-centre analysis of 316 consecutive lung SCC cases that underwent routine DNA- and RNA-based NGS. Actionable genomic alterations linked to approved targeted therapies were identified in a clinically relevant subset of cases, including patients with advanced age and substantial smoking history who would have been excluded by restrictive testing strategies. These findings demonstrate that comprehensive molecular profiling in SCC can reveal therapeutically relevant alterations that would be missed by selective testing strategies. The study therefore supports a histology-independent reflex testing workflow for all newly diagnosed NSCLC cases, thereby enabling equitable access to biomarker-driven targeted therapy.

5 Discussion

5.1 Integrative perspective on respiratory molecular pathology

Diseases of the respiratory tract often present with overlapping clinical and radiological findings (e.g., acute lung injury). However, their biological behavior and response to therapy can be highly heterogeneous. This heterogeneity reflects the unique structural and functional organization of the lung, in which host responses have to simultaneously ensure the efficient elimination of external stimuli and the preservation of the delicate tissue structures required for gas exchange. The resulting balance between antimicrobial defense and tissue tolerance generates distinct spatial and temporal reaction patterns that are not adequately captured by histopathology or molecular pathology approaches alone but require an integrative perspective. Temporal heterogeneity can only be addressed by examining tissue at pathogenetically relevant stages of disease. In the context of severe and lethal respiratory disorders, the postmortem setting represents a particularly informative but often underutilized time point. Research autopsies enable comprehensive tissue sampling and, when correlated with premortem diagnostic material, provide a unique opportunity to study terminal disease mechanisms in direct anatomical context. Spatial heterogeneity, in turn, is most comprehensively reflected by tissue-based analyses that preserve the structural organization of the respiratory tract. More easily accessible specimen types such as blood or respiratory fluids lack this tissue architectural context and therefore capture only a limited aspect of disease biology.

With the rise of next-generation sequencing and multi-omics technologies, molecular datasets have become increasingly available. However, their interpretation often remains separate from systematic histomorphological assessments. Integrating molecular readouts with tissue morphology is therefore essential for mechanistic studies but also for the implementation of reliable diagnostics. On the mechanistic level, this approach enables the characterization of tissue reaction patterns in response to diverse external stimuli, including neoplastic transformation and infections with pathogens of different composition and load. Emerging spatially resolved technologies such as spatial transcriptomics and multiplex imaging, technologies that have recently been awarded as methods of the year from the journal *Nature Methods* [229,230], further strengthen this concept by allowing the direct correlation of gene expression profiles with cellular localization and tissue architecture. The same principle applies

to diagnostic workflows. In infectious disease pathology, the distinction between true pathogen detection and contamination, which is particularly relevant in FFPE tissue, can only be achieved by correlating molecular findings with the corresponding immune reaction patterns. In tumor pathology, the interpretation of low variant allele frequencies depends on the histological estimation of tumor cell content, allowing discrimination between subclonal alterations and technical artefacts. Only within such a morphology-guided framework can the full diagnostic potential of molecular assays be realized.

The present cumulative thesis applies this integrative morpho-molecular concept to both infectious and neoplastic diseases of the respiratory tract. In the autopsy-based multi-omics analysis of Covid-19, this strategy enabled the identification of distinct tissue-level disease trajectories and provided mechanistic insight into lethal disease. Translated into diagnostic practice, the same framework improved pathogen detection, informed biosafety strategies in the postmortem setting, and facilitated the implementation and expansion of comprehensive reflex molecular testing in lung cancer. Together, these studies demonstrate that a structured integration of tissue morphology and molecular data represents a unifying principle for both the biological understanding and the clinical management of respiratory disease.

5.2 Tissue as the central reference for multi-omics studies

High-throughput omics technologies have profoundly advanced translational research in human respiratory disease. However, many molecular studies are based on biospecimens that lack direct anatomical context, largely because access to pulmonary tissue is limited and often requires invasive procedures. As a consequence, particularly immunological investigations frequently rely on peripheral blood, which reflects systemic rather than local immune responses and may therefore provide an incomplete or even misleading picture of the disease process within the lung. A classical example illustrating the discrepancy between systemic and local immunity is sarcoidosis. Whereas the pulmonary immune compartment is characterized by an accumulation of activated $CD4^+$ T cells with markedly increased CD4/CD8 ratio, peripheral blood typically shows reduced circulating $CD4^+$ T cell counts and a normal or decreased CD4/CD8 ratio [231–235]. Analysis of bronchoalveolar lavage fluid partially captures this local immune constellation and is therefore clinically useful. Nevertheless, fluid-based approaches cannot resolve the defining tissue architecture of sarcoidosis, which is the formation of well-structured non-necrotizing granulomas [236]. A recent single-cell and spatial transcriptomics

study has demonstrated that human sarcoidosis granulomas represent highly organized microenvironments resembling ectopic lymphoid structures driven by distinct cellular and metabolic programs. Notably, pharmacological inhibition of one of the identified processes attenuated granuloma formation in a sarcoidosis mouse model, pointing towards targetability of spatial programs in general [237]. Such spatially encoded biological mechanisms would remain inaccessible in studies based solely on blood or bronchoalveolar lavage fluid. Comparable observations have been made in neoplastic disease, where imaging mass cytometry has shown that the spatial organization of tumor cells and their microenvironment critically influences the response to immunotherapy, thereby highlighting the potential clinical relevance of tissue-based spatial analyses [238].

Within the present thesis, the integrative autopsy study of lethal Covid-19 serves as a proof of principle for a tissue-anchored multi-omics strategy. Comprehensive sampling enabled by autopsy combined with systematic histomorphological evaluation provided the essential backbone for the interpretation of transcriptomic and microbiome data. The clear morphological distinction between diffuse alveolar damage (DAD) and secondary pneumonia defined biologically meaningful disease categories that were consistently reflected at the molecular level. This histology-guided stratification prevented misinterpretation of complex RNA sequencing data and enabled the identification of distinct host response patterns within DAD. Likewise, microbial signals only became biologically interpretable when correlated with the corresponding tissue reaction patterns. This allowed us to link reduced microbial diversity and the emergence of prototypical respiratory pathogens to specific forms of lung injury and immune dysregulation. Beyond Covid-19, this concept has broader implications for infectious respiratory research. Studies that focus exclusively on host immune signatures may misinterpret neutrophil-dominant responses as intrinsic viral phenotypes when they in fact reflect bacterial or fungal superinfection. Conversely, pathogen- or microbiome-centered approaches that lack correlation with tissue morphology and host response risk overinterpreting contaminants, a well-recognized challenge in low-biomass pulmonary samples [129,172]. Even when microbial signals are biologically valid, the distinction between colonization and invasive infection cannot be made without assessing spatial relationships within tissue.

Taken together, these considerations demonstrate that tissue morphology provides the indispensable reference for the biologically meaningful interpretation of multi-omics data. An integrative morpho-molecular approach that places histopathology at the center of top-down

molecular analyses is therefore essential for both mechanistic studies and applied molecular diagnostics in infectious and neoplastic diseases of the respiratory tract.

5.3 Immunopathology of severe respiratory viral disease and superinfection

Severe respiratory viral disease is typically accompanied by markedly elevated systemic inflammatory markers, which hampers the clinical distinction between acute respiratory distress syndrome (ARDS) caused by the primary viral infection and superimposed bacterial or fungal pneumonia. This diagnostic uncertainty is likely one of the major reasons for the widely diverging rates of secondary infections reported in Covid-19 cohorts. While some studies describe bacterial superinfection in a substantial proportion of critically ill patients (up to 42% in Buehler et al [11]), others report considerably lower frequencies, and a large meta-analysis estimated an overall prevalence of approximately 8% among hospitalized patients [239,240]. These discrepancies likely reflect differences in patient selection and disease severity, but also in the timing, anatomical site, method and sensitivity of microbiological testing. In addition, the widespread empirical use of antibiotics (>70% in the meta-analysis by Langford et al [240]) probably influences detection rates, as prior antibiotic exposure may reduce pathogen recovery without preventing the development of infection-related tissue injury.

The autopsy-based analysis performed in this thesis [24] provides a tissue-level perspective that helps to elucidate these heterogeneous clinical observations. A dominant or contributory bacterial or fungal pneumonia was identified in a substantial proportion of lethal Covid-19 cases (8/20; 40%) and had frequently not been recognized during life. This discrepancy underscores the limited sensitivity of conventional ante-mortem microbiological testing in critically ill patients and highlights the importance of direct anatomical sampling at the site of injury. In general, tissue-based analysis might be able to yield higher detection rates than blood or other body fluids. Furthermore, only the combined assessment of pathogen detection and the corresponding histopathological reaction pattern allows the distinction between contamination or colonization and true invasive infection. In line with this, in one case of our autopsy cohort invasive mucormycosis caused by *Rhizopus microsporus* was identified exclusively postmortem, illustrating the diagnostic challenges encountered in the clinical setting to distinguish viral ARDS from invasive fungal superinfection [24,241]. These findings

emphasize that secondary infections represent a clinically relevant complication in a significant subset of patients with severe Covid-19.

Beyond its diagnostic implications, the integrative autopsy approach applied in our study exemplifies also the mechanistic concept developed in the preceding chapters of this thesis. By combining systematic histomorphology with transcriptomic, protein-based, microbiological, and virological analyses in a clinically well-defined cohort, we were able to relate spatially distinct host response patterns to microbial parameters and thereby gain insight into pathophysiological principles. Such “holistic” autopsy strategies have been proposed as a blueprint for investigating newly emerging diseases, as they enable unbiased characterization of terminal disease trajectories and can capture epidemiological and biological information directly from tissue [242]. Notably, the morphology-guided stratification applied in our study proved essential for the biological interpretation of the molecular data and enabled the identification of distinct subtypes of severe disease. At the tissue level, lethal Covid-19 did not present as a uniform pathological entity but segregated into two major immunopathological patterns: virus-associated diffuse alveolar damage (DAD) and secondary pneumonia [24]. These patterns were consistently mirrored across the different analysis modalities (histology, transcriptomics, microbiology). Importantly, virus-associated DAD alone was not accompanied by a prominent neutrophilic response, suggesting that neutrophil-dominated signatures reported in several Covid-19 studies may frequently reflect superimposed bacterial or fungal infection rather than intrinsic features of viral lung injury [153,243–246]. This highlights the importance of histomorphological pre-classification of tissue samples to avoid misleading conclusions in downstream analyses and reinforces the relevance of the overarching morpho-molecular framework presented in this cumulative thesis.

The lung microbiome represents an important factor contributing to disease heterogeneity. Alterations in the lung microbiome have been described not only specifically in Covid-19 but also more broadly in acute lung injury and in sepsis in general [170,247,248]. In our cohort, reduced microbial diversity and enrichment of pathogens were closely linked to secondary pneumonia [24]. Similar associations of bacterial and fungal superinfections contributing substantially to mortality have been described in other respiratory viral diseases, including influenza [14,249,250]. Furthermore, the frequent occurrence of polymicrobial infections and EBV in our autopsy cohort [24] supports the concept of broad immune impairment in a subset

of lethal Covid-19 cases, although the functional consequences of these findings require further investigation.

The development of secondary infection in severe respiratory virus disease is likely multifactorial. Mechanistically, the antiviral immune response has been shown to reduce the antibacterial defense by apoptosis in bone marrow granulocytes and reduction of granulocyte infiltrates at the site of bacterial superinfection [251]. Furthermore, Setdb2-mediated regulatory crosstalk between type I interferons and NF- κB pathways has been suggested to be an important mechanism of bacterial superinfection susceptibility induced by virus infection [252]. In addition to direct virus-induced immune modulation, other contributing factors might be preexisting comorbidities such as diabetes mellitus or chronic kidney disease, intensive care treatment, mechanical ventilation, and antimicrobial therapies [253–256], which were also common features in our Covid-19 autopsy cohort [24]. Antibiotic exposure represents a particularly complex variable in this context. While necessary in selected cases, extensive empirical use may alter the lung microbiome and contribute to antimicrobial resistance [257]. In analogy to well-known phenomena in the gastrointestinal tract where the depletion of resident microbial communities can reduce colonization resistance and promote overgrowth by opportunistic pathogens [258], comparable mechanisms may occur in the heavily remodeled lungs of critically ill Covid-19 patients.

The comprehensive data obtained in our multimodal autopsy study [24] are compatible with an evolutionary model of severe Covid-19 developing from an early more inflammatory phase dominated by myeloid cells, proinflammatory macrophages and predominantly exudative DAD histology, toward a phase characterized by immune exhaustion, tissue repair and predominantly organizing DAD histology. This later DAD phase may therefore be particularly susceptible to secondary infection. The evolutionary trajectories of severe Covid-19 occurred in the context of extensive complement activation, compatible with findings from other autopsy-based studies [188]. In general, complement activation in Covid-19 has mainly been discussed in relation to endothelial injury and thrombosis [259], however, our data suggest an additional role in the modulation of local immunity, possibly mediated by C1q [24].

C1q is involved in efferocytosis, which is the clearance of apoptotic and necrotic cells by phagocytes, and thereby likely contributes to the resolution of inflammation [260]. Because extensive cell death is a prominent feature of lung injury in Covid-19, increased C1q deposition

may promote efferocytosis and the differentiation of tolerogenic myeloid cells. It has been described that the interaction of C1q with inhibitory immune receptors such as LAIR-1 can attenuate type I interferon production and may subsequently impair antiviral defense [261]. In our study, one DAD subtype is specifically characterized by increased macrophage infiltration and substantial co-expression of C1q and LAIR-1, indicating a state of impaired immune activation. Furthermore, progressive extracellular matrix remodeling during organizing DAD might provide further immune inhibitory signals through collagen-binding receptors such as LAIR-1 and LILRB4, potentially linking structural tissue repair to immune modulation [262]. An additional layer of evidence for a local immunosuppressive milieu is our observation of the substantial upregulation of inhibitory immune checkpoint molecules in Covid-19 patients compared to controls [24]. Notably, similar mechanisms are well-known to be relevant for cancer immunotherapy [263], raising speculations if these pathways might also be therapeutically exploitable in selected cases of severe viral disease, although likely more nuanced in this context.

Taken together, the described findings indicate that the development of secondary infection in severe Covid-19 is not only caused by external clinical factors but also by intrinsic factors within host tissue. Such integrative insights emerging from our autopsy study were only possible by morphology-anchored interpretation of multi-omics data, a paradigm described throughout this cumulative thesis. Beyond the specific context of Covid-19, the observed progression from a phase dominated by proinflammatory lung injury to a phase dominated by tissue repair and immune exhaustion may represent a more general principle of severe respiratory viral disease. This provides also a possible immunopathological framework to understand the susceptibility to secondary pneumonia.

5.4 Integrating molecular pathogen detection into pathology workflows

The increasing availability of molecular assays has profoundly expanded the diagnostic armamentarium of infectious disease pathology. Of particular relevance for the field is the direct applicability of these assays on primary clinical specimens, specifically FFPE tissue, since most surgical pathology workflows rely on this specimen type. In contrast to the availability of the assays themselves, their implementation into routine diagnostic workflows is lagging behind. In most contexts of infectious disease pathology, molecular readouts have a histomorphological

pendant. In practice, however, these two modalities often stand in isolation, although they are in fact complementary and have mutual value when appropriately integrated. Without their incorporation into structured diagnostic workflows, the full potential of technically innovative molecular assays cannot be reached. One of the main challenges of the field is that molecular detection of microbes alone is not able to reliably distinguish between contamination, colonization, and infection. Especially the respiratory tract, with its low microbial biomass and constant environmental exposure, is prone to potential false-positive results, which would have substantial clinical consequences [129,264]. To avoid such overinterpretation, thorough correlation with histopathological or cytopathological as well as clinical and radiological findings is mandatory. Conversely, morphology alone may prove invasive infection but is limited in identifying pathogens with species-level resolution. Combining both modalities provides therefore complementary information that neither of them can achieve on its own. Such an integrative approach has been termed "morpho-molecular" or "histo-molecular" in the literature by us and others and has been shown to be of particular value in fungal infections [265].

Histopathology is often the first diagnostic modality to raise suspicion for mucormycosis by demonstrating tissue-invasive fungal hyphae with a predilection for blood vessels and associated ischemic necrosis. In principle, morphological criteria to differentiate *Mucorales* from other molds, such as *Aspergillus spp.*, have been suggested but may be unreliable, specifically in the tissue context. In their article titled "Histopathologic Diagnosis of Fungal Infections in the 21st Century", Guarner and Brandt state that "… histopathologic diagnosis should be primarily descriptive of the fungus and should include the presence or absence of tissue invasion and the host reaction to the infection." [266]. Thus, a specific diagnosis that includes the specific fungal species involved is only possible with ancillary tests. A comprehensive solution for this is ITS sequencing, and we could demonstrate its value and numerous advantages within the histopathological workup of mucormycosis [31]. First, in contrast to fungal culture, ITS sequencing can be performed on FFPE tissue. In this way, a histomorphology-based differential diagnosis can be confirmed immediately using the same FFPE block without the need for additional clinical sampling. Furthermore, our data suggest that ITS sequencing has a higher sensitivity than fungal culture in detecting tissue-invasive *Mucorales*. Possible reasons include challenging growth requirements of *Mucorales*, prior antifungal treatment, and limited representativeness of the specimen used for culture [267,268].

The latter can be more easily circumvented in FFPE-compatible workflows, as the most representative tissue region with histomorphologically verified fungal structures can be selected for subsequent molecular analysis. An additional advantage of integrating ITS sequencing is its ability to simultaneously detect other fungal DNA from the same specimen within the same sequencing run. This enables the identification of mixed fungal infections, which is particularly relevant for the frequently immunocompromised patient population affected by mucormycosis. Taken together, our mucormycosis workflow provides a bona fide example of the morpho-molecular framework in the context of infectious diseases.

Apart from histomorphology, molecular diagnostic strategies in infectious disease pathology can also be shaped by distinct clinical and public health demands. This is particularly relevant in emerging and pandemic infections, where rapid pathogen detection is crucial to contain transmission. During the SARS-CoV-2 pandemic, rapid antigen tests (RATs) were widely implemented in various settings, including screening programmes. However, for a long time, data on the use of RATs in the postmortem context were lacking. Our prospective cohort study [184], comparing postmortem RAT with qRT-PCR and virus cultivation, enabled us to determine the diagnostic performance of the antigen test, particularly with regard to approximating the infectivity of corpses. Despite its overall lower sensitivity than qRT-PCR, RAT detected all cases with virus concentrations above the threshold of cultivability. Thus, RAT-negative corpses may pose only minimal risks of infectivity, mirroring findings in the clinical setting [269]. One caveat for autopsy practice is, however, that a virus-negative nasopharyngeal swab specimen cannot exclude the possibility of viable virus in organs exposed during invasive postmortem procedures, as shown in our associated autopsy study [24], thereby supporting the need for additional biosafety measures when performing such procedures [192]. Taken together, our analyses suggest a potential value of RAT in guiding autopsy practice when interpreted cautiously and within the appropriate clinical and laboratory context, again stressing the importance of integrating novel diagnostic tests into existing workflows.

Collectively, the discussed examples demonstrate that the diagnostic value of a molecular assay in infectious disease pathology is not determined solely by its analytical performance, but by its appropriate integration into a structured diagnostic workflow. The application of such assays may be triggered by different factors, for example histomorphological suspicion (as in mucormycosis [31]) or infection control and public health requirements (as in the use of viral rapid antigen tests [184]). In both scenarios, the diagnostic question defines the molecular

testing strategy, going beyond the mere availability of the method. When guided by histomorphology, molecular analyses can be performed top-down in tissue areas with verified pathogen-associated alterations. This increases analytical sensitivity but also enables biological interpretation through correlation with the local host response. Conversely, in settings driven by infection control, assays such as rapid antigen tests enable risk stratification and guidance of clinical practice. In such ways, both approaches link analytical advancements to clinically meaningful decision-making and such a framework can also be applied to other areas of respiratory pathology.

5.5 Implementing and expanding comprehensive molecular profiling in NSCLC

Although lung cancer is still the leading cause of cancer-related death worldwide [217], treatment options have expanded substantially in recent years, particularly for NSCLC. A major driver of this progress has been the broad implementation of targeted therapies, most notably tyrosine kinase inhibitors (TKIs). Historically, gefitinib was the first TKI in NSCLC to (retrospectively) demonstrate that molecular stratification can result in profound clinical responses in defined patient subgroups. In two seminal NSCLC studies, performed both in patient cohorts and in cancer cell line models, it was convincingly shown that tumors harboring activating *EGFR* mutations are highly sensitive to EGFR inhibition, whereas *EGFR* wild-type tumors are less likely to respond [270,271]. As a consequence, *EGFR* mutation testing was rapidly incorporated into early molecular testing recommendations for lung cancer [272]. This marked the beginning of a steep increase in our understanding of oncogenic driver alterations within tumor cells, leading to the identification of numerous actionable molecular targets that now serve as predictive biomarkers for targeted therapies. Today, the spectrum of clinically actionable alterations in NSCLC is extensive and reflects the transformative impact that translational cancer research can have [219].

For the field of diagnostic and molecular pathology, this progress poses also some challenges. One of the most fundamental ones is that the primary diagnostic tissue specimens in NSCLC are often small and contain low numbers of tumor cells, while the demands to assess an increasing number of molecular targets continue to grow. This challenge is aggravated when immunohistochemistry is included in the diagnostic workup of biopsy specimens. Current diagnostic guidelines on NSCLC already suggest restricting diagnostic immunohistochemistry

to TTF1 (for adenocarcinoma) and p40 (for squamous cell carcinoma) [273]. If neither histomorphology nor the immunohistochemical expression profile allows an unambiguous diagnosis of adenocarcinoma or squamous cell carcinoma and if neuroendocrine neoplasms and metastases have also been excluded, the current WHO classification provides the entity "NSCLC not otherwise specified" (NSCLC-NOS) to avoid overinterpretation in small samples [92]. This diagnostic category is predominantly used in biopsies and reflects a paradigm shift toward accepting a less specific morphological diagnosis in order to preserve tissue for comprehensive predictive marker testing rather than exhausting the material in an attempt to completely subtype the tumor. However, PD-L1 immunohistochemistry has become an essential component of the routine diagnostic work-up in newly diagnosed NSCLC cases [274]. In the future, additional protein biomarkers may also be integrated, such as MTAP immunohistochemistry, which has been described to be more sensitive than some panel-based NGS assays for detecting MTAP loss [275]. To resolve these problems of tissue scarcity, optimal tissue management is essential.

From a technical perspective, there are several angles tissue management can be optimized for adequate predictive biomarker testing. One way to save tissue is by choosing comprehensive NGS-based assays over sequential single-gene tests or small panels. Moreover, there is scientific evidence that, compared with sequential testing strategies, NGS-based workflows can reduce turnaround time and be cost-effective [276]. Another tissue-saving measure is to avoid leveling steps in the tissue block of NSCLC biopsies as these use up tissue fast. To circumvent this, we have established a standardized tissue cutting workflow. After histomorphological verification of NSCLC as the most likely diagnosis and confirmation of sample representativeness, a comprehensive recutting program is performed cutting the tumor sample on blank slides reserved for both immunohistochemistry and molecular analysis, thus preventing additional leveling steps [223]. These unstained slides are then either stored until molecular testing is instructed by the clinical colleagues (clinician-initiated molecular testing) or are immediately further processed for seamless molecular testing within the pathology department (pathologist-initiated molecular testing or "reflex testing") [277].

Pathologist-initiated reflex testing is a dedicated workflow in which the pathologist responsible for the diagnostic case takes also the lead in initiating and managing the testing for a set of predefined biomarkers and, by definition, does not need a formal testing request from the treating clinician [277]. Such an approach has several advantages. Notably, reflex testing

democratizes access to biomarker testing since all NSCLC samples within a center are handled in the same way, supporting a more uniform standard of care at the local level. This seems particularly important since it has been shown that socioeconomic and racial factors may have an impact on biomarker testing rates [278,279]. Reflex molecular testing is increasingly recommended not only for late-stage NSCLC but also for earlier stages to inform neoadjuvant/adjuvant treatment decisions. Several recent clinical trials provided evidence for such an approach, particularly the ADAURA trial resulted in the approval of Osimertinib in the adjuvant setting of resectable *EGFR*-mutated NSCLC [280,281]. Furthermore, several real-world studies evaluating potential value after introducing reflex testing have shown that the overall mutation detection rate increased, while both the turnaround time and the time to optimal first-line therapy decreased [277,282,283]. Adding on to that, our own data shows that complementing a purely DNA-based workflow with RNA-based NGS results in more detected alterations but also in more patients receiving targeted therapies [223].

Comprehensive molecular profiling in NSCLC has traditionally been focused on adenocarcinoma due to its high rate of therapeutic targets [284]. Conversely, lung squamous cell carcinoma has a substantially lower rate and therefore the official molecular testing recommendations have been more controversial in this context. The International Association for the Study of Lung Cancer (IASLC), the College of American Pathologists (CAP), the Association of Molecular Pathology (AMP) and the European Society for Medical Oncology (ESMO) all recommend a selective testing approach for squamous cell carcinoma, with molecular analysis primarily advised in younger patients and in those with minimal or absent tobacco exposure [226,227,285], while the current National Comprehensive Cancer Network Clinical Practice Guidelines in Oncology (NCCN Guidelines) acknowledge a potential value in testing all patients with squamous cell carcinoma, independent of age or smoking history [225]. To help address these discrepancies, we conducted a retrospective single-center study assessing the value of DNA- and RNA-based NGS testing in 316 consecutive lung squamous cell carcinoma cases [224]. We identified established, targetable molecular alterations in 6.6% of cases, comprising *EGFR* mutations and fusions, *KRAS* G12C mutation, *ALK* fusions, and *MET* exon 14 skipping. The frequency of targetable alterations in our cohort was largely consistent with reports from other NSCLC series that included tumors with squamous histology [286–288], supporting the overall representativeness of our dataset. When Sands et al expanded their target definition from established to potential biomarkers, they reported alterations in 38% of

cases (e.g., *PIK3CA* mutations) [289], and applying a comparable definition to our cohort resulted in a prevalence of approximately 28%. Notably, all of our patients harboring an established targetable alteration would have been missed by restrictive testing algorithms based on age and smoking history [224]. This finding likely reflects the relatively high smoking prevalence in Austria [290], which resulted in a cohort with a large proportion of smokers and indicates that more selective testing strategies would have systematically denied these patients access to predictive biomarker testing.

Overall, both NSCLC studies included in this cumulative thesis [223,224] support the routine implementation of comprehensive NGS-based reflex testing for all newly diagnosed NSCLC cases without selection based on histology, age, or smoking history. Together, these data show that the shift towards upfront broad molecular profiling is not merely a technological upgrade. Rather, this encompasses a structural reorganization of diagnostic workflows that enables the optimal use of limited tissue and thereby facilitates uniform and comprehensive access to biomarker-driven precision oncology.

5.6 Conclusion and future directions

This cumulative thesis demonstrates that the integration of tissue morphology with multimodal molecular analysis is central to both advancing biological understanding and enabling innovative diagnostics in respiratory disease. Across infectious and neoplastic disease contexts, morphology served as the guiding principle for biological and clinical interpretation of complex molecular data. The studies included in this thesis show that the added value of novel molecular technologies lies not only in their analytical and high-throughput capacity, but to a large extent in their proper interpretation and integration with other findings, particularly histomorphology and clinical context. Academic pathology is in a unique position to lead such integrative approaches for both the study of pathogenesis and the optimization of diagnostics.

Mechanistically oriented translational research has been transformed by the increasing possibility to use omics technologies on patient-derived tissue. However, their true potential only emerges when they are applied to carefully phenotyped cohorts that allow systematic hypothesis testing. In our multi-omics autopsy study of lethal Covid-19, this integrative strategy enabled the identification of previously poorly described shifts in the pulmonary immune microenvironment that may predispose distinct patient subgroups to secondary infections. The

combination of deep sequencing with rigorous patient stratification based on histopathological and microbiological findings allowed RNA expression patterns to be interpreted in their appropriate biological context. This approach revealed a clear association between neutrophil-associated signatures and secondary infection, a result that is more consistent with fundamental pathophysiological principles than models derived from less stringently characterized Covid-19 cohorts. Research autopsy programs provide a particularly valuable translational platform when combined with cutting-edge sequencing technology. Both the volume of samples and the systematic way they are collected during an autopsy represent resources that are difficult to obtain by any other means.

Furthermore, this cumulative thesis shows that such an integrative approach embracing both histomorphology and molecular technology is also indispensable for developing and implementing diagnostic workflows. In the infectious disease context, we demonstrated that ITS sequencing has substantial diagnostic value in mucormycosis when guided by histopathology. This and our evaluation of rapid antigen testing in the postmortem setting illustrate how novel pathogen detection methods can be incorporated into established diagnostic workflows to maximize their clinical or public health benefit. A similar principle we applied in tumor molecular pathology. By systematically evaluating the incorporation and expansion of a comprehensive molecular profiling strategy in NSCLC, we could demonstrate both its feasibility and clinical value. Expanding this strategy to squamous cell carcinoma challenges traditional selection criteria and supports a histology-agnostic testing approach that ensures broad access to biomarker testing and subsequent precision oncology interventions.

Future developments will further strengthen the overarching morpho-molecular concept of respiratory disease outlined in this cumulative thesis. Ongoing technological innovations, such as spatially resolved transcriptomics and proteomics, will be key drivers of tissue-based translational research. Apart from studying the human tissue microenvironment, recent efforts in these technologies move toward the inclusion of non-human (e.g., microbial) reads, thus enabling assays such as spatial metatranscriptomics to study host-pathogen interactions. Furthermore, digital pathology and advanced artificial intelligence-assisted image analysis will likely increase our understanding of complex histomorphological patterns and their association with biological and clinical variables. Such pattern recognition could, for example, predict the likelihood of certain molecular alterations and thus influence subsequent diagnostic workflows. In parallel, research autopsy programs have gained renewed attention in recent years, not least

because of Covid-19, and are likely to become an increasingly important resource for the systematic study of pathogenesis. Their value has been clearly demonstrated in both neoplastic and infectious disease contexts and will increase further when combined with advanced molecular and computational methodologies. The future role of academic pathology will be defined by its willingness to embrace these developments. By doing so, it could position itself as a central discipline that drives and practices truly integrative molecular medicine.

6 References

[1] Watson JD, Crick FHC. Molecular Structure of Nucleic Acids: A Structure for Deoxyribose Nucleic Acid. Nature 1953;171:737–8. https://doi.org/10.1038/171737a0.

[2] Mullis KB, Faloona FA. Specific synthesis of DNA in vitro via a polymerase-catalyzed chain reaction. Methods Enzym 1987;155:335–50. https://doi.org/10.1016/0076-6879(87)55023-6.

[3] Collins FS, Green ED, Guttmacher AE, et al. A vision for the future of genomics research. Nature 2003;422:835–47. https://doi.org/10.1038/nature01626.

[4] Goodwin S, McPherson JD, McCombie WR. Coming of age: ten years of next-generation sequencing technologies. Nat Rev Genet 2016;17:333–51. https://doi.org/10.1038/nrg.2016.49.

[5] Margulies M, Egholm M, Altman WE, et al. Genome sequencing in microfabricated high-density picolitre reactors. Nature 2005;437:376–80. https://doi.org/10.1038/nature03959.

[6] Nimwegen KJ van, Soest RA van, Veltman JA, et al. Is the $1000 Genome as Near as We Think? A Cost Analysis of Next-Generation Sequencing. Clin Chem 2016;62:1458–64. https://doi.org/10.1373/clinchem.2016.258632.

[7] Hofman P, Lucas S, Jouvion G, et al. Pathology of infectious diseases: what does the future hold? Virchows Arch 2017;470:483–92. https://doi.org/10.1007/s00428-017-2082-6.

[8] Rosati LA. The microbe, creator of the pathologist: An inter-related history of pathology, microbiology, and infectious disease. Ann Diagn Pathol 2001;5:184–9. https://doi.org/10.1053/adpa.2001.25413.

[9] Shieh W-J, Zaki SR. Advanced Techniques in Diagnostic Microbiology. Adv Tech Diagn Microbiol 2012:873–90. https://doi.org/10.1007/978-1-4614-3970-7_45.

[10] Martín-Loeches I, Sanchez-Corral A, Diaz E, et al. Community-Acquired Respiratory Coinfection in Critically Ill Patients With Pandemic 2009 Influenza A(H1N1) Virus. Chest 2011;139:555–62. https://doi.org/10.1378/chest.10-1396.

[11] Buehler PK, Zinkernagel AS, Hofmaenner DA, et al. Bacterial pulmonary superinfections are associated with longer duration of ventilation in critically ill COVID-19 patients. Cell Rep Med 2021;2:100229. https://doi.org/10.1016/j.xcrm.2021.100229.

[12] Brundage JF, Shanks GD. Deaths from Bacterial Pneumonia during 1918–19 Influenza Pandemic - Volume 14, Number 8—August 2008 - Emerging Infectious Diseases journal - CDC. Emerg Infect Dis 2008;14:1193–9. https://doi.org/10.3201/eid1408.071313.

[13] Hartshorn KL. New Look at an Old Problem Bacterial Superinfection after Influenza. Am J Pathol 2010;176:536–9. https://doi.org/10.2353/ajpath.2010.090880.

[14] Morens DM., Taubenberger JK, Fauci AS. Predominant Role of Bacterial Pneumonia as a Cause of Death in Pandemic Influenza: Implications for Pandemic Influenza Preparedness. J Infect Dis 2008;198:962–70. https://doi.org/10.1086/591708.

[15] Goldsmith CS, Miller SE, Martines RB, et al. Electron microscopy of SARS-CoV-2: a challenging task. Lancet 2020;395:e99. https://doi.org/10.1016/s0140-6736(20)31188-0.

[16] Dittmayer C, Meinhardt J, Radbruch H, et al. Why misinterpretation of electron micrographs in SARS-CoV-2-infected tissue goes viral. Lancet 2020;396:e64–5. https://doi.org/10.1016/s0140-6736(20)32079-1.

[17] Bednarska K, Chowdhury R, Tobin JWD, et al. Epstein–Barr virus-associated lymphomas decoded. Br J Haematol 2024;204:415–33. https://doi.org/10.1111/bjh.19255.

[18] Quintanilla-Martinez L, Swerdlow SH, Tousseyn T, et al. New concepts in EBV-associated B, T, and NK cell lymphoproliferative disorders. Virchows Arch 2023;482:227–44. https://doi.org/10.1007/s00428-022-03414-4.

[19] Lefterova MI, Suarez CJ, Banaei N, et al. Next-Generation Sequencing for Infectious Disease Diagnosis and Management A Report of the Association for Molecular Pathology. J Mol Diagn 2015;17:623–34. https://doi.org/10.1016/j.jmoldx.2015.07.004.

[20] Janda JM, Abbott SL. 16S rRNA Gene Sequencing for Bacterial Identification in the Diagnostic Laboratory: Pluses, Perils, and Pitfalls. J Clin Microbiol 2007;45:2761–4. https://doi.org/10.1128/jcm.01228-07.

[21] Clarridge JE. Impact of 16S rRNA Gene Sequence Analysis for Identification of Bacteria on Clinical Microbiology and Infectious Diseases. Clin Microbiol Rev 2004;17:840–62. https://doi.org/10.1128/cmr.17.4.840-862.2004.

[22] Gorkiewicz G, Feierl G, Schober C, et al. Species-Specific Identification of Campylobacters by Partial 16S rRNA Gene Sequencing. J Clin Microbiol 2003;41:2537–46. https://doi.org/10.1128/jcm.41.6.2537-2546.2003.

[23] Fox GE, Stackebrandt E, Hespell RB, et al. The Phylogeny of Prokaryotes. Science 1980;209:457–63. https://doi.org/10.1126/science.6771870.

[24] Zacharias M, Kashofer K, Wurm P, et al. Host and microbiome features of secondary infections in lethal covid-19. Iscience 2022:104926. https://doi.org/10.1016/j.isci.2022.104926.

[25] Anderson BE, Dawson JE, Jones DC, et al. Ehrlichia chaffeensis, a new species associated with human ehrlichiosis. J Clin Microbiol 1991;29:2838–42. https://doi.org/10.1128/jcm.29.12.2838-2842.1991.

[26] Relman DA, Schmidt TM, MacDermott RP, et al. Identification of the Uncultured Bacillus of Whipple's Disease. N Engl J Med 1992;327:293–301. https://doi.org/10.1056/nejm199207303270501.

[27] Wilson KH, Frothingham R, Wilson JAP, et al. Phylogeny of the Whipple's-disease-associated bacterium. Lancet 1991;338:474–5. https://doi.org/10.1016/0140-6736(91)90545-z.

[28] Relman DA, Loutit JS, Schmidt TM, et al. The Agent of Bacillary Angiomatosis. N Engl J Med 1990;323:1573–80. https://doi.org/10.1056/nejm199012063232301.

[29] Halwachs B, Madhusudhan N, Krause R, et al. Critical Issues in Mycobiota Analysis. Front Microbiol 2017;8:180. https://doi.org/10.3389/fmicb.2017.00180.

[30] Schoch CL, Seifert KA, Huhndorf S, et al. Nuclear ribosomal internal transcribed spacer (ITS) region as a universal DNA barcode marker for Fungi. Proc Natl Acad Sci 2012;109:6241–6. https://doi.org/10.1073/pnas.1117018109.

[31] Zacharias M, Thüringer A, Krause R, et al. The mutual value of histopathology and ITS sequencing in the diagnosis of mucormycosis. Histopathology 2024;84:702–6. https://doi.org/10.1111/his.15131.

[32] Denning DW. Global incidence and mortality of severe fungal disease. Lancet Infect Dis 2024;24:e428–38. https://doi.org/10.1016/s1473-3099(23)00692-8.

[33] Quince C, Walker AW, Simpson JT, et al. Shotgun metagenomics, from sampling to analysis. Nat Biotechnol 2017;35:833–44. https://doi.org/10.1038/nbt.3935.

[34] Almeida A, Mitchell AL, Boland M, et al. A new genomic blueprint of the human gut microbiota. Nature 2019;568:499–504. https://doi.org/10.1038/s41586-019-0965-1.

[35] Kostic AD, Ojesina AI, Pedamallu CS, et al. PathSeq: software to identify or discover microbes by deep sequencing of human tissue. Nat Biotechnol 2011;29:393–6. https://doi.org/10.1038/nbt.1868.

[36] Walker MA, Pedamallu CS, Ojesina AI, et al. GATK PathSeq: a customizable computational tool for the discovery and identification of microbial sequences in libraries from eukaryotic hosts. Bioinformatics 2018;34:4287–9. https://doi.org/10.1093/bioinformatics/bty501.

[37] Guo Y, Li H, Chen H, et al. Metagenomic next-generation sequencing to identify pathogens and cancer in lung biopsy tissue. EBioMedicine 2021;73:103639. https://doi.org/10.1016/j.ebiom.2021.103639.

[38] Gu W, Talevich E, Hsu E, et al. Detection of cryptogenic malignancies from metagenomic whole genome sequencing of body fluids. Genome Med 2021;13:98. https://doi.org/10.1186/s13073-021-00912-z.

[39] Zheng Y, Chen Y, Yu K, et al. Fatal Infections Among Cancer Patients: A Population-Based Study in the United States. Infect Dis Ther 2021;10:871–95. https://doi.org/10.1007/s40121-021-00433-7.

[40] Rolston KVI. Infections in Cancer Patients with Solid Tumors: A Review. Infect Dis Ther 2017;6:69–83. https://doi.org/10.1007/s40121-017-0146-1.

[41] Song Q, Bates B, Shao YR, et al. Risk and Outcome of Breakthrough COVID-19 Infections in Vaccinated Patients With Cancer: Real-World Evidence From the National COVID Cohort Collaborative. J Clin Oncol 2022;40:1414–27. https://doi.org/10.1200/jco.21.02419.

[42] Landtblom AR, Andersson TM-L, Dickman PW, et al. Risk of infections in patients with myeloproliferative neoplasms—a population-based cohort study of 8363 patients. Leukemia 2021;35:476–84. https://doi.org/10.1038/s41375-020-0909-7.

[43] Huttenhower C, Gevers D, Knight R, et al. Structure, function and diversity of the healthy human microbiome. Nature 2012;486:207–14. https://doi.org/10.1038/nature11234.

[44] Turnbaugh PJ, Ley RE, Hamady M, et al. The Human Microbiome Project. Nature 2007;449:804–10. https://doi.org/10.1038/nature06244.

[45] Gorkiewicz G, Moschen A. Gut microbiome: a new player in gastrointestinal disease. Virchows Arch 2018;472:159–72. https://doi.org/10.1007/s00428-017-2277-x.

[46] Lynch SV, Pedersen O. The Human Intestinal Microbiome in Health and Disease. N Engl J Med 2016;375:2369–79. https://doi.org/10.1056/nejmra1600266.

[47] Qin J, Li R, Raes J, et al. A human gut microbial gene catalogue established by metagenomic sequencing. Nature 2010;464:59–65. https://doi.org/10.1038/nature08821.

[48] McCallum G, Tropini C. The gut microbiota and its biogeography. Nat Rev Microbiol 2024;22:105–18. https://doi.org/10.1038/s41579-023-00969-0.

[49] Saarenpää S, Shalev O, Ashkenazy H, et al. Spatial metatranscriptomics resolves host–bacteria–fungi interactomes. Nat Biotechnol 2024;42:1384–93. https://doi.org/10.1038/s41587-023-01979-2.

[50] Lötstedt B, Stražar M, Xavier R, et al. Spatial host–microbiome sequencing reveals niches in the mouse gut. Nat Biotechnol 2024;42:1394–403. https://doi.org/10.1038/s41587-023-01988-1.

[51] Zhu B, Bai Y, Yeo YY, et al. A multi-omics spatial framework for host-microbiome dissection within the intestinal tissue microenvironment. Nat Commun 2025;16:1230. https://doi.org/10.1038/s41467-025-56237-7.

[52] Haraoui L-P, Blaser MJ. The Microbiome and Infectious Diseases. Clin Infect Dis 2023;77:S441–6. https://doi.org/10.1093/cid/ciad577.

[53] Baty JJ, Stoner SN, Scoffield JA. Oral Commensal Streptococci: Gatekeepers of the Oral Cavity. J Bacteriol 2022;204:e00257-22. https://doi.org/10.1128/jb.00257-22.

[54] Klein RD, Hultgren SJ. Urinary tract infections: microbial pathogenesis, host–pathogen interactions and new treatment strategies. Nat Rev Microbiol 2020;18:211–26. https://doi.org/10.1038/s41579-020-0324-0.

[55] Atkinson AL, Atwood WJ. Fifty Years of JC Polyomavirus: A Brief Overview and Remaining Questions. Viruses 2020;12:969. https://doi.org/10.3390/v12090969.

[56] Tacconelli E, Carrara E, Savoldi A, et al. Discovery, research, and development of new antibiotics: the WHO priority list of antibiotic-resistant bacteria and tuberculosis. Lancet Infect Dis 2018;18:318–27. https://doi.org/10.1016/s1473-3099(17)30753-3.

[57] Cox LM, Yamanishi S, Sohn J, et al. Altering the Intestinal Microbiota during a Critical Developmental Window Has Lasting Metabolic Consequences. Cell 2014;158:705–21. https://doi.org/10.1016/j.cell.2014.05.052.

[58] Zhang X-S, Yin YS, Wang J, et al. Maternal cecal microbiota transfer rescues early-life antibiotic-induced enhancement of type 1 diabetes in mice. Cell Host Microbe 2021;29:1249-1265.e9. https://doi.org/10.1016/j.chom.2021.06.014.

[59] O'Riordan KJ, Moloney GM, Keane L, et al. The gut microbiota-immune-brain axis: Therapeutic implications. Cell Rep Med 2025;6:101982. https://doi.org/10.1016/j.xcrm.2025.101982.

[60] Gazzaniga FS, Kasper DL. The gut microbiome and cancer response to immune checkpoint inhibitors. J Clin Investig 2025;135:e184321. https://doi.org/10.1172/jci184321.

[61] Els van N, Vrieze A, Nieuwdorp M, et al. Duodenal Infusion of Donor Feces for Recurrent Clostridium difficile. N Engl J Med 2013;368:407–15. https://doi.org/10.1056/nejmoa1205037.

[62] Feuerstadt P, Louie TJ, Lashner B, et al. SER-109, an Oral Microbiome Therapy for Recurrent Clostridioides difficile Infection. N Engl J Med 2022;386:220–9. https://doi.org/10.1056/nejmoa2106516.

[63] Hanahan D, Weinberg RA. The Hallmarks of Cancer. Cell 2000;100:57–70. https://doi.org/10.1016/s0092-8674(00)81683-9.

[64] Virchow R. Die krankhaften Geschwülste. vol. 1–3. Berlin: August Hirschwald; 1863.

[65] Fletcher CDM. Diagnostic Histopathology of Tumors. 5th ed. Philadelphia: Elsevier; 2020.

[66] Hanahan D. Hallmarks of Cancer: New Dimensions. Cancer Discov 2022;12:31–46. https://doi.org/10.1158/2159-8290.cd-21-1059.

[67] Hanahan D, Weinberg RA. Hallmarks of Cancer: The Next Generation. Cell 2011;144:646–74. https://doi.org/10.1016/j.cell.2011.02.013.

[68] Harris TJR, McCormick F. The molecular pathology of cancer. Nat Rev Clin Oncol 2010;7:251–65. https://doi.org/10.1038/nrclinonc.2010.41.

[69] Garber JE, Offit K. Hereditary Cancer Predisposition Syndromes. J Clin Oncol 2005;23:276–92. https://doi.org/10.1200/jco.2005.10.042.

[70] Horak P, Griffith M, Danos AM, et al. Standards for the classification of pathogenicity of somatic variants in cancer (oncogenicity): Joint recommendations of Clinical Genome Resource (ClinGen), Cancer Genomics Consortium (CGC), and Variant Interpretation for Cancer Consortium (VICC). Genet Med 2022;24:986–98. https://doi.org/10.1016/j.gim.2022.01.001.

[71] Richards S, Aziz N, Bale S, et al. Standards and guidelines for the interpretation of sequence variants: a joint consensus recommendation of the American College of Medical Genetics and Genomics and the Association for Molecular Pathology. Genet Med 2015;17:405–23. https://doi.org/10.1038/gim.2015.30.

[72] Lindeman NI, Cagle PT, Aisner DL, et al. Updated Molecular Testing Guideline for the Selection of Lung Cancer Patients for Treatment With Targeted Tyrosine Kinase Inhibitors: Guideline From the College of American Pathologists, the International Association for the Study of Lung Cancer, and the Association for Molecular Pathology. Arch Pathol Lab Med 2018;142:321–46. https://doi.org/10.5858/arpa.2017-0388-cp.

[73] Li MM, Datto M, Duncavage EJ, et al. Standards and Guidelines for the Interpretation and Reporting of Sequence Variants in Cancer A Joint Consensus Recommendation of the Association for Molecular Pathology, American Society of Clinical Oncology, and College of American Pathologists. J Mol Diagn 2017;19:4–23. https://doi.org/10.1016/j.jmoldx.2016.10.002.

[74] Stratton MR, Campbell PJ, Futreal PA. The cancer genome. Nature 2009;458:719–24. https://doi.org/10.1038/nature07943.

[75] Vogelstein B, Papadopoulos N, Velculescu VE, et al. Cancer Genome Landscapes. Science 2013;339:1546–58. https://doi.org/10.1126/science.1235122.

[76] Deininger MWN, Goldman JM, Melo JV. The molecular biology of chronic myeloid leukemia. Blood 2000;96:3343–56. https://doi.org/10.1182/blood.v96.10.3343.

[77] André F, Rassy E, Marabelle A, et al. Forget lung, breast or prostate cancer: why tumour naming needs to change. Nature 2024;626:26–9. https://doi.org/10.1038/d41586-024-00216-3.

[78] WHO. Central nervous system tumours. WHO classification of tumors series, 5th ed.; vol. Lyon (France): International Agency for Research on Cancer; 2021.

[79] WHO. Haematolymphoid tumours. WHO classification of tumors series, 5th ed.; vol. 11. Lyon (France): International Agency for Research on Cancer; 2024.

[80] WHO. Soft tissue and bone tumours. WHO classification of tumors series, 5th ed.; vol. 3. Lyon (France): International Agency for Research on Cancer; 2020.

[81] Capper D, Jones DTW, Sill M, et al. DNA methylation-based classification of central nervous system tumours. Nature 2018;555:469–74. https://doi.org/10.1038/nature26000.

[82] Koelsche C, Schrimpf D, Stichel D, et al. Sarcoma classification by DNA methylation profiling. Nat Commun 2021;12:498. https://doi.org/10.1038/s41467-020-20603-4.

[83] Jurmeister P, Glöß S, Roller R, et al. DNA methylation-based classification of sinonasal tumors. Nat Commun 2022;13:7148. https://doi.org/10.1038/s41467-022-34815-3.

[84] Jurmeister P, Leitheiser M, Arnold A, et al. DNA Methylation Profiling of Salivary Gland Tumors Supports and Expands Conventional Classification. Mod Pathol 2024;37:100625. https://doi.org/10.1016/j.modpat.2024.100625.

[85] Jurmeister P, Bockmayr M, Seegerer P, et al. Machine learning analysis of DNA methylation profiles distinguishes primary lung squamous cell carcinomas from head and neck metastases. Sci Transl Med 2019;11:eaaw8513. https://doi.org/10.1126/scitranslmed.aaw8513.

[86] Jurmeister P, Schöler A, Arnold A, et al. DNA methylation profiling reliably distinguishes pulmonary enteric adenocarcinoma from metastatic colorectal cancer. Mod Pathol 2019;32:855–65. https://doi.org/10.1038/s41379-019-0207-y.

[87] Moran S, Martínez-Cardús A, Sayols S, et al. Epigenetic profiling to classify cancer of unknown primary: a multicentre, retrospective analysis. Lancet Oncol 2016;17:1386–95. https://doi.org/10.1016/s1470-2045(16)30297-2.

[88] Zhang S, He S, Zhu X, et al. DNA methylation profiling to determine the primary sites of metastatic cancers using formalin-fixed paraffin-embedded tissues. Nat Commun 2023;14:5686. https://doi.org/10.1038/s41467-023-41015-0.

[89] Zhang Z, Lu Y, Vosoughi S, et al. HiTAIC: hierarchical tumor artificial intelligence classifier traces tissue of origin and tumor type in primary and metastasized tumors using DNA methylation. NAR Cancer 2023;5:zcad017. https://doi.org/10.1093/narcan/zcad017.

[90] Sun M, Xu B, Chen C, et al. Tissue of origin prediction for cancer of unknown primary using a targeted methylation sequencing panel. Clin Epigenetics 2024;16:25. https://doi.org/10.1186/s13148-024-01638-6.

[91] Zhou Y, Tao L, Qiu J, et al. Tumor biomarkers for diagnosis, prognosis and targeted therapy. Signal Transduct Target Ther 2024;9:132. https://doi.org/10.1038/s41392-024-01823-2.

[92] WHO. Thoracic tumours. WHO classification of tumors series, 5th ed.; vol. 5. Lyon (France): International Agency for Research on Cancer; 2021.

[93] Petitjean A, Achatz MIW, Borresen-Dale AL, et al. TP53 mutations in human cancers: functional selection and impact on cancer prognosis and outcomes. Oncogene 2007;26:2157–65. https://doi.org/10.1038/sj.onc.1210302.

[94] Bowen D, Groves MJ, Burnett AK, et al. TP53 gene mutation is frequent in patients with acute myeloid leukemia and complex karyotype, and is associated with very poor prognosis. Leukemia 2009;23:203–6. https://doi.org/10.1038/leu.2008.173.

[95] Cronin M, Sangli C, Liu M-L, et al. Analytical Validation of the Oncotype DX Genomic Diagnostic Test for Recurrence Prognosis and Therapeutic Response Prediction in Node-Negative, Estrogen Receptor–Positive Breast Cancer. Clin Chem 2007;53:1084–91. https://doi.org/10.1373/clinchem.2006.076497.

[96] Thangue NBL, Kerr DJ. Predictive biomarkers: a paradigm shift towards personalized cancer medicine. Nat Rev Clin Oncol 2011;8:587–96. https://doi.org/10.1038/nrclinonc.2011.121.

[97] Doroshow DB, Bhalla S, Beasley MB, et al. PD-L1 as a biomarker of response to immune-checkpoint inhibitors. Nat Rev Clin Oncol 2021;18:345–62. https://doi.org/10.1038/s41571-021-00473-5.

[98] Aggarwal C, Ben-Shachar R, Gao Y, et al. Assessment of Tumor Mutational Burden and Outcomes in Patients With Diverse Advanced Cancers Treated With Immunotherapy. JAMA Netw Open 2023;6:e2311181. https://doi.org/10.1001/jamanetworkopen.2023.11181.

[99] Jardim DL, Goodman A, Gagliato D de M, et al. The Challenges of Tumor Mutational Burden as an Immunotherapy Biomarker. Cancer Cell 2021;39:154–73. https://doi.org/10.1016/j.ccell.2020.10.001.

[100] Routy B, Chatelier EL, Derosa L, et al. Gut microbiome influences efficacy of PD-1–based immunotherapy against epithelial tumors. Science 2018;359:91–7. https://doi.org/10.1126/science.aan3706.

[101] Gopalakrishnan V, Spencer CN, Nezi L, et al. Gut microbiome modulates response to anti–PD-1 immunotherapy in melanoma patients. Science 2018;359:97–103. https://doi.org/10.1126/science.aan4236.

[102] Visser KE de, Joyce JA. The evolving tumor microenvironment: From cancer initiation to metastatic outgrowth. Cancer Cell 2023;41:374–403. https://doi.org/10.1016/j.ccell.2023.02.016.

[103] Seferbekova Z, Lomakin A, Yates LR, et al. Spatial biology of cancer evolution. Nat Rev Genet 2023;24:295–313. https://doi.org/10.1038/s41576-022-00553-x.

[104] Sibai M, Zacharias M, McGranahan N, et al. Cancer in 4D: Towards Spatiotemporal Hallmark Ecosystems. Preprints 2025:202509.1469.v1. https://doi.org/10.20944/preprints202509.1469.v1.

[105] Cullin N, Antunes CA, Straussman R, et al. Microbiome and cancer. Cancer Cell 2021;39:1317–41. https://doi.org/10.1016/j.ccell.2021.08.006.

[106] Vétizou M, Pitt JM, Daillère R, et al. Anticancer immunotherapy by CTLA-4 blockade relies on the gut microbiota. Science 2015;350:1079–84. https://doi.org/10.1126/science.aad1329.

[107] Sivan A, Corrales L, Hubert N, et al. Commensal Bifidobacterium promotes antitumor immunity and facilitates anti–PD-L1 efficacy. Science 2015;350:1084–9. https://doi.org/10.1126/science.aac4255.

[108] Matson V, Fessler J, Bao R, et al. The commensal microbiome is associated with anti–PD-1 efficacy in metastatic melanoma patients. Science 2018;359:104–8. https://doi.org/10.1126/science.aao3290.

[109] Lee KA, Thomas AM, Bolte LA, et al. Cross-cohort gut microbiome associations with immune checkpoint inhibitor response in advanced melanoma. Nat Med 2022;28:535–44. https://doi.org/10.1038/s41591-022-01695-5.

[110] Lin NY-T, Fukuoka S, Koyama S, et al. Microbiota-driven antitumour immunity mediated by dendritic cell migration. Nature 2025;644:1058–68. https://doi.org/10.1038/s41586-025-09249-8.

[111] Davar D, Dzutsev AK, McCulloch JA, et al. Fecal microbiota transplant overcomes resistance to anti–PD-1 therapy in melanoma patients. Science 2021;371:595–602. https://doi.org/10.1126/science.abf3363.

[112] Baruch EN, Youngster I, Ben-Betzalel G, et al. Fecal microbiota transplant promotes response in immunotherapy-refractory melanoma patients. Science 2021;371:602–9. https://doi.org/10.1126/science.abb5920.

[113] Routy B, Lenehan JG, Miller WH, et al. Fecal microbiota transplantation plus anti-PD-1 immunotherapy in advanced melanoma: a phase I trial. Nat Med 2023;29:2121–32. https://doi.org/10.1038/s41591-023-02453-x.

[114] Duttagupta S, Messaoudene M, Hunter S, et al. Fecal microbiota transplantation plus immunotherapy in non-small cell lung cancer and melanoma: the phase 2 FMT-LUMINate trial. Nat Med 2026:1–14. https://doi.org/10.1038/s41591-025-04186-5.

[115] Porcari S, Ciccarese C, Heidrich V, et al. Fecal microbiota transplantation plus pembrolizumab and axitinib in metastatic renal cell carcinoma: the randomized phase 2 TACITO trial. Nat Med 2026:1–9. https://doi.org/10.1038/s41591-025-04189-2.

[116] Gur C, Ibrahim Y, Isaacson B, et al. Binding of the Fap2 Protein of Fusobacterium nucleatum to Human Inhibitory Receptor TIGIT Protects Tumors from Immune Cell Attack. Immunity 2015;42:344–55. https://doi.org/10.1016/j.immuni.2015.01.010.

[117] Gur C, Maalouf N, Shhadeh A, et al. Fusobacterium nucleatum supresses anti-tumor immunity by activating CEACAM1. OncoImmunology 2019;8:e1581531. https://doi.org/10.1080/2162402x.2019.1581531.

[118] Kostic AD, Chun E, Robertson L, et al. Fusobacterium nucleatum Potentiates Intestinal Tumorigenesis and Modulates the Tumor-Immune Microenvironment. Cell Host Microbe 2013;14:207–15. https://doi.org/10.1016/j.chom.2013.07.007.

[119] Rubinstein MR, Wang X, Liu W, et al. Fusobacterium nucleatum Promotes Colorectal Carcinogenesis by Modulating E-Cadherin/β-Catenin Signaling via its FadA Adhesin. Cell Host Microbe 2013;14:195–206. https://doi.org/10.1016/j.chom.2013.07.012.

[120] Rubinstein MR, Baik JE, Lagana SM, et al. Fusobacterium nucleatum promotes colorectal cancer by inducing Wnt/β-catenin modulator Annexin A1. EMBO Rep 2019;20:EMBR201847638. https://doi.org/10.15252/embr.201847638.

[121] Niño JLG, Ponath F, Ajisafe VA, et al. Tumor-infiltrating bacteria disrupt cancer epithelial cell interactions and induce cell-cycle arrest. Cancer Cell 2026;44:166-186.e16. https://doi.org/10.1016/j.ccell.2025.09.010.

[122] Pushalkar S, Hundeyin M, Daley D, et al. The Pancreatic Cancer Microbiome Promotes Oncogenesis by Induction of Innate and Adaptive Immune Suppression. Cancer Discov 2018;8:403–16. https://doi.org/10.1158/2159-8290.cd-17-1134.

[123] Fu A, Yao B, Dong T, et al. Tumor-resident intracellular microbiota promotes metastatic colonization in breast cancer. Cell 2022;185:1356-1372.e26. https://doi.org/10.1016/j.cell.2022.02.027.

[124] Silver NL, Dai J, Kerr TD, et al. Intratumoral bacteria are immunosuppressive and promote immunotherapy resistance in head and neck squamous cell carcinoma. Nat Cancer 2026;7:80–97. https://doi.org/10.1038/s43018-025-01067-1.

[125] Tsay J-CJ, Wu BG, Sulaiman I, et al. Lower Airway Dysbiosis Affects Lung Cancer Progression. Cancer Discov 2021;11:293–307. https://doi.org/10.1158/2159-8290.cd-20-0263.

[126] Nejman D, Livyatan I, Fuks G, et al. The human tumor microbiome is composed of tumor type–specific intracellular bacteria. Science 2020;368:973–80. https://doi.org/10.1126/science.aay9189.

[127] Morad G, Damania AV, Melendez B, et al. Microbial signals in primary and metastatic brain tumors. Nat Med 2025;31:3675–88. https://doi.org/10.1038/s41591-025-03957-4.

[128] Gigi E, Gavert N, Raijman-Nagar L, et al. Characterization of the tumor microbiome of brain metastases and glioblastoma reveals tumor-type-specific and location-specific microbial signatures. Nat Cancer 2025;6:1761–76. https://doi.org/10.1038/s43018-025-01073-3.

[129] Fierer N, Leung PM, Lappan R, et al. Guidelines for preventing and reporting contamination in low-biomass microbiome studies. Nat Microbiol 2025;10:1570–80. https://doi.org/10.1038/s41564-025-02035-2.

[130] Ge Y, Lu J, Puiu D, et al. Comprehensive analysis of microbial content in whole-genome sequencing samples from The Cancer Genome Atlas project. Sci Transl Med 2025;17:eads6335. https://doi.org/10.1126/scitranslmed.ads6335.

[131] Buja LM, Barth RF, Krueger GR, et al. The Importance of the Autopsy in Medicine: Perspectives of Pathology Colleagues. Acad Pathol 2019;6:2374289519834041. https://doi.org/10.1177/2374289519834041.

[132] Hill RB, Anderson RE. The recent history of the autopsy. Arch Pathol Lab Med 1996;120:702–12.

[133] Iacobuzio-Donahue CA, Michael C, Baez P, et al. Cancer biology as revealed by the research autopsy. Nat Rev Cancer 2019;19:686–97. https://doi.org/10.1038/s41568-019-0199-4.

[134] Kretzschmar H. Brain banking: opportunities, challenges and meaning for the future. Nat Rev Neurosci 2009;10:70–8. https://doi.org/10.1038/nrn2535.

[135] Wilson ML. Infectious Diseases and the Autopsy. Clin Infect Dis 2006;43:602–3. https://doi.org/10.1086/506574.

[136] Nolte KB. Infectious Disease Pathology and the Autopsy. Clin Infect Dis 2002;34:130–1. https://doi.org/10.1086/323750.

[137] Liu L, Callinan LS, Holman RC, et al. Determinants for Autopsy after Unexplained Deaths Possibly Resulting from Infectious Causes, United States - Volume 18, Number 4—April 2012 - Emerging Infectious Diseases journal - CDC. Emerg Infect Dis 2012;18:549–55. https://doi.org/10.3201/eid1804.111311.

[138] Lucas S. Investigating infectious diseases at autopsy. Diagn Histopathol 2018;24:357–64. https://doi.org/10.1016/j.mpdhp.2018.07.003.

[139] Scully T. Tuberculosis. Nature 2013;502:S1–S1. https://doi.org/10.1038/502s1a.

[140] Hunter RL. The Pathogenesis of Tuberculosis: The Early Infiltrate of Post-primary (Adult Pulmonary) Tuberculosis: A Distinct Disease Entity. Front Immunol 2018;9:2108. https://doi.org/10.3389/fimmu.2018.02108.

[141] Lucas SB, Hounnou A, Peacock C, et al. The mortality and pathology of HIV infection in a West African city. AIDS 1993;7:1569–79. https://doi.org/10.1097/00002030-199312000-00005.

[142] Afessa B, Green W, Chiao J, et al. Pulmonary Complications of HIV Infection Autopsy Findings. Chest 1998;113:1225–9. https://doi.org/10.1378/chest.113.5.1225.

[143] Duchin JS, Koster FT, Peters CJ, et al. Hantavirus Pulmonary Syndrome: A Clinical Description of 17 Patients with a Newly Recognized Disease. N Engl J Med 1994;330:949–55. https://doi.org/10.1056/nejm199404073301401.

[144] Nolte KB, Feddersen RM, Foucar K, et al. Hantavirus pulmonary syndrome in the United States: A pathological description of a disease caused by a new agent. Hum Pathol 1995;26:110–20. https://doi.org/10.1016/0046-8177(95)90123-x.

[145] Ding Y, Wang H, Shen H, et al. The clinical pathology of severe acute respiratory syndrome (SARS): a report from China. J Pathol 2003;200:282–9. https://doi.org/10.1002/path.1440.

[146] Franks TJ, Chong PY, Chui P, et al. Lung pathology of severe acute respiratory syndrome (SARS): a study of 8 autopsy cases from Singapore. Hum Pathol 2003;34:743–8. https://doi.org/10.1016/s0046-8177(03)00367-8.

[147] Menter T, Haslbauer JD, Nienhold R, et al. Postmortem examination of COVID-19 patients reveals diffuse alveolar damage with severe capillary congestion and variegated findings in lungs and other organs suggesting vascular dysfunction. Histopathology 2020;77:198–209. https://doi.org/10.1111/his.14134.

[148] Lax SF, Skok K, Zechner P, et al. Pulmonary Arterial Thrombosis in COVID-19 With Fatal Outcome: Results From a Prospective, Single-Center, Clinicopathologic Case Series. Ann Intern Med 2020;173:M20-2566. https://doi.org/10.7326/m20-2566.

[149] Bösmüller H, Traxler S, Bitzer M, et al. The evolution of pulmonary pathology in fatal COVID-19 disease: an autopsy study with clinical correlation. Virchows Arch 2020;477:349–57. https://doi.org/10.1007/s00428-020-02881-x.

[150] Rosen DG, Lopez AE, Anzalone ML, et al. Postmortem findings in eight cases of influenza A/H1N1. Mod Pathol 2010;23:1449–57. https://doi.org/10.1038/modpathol.2010.148.

[151] Taubenberger JK, Morens DM. The Pathology of Influenza Virus Infections. Annu Rev Pathol: Mech Dis 2008;3:499–522. https://doi.org/10.1146/annurev.pathmechdis.3.121806.154316.

[152] Sheng Z-M, Chertow DS, Ambroggio X, et al. Autopsy series of 68 cases dying before and during the 1918 influenza pandemic peak. Proc Natl Acad Sci 2011;108:16416–21. https://doi.org/10.1073/pnas.1111179108.

[153] Melms JC, Biermann J, Huang H, et al. A molecular single-cell lung atlas of lethal COVID-19. Nature 2021;595:114–9. https://doi.org/10.1038/s41586-021-03569-1.

[154] Delorey TM, Ziegler CGK, Heimberg G, et al. COVID-19 tissue atlases reveal SARS-CoV-2 pathology and cellular targets. Nature 2021;595:107–13. https://doi.org/10.1038/s41586-021-03570-8.

[155] Rendeiro AF, Ravichandran H, Bram Y, et al. The spatial landscape of lung pathology during COVID-19 progression. Nature 2021;593:564–9. https://doi.org/10.1038/s41586-021-03475-6.

[156] Kanazawa J, Rawlings SA, Hendrickx S, et al. Lessons learned from the Last Gift study: ethical and practical challenges faced while conducting HIV cure-related research at the end of life. J Méd Ethics 2023;49:305–10. https://doi.org/10.1136/medethics-2021-107512.

[157] Paget S. THE DISTRIBUTION OF SECONDARY GROWTHS IN CANCER OF THE BREAST. Lancet 1889;133:571–3. https://doi.org/10.1016/s0140-6736(00)49915-0.

[158] Rubin MA, Putzi M, Mucci N, et al. Rapid ("warm") autopsy study for procurement of metastatic prostate cancer. Clin Cancer Res : Off J Am Assoc Cancer Res 2000;6:1038–45.

[159] Geukens T, Maetens M, Hooper JE, et al. Research autopsy programmes in oncology: shared experience from 14 centres across the world. J Pathol 2024;263:150–65. https://doi.org/10.1002/path.6271.

[160] Cottrell T, Zhang J, Zhang B, et al. Evaluating T-cell cross-reactivity between tumors and immune-related adverse events with TCR sequencing: pitfalls in interpretations of functional relevance. J Immunother Cancer 2021;9:e002642. https://doi.org/10.1136/jitc-2021-002642.

[161] Takai E, Maeda D, Li Z, et al. Post-mortem Plasma Cell-Free DNA Sequencing: Proof-of-Concept Study for the "Liquid Autopsy." Sci Rep 2020;10:2120. https://doi.org/10.1038/s41598-020-59193-y.

[162] Pich O, Ward S, Rowan A, et al. Somatic evolution following cancer treatment in normal tissue. Nature 2025:1–11. https://doi.org/10.1038/s41586-025-09792-4.

[163] Mills SE. Histology for Pathologists. 5th ed. Lippincott Williams and Wilkins; 2019.

[164] Dickson RP, Erb-Downward JR, Martinez FJ, et al. The Microbiome and the Respiratory Tract. Annu Rev Physiol 2015;78:1–24. https://doi.org/10.1146/annurev-physiol-021115-105238.

[165] Gopallawa I, Dehinwal R, Bhatia V, et al. A four-part guide to lung immunology: Invasion, inflammation, immunity, and intervention. Front Immunol 2023;14:1119564. https://doi.org/10.3389/fimmu.2023.1119564.

[166] Huffnagle GB, Dickson RP, Lukacs NW. The respiratory tract microbiome and lung inflammation: a two-way street. Mucosal Immunol 2017;10:299–306. https://doi.org/10.1038/mi.2016.108.

[167] Mettelman RC, Allen EK, Thomas PG. Mucosal immune responses to infection and vaccination in the respiratory tract. Immunity 2022;55:749–80. https://doi.org/10.1016/j.immuni.2022.04.013.

[168] Charlson ES, Bittinger K, Haas AR, et al. Topographical Continuity of Bacterial Populations in the Healthy Human Respiratory Tract. Am J Respir Crit Care Med 2011;184:957–63. https://doi.org/10.1164/rccm.201104-0655oc.

[169] Dickson RP, Erb-Downward JR, Freeman CM, et al. Spatial Variation in the Healthy Human Lung Microbiome and the Adapted Island Model of Lung Biogeography. Ann Am Thorac Soc 2015;12:821–30. https://doi.org/10.1513/annalsats.201501-029oc.

[170] Natalini JG, Singh S, Segal LN. The dynamic lung microbiome in health and disease. Nat Rev Microbiol 2023;21:222–35. https://doi.org/10.1038/s41579-022-00821-x.

[171] Hilty M, Burke C, Pedro H, et al. Disordered Microbial Communities in Asthmatic Airways. PLoS ONE 2010;5:e8578. https://doi.org/10.1371/journal.pone.0008578.

[172] Dickson RP, Erb-Downward JR, Freeman CM, et al. Bacterial Topography of the Healthy Human Lower Respiratory Tract. mBio 2017;8:10.1128/mbio.02287-16. https://doi.org/10.1128/mbio.02287-16.

[173] Krause R, Moissl-Eichinger C, Halwachs B, et al. Mycobiome in the Lower Respiratory Tract – A Clinical Perspective. Front Microbiol 2017;07:2169. https://doi.org/10.3389/fmicb.2016.02169.

[174] Koskinen K, Pausan MR, Perras AK, et al. First Insights into the Diverse Human Archaeome: Specific Detection of Archaea in the Gastrointestinal Tract, Lung, and Nose and on Skin. mBio 2017;8:10.1128/mbio.00824-17. https://doi.org/10.1128/mbio.00824-17.

[175] Purcell M, Ackland J, Staples KJ, et al. The respiratory tract virome: unravelling the role of viral dark matter in respiratory health and disease. Eur Respir Rev 2025;34:240284. https://doi.org/10.1183/16000617.0284-2024.

[176] DOCK W. EFFECT OF POSTURE ON ALVEOLAR GAS TENSION IN TUBERCULOSIS: Explanation for Favored Sites of Chronic Pulmonary Lesions. AMA Arch Intern Med 1954;94:700–8. https://doi.org/10.1001/archinte.1954.00250050014003.

[177] Murray JF. Bill Dock and the Location of Pulmonary Tuberculosis. Am J Respir Crit Care Med 2003;168:1029–33. https://doi.org/10.1164/rccm.200307-1016oe.

[178] Corman VM, Landt O, Kaiser M, et al. Detection of 2019 novel coronavirus (2019-nCoV) by real-time RT-PCR. Eurosurveillance 2020;25:2000045. https://doi.org/10.2807/1560-7917.es.2020.25.3.2000045.

[179] Vogels CBF, Brito AF, Wyllie AL, et al. Analytical sensitivity and efficiency comparisons of SARS-CoV-2 RT–qPCR primer–probe sets. Nat Microbiol 2020;5:1299–305. https://doi.org/10.1038/s41564-020-0761-6.

[180] Nalla AK, Casto AM, Huang M-LW, et al. Comparative Performance of SARS-CoV-2 Detection Assays Using Seven Different Primer-Probe Sets and One Assay Kit. J Clin Microbiol 2020;58:10.1128/jcm.00557-20. https://doi.org/10.1128/jcm.00557-20.

[181] Corman VM, Haage VC, Bleicker T, et al. Comparison of seven commercial SARS-CoV-2 rapid point-of-care antigen tests: a single-centre laboratory evaluation study. Lancet Microbe 2021;2:e311–9. https://doi.org/10.1016/s2666-5247(21)00056-2.

[182] Dinnes J, Deeks JJ, Berhane S, et al. Rapid, point-of-care antigen and molecular-based tests for diagnosis of SARS-CoV-2 infection. Cochrane Db Syst Rev 2021;3:CD013705. https://doi.org/10.1002/14651858.cd013705.pub2.

[183] Brümmer LE, Katzenschlager S, Gaeddert M, et al. Accuracy of novel antigen rapid diagnostics for SARS-CoV-2: A living systematic review and meta-analysis. PLoS Med 2021;18:e1003735. https://doi.org/10.1371/journal.pmed.1003735.

[184] Zacharias M, Stangl V, Thüringer A, et al. Rapid Antigen Test for Postmortem Evaluation of SARS-CoV-2 Carriage. Emerg Infect Dis 2021;27:1734–7. https://doi.org/10.3201/eid2706.210226.

[185] Wiersinga WJ, Rhodes A, Cheng AC, et al. Pathophysiology, Transmission, Diagnosis, and Treatment of Coronavirus Disease 2019 (COVID-19). JAMA 2020;324:782–93. https://doi.org/10.1001/jama.2020.12839.

[186] Merad M, Blish CA, Sallusto F, et al. The immunology and immunopathology of COVID-19. Science 2022;375:1122–7. https://doi.org/10.1126/science.abm8108.

[187] Bryce C, Grimes Z, Pujadas E, et al. Pathophysiology of SARS-CoV-2: the Mount Sinai COVID-19 autopsy experience. Mod Pathol 2021;34:1456–67. https://doi.org/10.1038/s41379-021-00793-y.

[188] Nienhold R, Ciani Y, Koelzer VH, et al. Two distinct immunopathological profiles in autopsy lungs of COVID-19. Nat Commun 2020;11:5086. https://doi.org/10.1038/s41467-020-18854-2.

[189] Hoenigl M, Seidel D, Carvalho A, et al. The emergence of COVID-19 associated mucormycosis: a review of cases from 18 countries. Lancet Microbe 2022;3:e543–52. https://doi.org/10.1016/s2666-5247(21)00237-8.

[190] Heinrich F, Mertz KD, Glatzel M, et al. Using autopsies to dissect COVID-19 pathogenesis. Nat Microbiol 2023;8:1986–94. https://doi.org/10.1038/s41564-023-01488-7.

[191] Fusco FM, Scappaticci L, Schilling S, et al. A 2009 cross-sectional survey of procedures for post-mortem management of highly infectious disease patients in 48

isolation facilities in 16 countries: data from EuroNHID. Infection 2016;44:57–64. https://doi.org/10.1007/s15010-015-0831-5.

[192] Loibner M, Langner C, Regitnig P, et al. Biosafety Requirements for Autopsies of Patients with COVID-19: Example of a BSL-3 Autopsy Facility Designed for Highly Pathogenic Agents. Pathobiology 2021;88:37–45. https://doi.org/10.1159/000513438.

[193] Roberts DJ, Njuguna HN, Fields B, et al. Comparison of Minimally Invasive Tissue Sampling With Conventional Autopsy to Detect Pulmonary Pathology Among Respiratory Deaths in a Resource-Limited Setting. Am J Clin Pathol 2019;152:36–49. https://doi.org/10.1093/ajcp/aqz016.

[194] Noack P, Grosse C, Bodingbauer J, et al. Minimally invasive autopsies for the investigation of pulmonary pathology of COVID-19—experiences of a longitudinal series of 92 patients. Virchows Arch 2023;483:611–9. https://doi.org/10.1007/s00428-023-03622-6.

[195] Letang E, Rakislova N, Martinez MJ, et al. Minimally Invasive Tissue Sampling: A Tool to Guide Efforts to Reduce AIDS-Related Mortality in Resource-Limited Settings. Clin Infect Dis 2021;73:S343–50. https://doi.org/10.1093/cid/ciab789.

[196] Lahmer T, Weirich G, Porubsky S, et al. Postmortem Minimally Invasive Autopsy in Critically Ill COVID-19 Patients at the Bedside: A Proof-of-Concept Study at the ICU. Diagnostics 2024;14:294. https://doi.org/10.3390/diagnostics14030294.

[197] Kontoyiannis DP, Walsh TJ. Mucormycosis. N Engl J Med 2026;394:684–98. https://doi.org/10.1056/nejmra2412565.

[198] Roden MM, Zaoutis TE, Buchanan WL, et al. Epidemiology and Outcome of Zygomycosis: A Review of 929 Reported Cases. Clin Infect Dis 2005;41:634–53. https://doi.org/10.1086/432579.

[199] Özbek L, Topçu U, Manay M, et al. COVID-19–associated mucormycosis: a systematic review and meta-analysis of 958 cases. Clin Microbiol Infect 2023;29:722–31. https://doi.org/10.1016/j.cmi.2023.03.008.

[200] Cheok KPL, Farrow A, Springell D, et al. Mucormycosis after CD19 chimeric antigen receptor T-cell therapy: results of a US Food and Drug Administration adverse events reporting system analysis and a review of the literature. Lancet Infect Dis 2024;24:e256–65. https://doi.org/10.1016/s1473-3099(23)00563-7.

[201] Anastasopoulou A, DiPippo AJ, Kontoyiannis DP. Non-Aspergillus invasive mould infections in patients treated with ibrutinib. Mycoses 2020;63:787–93. https://doi.org/10.1111/myc.13120.

[202] Gomes MZR, Lewis RE, Kontoyiannis DP. Mucormycosis Caused by Unusual Mucormycetes, Non-Rhizopus, -Mucor, and -Lichtheimia Species. Clin Microbiol Rev 2011;24:411–45. https://doi.org/10.1128/cmr.00056-10.

[203] Petraitis V, Petraitiene R, Antachopoulos C, et al. Increased virulence of Cunninghamella bertholletiae in experimental pulmonary mucormycosis: correlation with circulating molecular biomarkers, sporangiospore germination and hyphal metabolism. Méd Mycol 2013;51:72–82. https://doi.org/10.3109/13693786.2012.690107.

[204] Walther G, Wagner L, Kurzai O. Updates on the Taxonomy of Mucorales with an Emphasis on Clinically Important Taxa. J Fungi 2019;5:106. https://doi.org/10.3390/jof5040106.

[205] Steinbrink JM, Miceli MH. Mucormycosis. Infect Dis Clin North Am 2021;35:435–52. https://doi.org/10.1016/j.idc.2021.03.009.

[206] Chamilos G, Lewis RE, Kontoyiannis DP. Delaying Amphotericin B–Based Frontline Therapy Significantly Increases Mortality among Patients with Hematologic Malignancy Who Have Zygomycosis. Clin Infect Dis 2008;47:503–9. https://doi.org/10.1086/590004.

[207] Lackner N, Posch W, Lass-Flörl C. Microbiological and Molecular Diagnosis of Mucormycosis: From Old to New. Microorganisms 2021;9:1518. https://doi.org/10.3390/microorganisms9071518.

[208] Kontoyiannis DP, Chamilos G, Hassan SA, et al. Increased Culture Recovery of Zygomycetes Under Physiologic Temperature Conditions. Am J Clin Pathol 2007;127:208–12. https://doi.org/10.1309/7ku5xwurym0151yn.

[209] Dekio F, Bhatti TR, Zhang SX, et al. Positive Impact of Fungal Histopathology on Immunocompromised Pediatric Patients With Histology-Proven Invasive Fungal Infection. Am J Clin Pathol 2015;144:61–7. https://doi.org/10.1309/ajcpemvyt88avfkg.

[210] Spallone A, Moran CA, Wurster S, et al. Taking a Closer Look: Clinical and Histopathological Characteristics of Culture-Positive versus Culture-Negative Pulmonary Mucormycosis. J Fungi 2022;8:380. https://doi.org/10.3390/jof8040380.

[211] Imbert S, Portejoie L, Pfister E, et al. A Multiplex PCR and DNA-Sequencing Workflow on Serum for the Diagnosis and Species Identification for Invasive Aspergillosis and Mucormycosis. J Clin Microbiol 2022;61:e01409-22. https://doi.org/10.1128/jcm.01409-22.

[212] Millon L, Caillot D, Berceanu A, et al. Evaluation of Serum Mucorales Polymerase Chain Reaction (PCR) for the Diagnosis of Mucormycoses: The MODIMUCOR Prospective Trial. Clin Infect Dis 2022;75:777–85. https://doi.org/10.1093/cid/ciab1066.

[213] Fissel JA, Holdren-Serrell CK, Memon W, et al. Performance of a Matrix-Assisted Laser Desorption/Ionization Time-of-Flight Mass Spectrometry Testing Algorithm for the Rapid Identification of Clinical Filamentous Molds. Front Cell Infect Microbiol 2022;12:915049. https://doi.org/10.3389/fcimb.2022.915049.

[214] Walsh TJ, McCarthy MW. The expanding use of matrix-assisted laser desorption/ionization-time of flight mass spectroscopy in the diagnosis of patients with mycotic diseases. Expert Rev Mol Diagn 2019;19:241–8. https://doi.org/10.1080/14737159.2019.1574572.

[215] Faure E, Cordier C, Delacoste H, et al. Weekly Screening of Circulating Mucorales DNA and Early Treatment in Severely Burned Patients Improves Survival: Real-Life Bi-center Experience in France. Clin Infect Dis 2025;81:907–13. https://doi.org/10.1093/cid/ciaf423.

[216] Sim BZ, Mah JK, Heldman MR, et al. Plasma Microbial Cell-free DNA Metagenomic Sequencing for Diagnosis of Invasive Fungal Diseases Among High-risk Outpatient and Inpatient Immunocompromised Hosts. Clin Infect Dis 2025;81:1008–14. https://doi.org/10.1093/cid/ciaf170.

[217] Bray F, Laversanne M, Sung H, et al. Global cancer statistics 2022: GLOBOCAN estimates of incidence and mortality worldwide for 36 cancers in 185 countries. CA: A Cancer J Clin 2024;74:229–63. https://doi.org/10.3322/caac.21834.

[218] Ganti AK, Klein AB, Cotarla I, et al. Update of Incidence, Prevalence, Survival, and Initial Treatment in Patients With Non–Small Cell Lung Cancer in the US. JAMA Oncol 2021;7:1824–32. https://doi.org/10.1001/jamaoncol.2021.4932.

[219] Carbone M, Amos C, Attanoos RL, et al. Advances in the Basic Sciences in Thoracic Oncology in the Last 20 Years and Their Translational Impact. J Thorac Oncol 2026;21:41–76. https://doi.org/10.1016/j.jtho.2025.11.002.

[220] Camidge DR, Doebele RC, Kerr KM. Comparing and contrasting predictive biomarkers for immunotherapy and targeted therapy of NSCLC. Nat Rev Clin Oncol 2019;16:341–55. https://doi.org/10.1038/s41571-019-0173-9.

[221] Tan AC, Tan DSW. Targeted Therapies for Lung Cancer Patients With Oncogenic Driver Molecular Alterations. J Clin Oncol 2022;40:611–25. https://doi.org/10.1200/jco.21.01626.

[222] Kerr KM, Bibeau F, Thunnissen E, et al. The evolving landscape of biomarker testing for non-small cell lung cancer in Europe. Lung Cancer 2021;154:161–75. https://doi.org/10.1016/j.lungcan.2021.02.026.

[223] Zacharias M, Absenger G, Kashofer K, et al. Reflex testing in non-small cell lung carcinoma using DNA- and RNA-based next-generation sequencing—a single-center experience. Transl Lung Cancer Res 2021;0:0–0. https://doi.org/10.21037/tlcr-21-570.

[224] Zacharias M, Konjic S, Kratochwill N, et al. Expanding Broad Molecular Reflex Testing in Non-Small Cell Lung Cancer to Squamous Histology. Cancers 2024;16:903. https://doi.org/10.3390/cancers16050903.

[225] Riely GJ, Wood DE, Ettinger DS, et al. Non–Small Cell Lung Cancer, Version 4.2024. J Natl Compr Cancer Netw 2024;22:249–74. https://doi.org/10.6004/jnccn.2204.0023.

[226] Lindeman NI, Cagle PT, Aisner DL, et al. Updated Molecular Testing Guideline for the Selection of Lung Cancer Patients for Treatment With Targeted Tyrosine Kinase Inhibitors Guideline From the College of American Pathologists, the International Association for the Study of Lung Cancer, and the Association for Molecular Pathology. J Thorac Oncol 2018;13:323–58. https://doi.org/10.1016/j.jtho.2017.12.001.

[227] Hendriks LE, Kerr K, Menis J, et al. Oncogene-addicted metastatic non-small-cell lung cancer: ESMO Clinical Practice Guideline for diagnosis, treatment and follow-up †. Ann Oncol 2023. https://doi.org/10.1016/j.annonc.2022.12.009.

[228] Aggarwal C, Marmarelis ME, Hwang W-T, et al. Association Between Availability of Molecular Genotyping Results and Overall Survival in Patients With Advanced Nonsquamous Non–Small-Cell Lung Cancer. JCO Precis Oncol 2023;7:e2300191. https://doi.org/10.1200/po.23.00191.

[229] Marx V. Method of the Year 2024: spatial proteomics. Nat Methods 2024;21:2195–6. https://doi.org/10.1038/s41592-024-02565-3.

[230] Marx V. Method of the Year: spatially resolved transcriptomics. Nat Methods 2021;18:9–14. https://doi.org/10.1038/s41592-020-01033-y.

[231] Shen Y, Pang C, Wu Y, et al. Diagnostic Performance of Bronchoalveolar Lavage Fluid CD4/CD8 Ratio for Sarcoidosis: A Meta-analysis. EBioMedicine 2016;8:302–8. https://doi.org/10.1016/j.ebiom.2016.04.024.

[232] Winterbauer RH, Lammert J, Sellami M, et al. Bronchoalveolar Lavage Cell Populations in the Diagnosis of Sarcoidosis. Chest 1993;104:352–61. https://doi.org/10.1378/chest.104.2.352.

[233] Reichenberger F, Kleiber B, Baschiera B, et al. Bronchoalveolar lavage quality influences the T4/T8 ratio in sarcoidosis. Respir Med 2007;101:2025–30. https://doi.org/10.1016/j.rmed.2006.11.027.

[234] WAHLSTRÖM J, KATCHAR K, WIGZELL H, et al. Analysis of Intracellular Cytokines in CD4+ and CD8+ Lung and Blood T Cells in Sarcoidosis. Am J Respir Crit Care Med 2001;163:115–21. https://doi.org/10.1164/ajrccm.163.1.9906071.

[235] Wahlström J, Berlin M, Sköld CM, et al. Phenotypic analysis of lymphocytes and monocytes/macrophages in peripheral blood and bronchoalveolar lavage fluid from patients with pulmonary sarcoidosis. Thorax 1999;54:339. https://doi.org/10.1136/thx.54.4.339.

[236] Grunewald J, Grutters JC, Arkema EV, et al. Sarcoidosis. Nat Rev Dis Prim 2019;5:45. https://doi.org/10.1038/s41572-019-0096-x.

[237] Krausgruber T, Redl A, Barreca D, et al. Single-cell and spatial transcriptomics reveal aberrant lymphoid developmental programs driving granuloma formation. Immunity 2023;56:289-306.e7. https://doi.org/10.1016/j.immuni.2023.01.014.

[238] Wang XQ, Danenberg E, Huang C-S, et al. Spatial predictors of immunotherapy response in triple-negative breast cancer. Nature 2023;621:868–76. https://doi.org/10.1038/s41586-023-06498-3.

[239] Russell CD, Fairfield CJ, Drake TM, et al. Co-infections, secondary infections, and antimicrobial use in patients hospitalised with COVID-19 during the first pandemic wave from the ISARIC WHO CCP-UK study: a multicentre, prospective cohort study. Lancet Microbe 2021;2:e354–65. https://doi.org/10.1016/s2666-5247(21)00090-2.

[240] Langford BJ, So M, Raybardhan S, et al. Bacterial co-infection and secondary infection in patients with COVID-19: a living rapid review and meta-analysis. Clin Microbiol Infect 2020;26:1622–9. https://doi.org/10.1016/j.cmi.2020.07.016.

[241] Zurl C, Hoenigl M, Schulz E, et al. Autopsy Proven Pulmonary Mucormycosis Due to Rhizopus microsporus in a Critically Ill COVID-19 Patient with Underlying Hematological Malignancy. J Fungi 2021;7:88. https://doi.org/10.3390/jof7020088.

[242] Layne SP, Walters K-A, Kash JC, et al. More autopsy studies are needed to understand the pathogenesis of severe COVID-19. Nat Med 2022;28:427–8. https://doi.org/10.1038/s41591-022-01684-8.

[243] Liao M, Liu Y, Yuan J, et al. Single-cell landscape of bronchoalveolar immune cells in patients with COVID-19. Nat Med 2020;26:842–4. https://doi.org/10.1038/s41591-020-0901-9.

[244] Xu G, Qi F, Li H, et al. The differential immune responses to COVID-19 in peripheral and lung revealed by single-cell RNA sequencing. Cell Discov 2020;6:73. https://doi.org/10.1038/s41421-020-00225-2.

[245] Nie X, Qian L, Sun R, et al. Multi-organ proteomic landscape of COVID-19 autopsies. Cell 2021;184:775-791.e14. https://doi.org/10.1016/j.cell.2021.01.004.

[246] Wauters E, Mol PV, Garg AD, et al. Discriminating mild from critical COVID-19 by innate and adaptive immune single-cell profiling of bronchoalveolar lavages. Cell Res 2021;31:272–90. https://doi.org/10.1038/s41422-020-00455-9.

[247] Dickson RP, Singer BH, Newstead MW, et al. Enrichment of the lung microbiome with gut bacteria in sepsis and the acute respiratory distress syndrome. Nat Microbiol 2016;1:16113. https://doi.org/10.1038/nmicrobiol.2016.113.

[248] Luyt C-E, Bouadma L, Morris AC, et al. Pulmonary infections complicating ARDS. Intensiv Care Med 2020;46:2168–83. https://doi.org/10.1007/s00134-020-06292-z.

[249] Klein EY, Monteforte B, Gupta A, et al. The frequency of influenza and bacterial coinfection: a systematic review and meta-analysis. Influ Other Respir Viruses 2016;10:394–403. https://doi.org/10.1111/irv.12398.

[250] Crum-Cianflone NF. Invasive Aspergillosis Associated With Severe Influenza Infections. Open Forum Infect Dis 2016;3:ofw171. https://doi.org/10.1093/ofid/ofw171.

[251] Navarini AA, Recher M, Lang KS, et al. Increased susceptibility to bacterial superinfection as a consequence of innate antiviral responses. Proc Natl Acad Sci 2006;103:15535–9. https://doi.org/10.1073/pnas.0607325103.

[252] Schliehe C, Flynn EK, Vilagos B, et al. The methyltransferase Setdb2 mediates virus-induced susceptibility to bacterial superinfection. Nat Immunol 2015;16:67–74. https://doi.org/10.1038/ni.3046.

[253] Callender LA, Curran M, Bates SM, et al. The Impact of Pre-existing Comorbidities and Therapeutic Interventions on COVID-19. Front Immunol 2020;11:1991. https://doi.org/10.3389/fimmu.2020.01991.

[254] Carey IM, Critchley JA, DeWilde S, et al. Risk of Infection in Type 1 and Type 2 Diabetes Compared With the General Population: A Matched Cohort Study. Diabetes Care 2018;41:513–21. https://doi.org/10.2337/dc17-2131.

[255] Syed-Ahmed M, Narayanan M. Immune Dysfunction and Risk of Infection in Chronic Kidney Disease. Adv Chronic Kidney Dis 2019;26:8–15. https://doi.org/10.1053/j.ackd.2019.01.004.

[256] Wu D, Wu C, Zhang S, et al. Risk Factors of Ventilator-Associated Pneumonia in Critically III Patients. Front Pharmacol 2019;10:482. https://doi.org/10.3389/fphar.2019.00482.

[257] Sieswerda E, Boer MGJ de, Bonten MMJ, et al. Recommendations for antibacterial therapy in adults with COVID-19 – an evidence based guideline. Clin Microbiol Infect 2021;27:61–6. https://doi.org/10.1016/j.cmi.2020.09.041.

[258] Chang JY, Antonopoulos DA, Kalra A, et al. Decreased Diversity of the Fecal Microbiome in Recurrent Clostridium difficile—Associated Diarrhea. J Infect Dis 2008;197:435–8. https://doi.org/10.1086/525047.

[259] Perico L, Benigni A, Casiraghi F, et al. Immunity, endothelial injury and complement-induced coagulopathy in COVID-19. Nat Rev Nephrol 2021;17:46–64. https://doi.org/10.1038/s41581-020-00357-4.

[260] Doran AC, Yurdagul A, Tabas I. Efferocytosis in health and disease. Nat Rev Immunol 2020;20:254–67. https://doi.org/10.1038/s41577-019-0240-6.

[261] Son M, Santiago-Schwarz F, Al-Abed Y, et al. C1q limits dendritic cell differentiation and activation by engaging LAIR-1. Proc Natl Acad Sci 2012;109:E3160–7. https://doi.org/10.1073/pnas.1212753109.

[262] Fouët G, Bally I, Chouquet A, et al. Molecular Basis of Complement C1q Collagen-Like Region Interaction with the Immunoglobulin-Like Receptor LAIR-1. Int J Mol Sci 2021;22:5125. https://doi.org/10.3390/ijms22105125.

[263] Tang Z, Veillette A. Inhibitory immune checkpoints in cancer immunotherapy. Sci Immunol 2025;10:eadv6870. https://doi.org/10.1126/sciimmunol.adv6870.

[264] Hanson KE, Azar MM, Banerjee R, et al. Molecular Testing for Acute Respiratory Tract Infections: Clinical and Diagnostic Recommendations From the IDSA's Diagnostics Committee. Clin Infect Dis 2020;71:2744–51. https://doi.org/10.1093/cid/ciaa508.

[265] Trecourt A, Rabodonirina M, Devouassoux-Shisheboran M, et al. Pathologists' role in fungal infection diagnosis using an integrated histomolecular approach: highlighting novelties and the need for real-life pragmatic guidelines. Virchows Arch 2025:1–3. https://doi.org/10.1007/s00428-025-04245-9.

[266] Guarner J, Brandt ME. Histopathologic Diagnosis of Fungal Infections in the 21st Century. Clin Microbiol Rev 2011;24:247–80. https://doi.org/10.1128/cmr.00053-10.

[267] Haas A, Hanson K. Clinical Test Comparison for Improved Diagnosis of Mucormycosis. Am J Clin Pathol 2024;162:S165–S165. https://doi.org/10.1093/ajcp/aqae129.364.

[268] Cornely OA, Alastruey-Izquierdo A, Arenz D, et al. Global guideline for the diagnosis and management of mucormycosis: an initiative of the European Confederation of Medical Mycology in cooperation with the Mycoses Study Group Education and Research Consortium. Lancet Infect Dis 2019;19:e405–21. https://doi.org/10.1016/s1473-3099(19)30312-3.

[269] Lopera TJ, Alzate-Ángel JC, Díaz FJ, et al. The Usefulness of Antigen Testing in Predicting Contagiousness in COVID-19. Microbiol Spectr 2022;10:e01962-21. https://doi.org/10.1128/spectrum.01962-21.

[270] Paez JG, Jänne PA, Lee JC, et al. EGFR Mutations in Lung Cancer: Correlation with Clinical Response to Gefitinib Therapy. Science 2004;304:1497–500. https://doi.org/10.1126/science.1099314.

[271] Lynch TJ, Bell DW, Sordella R, et al. Activating Mutations in the Epidermal Growth Factor Receptor Underlying Responsiveness of Non–Small-Cell Lung Cancer to Gefitinib. N Engl J Med 2004;350:2129–39. https://doi.org/10.1056/nejmoa040938.

[272] Pirker R, Herth FJF, Kerr KM, et al. Consensus for EGFR Mutation Testing in Non-small Cell Lung Cancer: Results from a European Workshop. J Thorac Oncol 2010;5:1706–13. https://doi.org/10.1097/jto.0b013e3181f1c8de.

[273] Yatabe Y, Dacic S, Borczuk AC, et al. Best Practices Recommendations for Diagnostic Immunohistochemistry in Lung Cancer. J Thorac Oncol 2019;14:377–407. https://doi.org/10.1016/j.jtho.2018.12.005.

[274] Lantuejoul S, Sound-Tsao M, Cooper WA, et al. PD-L1 Testing for Lung Cancer in 2019: Perspective From the IASLC Pathology Committee. J Thorac Oncol 2020;15:499–519. https://doi.org/10.1016/j.jtho.2019.12.107.

[275] Brune MM, Roma L, Chijioke O, et al. MTAP Expression by Immunohistochemistry: A Novel Biomarker in NSCLC. J Thorac Oncol 2026;21:112–23. https://doi.org/10.1016/j.jtho.2025.08.014.

[276] Pennell NA, Mutebi A, Zhou Z-Y, et al. Economic Impact of Next-Generation Sequencing Versus Single-Gene Testing to Detect Genomic Alterations in Metastatic Non–Small-Cell Lung Cancer Using a Decision Analytic Model. JCO Precis Oncol 2019;3:1–9. https://doi.org/10.1200/po.18.00356.

[277] Gosney JR, Paz-Ares L, Jänne P, et al. Pathologist-initiated reflex testing for biomarkers in non-small-cell lung cancer: expert consensus on the rationale and

considerations for implementation. ESMO Open 2023;8:101587. https://doi.org/10.1016/j.esmoop.2023.101587.

[278] Bruno DS, Li X, Hess LM. Biomarker Testing, Targeted Therapy and Clinical Trial Participation by Race Among Patients With Lung Cancer: A Real-World Medicaid Database Study. JTO Clin Res Rep 2024;5:100643. https://doi.org/10.1016/j.jtocrr.2024.100643.

[279] Bruno DS, Hess LM, Li X, et al. Disparities in Biomarker Testing and Clinical Trial Enrollment Among Patients With Lung, Breast, or Colorectal Cancers in the United States. JCO Precis Oncol 2022;6:e2100427. https://doi.org/10.1200/po.21.00427.

[280] Tsuboi M, Herbst RS, John T, et al. Overall Survival with Osimertinib in Resected EGFR-Mutated NSCLC. N Engl J Med 2023;389:137–47. https://doi.org/10.1056/nejmoa2304594.

[281] Wu Y-L, Tsuboi M, He J, et al. Osimertinib in Resected EGFR-Mutated Non–Small-Cell Lung Cancer. New Engl J Med 2020;383:1711–23. https://doi.org/10.1056/nejmoa2027071.

[282] Miller TE, Yang M, Bajor D, et al. Clinical utility of reflex testing using focused next-generation sequencing for management of patients with advanced lung adenocarcinoma. J Clin Pathol 2018;71:1108. https://doi.org/10.1136/jclinpath-2018-205396.

[283] Takahashi T, Nishio M, Nishino K, et al. Real-world study of next-generation sequencing diagnostic biomarker testing for patients with lung cancer in Japan. Cancer Sci 2023;114:2524–33. https://doi.org/10.1111/cas.15752.

[284] Devarakonda S, Morgensztern D, Govindan R. Genomic alterations in lung adenocarcinoma. Lancet Oncol 2015;16:e342–51. https://doi.org/10.1016/s1470-2045(15)00077-7.

[285] Kalemkerian GP, Narula N, Kennedy EB, et al. Molecular Testing Guideline for the Selection of Patients With Lung Cancer for Treatment With Targeted Tyrosine Kinase Inhibitors: American Society of Clinical Oncology Endorsement of the College of American Pathologists/International Association for the Study of Lung Cancer/Association for Molecular Pathology Clinical Practice Guideline Update. J Clin Oncol 2018;36:JCO.2017.76.729. https://doi.org/10.1200/jco.2017.76.7293.

[286] Kron A, Scheffler M, Heydt C, et al. Genetic Heterogeneity of MET-Aberrant NSCLC and Its Impact on the Outcome of Immunotherapy. J Thorac Oncol 2021;16:572–82. https://doi.org/10.1016/j.jtho.2020.11.017.

[287] Griesinger F, Eberhardt W, Nusch A, et al. Biomarker testing in non-small cell lung cancer in routine care: Analysis of the first 3,717 patients in the German prospective, observational, nation-wide CRISP Registry (AIO-TRK-0315). Lung Cancer 2021;152:174–84. https://doi.org/10.1016/j.lungcan.2020.10.012.

[288] Adib E, Nassar AH, Alaiwi SA, et al. Variation in targetable genomic alterations in non-small cell lung cancer by genetic ancestry, sex, smoking history, and histology. Genome Med 2022;14:39. https://doi.org/10.1186/s13073-022-01041-x.

[289] Sands JM, Nguyen T, Shivdasani P, et al. Next-generation sequencing informs diagnosis and identifies unexpected therapeutic targets in lung squamous cell carcinomas. Lung Cancer 2020;140:35–41. https://doi.org/10.1016/j.lungcan.2019.12.005.

[290] Pirker R, Prosch H, Popper H, et al. Lung Cancer in Austria. J Thorac Oncol 2021;16:725–33. https://doi.org/10.1016/j.jtho.2020.10.158.

7 Appendix - Publications I-V (full text PDFs)

Publication I:
Zacharias, M*; Kashofer, K*; Wurm, P*; Regitnig, P; Schütte, M; Neger, M; Ehmann, S; Marsh, LM; Kwapiszewska, G; Loibner, M; Birnhuber, A; Leitner, E; Thüringer, A; Winter, E; Sauer, S; Pollheimer, MJ; Vagena, FR; Lackner, C; Jelusic, B; Ogilvie, L; Durdevic, M; Timmermann, B; Lehrach, H; Zatloukal, K; Gorkiewicz, G.
Host and microbiome features of secondary infections in lethal covid-19.
iScience. 2022. https://doi.org/10.1016/j.isci.2022.104926

Publication II:
Zacharias, M; Stangl, V; Thüringer, A; Loibner, M; Wurm, P; Wolfgruber, S; Zatloukal, K; Kashofer, K; Gorkiewicz, G.
Rapid antigen test for postmortem evaluation of SARS-CoV-2 carriage.
Emerg Infect Dis. 2021. https://doi.org/10.3201/eid2706.210226

Publication III:
Zacharias, M; Thüringer, A; Krause, R; Kashofer, K; Gorkiewicz, G.
The mutual value of histopathology and ITS sequencing in the diagnosis of mucormycosis.
Histopathology. 2024. https://doi.org/10.1111/his.15131

Publication IV:
Zacharias, M*; Absenger, G*; Kashofer, K; Wurm, R; Lindenmann, J; Terbuch, A; Konjic, S; Sauer, S; Gollowitsch, F; Gorkiewicz, G; Brcic, L.
Reflex testing in non-small cell lung carcinoma using DNA- and RNA-based next-generation sequencing - a single-center experience.
Transl Lung Cancer Res. 2021. https://doi.org/10.21037/tlcr-21-570

Publication V:
Zacharias, M; Konjic, S; Kratochwill, N; Absenger, G; Terbuch, A; Jost, PJ; Wurm, R; Lindenmann, J; Kashofer, K; Gollowitsch, F; Gorkiewicz, G; Brcic, L.
Expanding broad molecular reflex testing in non-small cell lung cancer to squamous histology.
Cancers. 2024. https://doi.org/10.3390/cancers16050903

*contributed equally

iScience

CellPress
OPEN ACCESS

Article

Host and microbiome features of secondary infections in lethal covid-19

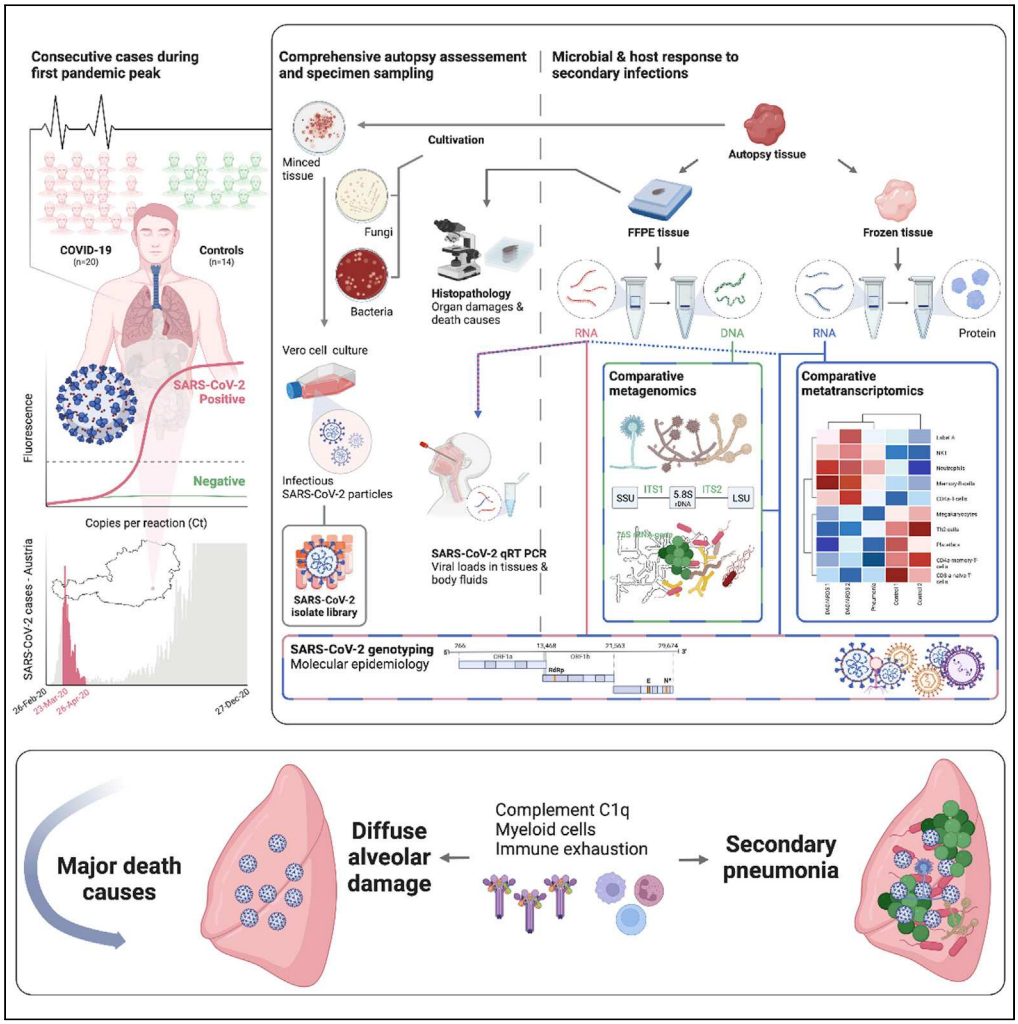

Martin Zacharias, Karl Kashofer, Philipp Wurm, ..., Hans Lehrach, Kurt Zatloukal, Gregor Gorkiewicz

kurt.zatloukal@medunigraz.at (K.Z.)
gregor.gorkiewicz@medunigraz.at (G.G.)

Highlights

Covid-19 autopsy cohort complemented with microbial cultivation and deep sequencing

Major death causes stratify into DAD and secondary pneumonias

Prototypical bacterial and fungal agents are found in secondary pneumonias

Macrophages and C1q stratify DAD subgroups and indicate immune impairment in lungs

Zacharias et al., iScience 25, 104926
September 16, 2022
https://doi.org/10.1016/j.isci.2022.104926

iScience

CellPress
OPEN ACCESS

Article

Host and microbiome features of secondary infections in lethal covid-19

Martin Zacharias,[1,6] Karl Kashofer,[1,6] Philipp Wurm,[1,6] Peter Regitnig,[1] Moritz Schütte,[2] Margit Neger,[1] Sandra Ehmann,[1] Leigh M. Marsh,[3] Grazyna Kwapiszewska,[3] Martina Loibner,[1] Anna Birnhuber,[3] Eva Leitner,[4] Andrea Thüringer,[1] Elke Winter,[1] Stefan Sauer,[1] Marion J. Pollheimer,[1] Fotini R. Vagena,[1] Carolin Lackner,[1] Barbara Jelusic,[1] Lesley Ogilvie,[2] Marija Durdevic,[1] Bernd Timmermann,[5] Hans Lehrach,[2,5] Kurt Zatloukal,[1,*] and Gregor Gorkiewicz[1,7,*]

SUMMARY

Secondary infections contribute significantly to covid-19 mortality but driving factors remain poorly understood. Autopsies of 20 covid-19 cases and 14 controls from the first pandemic wave complemented with microbial cultivation and RNA-seq from lung tissues enabled description of major organ pathologies and specification of secondary infections. Lethal covid-19 segregated into two main death causes with either dominant diffuse alveolar damage (DAD) or secondary pneumonias. The lung microbiome in covid-19 showed a reduced biodiversity and increased prototypical bacterial and fungal pathogens in cases of secondary pneumonias. RNA-seq distinctly mirrored death causes and stratified DAD cases into subgroups with differing cellular compositions identifying myeloid cells, macrophages and complement C1q as strong separating factors suggesting a pathophysiological link. Together with a prominent induction of inhibitory immune-checkpoints our study highlights profound alterations of the lung immunity in covid-19 wherein a reduced antimicrobial defense likely drives development of secondary infections on top of SARS-CoV-2 infection.

INTRODUCTION

Covid-19 originates from infection of the upper respiratory tract with SARS-CoV-2, which can progress into severe acute lung injury (ALI). Based on the tissue-typic expression of the viral host-entry receptor ACE2 and certain proteases (e.g. TMPRSS2) facilitating cellular uptake, also other organs like the kidney could be directly infected (Hou et al., 2020b). In addition, severe disturbances of immune and coagulation systems during covid-19 lead to a multifaceted disease with variable multi-organ damages (Ramlall et al., 2020). A consistent finding in severe covid-19 is initial immune hyperactivation (called "cytokine storm") leading to subsequent immune exhaustion, a phenomenon also known in other severe infections (Blanco-Melo et al., 2020; Lowery et al., 2021; Roquilly et al., 2020; Wang et al., 2021). Consequently, secondary infections which develop on top of SARS-CoV-2 infection contribute significantly to covid-19 mortality similar to severe influenza (Buehler et al., 2021). Curiously, the pathophysiology leading to the development of secondary lung infections is generally poorly understood. We performed an autopsy study of 20 consecutive covid-19 patients who died during the first pandemic wave. Full autopsies were performed and various specimen types were collected for tissue-based investigations, molecular measures including deep sequencing and cultivation of virus and other microbes. Integrating all information gained from this "holistic" autopsy approach allowed us to gain a deeper understanding of host and microbial factors contributing to secondary infections as a major sequel of lethal covid-19.

RESULTS

Autopsy cohort, SARS-CoV-2 body distribution and genotyping

Twenty consecutive covid-19 patients were examined post-mortem (Figure S1). Thirteen cases were males and 7 were females; their ages ranged from 53 to 93 years (median: 79 years). All had multiple comorbidities typically prevalent in severe covid-19. In addition, 14 age-matched non-covid-19 controls who died

[1]Diagnostic and Research Institute of Pathology, Medical University of Graz, Neue Stiftingtalstrasse 6, 8010 Graz, Austria

[2]Alacris Theranostics GmbH, Max-Planck-Strasse 3, 12489 Berlin, Germany

[3]Ludwig Boltzmann Institute for Lung Vascular Research, Neue Stiftingtalstrasse 6/VI, 8010 Graz, Austria

[4]Diagnostic and Research Institute of Hygiene, Microbiology and Environmental Medicine, Medical University of Graz, Neue Stiftingtalstrasse 6, 8010 Graz, Austria

[5]Max Planck Institute for Molecular Genetics, Ihnestrasse 63, 14195 Berlin, Germany

[6]These authors contributed equally

[7]Lead contact

*Correspondence: kurt.zatloukal@medunigraz.at (K.Z.), gregor.gorkiewicz@medunigraz.at (G.G.)

https://doi.org/10.1016/j.isci.2022.104926

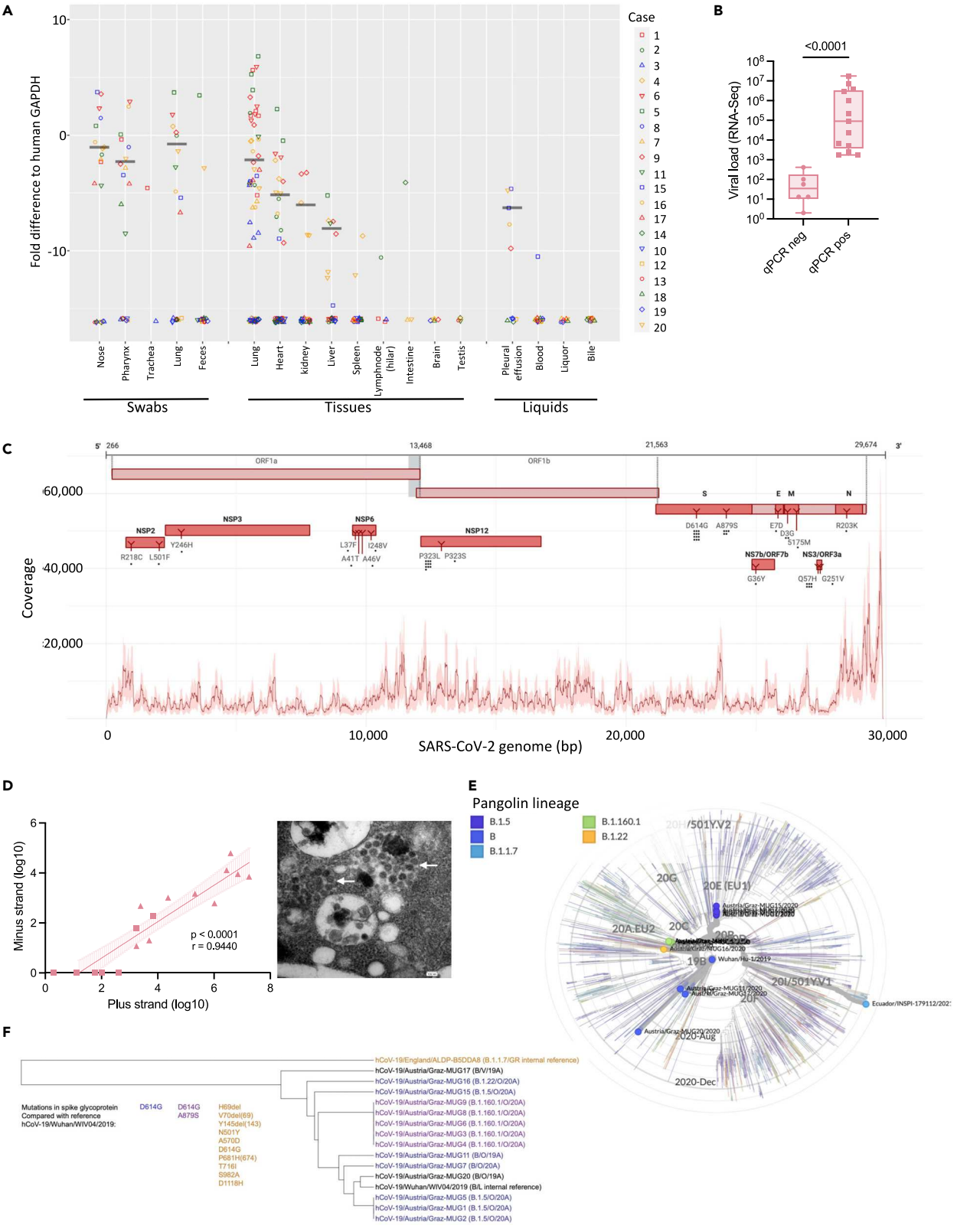
A
Fold difference to human GAPDH
Case
Nose
Pharynx
Trachea
Lung
Feces
Lung
Heart
kidney
Liver
Spleen
Lymphnode (hilar)
Intestine
Brain
Testis
Pleural effusion
Blood
Liquor
Bile
Swabs
Tissues
Liquids
B
<0.0001
Viral load (RNA-Seq)
qPCR neg
qPCR pos
C
ORF1a
ORF1b
S
E
M
N
NSP2
NSP3
NSP6
NSP12
NS7b/ORF7b
NS3/ORF3a
Coverage
SARS-CoV-2 genome (bp)
D
Minus strand (log10)
Plus strand (log10)
p < 0.0001
r = 0.9440
E
Pangolin lineage
B.1.5
B
B.1.1.7
B.1.160.1
B.1.22
/501YV2
20G
20E (EU1)
20A.EU2
20C
19B
20I/501YV1
2020-Aug
2020-Dec
F
Mutations in spike glycoprotein
Compared with reference
hCoV-19/Wuhan/WIV04/2019:
D614G
D614G
A879S
H69del
V70del(69)
Y145del(143)
N501Y
A570D
D614G
P681H(674)
T716I
S982A
D1118H
hCoV-19/England/ALDP-B5DDA8 (B.1.1.7/GR internal reference)
hCoV-19/Austria/Graz-MUG17 (B/V/19A)
hCoV-19/Austria/Graz-MUG16 (B.1.22/O/20A)
hCoV-19/Austria/Graz-MUG15 (B.1.5/O/20A)
hCoV-19/Austria/Graz-MUG9 (B.1.160.1/O/20A)
hCoV-19/Austria/Graz-MUG8 (B.1.160.1/O/20A)
hCoV-19/Austria/Graz-MUG6 (B.1.160.1/O/20A)
hCoV-19/Austria/Graz-MUG3 (B.1.160.1/O/20A)
hCoV-19/Austria/Graz-MUG4 (B.1.160.1/O/20A)
hCoV-19/Austria/Graz-MUG11 (B/O/19A)
hCoV-19/Austria/Graz-MUG7 (B/O/20A)
hCoV-19/Austria/Graz-MUG20 (B/O/19A)
hCoV-19/Wuhan/WIV04/2019 (B/L internal reference)
hCoV-19/Austria/Graz-MUG5 (B.1.5/O/20A)
hCoV-19/Austria/Graz-MUG1 (B.1.5/O/20A)
hCoV-19/Austria/Graz-MUG2 (B.1.5/O/20A)

Figure 1. SARS-CoV-2 tissue distributions, genotyping and virus cultivation

(A) SARS-CoV-2 loads (compared to human glyceraldehyde 3-phosphate dehydrogenase, GAPDH) and tissue distributions derived from postmortem sampling (median highlighted). Case numbers are given on the right.

(B) Significant association of qRT-PCR positivity (n-gene) with viral loads determined by RNAseq of lung tissues (Mann-Whitney test).

(C) Distribution of viral reads generated from lung tissues along the SARS-CoV-2 genome. Cumulative coverage of plus and minus strand transcripts is shown (median in bold). Identified nucleotide and amino-acid changes in comparison to the Wuhan reference strain are indicated.

(D) Correlation of SARS-CoV-2 plus and minus strand reads with cultivation (Spearman correlation). Triangles specify cultivation-positive samples. EM picture showing viral particles in Vero CCL-81 cells (arrows).

(E) Cladogram showing detected virus genotypes within a global context. The Wuhan reference strain (center) and the UK variant B.1.1.7 (Ecuador/INSPI-179112/2021) are included for comparisons. The pangolin lineage designation is used to specify viral genotypes.

(F) Dendrogram showing detected viral genotypes. Corresponding mutations in the S protein are indicated and virus strains are color coded accordingly.

within the same time period were included for comparisons (Tables S1 and S2). Patients were tested for SARS-CoV-2 tissue distributions by quantitative RT-PCR (target: nucleocapsid-gene) and most positive samples with the highest viral loads originated from the respiratory tract, followed by myocardium, liver, kidney and pleural effusions. Other tissues and body liquids were positive only in single cases or tested overall negative (Figure 1A). Notably, deep RNA-seq generated from lung tissues revealed SARS-CoV-2 transcripts in each covid-19 case, including the four qRT-PCR negative ones, showing increased sensitivity of deep transcriptomic analysis (127 $\pm$ 29 million reads were generated per sample on average; Figure 1B). The viral genome was entirely captured by RNA-seq yielding more plus-strand reads (mean: 37.89 reads per million; range: 0.02–131,165.41) than minus-strand reads (mean: 1.81 reads per million; range: 0–484.81; Figure 1C). In addition, 11 SARS-CoV-2 strains could be cultivated from post-mortem lung tissues using Vero cells (Table S3). Successful virus cultivation significantly correlated with abundance of SARS-CoV-2 reads (Figures 1D and S2).

SARS-CoV-2 genotyping facilitated by PCR and sequencing directly from autopsy specimens yielded 14 complete viral genomes (Table S4). Nine different sequence variants were detected showing up to 12 nucleotide changes compared to the reference (SARS-CoV-2 Wuhan-Hu-1; total genome size 29,903 bp; Table S5). Strains corresponded to the pangolin lineages B.1.22, B1.5, B and B.1.160.1, respectively (clades 19A and 20A), representing the dominant genotypes of the first pandemic wave (Figure 1E). Twelve strains harbored a D614G mutation in the spike (S) protein, which leads to increased viral transmissibility and, therefore, this genotype superseded the wild-type strain already early in the pandemic (Hou et al., 2020a). We identified also 2 viral clusters in our cohort, cluster 1 (case 3, 4, 6, 8, and 9) and cluster 2 (case 1, 2, and 5), respectively (Figure 1F). Notably, cases 6, 8 and 9 from cluster 1 originated from the same residential care home and all cases from cluster 2 stayed in the same hospital ward before covid-19. Thus, it is very likely that these individuals were infected from the same sources and/or transmission occurred.

Major organ pathologies and death causes

Lungs showed the dominant pathologies in relation to covid-19, only one case (#1) presented with acute myocardial infarction as the ascribed death cause. Diffuse alveolar damage (DAD), the histopathological representation of ALI, in a patchy distribution and often prevalent in multiple lung segments was the major finding in 11 cases. Early exudative stages and later organizing stages of DAD were found within the same patient together, often adjacent to nearly normal or less affected parenchyma indicating ongoing tissue damage (Figures 2A and S3–S5). Also, a significant positive correlation of SARS-CoV-2 loads from nasopharyngeal tissues to lungs was found (Figure 2B) likely suggesting active seeding of infectious particles from the upper respiratory tract via micro-aspiration (Hou et al., 2020b). We extensively assessed microscopic lung features (see STAR Methods for details of histopathological scoring) to specify and grade the severity of lesions and also to capture the heterogeneity of different lung pathologies. Features greatly varied between cases and the majority of patterns did not correlate with disease duration (defined as the interval between the first SARS-CoV-2 positive PCR and death) or viral loads (Figure 2C). Although early DAD features (intra-alveolar edema, hyaline membranes) correlated positively with shorter disease duration and late features (fibrosis) increased with disease duration, early and late features were often intermixed showing no inverse correlation (Figure 2D) corroborating findings also by other studies (Borczuk et al., 2020). Of importance, the clearest discriminating feature of cases was the presence of neutrophilic granulocytes, indicative of secondary infections (i.e., "pneumonia"), in comparison to DAD. Three cases showed DAD superimposed with acute inflammation and 5 cases showed mainly pneumonia as the dominant pathology, wherein DAD was only focally visible overlaid with dense inflammation. Altogether, 16 cases

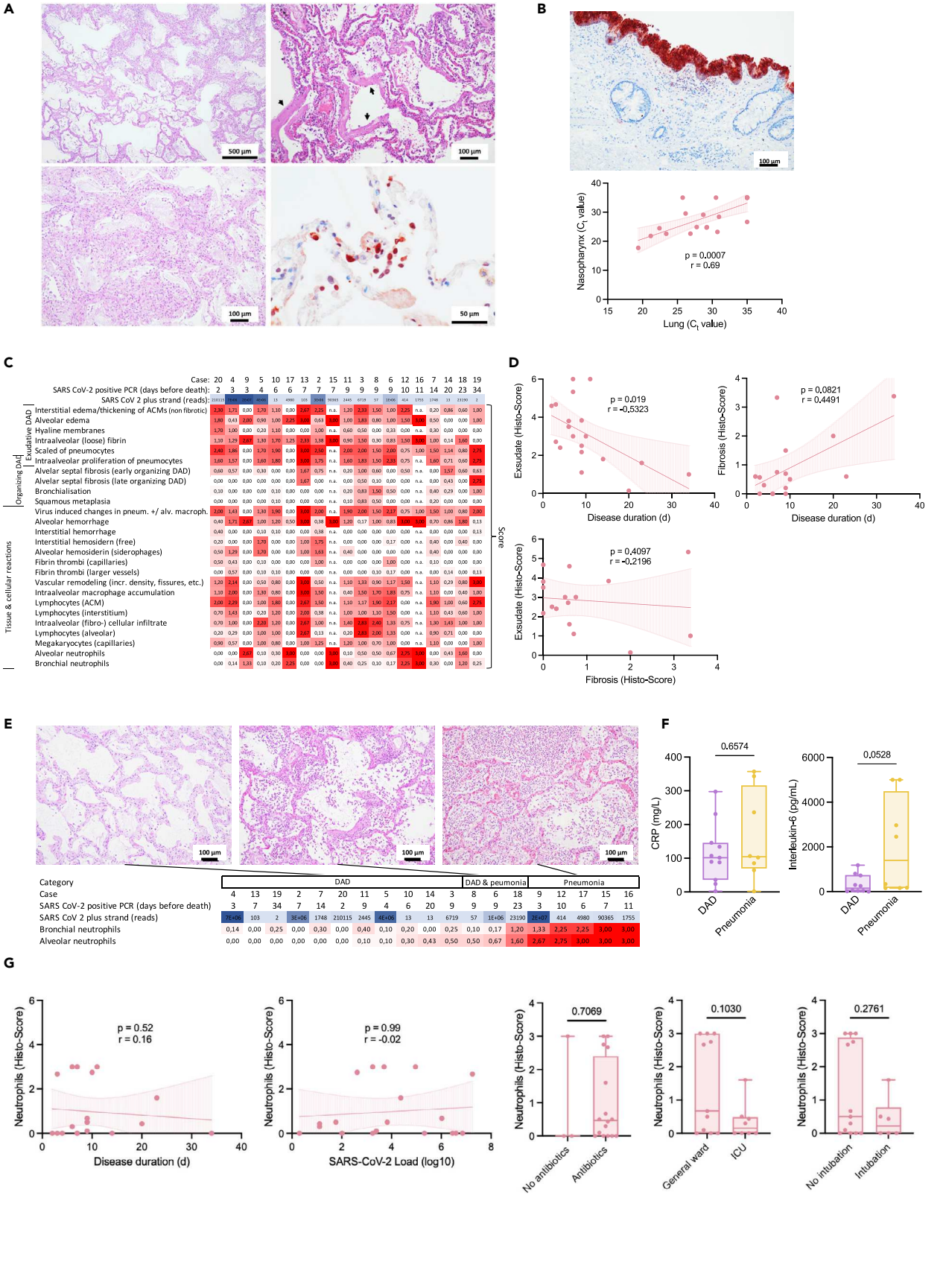
A
500 µm
100 µm
100 µm
50 µm
B
100 µm
Nasopharynx (C$_t$ value)
Lung (C$_t$ value)
p = 0.0007
r = 0.69
C
Case: 20 4 9 5 10 17 13 2 15 11 3 8 6 12 16 7 14 18 19
SARS-CoV-2 positive PCR (days before death): 2 3 3 4 6 6 7 7 7 9 9 9 9 10 11 14 20 23 34
SARS CoV 2 plus strand (reads):
Exudative DAD
Organizing DAD
Tissue & cellular reactions
Interstitial edema/thickening of ACMs (non fibrotic)
Alveolar edema
Hyaline membranes
Intraalveolar (loose) fibrin
Scaled of pneumocytes
Intraalveolar proliferation of pneumocytes
Alvelar septal fibrosis (early organizing DAD)
Alvelar septal fibrosis (late organizing DAD)
Bronchialisation
Squamous metaplasia
Virus induced changes in pneum. +/ alv. macroph.
Alveolar hemorrhage
Interstitial hemorrhage
Interstitial hemosidern (free)
Alveolar hemosiderin (siderophages)
Fibrin thrombi (capillaries)
Fibrin thrombi (larger vessels)
Vascular remodeling (incr. density, fissures, etc.)
Intraalveolar macrophage accumulation
Lymphocytes (ACM)
Lymphocytes (interstitium)
Intraalveolar (fibro-) cellular infiltrate
Lymphocytes (alveolar)
Megakaryocytes (capillaries)
Alveolar neutrophils
Bronchial neutrophils
score
D
Exsudate (Histo-Score)
Disease duration (d)
p = 0.019
r = -0.5323
Fibrosis (Histo-Score)
p = 0.0821
r = 0.4491
p = 0.4097
r = -0.2196
Fibrosis (Histo-Score)
E
100 µm
100 µm
100 µm
Category DAD DAD & peumonia Pneumonia
Case 4 13 19 2 7 20 11 5 10 14 3 8 6 18 9 12 17 15 16
SARS CoV-2 positive PCR (days before death) 3 7 34 7 14 2 9 4 6 20 9 9 9 23 3 10 6 7 11
SARS CoV 2 plus strand (reads) 7E+08 103 2 3E+06 1748 210115 2445 4E+06 13 13 6719 57 1E+06 23190 2E+07 414 4980 90365 1755
Bronchial neutrophils 0,14 0,00 0,25 0,00 0,30 0,00 0,40 0,10 0,20 0,00 0,25 0,10 0,17 1,20 1,33 2,25 2,25 3,00 3,00
Alveolar neutrophils 0,00 0,00 0,00 0,00 0,00 0,00 0,10 0,10 0,30 0,43 0,50 0,50 0,67 1,60 2,67 2,75 3,00 3,00 3,00
F
CRP (mg/L)
0.6574
DAD
Pneumonia
Interleukin-6 (pg/mL)
0.0528
DAD
Pneumonia
G
Neutrophils (Histo-Score)
Disease duration (d)
p = 0.52
r = 0.16
SARS-CoV-2 Load (log10)
p = 0.99
r = -0.02
0.7069
No antibiotics
Antibiotics
0.1030
General ward
ICU
0.2761
No intubation
Intubation

Figure 2. Lung pathology of lethal covid-19 stratifies into DAD and pneumonia

(A) Histological representation of DAD in lungs. A patchy representation of DAD is shown (left). Hyaline membranes (arrows) as a hallmark lesion of early DAD (top right). Immunohistochemical detection (nucleoprotein antibody) of SARS-CoV-2 infected pneumocytes (bottom right).

(B) (Top) Immunohistochemical detection of SARS-CoV-2 infected respiratory epithelium of the nasopharynx. (Bottom) Correlation between SARS-CoV-2 loads in the nasopharyngeal mucosa and lung tissue determined by qRT-PCR (Spearman correlation).

(C) Scoring of prevalent histopathology patterns in lungs. Cases are ordered according to duration of disease.

(D) Correlation analysis of early and late DAD histopathology features and disease duration (Spearman r).

(E) Main discrimination of lung pathology according to DAD and pneumonia patterns. Cases are ordered according to alveolar neutrophil scores.

(F) Serum C-reactive protein (CRP) and interleukin-6 (IL-6) levels in DAD and pneumonia cases (Mann-Whitney test).

(G) Correlation analyses of neutrophil abundance and clinical parameters (Spearman r; Mann-Whitney test).

showed neutrophilic granulocytes present in bronchi, bronchioli, or alveoli suggestive of secondary infections. Thus, lung histopathology in lethal covid-19 could be stratified into DAD, DAD superimposed with pneumonia and dominating pneumonia (Figures 2E and S3). Pneumonia cases showed increased IL-6 levels compared with pure DAD cases, whereas CRP levels were weaker discriminators (Figure 2F). It is noteworthy that neither disease duration nor viral loads correlated with the presence of neutrophils, nor did any other clinical parameter (Figures 2G and S6). Other organs showed features of preexisting comorbidities including arteriosclerosis, hypertension and diabetes, especially in the kidneys, wherein SARS-CoV-2 could be detected in tubular epithelia by positive immunohistochemistry (Figure S7). Heart and liver specimens revealed no clear evidence of direct SARS-CoV-2 carriage or features of myocarditis or hepatitis (Figures S8 and S9). A detailed summary of organ histopathologies is given in the supplementary material (Table S6).

Lung microbiome alterations and secondary infections in lethal covid-19

The lung microbiome is altered in DAD and thought to be a relevant factor for the development of secondary infections (Dickson et al., 2016; Luyt et al., 2020). RNA-seq from lung tissues was screened for microbial sequences and bacterial (16S rRNA gene) and fungal (internal transcribed spacer, ITS) marker genes were amplified to additionally specify microbial changes. On average 6573.33 $\pm$ 2552.32 (MW$\pm$SD) reads per million (rpm) per sample were not human in RNA-seq and likely of microbial origin, of those 2.02 $\pm$ 4.00% and 0.03 $\pm$ 0.05% could be clearly annotated to specific microbes with different microbial annotation pipelines (Figure 3A). Excluding SARS-CoV-2 reads, which were the dominant microbial component in several cases (range: 0.01–131218.36 rpm), bacterial sequences were dominant, significantly increased in covid-19 cases with pneumonia compared to DAD and controls. Fungal and viral sequences other than SARS-CoV-2 were also significantly enriched in covid-19 cases with pneumonia (Figure 3B). Number of bacterial reads significantly correlated with neutrophil scores suggesting that their presence is a sign of secondary infections, however, the post-mortem interval did not, precluding a strong influence of post-mortal bacterial overgrowth in our investigation (Figure 3C). Bacteria are assumed to be the dominant microbiome component in lungs (Huffnagle et al., 2017). Analysis based on the bacterial 16S rRNA gene marker showed that richness was significantly decreased in the DAD and pneumonia cases of covid-19 compared to controls indicating an overall reduced biodiversity (Figure 3D). In contrast, evenness was significantly decreased in the pneumonia group of covid-19 only, suggesting a dominance of certain taxa, possibly representing the agents of secondary infections (pairwise Kruskal-Wallis; *$p < 0.05$, **$p < 0.005$). Principal component analysis (PCA) clearly separated controls from covid-19 cases with DAD and cases with pneumonia indicating significantly different bacterial community compositions (Figure 3E). Lung tissues were also cultured for bacteria and fungi and both—covid-19 cases and controls—yielded cultivable microorganisms but in different quantities and taxonomic constellations (Table S7).

Finally, we integrated RNA-seq, 16S, ITS, and culture data to define dominant pathogens, most likely representing the agents of secondary infections and to account for the different samples used for microbial identifications in the light of the patchy disease representations likely impacting the microbial repertoires (Figure S10 and Table S8). Dominant pathogens were defined if they were dominant in the RNA and/or DNA data (representing >10% of microbial reads excluding SARS-CoV-2) and if they also yielded a reasonable culture growth ($\geq 10^4$ cfu/mL). Dominant taxa were typical agents of pulmonary secondary infections like *Staphylococcus aureus*, *Enterococcus faecium*, or *Klebsiella pneumoniae*, as well as fungi like *Candida* spp. or the mold *Rhizopus microsporus* identified in one case (#18; (Zurl et al., 2021)). Often multiple pathogens were found simultaneously indicating polymicrobial infections (e.g., in case #16 wherein *K. pneumonia*, *S. aureus* and *Candida glabrata* were cultivated in reasonable amounts and were also captured by RNA-seq). In addition, 5 covid-19 cases yielded transcripts of Epstein-Barr virus (EBV), which were also

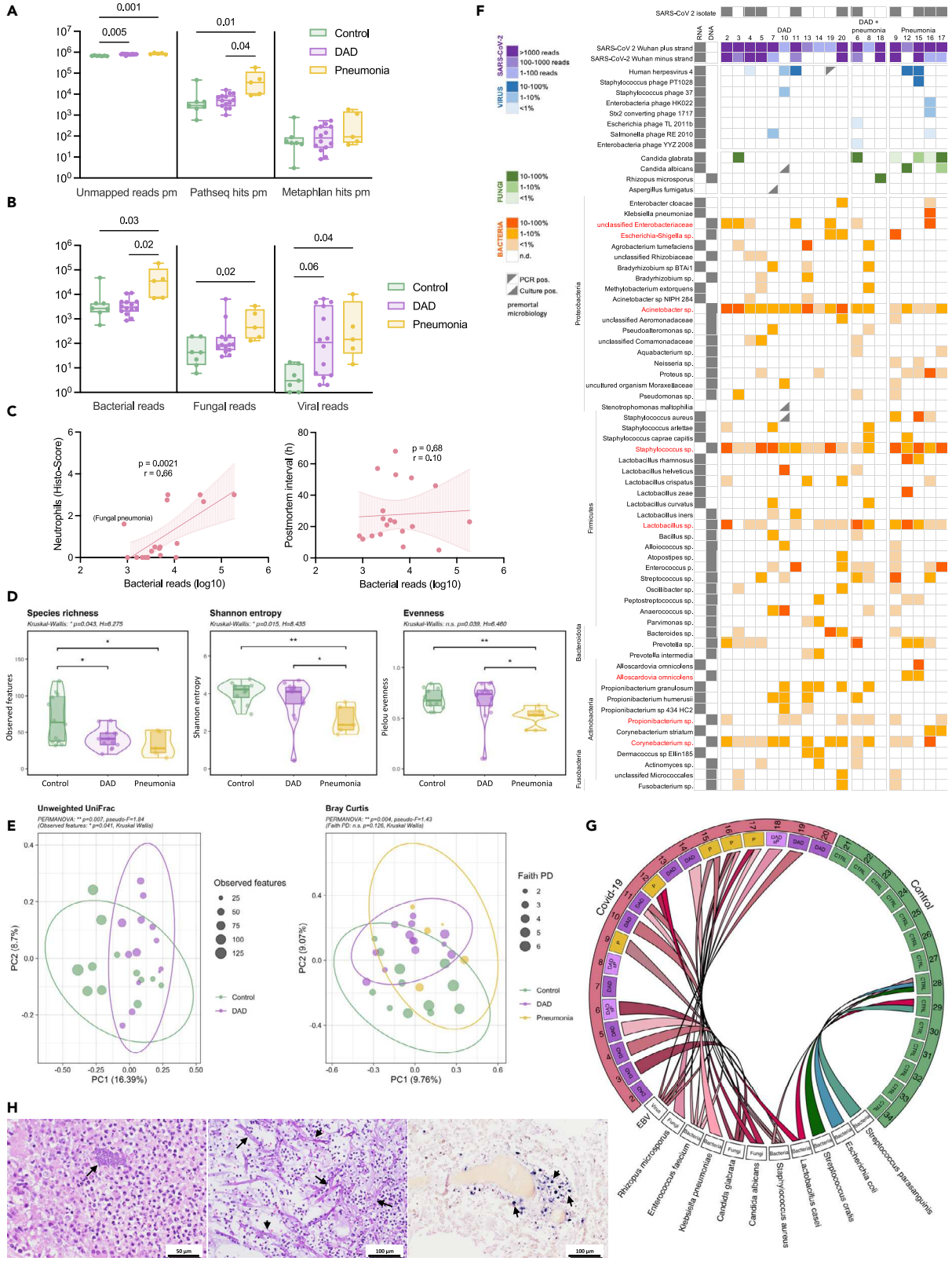
A
0.001
0.005
0.01
0.04
Control
DAD
Pneumonia
Unmapped reads pm
Pathseq hits pm
Metaphlan hits pm
B
0.03
0.02
0.02
0.04
0.06
Control
DAD
Pneumonia
Bacterial reads
Fungal reads
Viral reads
C
p = 0.0021
r = 0.66
(Fungal pneumonia)
Neutrophils (Histo-Score)
Bacterial reads (log10)
p = 0.68
r = 0.10
Postmortem interval (h)
Bacterial reads (log10)
D
Species richness
Kruskal-Wallis: * p=0.043, H=6.275
Shannon entropy
Kruskal-Wallis: * p=0.015, H=8.435
Evenness
Kruskal-Wallis: n.s. p=0.039, H=6.460
Observed features
Shannon entropy
Pielou evenness
Control
DAD
Pneumonia
E
Unweighted UniFrac
PERMANOVA: ** p=0.007, pseudo-F=1.84
(Observed features: * p=0.041, Kruskal Wallis)
Bray Curtis
PERMANOVA: ** p=0.004, pseudo-F=1.43
(Faith PD: n.s. p=0.126, Kruskal Wallis)
PC2 (8.7%)
PC1 (16.39%)
PC2 (9.07%)
PC1 (9.76%)
Observed features
Faith PD
Control
DAD
Pneumonia
F
SARS-CoV 2 isolate
RNA
DNA
DAD
DAD + pneumonia
Pneumonia
SARS-CoV-2
>1000 reads
100-1000 reads
1-100 reads
VIRUS
10-100%
1-10%
<1%
FUNGI
BACTERIA
n.d.
PCR pos.
Culture pos.
premortal microbiology
SARS-CoV 2 Wuhan plus strand
SARS-CoV-2 Wuhan minus strand
Human herpesvirus 4
Staphylococcus phage PT1028
Staphylococcus phage 37
Enterobacteria phage HK022
Stx2 converting phage 1717
Escherichia phage TL 2011b
Salmonella phage RE 2010
Enterobacteria phage YYZ 2008
Candida glabrata
Candida albicans
Rhizopus microsporus
Aspergillus fumigatus
Enterobacter cloacae
Klebsiella pneumoniae
unclassified Enterobacteriaceae
Escherichia-Shigella sp.
Agrobacterium tumefaciens
unclassified Rhizobiaceae
Bradyrhizobium sp BTAi1
Bradyrhizobium sp.
Methylobacterium extorquens
Acinetobacter sp NIPH 284
Acinetobacter sp.
unclassified Aeromonadaceae
Pseudoalteromonas sp.
unclassified Comamonadaceae
Aquabacterium sp.
Neisseria sp.
Proteus sp.
uncultured organism Moraxellaceae
Pseudomonas sp.
Stenotrophomonas maltophilia
Staphylococcus aureus
Staphylococcus arlettae
Staphylococcus caprae capitis
Staphylococcus sp.
Lactobacillus rhamnosus
Lactobacillus helveticus
Lactobacillus crispatus
Lactobacillus zeae
Lactobacillus curvatus
Lactobacillus iners
Lactobacillus sp.
Bacillus sp.
Alloiococcus sp.
Atopostipes sp.
Enterococcus p.
Streptococcus sp.
Oscillibacter sp.
Peptostreptococcus sp.
Anaerococcus sp.
Parvimonas sp.
Bacteroides sp.
Prevotella sp.
Prevotella intermedia
Alloscardovia omnicolens
Alloscardovia omnicolens
Propionibacterium granulosum
Propionibacterium humerusii
Propionibacterium sp 434 HC2
Propionibacterium sp.
Corynebacterium striatum
Corynebacterium sp.
Dermacoccus sp Ellin185
Actinomyces sp.
unclassified Micrococcales
Fusobacterium sp.
Proteobacteria
Firmicutes
Bacteroidota
Actinobacteria
Fusobacteria
G
Covid-19
Control
EBV
Rhizopus microsporus
Enterococcus faecium
Klebsiella pneumoniae
Candida glabrata
Candida albicans
Staphylococcus aureus
Lactobacillus casei
Streptococcus oralis
Escherichia coli
Streptococcus parasanguinis
H
50 µm
100 µm
100 µm

Figure 3. Microbiome alterations and agents of secondary infections in covid-19 lungs

(A) Annotation of non-human transcripts to microbial sequences with PathSeq and MetaPhlAn, respectively (hits per million; Kruskal-Wallis test).

(B) Significantly increased bacterial, fungal and viral reads in the pneumonia category of covid-19 (PathSeq annotation, Kruskal-Wallis test).

(C) Bacterial reads significantly correlate with neutrophil counts but not with the post-mortem interval (Spearman correlation).

(D) Richness and evenness in the bacterial component of the lung microbiome (based on the 16S rRNA gene marker; Kruskal-Wallis test).

(E) Beta-diversity analysis (PCA based on unweighted UniFrac and Bray-Curtis distance) clearly separates DAD and pneumonia cases of covid-19 from controls (16S rRNA gene; PERMANOVA, Kruskal-Wallis test).

(F) Summary of bacterial, fungal and viral microbes prevalent in covid-19 lungs. Shown are microbes detected by cultivation, RNA and/or DNA sequencing (red labeled taxa were also spuriously found in controls).

(G) Dominant pathogens causing secondary infections in covid-19 lungs compared to controls (summary of cultivation and deep sequencing).

(H) Microscopic representation (H&E) of bacterial (left, case #16) and fungal (middle, case #18) pathogens in lung tissues. Epstein-Barr virus RNA positivity in lung tissue (EBV RNA in-situ hybridization, case #11).

detectable by RNA *in-situ* hybridization of lung tissues but not in controls (Figure 3H). EBV often emerges because of endogenous reactivation in the context of impaired immunity (Tangye et al., 2017). Control cases yielded microbial sequences and cultivable microbes in lower quantity and they often belonged to known contaminants like *Lactobacillus* sp. or *Propionibacterium* sp. (Table S8). In summary, the lung microbiome in covid-19 shows a reduced taxonomic richness but harbors a diverse spectrum of bacterial and fungal pathogens typically associated with secondary lung infections. Prominent pathogens like *S. aureus*, *Klebsiella* or *Candida* spp. are also known agents of secondary infection in influenza, SARS, and MERS (Klein et al., 2016; Morens et al., 2008). Notably, secondary infections were rarely detected ante-mortem in our cohort (Table S8). The presence of poly-microbial infections and the relatively high proportion of EBV positivity suggest an overall impaired immunity in covid-19 lungs.

The lung metatranscriptome mirrors the major death categories DAD and pneumonia

Deep RNA-seq of lung tissue revealed 4,547 differentially expressed genes between covid-19 cases and controls (adj. $p < 0.05$). Hierarchical clustering indicated depleted (cluster 1) or enriched (cluster 2) genes in covid-19 compared to controls (Figure 4A). Pathway analysis indicated impaired central cellular functions within mRNA metabolism, post-translational protein modification, the respiratory chain, VEGFA signaling and extracellular matrix organization in covid-19. Enriched pathways consisted mainly of innate and adaptive immune functions, neutrophil degranulation, cytokine signaling as well as complement activation (Figure 4B). Overall, these data confirm profound and complex transcriptional alterations in covid-19 lung tissue (Delorey et al., 2021; Liao et al., 2020; Wu et al., 2020). Unsupervised principal components analysis (PCA) of differentially expressed genes clearly separated covid-19 samples on principal component 1 (PC1) from controls but also clearly separated pneumonia samples from pure DAD cases (Figure 4C). Comparison of differentially expressed genes between these major death categories indicated that the major discriminator from controls was DAD showing 3862 unique differentially expressed genes (adj. $P < 0.05$ and abs. LFC >= 0.58) followed by pneumonia with 1673 unique differentially expressed genes (Figure 4D). DAD and pneumonia differed by only 226 differentially expressed genes. Notably, among the top 50 differential expressed genes enriched in pneumonia cases several macrophage markers were evident, including the receptor *ADGRE1* (murine homolog F4/80) as top-hit, the interleukin-1 receptor-associated kinase-like 2 (*IRAK2*) or *PSTPIP2*, which is involved in macrophage polarization (Figure 4E). Thus, macrophages seem to be implicated in covid-19 secondary infections. In summary, deep transcriptomic analyses specified multiple dysregulated processes in covid-19, including vascular and coagulation systems, connective tissue remodeling as well as activated immunity and complement (Nie et al., 2021). Similar to histopathology, the major discriminator from controls based on gene expression was DAD followed by pneumonia likely mirroring the development of secondary infections on top of ALI caused by the virus.

Cellular deconvolution subgroups covid-19 lung pathology

Cellular compositions were inferred from RNA-seq by using xCell (Aran et al., 2017). Hierarchical clustering based on cellular compositions clearly separated samples into four distinct groups. Group 1 (“control”) consisted only of control cases and was related to group 2 (“DAD1”) consisting of covid-19 cases with pure DAD (in addition to one control case #22). Group 3 (“DAD2”) also contained DAD cases, including one sample with the histological category DAD and secondary pneumonia. This group was related to group 4 (“pneumonia”) composed of all pneumonia cases, in addition to 3 DAD cases and the two remaining DAD cases with secondary pneumonia (Figure 5A). It is noteworthy that neither disease duration nor early versus late DAD histological features or SARS-CoV-2 loads significantly correlated with a specific grouping (Figure S11). Cell types discriminating these groups showed a specific assembly (Figure 5B).

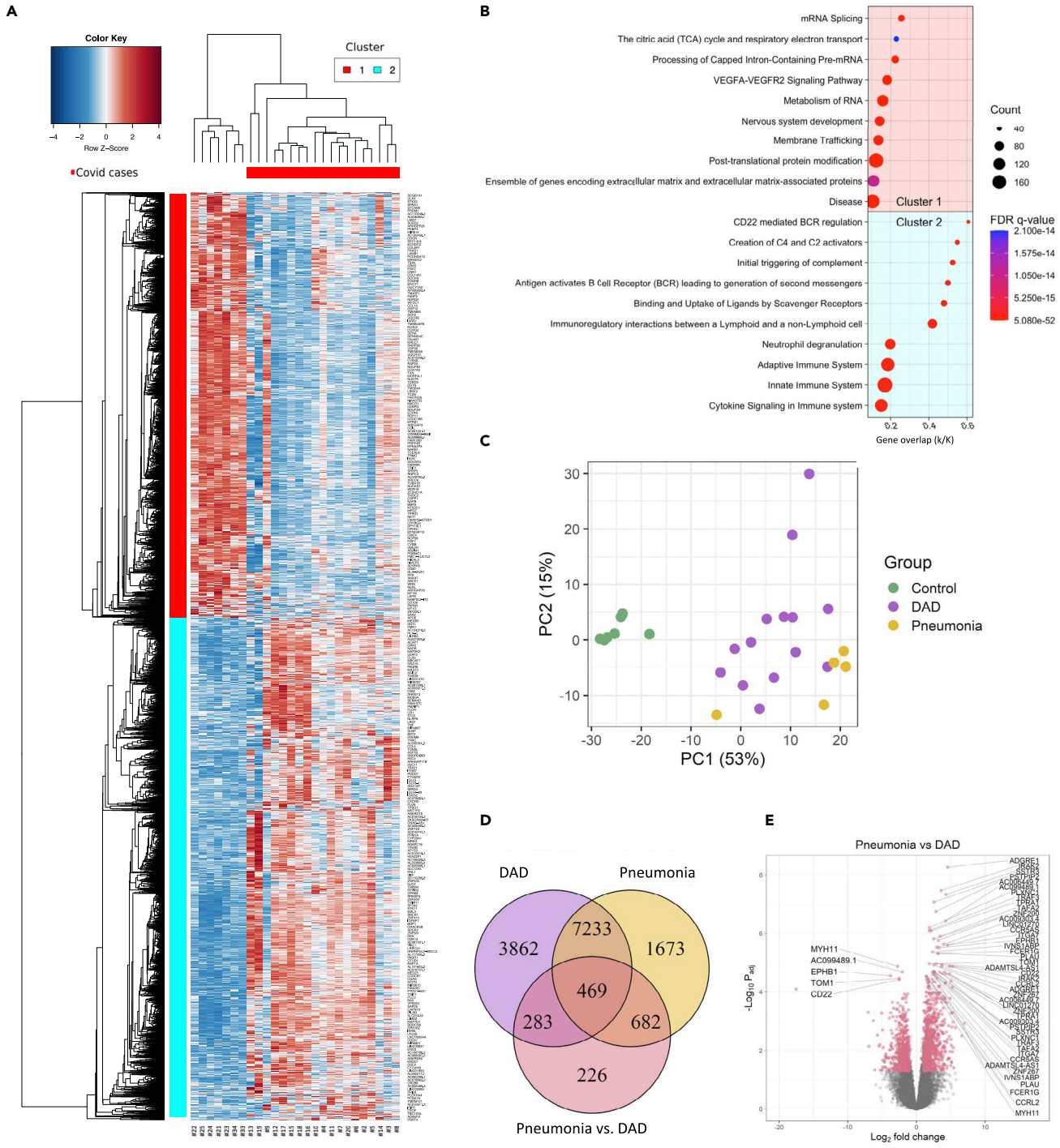

Figure 4. The lung metatranscriptome mirrors the major death categories DAD and pneumonia

(A) Hierarchical clustering shows depleted (cluster 1) and enriched (cluster 2) genes (n = 4,547; adj. P< 0.05) in lung tissue of covid-19 cases compared to controls.

(B) Gen set enrichment analysis (canonical pathways) of major depleted (top) and enriched (bottom) pathways in covid-19 lungs.

(C) PCA based on differentially expressed genes clearly discriminates DAD cases and cases with secondary pneumonia of covid-19 from controls.

(D) Venn diagram specifying differentially expressed genes in DAD as the major discriminator followed by pneumonia (adj. P< 0.05, LFC≥0.58).

(E) Volcano plot showing the top 25 significantly deregulated genes in secondary pneumonia versus DAD. Several macrophage genes are increased.

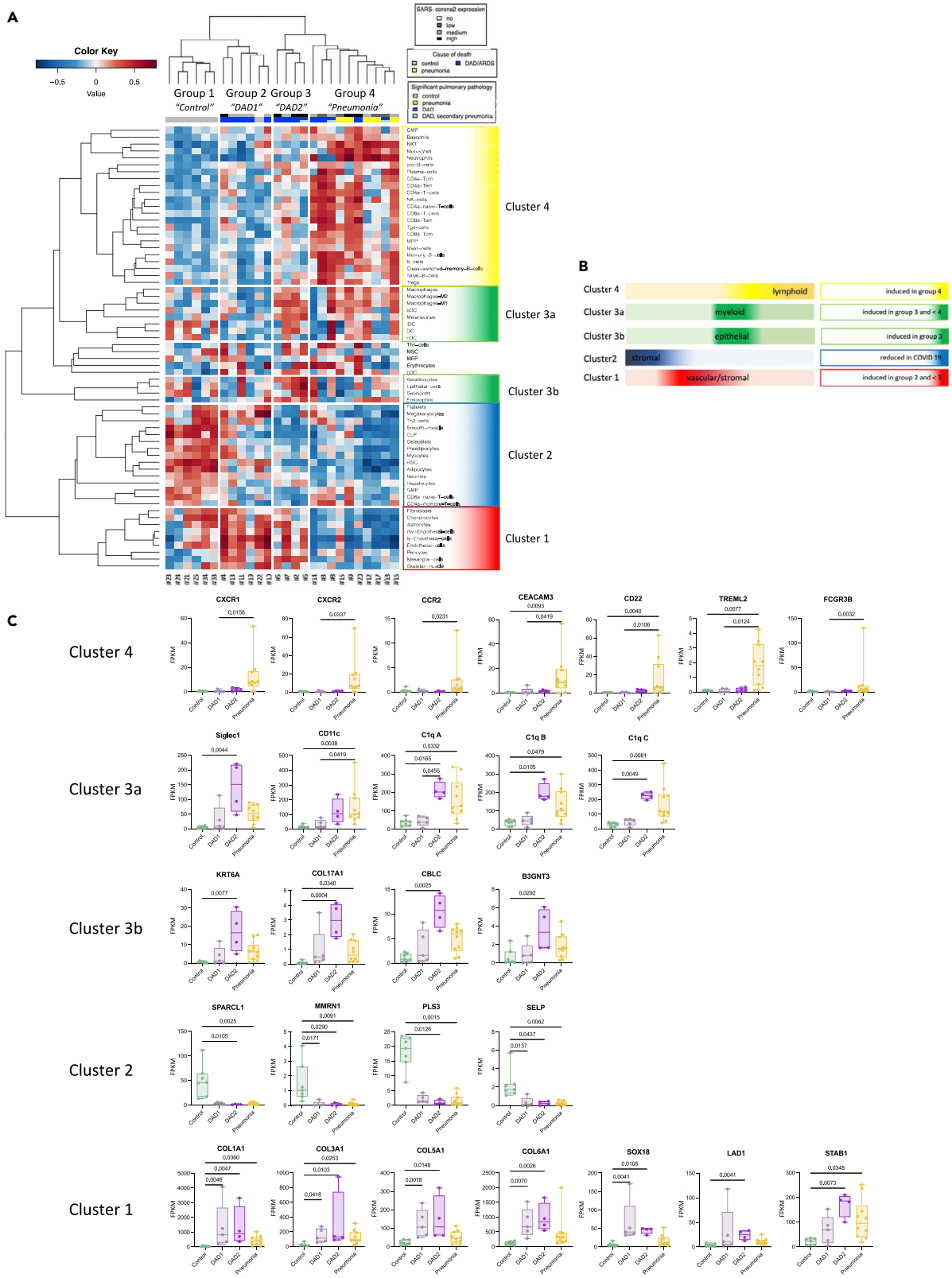
A
Color Key
−0.5
0
0.5
Value
Group 1
"Control"
Group 2
"DAD1"
Group 3
"DAD2"
Group 4
"Pneumonia"
SARS−corona2 expression
no
low
medium
high
Cause of death
control
pneumonia
DAD/ARDS
Significant pulmonary pathology
control
pneumonia
DAD
DAD, secondary pneumonia
Cluster 4
Cluster 3a
Cluster 3b
Cluster 2
Cluster 1
B
Cluster 4
lymphoid
induced in group 4
Cluster 3a
myeloid
induced in group 3 and < 4
Cluster 3b
epithelial
induced in group 3
Cluster2
stromal
reduced in COVID 19
Cluster 1
vascular/stromal
induced in group 2 and < 3
C
Cluster 4
CXCR1
CXCR2
CCR2
CEACAM3
CD22
TREML2
FCGR3B
Cluster 3a
Siglec1
CD11c
C1q A
C1q B
C1q C
Cluster 3b
KRT6A
COL17A1
CBLC
B3GNT3
Cluster 2
SPARCL1
MMRN1
PLS3
SELP
Cluster 1
COL1A1
COL3A1
COL5A1
COL6A1
SOX18
LAD1
STAB1
FPKM
Control
DAD1
DAD2
Pneumonia

Figure 5. Cellular deconvolution stratifies lung pathology sub-groups

(A) Hierarchical clustering based on cell-type enrichments derived from xCell analysis indicates a specific grouping of samples.

(B) Scheme indicating cell clusters which discriminate different groups.

(C) Top induced genes in the respective cell clusters determining the specific grouping (Kruskal-Wallis test).

Cluster 1 consisted mainly of vascular and stromal cell types like endothelial cells, pericytes and fibroblasts, enriched in "DAD1" and "DAD2". Top enriched genes in this cluster were certain collagen genes, the vascular transcription factor *sox 18*, the basement membrane protein *ladinin-1* or the endothelial protein *stabilin-1* (Figure 5C). Cell types of cluster 2 consisted mainly of structural and stromal cells, in addition to certain immune and blood cell types and they were overall reduced in covid-19. Top down-regulated genes included the extracellular matrix proteins *sparc-like 1*, *multimerin-1* and *plastin-3* or the cell adhesion molecule *p-selectin* important for the recruitment of leukocytes typically prevalent on activated endothelial cells and platelets (Figure 5C). Together these alterations highlight the vascular and connective tissue changes emerging during DAD development (Figure 2B) (Ackermann et al., 2020; Hughes and Beasley, 2017). Cell types of cluster 3, which were dominantly induced in "DAD2" and to a lesser extent in "pneumonia" showed enrichment of myeloid (cluster 3a) and epithelial cell types (cluster 3b). Top induced genes in cluster 3a were the myeloid cell specific genes *siglec-1*, *CD11c* and complement factor *C1q*. Top induced genes in cluster 3b consisted of keratin 6A, collagen XVII, the tyrosine kinase signaling protein *cbl-c* and beta-1,3-N-acetylglucosaminyltransferase 3 (*b3gnt3*), typically expressed in epithelia and also involved in lymphocyte trafficking and homing. Cell types in cluster 4, strongly increased in "pneumonia" consisted of different leukocyte classes including B-, T-cells and (neutrophilic) granulocytes. Top induced genes consisted of the interleukin 8 receptor genes *cxcr1* and *cxcr2*, the chemokine receptor type 2 (*CCR2*), *CEACAM3*, *CD22* (B cell marker), and the cell surface receptors *TREML2* and *FCGR3B*.

In summary, cellular deconvolution clearly sub-stratified the major categories DAD and pneumonia of covid-19 lung pathology. Noteworthy, DAD subclustered into two different groups, one showing mainly induction of vascular and stromal cell elements ("DAD1"), the other dominant induction of genes related to myeloid and epithelial cells ("DAD2"), and this subgroup showed more commonalities with the pneumonia group.

Macrophages complement c1q and immune impairment in covid-19 lungs

Myeloid cells including macrophages play a central role in the pathogenesis of DAD (Chen et al., 2020; Fan and Fan, 2018; Huang et al., 2018), and bronchalveolar lavage fluids (BALFs) of patients with severe covid-19 reveal high proportions of macrophages (Liao et al., 2020; Wang et al., 2020). We confirmed significantly increased macrophages in covid-19 lungs by CD163 immunohistochemistry, depicting a M2-type macrophage marker (Figure 6A), corroborating a recent proteomic study wherein CD163 was found among the most induced proteins in lungs and spleens derived from covid-19 autopsies (Nie et al., 2021). Deconvolution indicated both M1- and M2-type macrophages significantly enriched predominantly in "DAD2" whereas monocytes were mainly induced in the "pneumonia" group (Figure 6B). Increased CD163 positive macrophages gathering around virus positive cells were recently shown also in a macaque model of SARS-CoV infection, indicating that infected pneumocytes may lead to macrophage recruitment in coronavirus infections (Liu et al., 2019).

Among the most discriminative genes between DAD subtypes we found complement factor *C1q* dominantly induced in "DAD2" (Figure 5C). Complement activation is implicated in DAD pathogenesis and linked to severe covid-19 (Holter et al., 2020; Java et al., 2020; Perico et al., 2021). Other complement factors showed no discriminative expression pattern between pathological subgroups in our cohort, except certain complement receptors and properdin mainly induced in pneumonia cases (Figure 6C). C1q levels did not correlate with survival times of patients (Figure S12). Western blots generated from extracts of lungs confirmed significantly increased C1q protein (Figure 6D). A major source of C1q are macrophages corroborated also by a recent single-cell transcriptomic analysis of covid-19 lungs (Figure S13) (Lu et al., 2008; Xu et al., 2020) suggesting a strong connection between macrophages and complement C1q in covid-19 (Carvelli et al., 2020). Immunohistochemical analysis of lung tissues with a C1q specific antibody showed staining of the vasculature, the interstitial and alveolar space but also of alveolar cells including macrophages and pneumocytes, indicating a multifaceted deposition of C1q in the context of covid-19 in our series (Figure 6E).

C1q is the initiating component of the classical complement cascade but exhibits also immune regulatory functions. It induces the development of pro-resolving M2 type macrophages and is involved in the

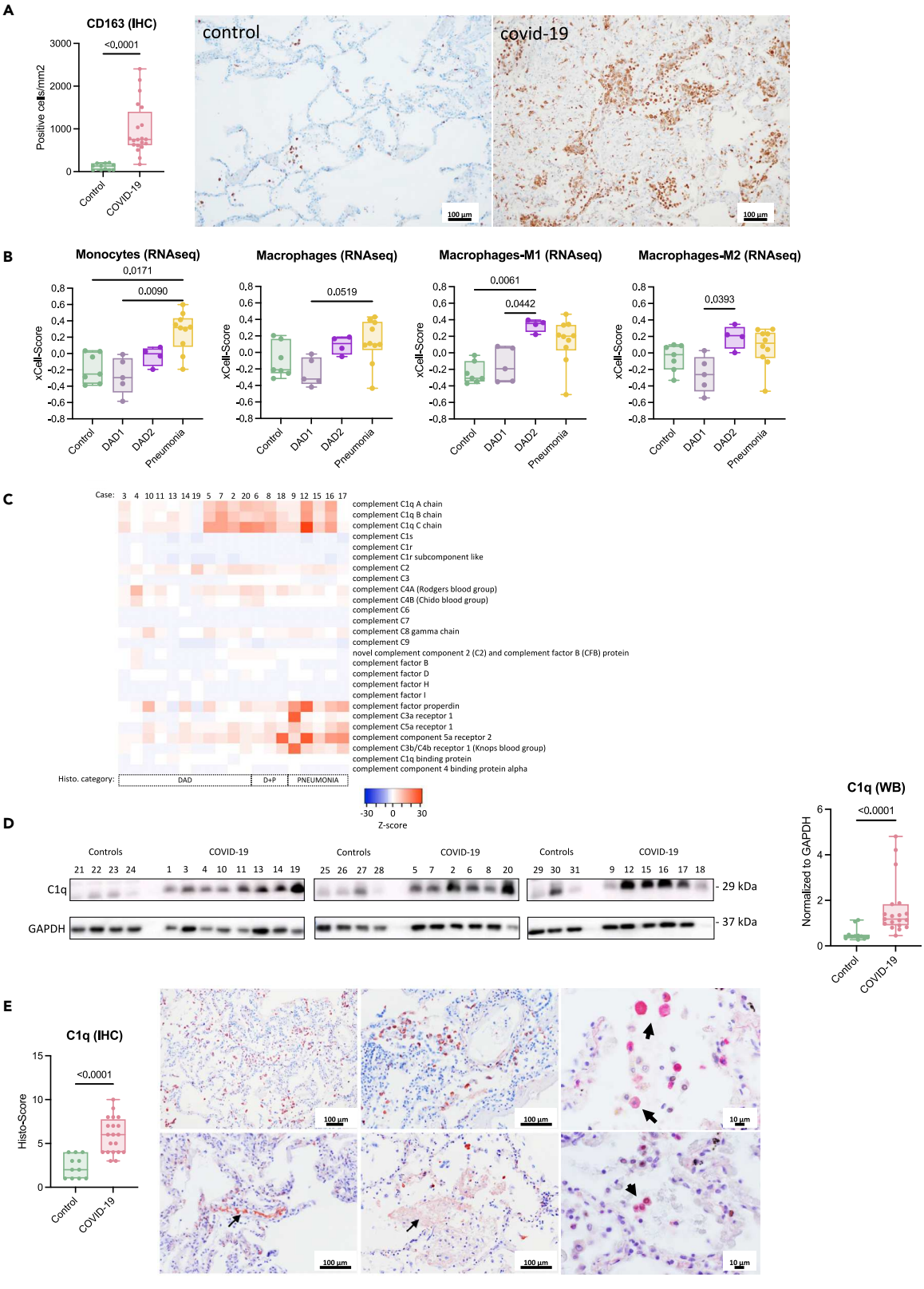
A
CD163 (IHC)
<0.0001
Positive cells/mm2
3000
2000
1000
0
Control
COVID-19
control
covid-19
100 µm
B
Monocytes (RNAseq)
0.0171
0.0090
Macrophages (RNAseq)
0.0519
Macrophages-M1 (RNAseq)
0.0061
0.0442
Macrophages-M2 (RNAseq)
0.0393
xCell-Score
Control
DAD1
DAD2
Pneumonia
C
Case: 3 4 10 11 13 14 19 5 7 2 20 6 8 18 9 12 15 16 17
complement C1q A chain
complement C1q B chain
complement C1q C chain
complement C1s
complement C1r
complement C1r subcomponent like
complement C2
complement C3
complement C4A (Rodgers blood group)
complement C4B (Chido blood group)
complement C6
complement C7
complement C8 gamma chain
complement C9
novel complement component 2 (C2) and complement factor B (CFB) protein
complement factor B
complement factor D
complement factor H
complement factor I
complement factor properdin
complement C3a receptor 1
complement C5a receptor 1
complement component 5a receptor 2
complement C3b/C4b receptor 1 (Knops blood group)
complement C1q binding protein
complement component 4 binding protein alpha
Histo. category:
DAD
D+P
PNEUMONIA
-30 0 30
Z-score
D
Controls
COVID-19
21 22 23 24 1 3 4 10 11 13 14 19 25 26 27 28 5 7 2 6 8 20 29 30 31 9 12 15 16 17 18
C1q
GAPDH
29 kDa
37 kDa
C1q (WB)
<0.0001
Normalized to GAPDH
E
C1q (IHC)
<0.0001
Histo-Score
100 µm
10 µm

Figure 6. Macrophage and complement C1q induction in covid-19 lungs

(A) Immunohistochemical counting of CD163 positive macrophages shows induction in covid-19 compared to controls (Mann-Whitney test).
(B) Both M1 and M2 macrophages are specifically increased in "DAD2" compared to "DAD1" (grouping according to xCell analysis; Kruskal-Wallis test).
(C) Heatmap of complement genes specifies C1q induction in a subgroup of DAD cases and in pneumonia.
(D) C1q protein (29 kDa) is significantly increased in covid-19 lung tissue compared to controls (reference human GAPDH; Mann-Whitney test).
(E) Significant induction of C1q detected by immunohistochemistry (Mann–Whitney test) and different staining patterns in covid-19 lungs; top left & middle: C1q staining of alveolar cells; top right: double immunohistochemistry staining (red: C1q, nuclear black: TTF-1) shows C1q staining of alveolar macrophages; bottom left: intravascular C1q staining; bottom middle: free C1q specific staining of proteinaceous fluid in the alveolar space; bottom right: double immunohistochemistry staining (red: C1q, nuclear black: TTF-1) shows C1q staining of pneumocytes (TTF-1 positive).

clearance of apoptotic and necrotic cells, which are highly increased in covid-19 lungs (Bohlson et al., 2014; Li et al., 2020b; Mulay et al., 2021). In this process C1q binds to cellular break-down products and is subsequently recognized by phagocyte receptors like the leukocyte-associated immunoglobulin-like receptor 1 (LAIR-1; syn.: CD305) conferring uptake and triggering a tolerogenic state in the phagocyte (Son et al., 2015; Thielens et al., 2017). As shown by a recent single-cell transcriptomics analysis of covid-19 lungs, *LAIR-1* is mainly present in macrophages (Figure S14) (Delorey et al., 2021). LAIR-1 together with LILRB4 (leukocyte immunoglobulin-like receptor subfamily B member 4; syn.: ILT3) belong to immunoglobulin-like receptors recognizing collagen domains such as present in C1q, thereby inhibiting immune activation (Lebbink et al., 2006; Son et al., 2012). RNA-seq confirmed significant induction of *LAIR-1* and *LILRB4* dominantly in "DAD2" followed by "pneumonia" (Figure 7A). Expressions of all 3 *C1q* polypeptide chains (*A, B, & C*) significantly correlated with *LAIR-1* and *LILRB4* expression but not with induced collagens (Figures 7B and S15). This might suggest a functional link between C1q and the immune inhibitory receptors LAIR-1 and LILRB4.

Because the development of secondary infections is likely driven by local immune-impairment we screened for other anti-inflammatory markers. TGF-β1 is a key factor in the development and healing response of ALI and also implicated in covid-19 lung pathology (Peters et al., 2014; Vaz dePaula et al., 2021). *TGF-β1* transcription was significantly increased in covid-19, showing a huge variability, however, TGF-β1 protein measured by immunohistochemistry and western blotting showed no significant induction compared to controls (Figures 7C and S16). Because several immune and non-immune cell types are able to produce TGF-β1, the observed variability in expression might reflect the temporal heterogeneity of lung pathologies in our cohort. Induction of certain inhibitory immune-checkpoints is reported in covid-19 (Bobcakova et al., 2021; Diao et al., 2020; Files et al., 2021; Jeannet et al., 2020; Li et al., 2020a). We confirmed transcriptional induction of several inhibitory immune-checkpoints in covid-19 lungs (*LAG3*, *PDCD1*, *ADORA2A*, *VSIR*, *CTLA4*, *SIRPA*, *LAIR1*, *SIGLEC9*, *LILRB4*, *SIGLEC7*, and *HAVCR2*), whereas some showed no induction (*CD276*, *SP140*, *IDO1*, *KLRG1*, and *CD274*) or were even reduced (*GGT1* and *CD80*) compared with controls (Figures 7D and S17). Of note, the top induced inhibitory immune-checkpoint was found to be *LAG3* (lymphocyte-activation gene 3; syn.: CD223), dominantly induced in "DAD2" and "pneumonia" based on RNA-seq, which was also confirmed by immunohistochemistry wherein mainly lymphocytes showed strong staining signals (Figures 7E and S18). LAG3 was recently described as a major increased factor in a plasma proteomic study of severe covid-19 (Filbin et al., 2021). During immune exhaustion multiple inhibitory receptors act often in synergy amplifying immune impairment, like LAG3 and PD-1 co-induced during chronic viral infections (Blackburn et al., 2009). We confirmed synergistic induction of several inhibitory immune-checkpoints in covid-19 lungs, which showed a different costimulatory pattern compared to controls (Figure 7F). Of interest, co-expression patterns discriminated cases with high viral loads (*KLRG1*, *CTLA4*, *SP140*, *CD274*, *IDO1*, *LAG3*, *PDCD1*, *HAVCR2*, and *CD80*) from samples with pneumonia (*CD276*, *TGFB1*, *ADORA2A*, *LILRB4*, *LAIR1*, *VSIR*, *SIRPA*, *SIGLEC7*, and *SIGLEC9*) suggesting a divergent pattern of induction of inhibitory immune-checkpoints during the course of covid-19 lung pathology (Figure 7G). In summary, these data highlight that multiple pillars of immune impairment act in severe covid-19, leading to a reduced antimicrobial defense in lungs driving the development of secondary infections. The molecular dissection of cell types and immune inhibitory signals might enable the development of specific measures counteracting this potentially lethal complication.

DISCUSSION

We performed a systematic autopsy study of 20 consecutive covid-19 cases and 14 controls to gain unbiased information about lethal disease courses from the early pandemic. Integration of autopsy, cultivation and deep sequencing provided important clues about host and microbial factors involved in the development of secondary infections as a major sequel of lethal covid-19. Thus, our study might serve

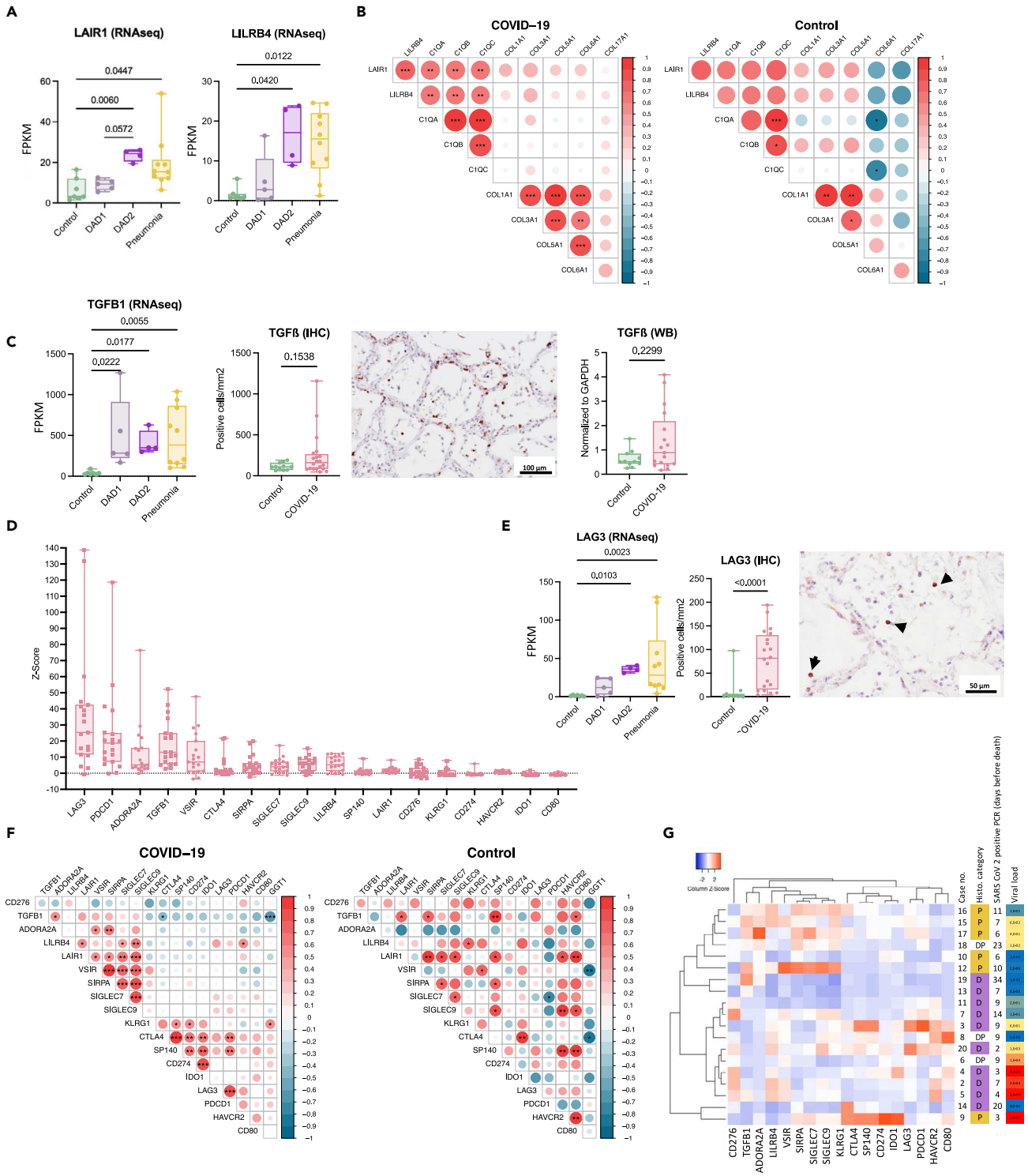

Figure 7. Signatures of immune-impairment in covid-19 lungs

(A) The tolerogenic leukocyte receptors *LAIR-1* and *LILRB4* are mainly induced in "DAD2" and "pneumonia" (Kruskal–Wallis test).

(B) Spearman correlation of RNA expression of *LAIR-1* and *LILRB4* with *C1q* chains and induced collagen types (Spearman r; p*<0.05 to p***<0.001).

(C) Significant induction of *TGFβ1* transcription (Kruskal-Wallis test). Protein measurement by immunohistochemistry and western blotting does not reveal a significant difference of covid-19 lungs to controls (Mann-Whitney test).

(D) Strong induction of immune checkpoint inhibitors in covid-19 (order according to z-score).

Figure 7. *Continued*

(E) *LAG3* transcriptional induction (Kruskal-Wallis test) and increased lymphocyte staining with LAG3 immunohistochemistry in covid-19 lung tissue (Mann-Whitney test).

(F) Simultaneous transcriptional induction of immune checkpoint inhibitors in covid-19 lungs compared to controls (Pearson correlation; p*<0.05, p***<0.001).

(G) Hierarchical clustering of immune checkpoint inhibitors in covid-19 cases shows a different grouping of samples with high viral loads (transcript abundance) versus samples with the histological pneumonia category (clustering: average linkage; distance measure: Pearson).

as a blue-print for a "holistic" autopsy approach tempting to gain relevant pathophysiological insights from a newly emerging disease (Layne et al., 2022). Viral genotyping facilitated directly from autopsy material provided epidemiologic clues about transmission and captured already early events of viral genetic adaptation. Of note, a significant proportion of corpses yielded cultivable SARS-CoV-2 indicating that autopsy might facilitate virus spread and that special safety requirements should be applied during post-mortem examinations of covid-19 patients (Loibner et al., 2021). Our investigation showed that covid-19 lung pathology is multifaceted and that a major discriminator of lethal courses is DAD and the presence of secondary infections. This was evident by histology but also mirrored by the deep transcriptomic analysis and microbiology. Secondary infections are reported to develop in up to 42% of patients with covid-19 (Buehler et al., 2021). Notably, DAD caused by the virus itself and secondary infections are chronologically divergent and provoke overtly different host reactions. It is also noteworthy that SARS-CoV-2 infection alone might not trigger prominent neutrophil recruitment to the lung at all and neutrophil signatures found in recent covid-19 studies might likely already indicate secondary infections (Liao et al., 2020; Melms et al., 2021; Nie et al., 2021; Wauters et al., 2021; Xu et al., 2020). Thus, it is important to seek for a proper pre-classification of tissue samples based on histology to omit wrong conclusions in molecular down-stream analyses.

The resident lung microbiome is a relevant factor in the pathogenesis of lung infections and reported to be altered in sepsis and DAD (Dickson et al., 2016; Luyt et al., 2020). Secondary lung infections are also complicating influenza, SARS and MERS, wherein bacteria like *S. aureus* or *Klebsiella* spp. and fungi such as *Candida* or *Aspergillus* spp. are found (Klein et al., 2016; Morens et al., 2008). Such microbial agents were also present in our cohort. Curiously, the mechanistic understanding why secondary infections develop on top of viral infections is still limited. We could not identify any associated clinical parameter clearly correlated with secondary infections but showed that lung immunity is impaired in covid-19, which might drive these infections. This finding was also underscored by the presence of polymicrobial infections and EBV indicative for a general decreased immunity (Tangye et al., 2017). Typical comorbidities of covid-19, like chronic kidney disease or diabetes, are already signified by a lowered immunity increasing the infection risk (Carey et al., 2018; Syed-Ahmed and Narayanan, 2019). Moreover, ICU admission and mechanical ventilation are established risk factors for the development of pneumonias (Wu et al., 2019). Thus, secondary lung infections in covid-19 could originate from different sources including direct immune challenge by SARS-CoV-2, the underlying condition and medical interventions (Callender et al., 2020). Curiously, the majority of our patients received antibiotics, which failed to effectively protect against secondary infections. This circumstance might have been influenced by underdeveloped antibiotic regimens or ineffective substances (e.g., chloroquine; (Axfors et al., 2021)) given during the early pandemic but also from concomitant therapeutic immunosuppression (e.g., corticosteroids) altogether modulating the infection risk on an individual base. Notably, ICU admission and intubation, however, were generally associated with lower neutrophil scores. Because all intubated patients received antibiotics in our series, this therapy might have delayed secondary pneumonia development.

Severe cases of covid-19 typically present with high inflammatory markers complicating the distinction between severe courses with pure DAD or bacterial or fungal secondary infections. As in our cohort, hospitalized covid-19 patients are empirically treated with broad-spectrum antibiotics but efficacy of this therapy is still debated (Sieswerda et al., 2021). Because patients frequently need prolonged hospitalizations and respiratory support, unnecessary antibiotic therapy also likely increases the risk of hospital-acquired pneumonias caused by resistant bacteria. On a population level increased antibiotic usage likely leads to rising antimicrobial resistance further complicating management of the pandemic (Chong et al., 2021; Sopirala, 2021). Noteworthy, antibiotic challenge of the resident lung microbiome might also impact secondary infection development. In analogy to the GI tract wherein depletion of the resident microbiome potentially provokes overgrowth of pathogens (e.g., in *C. difficile* colitis; (Chang et al., 2008)), similar mechanisms might happen in the respiratory tract. Notably, we detected a significant reduced biodiversity in

lungs of our covid-19 patients which was likely influenced by antibiotics. Single reports indicate a rise of secondary infections in the second pandemic wave compared to the initial phase indicating a fluctuating picture of secondary infections (Fortarezza et al., 2022; Hedberg et al., 2022). This development might have been influenced by several factors including a changed epidemiology of patients (different comorbidities and ages), seasonal effects, which seem to be particularly important for the development of fungal pneumonias but also changes in clinical practice (Ayzac et al., 2016; Group et al., 2021).

Immune exhaustion seems to follow the systemic immune hyperactivation in severe covid-19 and myeloid cells, which are important for the recognition of virus infected cells, are key to initiate the proinflammatory response (McGonagle et al., 2020; Merad and Martin, 2020). Recent single-cell transcriptomic studies of covid-19 patients identified myeloid cells as a major induced cell type in BALF specimens with high proportions of proinflammatory macrophages (Liao et al., 2020; Melms et al., 2021). Generally, M1-type macrophages dominate early DAD, whereas later DAD stages show increased M2-types involved in tissue repair with immunosuppressive features (Huang et al., 2018). Thus, later (organizing) phases of DAD might be specifically prone to acquire secondary infections. Respiratory failure in covid-19 is linked to strong complement activation (Holter et al., 2020; Java et al., 2020; Messner et al., 2020), which likely occurs when the disease progresses (Nienhold et al., 2020). Extensive deposition of complement factors, including C1q, in vessels and epithelial cells of lungs and skin was reported in covid-19 (Macor et al., 2021; Magro et al., 2020). Notably, the SARS-CoV-2 spike-protein might directly activate complement via the alternative pathway (Yu et al., 2020). Complement in covid-19 is currently discussed mainly in the context of endothelial injury and fibrin-clot formation (Perico et al., 2021). Our study suggests another pathophysiological role, wherein C1q and macrophages might perpetuate immune impairment. Immune complexes formed by viral antigens and antibodies can activate factor C1 as shown in SARS-CoV infection (Yang et al., 2005). C1q is involved in the clearance of apoptotic and necrotic cells by phagocytes, a process termed efferocytosis (Doran et al., 2020). Apoptosis and necrosis are prominent in covid-19 lungs (Filbin et al., 2021; Li et al., 2020b; Mulay et al., 2021). During efferocytosis suppression of overwhelming inflammation is important and phagocytes involved in this process are producing anti-inflammatory cytokines. Therefore, C1q binds to molecules released from apoptotic and necrotic cells (e.g., phosphatidylserine, nucleic acids, etc.) and these complexes are recognized by receptors present on phagocytes, like LAIR-1, conferring uptake and inducing a tolerogenic state (Bohlson et al., 2014; Lu et al., 2008; Son et al., 2015; Thielens et al., 2017). Noteworthy, binding of C1q to LAIR-1 on plasmacytoid DCs restricts the production of type I interferons impairing antiviral defense, which also occurs in covid-19 (Son et al., 2012, 2015). The "DAD2" subtype in our study shows increased macrophages, C1q and LAIR-1 and might therefore represent cases with a lowered immune tone prone for the development of secondary infections. Overall the progression of early (exudative) DAD into late (fibrotic) DAD indicates healing of ALI characterized by significant connective tissue remodeling and a reduced inflammatory tone (Margaroli et al., 2021; Matthay et al., 2019). Immune suppressive factors such as TGF-β1 are known to be involved in this process and also LAIR-1 and LILRB4 recognizing collagens or collagen-like proteins might act anti-inflammatory during this disease phase (Fernandez and Eickelberg, 2012; Fouet et al., 2021; Paavola et al., 2021; Son et al., 2012; Tomic et al., 2021). Moreover, the synergistic induction of several tolerogenic factors including inhibitory immune-checkpoints (Bobcakova et al., 2021; Diao et al., 2020; Filbin et al., 2021; Files et al., 2021; Hadjadj et al., 2020; Jeannet et al., 2020; Li et al., 2020a) and increased (apoptotic) cell death of immune-cells (Cizmecioglu et al., 2021; Feng et al., 2020) altogether perpetuate immune failure in covid-19.

Limitations of the study

The limitations of our descriptive study are that causalities cannot be directly inferred and that the relatively small cohort cannot reveal the entire picture of severe covid-19 and associated secondary infections. Varying clinical courses and different comorbidities might also have influenced our findings. In addition, treatment of covid-19 has changed since the early pandemic, thus, current severe courses and developing sequels might also have changed. We also cannot be sure whether the two described forms of DAD might represent just a spectrum of pathophysiological states or are specific pathotypes. Moreover, post-mortem effects like RNA degradation might have introduced additional noise in our investigation. Nevertheless, we found autopsy complemented with microbiology and molecular measures as a powerful tool to gain relevant clues about covid-19 pathophysiology. Of importance, there exists an obvious knowledge gap in the understanding of the molecular mechanisms driving the development of secondary infections on top of in viral lung diseases. This should initiate further studies to understand the molecular pathways in more detail and to unravel chronological phases of immuno-suppression which could also lead to development of

rational therapies counteracting this sequel not only in covid-19. For these investigations, autopsy specimens and associated molecular data might serve as a valuable resource.

STAR★METHODS

Detailed methods are provided in the online version of this paper and include the following:

- KEY RESOURCES TABLE
- RESOURCE AVAILABILITY
  - Lead contact
  - Materials availability
  - Data and code availability
- EXPERIMENTAL MODEL AND SUBJECT DETAILS
- METHOD DETAILS
  - Autopsy procedure & specimen collection
  - Histopathology and immunohistochemistry
  - Scoring of histological lung features
  - Microbial culture and identification
  - Virus isolation
  - RNA extraction
  - SARS-CoV-2 quantitative RT-PCR
  - Viral genome sequencing
  - RNA sequencing
  - RNA profiling
  - Single cell transcriptomic metanalysis
  - Microbiome analysis based on RNAseq
  - Microbiome analysis based on the 16S rRNA gene and internal transcribed spacers (ITS)
  - Protein isolation and western blot
- QUANTIFICATION AND STATISTICAL ANALYSIS

SUPPLEMENTAL INFORMATION

Supplemental information can be found online at https://doi.org/10.1016/j.isci.2022.104926.

ACKNOWLEDGMENTS

We are grateful to Tanja V. Mascher, Birgit Gangl, Margit Gogg-Kamerer, Iris Kufferath, Sylvia Eidenhammer, Christine Langner, Stella Wolfgruber, Daniela Pabst, Iris Kreuzmann, Helmut Donnerer, and Lajos Redecsi for their technical assistance and support from the Medical University of Graz, the Austrian Science Fund (FWF, DK-MOLIN W1241) and the European Union's Horizon 2020 Research & Innovation Program (ERINHA-Advance project, grant agreement no. 824061).

AUTHOR CONTRIBUTIONS

Conceptualization and methodology, M.Z., G.G., K.K., P.R., and K.Z. Investigation and formal analysis, M.Z., K.K., P.W., P.R., M.S., M.N., S.E., L.M-M., G.K., M.L., A.B., E.L., A.T., E.W., S.S., M-J.P., F-R.V., C.L., B.J., L.O., and G.G. Resources, K.Z., P.R., G.G., B.T., and H.L. Writing of original draft G.G. Writing, review and editing, all authors. Funding acquisition, K.Z., G.G., and H.L. Supervision, G.G., P.R., and K.Z. All authors have read and agreed to the published version of the manuscript.

DECLARATION OF INTERESTS

H.L. is founder of Alacris Theranostics GmbH and M.S. and L.O. are employees of Alacris Theranostics GmbH. K. Z. is CEO and founder of Zatloukal Innovations GmbH. All other authors declare no conflicts of interest.

Received: February 24, 2022
Revised: July 12, 2022
Accepted: August 9, 2022
Published: September 16, 2022

REFERENCES

Ackermann, M., Verleden, S.E., Kuehnel, M., Haverich, A., Welte, T., Laenger, F., Vanstapel, A., Werlein, C., Stark, H., Tzankov, A., et al. (2020). Pulmonary vascular endothelialitis, thrombosis, and angiogenesis in covid-19. N. Engl. J. Med. *383*, 120–128. https://doi.org/10.1056/NEJMoa2015432.

Anders, S., Pyl, P.T., and Huber, W. (2015). HTSeq–a Python framework to work with high-throughput sequencing data. Bioinformatics *31*, 166–169. https://doi.org/10.1093/bioinformatics/btu638.

Aran, D., Hu, Z., and Butte, A.J. (2017). xCell: digitally portraying the tissue cellular heterogeneity landscape. Genome Biol. *18*, 220. https://doi.org/10.1186/s13059-017-1349-1.

Axfors, C., Schmitt, A.M., Janiaud, P., Van't Hooft, J., Abd-Elsalam, S., Abdo, E.F., Abella, B.S., Akram, J., Amaravadi, R.K., Angus, D.C., et al. (2021). Mortality outcomes with hydroxychloroquine and chloroquine in COVID-19 from an international collaborative meta-analysis of randomized trials. Nat. Commun. *12*, 2349. https://doi.org/10.1038/s41467-021-22446-z.

Ayzac, L., Girard, R., Baboi, L., Beuret, P., Rabilloud, M., Richard, J.C., and Guérin, C. (2016). Ventilator-associated pneumonia in ARDS patients: the impact of prone positioning. A secondary analysis of the PROSEVA trial. Intensive Care Med. *42*, 871–878. https://doi.org/10.1007/s00134-015-4167-5.

Blackburn, S.D., Shin, H., Haining, W.N., Zou, T., Workman, C.J., Polley, A., Betts, M.R., Freeman, G.J., Vignali, D.A.A., and Wherry, E.J. (2009). Coregulation of CD8+ T cell exhaustion by multiple inhibitory receptors during chronic viral infection. Nat. Immunol. *10*, 29–37. https://doi.org/10.1038/ni.1679.

Blanco-Melo, D., Nilsson-Payant, B.E., Liu, W.C., Uhl, S., Hoagland, D., Møller, R., Jordan, T.X., Oishi, K., Panis, M., Sachs, D., et al. (2020). Imbalanced host response to SARS-CoV-2 drives development of COVID-19. Cell *181*, 1036–1045.e9. https://doi.org/10.1016/j.cell.2020.04.026.

Bobcakova, A., Petriskova, J., Vysehradsky, R., Kocan, I., Kapustova, L., Barnova, M., Diamant, Z., and Jesenak, M. (2021). Immune profile in patients with COVID-19: lymphocytes exhaustion markers in relationship to clinical outcome. Front. Cell. Infect. Microbiol. *11*, 646688. https://doi.org/10.3389/fcimb.2021.646688.

Bohlson, S.S., O'Conner, S.D., Hulsebus, H.J., Ho, M.M., and Fraser, D.A. (2014). Complement, c1q, and c1q-related molecules regulate macrophage polarization. Front. Immunol. *5*, 402. https://doi.org/10.3389/fimmu.2014.00402.

Bolyen, E., Rideout, J.R., Dillon, M.R., Bokulich, N.A., Abnet, C.C., Al-Ghalith, G.A., Alexander, H., Alm, E.J., Arumugam, M., Asnicar, F., et al. (2019). Reproducible, interactive, scalable and extensible microbiome data science using QIIME 2. Nat. Biotechnol. *37*, 852–857. https://doi.org/10.1038/s41587-019-0209-9.

Borczuk, A.C., Salvatore, S.P., Seshan, S.V., Patel, S.S., Bussel, J.B., Mostyka, M., Elsoukkary, S., He, B., Del Vecchio, C., Fortarezza, F., et al. (2020). COVID-19 pulmonary pathology: a multi-institutional autopsy cohort from Italy and New York City. Mod. Pathol. *33*, 2156–2168. https://doi.org/10.1038/s41379-020-00661-1.

Buehler, P.K., Zinkernagel, A.S., Hofmaenner, D.A., Wendel Garcia, P.D., Acevedo, C.T., Gómez-Mejia, A., Mairpady Shambat, S., Andreoni, F., Maibach, M.A., Bartussek, J., et al. (2021). Bacterial pulmonary superinfections are associated with longer duration of ventilation in critically ill COVID-19 patients. Cell Rep. Med. *2*, 100229. https://doi.org/10.1016/j.xcrm.2021.100229.

Callahan, B.J., McMurdie, P.J., Rosen, M.J., Han, A.W., Johnson, A.J.A., and Holmes, S.P. (2016). DADA2: high-resolution sample inference from Illumina amplicon data. Nat. Methods *13*, 581–583. https://doi.org/10.1038/nmeth.3869.

Callender, L.A., Curran, M., Bates, S.M., Mairesse, M., Weigandt, J., and Betts, C.J. (2020). The impact of pre-existing comorbidities and therapeutic interventions on COVID-19. Front. Immunol. *11*, 1991. https://doi.org/10.3389/fimmu.2020.01991.

Carey, I.M., Critchley, J.A., DeWilde, S., Harris, T., Hosking, F.J., and Cook, D.G. (2018). Risk of infection in type 1 and type 2 diabetes compared with the general population: a matched cohort study. Diabetes Care *41*, 513–521. https://doi.org/10.2337/dc17-2131.

Carvelli, J., Demaria, O., Vély, F., Batista, L., Chouaki Benmansour, N., Fares, J., Carpentier, S., Thibult, M.L., Morel, A., Remark, R., et al. (2020). Association of COVID-19 inflammation with activation of the C5a-C5aR1 axis. Nature *588*, 146–150. https://doi.org/10.1038/s41586-020-2600-6.

Castro, C.Y. (2006). ARDS and diffuse alveolar damage: a pathologist's perspective. Semin. Thorac. Cardiovasc. Surg. *18*, 13–19. https://doi.org/10.1053/j.semtcvs.2006.02.001.

Chang, J.Y., Antonopoulos, D.A., Kalra, A., Tonelli, A., Khalife, W.T., Schmidt, T.M., and Young, V.B. (2008). Decreased diversity of the fecal Microbiome in recurrent Clostridium difficile-associated diarrhea. J. Infect. Dis. *197*, 435–438. https://doi.org/10.1086/525047.

Chen, X., Tang, J., Shuai, W., Meng, J., Feng, J., and Han, Z. (2020). Macrophage polarization and its role in the pathogenesis of acute lung injury/acute respiratory distress syndrome. Inflamm. Res. *69*, 883–895. https://doi.org/10.1007/s00011-020-01378-2.

Chong, W.H., Saha, B.K., Ananthakrishnan, R., and Chopra, A. (2021). State-of-the-art review of secondary pulmonary infections in patients with COVID-19 pneumonia. Infection *49*, 591–605. https://doi.org/10.1007/s15010-021-01602-z.

Cizmecioglu, A., Akay Cizmecioglu, H., Goktepe, M.H., Emsen, A., Korkmaz, C., Esenkaya Tasbent, F., Colkesen, F., and Artac, H. (2021). Apoptosis-induced T-cell lymphopenia is related to COVID-19 severity. J. Med. Virol. *93*, 2867–2874. https://doi.org/10.1002/jmv.26742.

Corman, V.M., Landt, O., Kaiser, M., Molenkamp, R., Meijer, A., Chu, D.K., Bleicker, T., Brünink, S., Schneider, J., Schmidt, M.L., et al. (2020). Detection of 2019 novel coronavirus (2019-nCoV) by real-time RT-PCR. Euro Surveill. *25*. https://doi.org/10.2807/1560-7917.ES.2020.25.3.2000045.

Danecek, P., Bonfield, J.K., Liddle, J., Marshall, J., Ohan, V., Pollard, M.O., Whitwham, A., Keane, T., McCarthy, S.A., Davies, R.M., and Li, H. (2021). Twelve years of SAMtools and BCFtools. GigaScience *10*, giab008. https://doi.org/10.1093/gigascience/giab008.

Delorey, T.M., Ziegler, C.G.K., Heimberg, G., Normand, R., Yang, Y., Segerstolpe, Å., Abbondanza, D., Fleming, S.J., Subramanian, A., Montoro, D.T., et al. (2021). COVID-19 tissue atlases reveal SARS-CoV-2 pathology and cellular targets. Nature *595*, 107–113. https://doi.org/10.1038/s41586-021-03570-8.

Diao, B., Wang, C., Tan, Y., Chen, X., Liu, Y., Ning, L., Chen, L., Li, M., Liu, Y., Wang, G., et al. (2020). Reduction and functional exhaustion of T cells in patients with coronavirus disease 2019 (COVID-19). Front. Immunol. *11*, 827. https://doi.org/10.3389/fimmu.2020.00827.

Dickson, R.P., Singer, B.H., Newstead, M.W., Falkowski, N.R., Erb-Downward, J.R., Standiford, T.J., and Huffnagle, G.B. (2016). Enrichment of the lung microbiome with gut bacteria in sepsis and the acute respiratory distress syndrome. Nat. Microbiol. *1*, 16113. https://doi.org/10.1038/nmicrobiol.2016.113.

Dobin, A., Davis, C.A., Schlesinger, F., Drenkow, J., Zaleski, C., Jha, S., Batut, P., Chaisson, M., and Gingeras, T.R. (2013). STAR: ultrafast universal RNA-seq aligner. Bioinformatics *29*, 15–21. https://doi.org/10.1093/bioinformatics/bts635.

Doran, A.C., Yurdagul, A., Jr., and Tabas, I. (2020). Efferocytosis in health and disease. Nat. Rev. Immunol. *20*, 254–267. https://doi.org/10.1038/s41577-019-0240-6.

Fan, E.K.Y., and Fan, J. (2018). Regulation of alveolar macrophage death in acute lung inflammation. Respir. Res. *19*, 50. https://doi.org/10.1186/s12931-018-0756-5.

Feng, Z., Diao, B., Wang, R., Wang, G., Wang, C., Tan, Y., Liu, L., Wang, C., Liu, Y., Liu, Y., et al. (2020). The novel severe acute respiratory syndrome coronavirus 2 (SARS-CoV-2) directly decimates human spleens and lymph nodes. Preprint at medRxiv. https://doi.org/10.1101/2020.03.27.20045427.

Fernandez, I.E., and Eickelberg, O. (2012). The impact of TGF-beta on lung fibrosis: from targeting to biomarkers. Proc. Am. Thorac. Soc. *9*, 111–116. https://doi.org/10.1513/pats.201203-023AW.

Filbin, M.R., Mehta, A., Schneider, A.M., Kays, K.R., Guess, J.R., Gentili, M., Fenyves, B.G., Charland, N.C., Gonye, A.L.K., Gushterova, I., et al. (2021). Longitudinal proteomic analysis of severe COVID-19 reveals survival-associated signatures, tissue-specific cell death, and cell-cell interactions. Cell Rep. Med. *2*, 100287. https://doi.org/10.1016/j.xcrm.2021.100287.

Files, J.K., Boppana, S., Perez, M.D., Sarkar, S., Lowman, K.E., Qin, K., Sterrett, S., Carlin, E., Bansal, A., Sabbaj, S., et al. (2021). Sustained

cellular immune dysregulation in individuals recovering from SARS-CoV-2 infection. J. Clin. Invest. *131*, 140491. https://doi.org/10.1172/JCI140491.

Fortarezza, F., Pezzuto, F., Hofman, P., Kern, I., Panizo, A., von der Thüsen, J., Timofeev, S., Gorkiewicz, G., Berezowska, S., de Leval, L., et al. (2022). COVID-19 pulmonary pathology: the experience of European pulmonary pathologists throughout the first two waves of the pandemic. Diagnostics *12*, 95. https://doi.org/10.3390/diagnostics12010095.

Fouët, G., Bally, I., Chouquet, A., Reiser, J.B., Thielens, N.M., Gaboriaud, C., and Rossi, V. (2021). Molecular basis of complement C1q collagen-like region interaction with the immunoglobulin-like receptor LAIR-1. Int. J. Mol. Sci. *22*, 5125. https://doi.org/10.3390/ijms22105125.

Gorkiewicz, G., Feierl, G., Schober, C., Dieber, F., Köfer, J., Zechner, R., and Zechner, E.L. (2003). Species-specific identification of campylobacters by partial 16S rRNA gene sequencing. J. Clin. Microbiol. *41*, 2537–2546. https://doi.org/10.1128/JCM.41.6.2537-2546.2003.

Group, R.C., Horby, P., Lim, W.S., Emberson, J.R., Mafham, M., Bell, J.L., Linsell, L., Staplin, N., Brightling, C., Ustianowski, A., et al. (2021). Dexamethasone in hospitalized patients with covid-19. N. Engl. J. Med. Overseas. Ed. *384*, 693–704. https://doi.org/10.1056/NEJMoa2021436.

Hadfield, J., Megill, C., Bell, S.M., Huddleston, J., Potter, B., Callender, C., Sagulenko, P., Bedford, T., and Neher, R.A. (2018). Nextstrain: real-time tracking of pathogen evolution. Bioinformatics *34*, 4121–4123. https://doi.org/10.1093/bioinformatics/bty407.

Hadjadj, J., Yatim, N., Barnabei, L., Corneau, A., Boussier, J., Smith, N., Péré, H., Charbit, B., Bondet, V., Chenevier-Gobeaux, C., et al. (2020). Impaired type I interferon activity and inflammatory responses in severe COVID-19 patients. Science *369*, 718–724. https://doi.org/10.1126/science.abc6027.

Halwachs, B., Madhusudhan, N., Krause, R., Nilsson, R.H., Moissl-Eichinger, C., Högenauer, C., Thallinger, G.G., and Gorkiewicz, G. (2017). Critical issues in mycobiota analysis. Front. Microbiol. *8*, 180. https://doi.org/10.3389/fmicb.2017.00180.

Hedberg, P., Ternhag, A., Giske, C.G., Strålin, K., Özenci, V., Johansson, N., Spindler, C., Hedlund, J., Mårtensson, J., and Nauclér, P. (2022). Ventilator-associated lower respiratory tract bacterial infections in COVID-19 compared with non-COVID-19 patients. Crit. Care Med. *50*, 825–836. https://doi.org/10.1097/CCM.0000000000005462.

Holter, J.C., Pischke, S.E., de Boer, E., Lind, A., Jenum, S., Holten, A.R., Tonby, K., Barratt-Due, A., Sokolova, M., Schjalm, C., et al. (2020). Systemic complement activation is associated with respiratory failure in COVID-19 hospitalized patients. Proc. Natl. Acad. Sci. USA *117*, 25018–25025. https://doi.org/10.1073/pnas.2010540117.

Hou, Y.J., Chiba, S., Halfmann, P., Ehre, C., Kuroda, M., Dinnon, K.H., 3rd, Leist, S.R., Schäfer, A., Nakajima, N., Takahashi, K., et al. (2020a). SARS-CoV-2 D614G variant exhibits efficient replication ex vivo and transmission in vivo. Science *370*, 1464–1468. https://doi.org/10.1126/science.abe8499.

Hou, Y.J., Okuda, K., Edwards, C.E., Martinez, D.R., Asakura, T., Dinnon, K.H., 3rd, Kato, T., Lee, R.E., Yount, B.L., Mascenik, T.M., et al. (2020b). SARS-CoV-2 Reverse genetics reveals a variable infection gradient in the respiratory tract. Cell *182*, 429–446.e14. https://doi.org/10.1016/j.cell.2020.05.042.

Huang, X., Xiu, H., Zhang, S., and Zhang, G. (2018). The role of macrophages in the pathogenesis of ALI/ARDS. Mediators Inflamm. *2018*, 1264913. https://doi.org/10.1155/2018/1264913.

Huffnagle, G.B., Dickson, R.P., and Lukacs, N.W. (2017). The respiratory tract microbiome and lung inflammation: a two-way street. Mucosal Immunol. *10*, 299–306. https://doi.org/10.1038/mi.2016.108.

Hughes, K.T., and Beasley, M.B. (2017). Pulmonary manifestations of acute lung injury: more than just diffuse alveolar damage. Arch. Pathol. Lab Med. *141*, 916–922. https://doi.org/10.5858/arpa.2016-0342-RA.

Ishak, K., Baptista, A., Bianchi, L., Callea, F., De Groote, J., Gudat, F., Denk, H., Desmet, V., Korb, G., MacSween, R.N., et al. (1995). Histological grading and staging of chronic hepatitis. J. Hepatol. *22*, 696–699. https://doi.org/10.1016/0168-8278(95)80226-6.

Java, A., Apicelli, A.J., Liszewski, M.K., Coler-Reilly, A., Atkinson, J.P., Kim, A.H., and Kulkarni, H.S. (2020). The complement system in COVID-19: friend and foe? JCI Insight *5*, 140711. https://doi.org/10.1172/jci.insight.140711.

Jeannet, R., Daix, T., Formento, R., Feuillard, J., and François, B. (2020). Severe COVID-19 is associated with deep and sustained multifaceted cellular immunosuppression. Intensive Care Med. *46*, 1769–1771. https://doi.org/10.1007/s00134-020-06127-x.

Klein, E.Y., Monteforte, B., Gupta, A., Jiang, W., May, L., Hsieh, Y.H., and Dugas, A. (2016). The frequency of influenza and bacterial coinfection: a systematic review and meta-analysis. Influenza Other Respir. Viruses *10*, 394–403. https://doi.org/10.1111/irv.12398.

Kostic, A.D., Ojesina, A.I., Pedamallu, C.S., Jung, J., Verhaak, R.G.W., Getz, G., and Meyerson, M. (2011). PathSeq: software to identify or discover microbes by deep sequencing of human tissue. Nat. Biotechnol. *29*, 393–396. https://doi.org/10.1038/nbt.1868.

Langmead, B., and Salzberg, S.L. (2012). Fast gapped-read alignment with Bowtie 2. Nat. Methods *9*, 357–359. https://doi.org/10.1038/nmeth.1923.

Larkin, M.A., Blackshields, G., Brown, N.P., Chenna, R., McGettigan, P.A., McWilliam, H., Valentin, F., Wallace, I.M., Wilm, A., Lopez, R., et al. (2007). Clustal W and clustal X version 2.0. Bioinformatics *23*, 2947–2948. https://doi.org/10.1093/bioinformatics/btm404.

Layne, S.P., Walters, K.A., Kash, J.C., and Taubenberger, J.K. (2022). More autopsy studies are needed to understand the pathogenesis of severe COVID-19. Nat. Med. *28*, 427–428. https://doi.org/10.1038/s41591-022-01684-8.

Lebbink, R.J., de Ruiter, T., Adelmeijer, J., Brenkman, A.B., van Helvoort, J.M., Koch, M., Farndale, R.W., Lisman, T., Sonnenberg, A., Lenting, P.J., and Meyaard, L. (2006). Collagens are functional, high affinity ligands for the inhibitory immune receptor LAIR-1. J. Exp. Med. *203*, 1419–1425. https://doi.org/10.1084/jem.20052554.

Li, M., Guo, W., Dong, Y., Wang, X., Dai, D., Liu, X., Wu, Y., Li, M., Zhang, W., Zhou, H., et al. (2020a). Elevated exhaustion levels of NK and CD8(+) T cells as indicators for progression and prognosis of COVID-19 disease. Front. Immunol. *11*, 580237. https://doi.org/10.3389/fimmu.2020.580237.

Li, S., Zhang, Y., Guan, Z., Li, H., Ye, M., Chen, X., Shen, J., Zhou, Y., Shi, Z.L., Zhou, P., and Peng, K. (2020b). SARS-CoV-2 triggers inflammatory responses and cell death through caspase-8 activation. Signal Transduct. Target. Ther. *5*, 235. https://doi.org/10.1038/s41392-020-00334-0.

Liao, M., Liu, Y., Yuan, J., Wen, Y., Xu, G., Zhao, J., Cheng, L., Li, J., Wang, X., Wang, F., et al. (2020). Single-cell landscape of bronchoalveolar immune cells in patients with COVID-19. Nat. Med. *26*, 842–844. https://doi.org/10.1038/s41591-020-0901-9.

Liu, L., Wei, Q., Lin, Q., Fang, J., Wang, H., Kwok, H., Tang, H., Nishiura, K., Peng, J., Tan, Z., et al. (2019). Anti-spike IgG causes severe acute lung injury by skewing macrophage responses during acute SARS-CoV infection. JCI Insight *4*, 123158. https://doi.org/10.1172/jci.insight.123158.

Loibner, M., Langner, C., Regitnig, P., Gorkiewicz, G., and Zatloukal, K. (2021). Biosafety requirements for autopsies of patients with COVID-19: example of a BSL-3 autopsy facility designed for highly pathogenic agents. Pathobiology *88*, 37–45. https://doi.org/10.1159/000513438.

Lowery, S.A., Sariol, A., and Perlman, S. (2021). Innate immune and inflammatory responses to SARS-CoV-2: implications for COVID-19. Cell Host Microbe *29*, 1052–1062. https://doi.org/10.1016/j.chom.2021.05.004.

Lu, J.H., Teh, B.K., Wang, L.d., Wang, Y.N., Tan, Y.S., Lai, M.C., and Reid, K.B.M. (2008). The classical and regulatory functions of C1q in immunity and autoimmunity. Cell. Mol. Immunol. *5*, 9–21. https://doi.org/10.1038/cmi.2008.2.

Luyt, C.E., Bouadma, L., Morris, A.C., Dhanani, J.A., Kollef, M., Lipman, J., Martin-Loeches, I., Nseir, S., Ranzani, O.T., Roquilly, A., et al. (2020). Pulmonary infections complicating ARDS. Intensive Care Med. *46*, 2168–2183. https://doi.org/10.1007/s00134-020-06292-z.

Macor, P., Durigutto, P., Mangogna, A., Bussani, R., De Maso, L., D'Errico, S., Zanon, M., Pozzi, N., Meroni, P.L., and Tedesco, F. (2021). Multiple-organ complement deposition on vascular endothelium in COVID-19 patients. Biomedicines *9*, 1003. https://doi.org/10.3390/biomedicines9081003.

Magro, C., Mulvey, J.J., Berlin, D., Nuovo, G., Salvatore, S., Harp, J., Baxter-Stoltzfus, A., and Laurence, J. (2020). Complement associated microvascular injury and thrombosis in the pathogenesis of severe COVID-19 infection: a report of five cases. Transl. Res. *220*, 1–13. https://doi.org/10.1016/j.trsl.2020.04.007.

Maiwald, M. (2011). Broad-range PCR for detection and identification of bacteria. In Molecular Microbiology: Diagnostic Principles and Practice, 2nd Ed., D.H.E.A. Persing, ed. (ASM Press), pp. 491–505.

Margaroli, C., Benson, P., Sharma, N.S., Madison, M.C., Robison, S.W., Arora, N., Ton, K., Liang, Y., Zhang, L., Patel, R.P., and Gaggar, A. (2021). Spatial mapping of SARS-CoV-2 and H1N1 lung injury identifies differential transcriptional signatures. Cell Rep. Med. *2*, 100242. https://doi.org/10.1016/j.xcrm.2021.100242.

Matthay, M.A., Zemans, R.L., Zimmerman, G.A., Arabi, Y.M., Beitler, J.R., Mercat, A., Herridge, M., Randolph, A.G., and Calfee, C.S. (2019). Acute respiratory distress syndrome. Nat. Rev. Dis. Primers *5*, 18. https://doi.org/10.1038/s41572-019-0069-0.

McGonagle, D., Sharif, K., O'Regan, A., and Bridgewood, C. (2020). The role of cytokines including interleukin-6 in COVID-19 induced pneumonia and macrophage activation syndrome-like disease. Autoimmun. Rev. *19*, 102537. https://doi.org/10.1016/j.autrev.2020.102537.

Melms, J.C., Biermann, J., Huang, H., Wang, Y., Nair, A., Tagore, S., Katsyv, I., Rendeiro, A.F., Amin, A.D., Schapiro, D., et al. (2021). A molecular single-cell lung atlas of lethal COVID-19. Nature *595*, 114–119. https://doi.org/10.1038/s41586-021-03569-1.

Merad, M., and Martin, J.C. (2020). Pathological inflammation in patients with COVID-19: a key role for monocytes and macrophages. Nat. Rev. Immunol. *20*, 355–362. https://doi.org/10.1038/s41577-020-0331-4.

Messner, C.B., Demichev, V., Wendisch, D., Michalick, L., White, M., Freiwald, A., Textoris-Taube, K., Vernardis, S.I., Egger, A.S., Kreidl, M., et al. (2020). Ultra-high-Throughput clinical proteomics reveals classifiers of COVID-19 infection. Cell Syst. *11*, 11–24.e4. https://doi.org/10.1016/j.cels.2020.05.012.

Morens, D.M., Taubenberger, J.K., and Fauci, A.S. (2008). Predominant role of bacterial pneumonia as a cause of death in pandemic influenza: implications for pandemic influenza preparedness. J. Infect. Dis. *198*, 962–970. https://doi.org/10.1086/591708.

Mulay, A., Konda, B., Garcia, G., Jr., Yao, C., Beil, S., Villalba, J.M., Koziol, C., Sen, C., Purkayastha, A., Kolls, J.K., et al. (2021). SARS-CoV-2 infection of primary human lung epithelium for COVID-19 modeling and drug discovery. Cell Rep. *35*, 109055. https://doi.org/10.1016/j.celrep.2021.109055.

Nie, X., Qian, L., Sun, R., Huang, B., Dong, X., Xiao, Q., Zhang, Q., Lu, T., Yue, L., Chen, S., et al. (2021). Multi-organ proteomic landscape of COVID-19 autopsies. Cell *184*, 775–791.e14. https://doi.org/10.1016/j.cell.2021.01.004.

Nienhold, R., Ciani, Y., Koelzer, V.H., Tzankov, A., Haslbauer, J.D., Menter, T., Schwab, N., Henkel, M., Frank, A., Zsikla, V., et al. (2020). Two distinct immunopathological profiles in autopsy lungs of COVID-19. Nat. Commun. *11*, 5086. https://doi.org/10.1038/s41467-020-18854-2.

Nilsson, R.H., Larsson, K.H., Taylor, A.F.S., Bengtsson-Palme, J., Jeppesen, T.S., Schigel, D., Kennedy, P., Picard, K., Glöckner, F.O., Tedersoo, L., et al. (2019). The UNITE database for molecular identification of fungi: handling dark taxa and parallel taxonomic classifications. Nucleic Acids Res. *47*, D259–D264. https://doi.org/10.1093/nar/gky1022.

Paavola, K.J., Roda, J.M., Lin, V.Y., Chen, P., O'Hollaren, K.P., Ventura, R., Crawley, S.C., Li, B., Chen, H.I.H., Malmersjö, S., et al. (2021). The Fibronectin-ILT3 interaction functions as a stromal checkpoint that Suppresses myeloid cells. Cancer Immunol. Res. *9*, 1283–1297. https://doi.org/10.1158/2326-6066.CIR-21-0240.

Perico, L., Benigni, A., Casiraghi, F., Ng, L.F.P., Renia, L., and Remuzzi, G. (2021). Immunity, endothelial injury and complement-induced coagulopathy in COVID-19. Nat. Rev. Nephrol. *17*, 46–64. https://doi.org/10.1038/s41581-020-00357-4.

Peters, D.M., Vadász, I., Wujak, L., Wygrecka, M., Olschewski, A., Becker, C., Herold, S., Papp, R., Mayer, K., Rummel, S., et al. (2014). TGF-beta directs trafficking of the epithelial sodium channel ENaC which has implications for ion and fluid transport in acute lung injury. Proc. Natl. Acad. Sci. USA *111*, E374–E383. https://doi.org/10.1073/pnas.1306798111.

Qi, C., Wang, C., Zhao, L., Zhu, Z., Wang, P., Zhang, S., Cheng, L., and Zhang, X. (2022). SCovid: single-cell atlases for exposing molecular characteristics of COVID-19 across 10 human tissues. Nucleic Acids Res. *50*, D867–D874. https://doi.org/10.1093/nar/gkab881.

Quast, C., Pruesse, E., Yilmaz, P., Gerken, J., Schweer, T., Yarza, P., Peplies, J., and Glöckner, F.O. (2013). The SILVA ribosomal RNA gene database project: improved data processing and web-based tools. Nucleic Acids Res. *41*, D590–D596. https://doi.org/10.1093/nar/gks1219.

Ramlall, V., Thangaraj, P.M., Meydan, C., Foox, J., Butler, D., Kim, J., May, B., De Freitas, J.K., Glicksberg, B.S., Mason, C.E., et al. (2020). Immune complement and coagulation dysfunction in adverse outcomes of SARS-CoV-2 infection. Nat. Med. *26*, 1609–1615. https://doi.org/10.1038/s41591-020-1021-2.

Robinson, M.D., McCarthy, D.J., and Smyth, G.K. (2010). edgeR: a Bioconductor package for differential expression analysis of digital gene expression data. Bioinformatics *26*, 139–140. https://doi.org/10.1093/bioinformatics/btp616.

Roquilly, A., Jacqueline, C., Davieau, M., Mollé, A., Sadek, A., Fourgeux, C., Rooze, P., Broquet, A., Misme-Aucouturier, B., Chaumette, T., et al. (2020). Alveolar macrophages are epigenetically altered after inflammation, leading to long-term lung immunoparalysis. Nat. Immunol. *21*, 636–648. https://doi.org/10.1038/s41590-020-0673-x.

Sagulenko, P., Puller, V., and Neher, R.A. (2018). TreeTime: maximum-likelihood phylodynamic analysis. Virus Evol. *4*, vex042. https://doi.org/10.1093/ve/vex042.

Segata, N., Izard, J., Waldron, L., Gevers, D., Miropolsky, L., Garrett, W.S., and Huttenhower, C. (2011). Metagenomic biomarker discovery and explanation. Genome Biol. *12*, R60. https://doi.org/10.1186/gb-2011-12-6-r60.

Segata, N., Waldron, L., Ballarini, A., Narasimhan, V., Jousson, O., and Huttenhower, C. (2012). Metagenomic microbial community profiling using unique clade-specific marker genes. Nat. Methods *9*, 811–814. https://doi.org/10.1038/nmeth.2066.

Sethi, S., D'Agati, V.D., Nast, C.C., Fogo, A.B., De Vriese, A.S., Markowitz, G.S., Glassock, R.J., Fervenza, F.C., Seshan, S.V., Rule, A., et al. (2017). A proposal for standardized grading of chronic changes in native kidney biopsy specimens. Kidney Int. *91*, 787–789. https://doi.org/10.1016/j.kint.2017.01.002.

Sieswerda, E., de Boer, M.G.J., Bonten, M.M.J., Boersma, W.G., Jonkers, R.E., Aleva, R.M., Kullberg, B.J., Schouten, J.A., van de Garde, E.M.W., Verheij, T.J., et al. (2021). Recommendations for antibacterial therapy in adults with COVID-19 - an evidence based guideline. Clin. Microbiol. Infect. *27*, 61–66. https://doi.org/10.1016/j.cmi.2020.09.041.

Son, M., Diamond, B., and Santiago-Schwarz, F. (2015). Fundamental role of C1q in autoimmunity and inflammation. Immunol. Res. *63*, 101–106. https://doi.org/10.1007/s12026-015-8705-6.

Son, M., Santiago-Schwarz, F., Al-Abed, Y., and Diamond, B. (2012). C1q limits dendritic cell differentiation and activation by engaging LAIR-1. Proc. Natl. Acad. Sci. USA *109*, E3160–E3167. https://doi.org/10.1073/pnas.1212753109.

Sopirala, M.M. (2021). Predisposition of COVID-19 patients to secondary infections: set in stone or subject to change? Curr. Opin. Infect. Dis. *34*, 357–364. https://doi.org/10.1097/QCO.0000000000000736.

Subramanian, A., Tamayo, P., Mootha, V.K., Mukherjee, S., Ebert, B.L., Gillette, M.A., Paulovich, A., Pomeroy, S.L., Golub, T.R., Lander, E.S., and Mesirov, J.P. (2005). Gene set enrichment analysis: a knowledge-based approach for interpreting genome-wide expression profiles. Proc. Natl. Acad. Sci. USA *102*, 15545–15550. https://doi.org/10.1073/pnas.0506580102.

Syed-Ahmed, M., and Narayanan, M. (2019). Immune dysfunction and risk of infection in chronic kidney disease. Adv. Chronic Kidney Dis. *26*, 8–15. https://doi.org/10.1053/j.ackd.2019.01.004.

Tangye, S.G., Palendira, U., and Edwards, E.S.J. (2017). Human immunity against EBV-lessons from the clinic. J. Exp. Med. *214*, 269–283. https://doi.org/10.1084/jem.20161846.

Thielens, N.M., Tedesco, F., Bohlson, S.S., Gaboriaud, C., and Tenner, A.J. (2017). C1q: a fresh look upon an old molecule. Mol. Immunol. *89*, 73–83. https://doi.org/10.1016/j.molimm.2017.05.025.

Tomic, S., Đokić, J., Stevanović, D., Ilić, N., Gruden-Movsesijan, A., Dinić, M., Radojević, D.,

Bekić, M., Mitrović, N., Tomašević, R., et al. (2021). Reduced expression of autophagy markers and expansion of myeloid-derived suppressor cells correlate with poor T cell response in severe COVID-19 patients. Front. Immunol. *12*, 614599. https://doi.org/10.3389/fimmu.2021.614599.

Vaz de Paula, C.B., Nagashima, S., Liberalesso, V., Collete, M., da Silva, F.P.G., Oricil, A.G.G., Barbosa, G.S., da Silva, G.V.C., Wiedmer, D.B., da Silva Dezidério, F., and Noronha, L. (2021). COVID-19: immunohistochemical analysis of TGF-beta signaling pathways in pulmonary fibrosis. Int. J. Mol. Sci. *23*, 168. https://doi.org/10.3390/ijms23010168.

Wang, C., Xie, J., Zhao, L., Fei, X., Zhang, H., Tan, Y., Nie, X., Zhou, L., Liu, Z., Ren, Y., et al. (2020). Alveolar macrophage dysfunction and cytokine storm in the pathogenesis of two severe COVID-19 patients. EBioMedicine *57*, 102833. https://doi.org/10.1016/j.ebiom.2020.102833.

Wang, T., Zhang, X., Liu, Z., Yao, T., Zheng, D., Gan, J., Yu, S., Li, L., Chen, P., and Sun, J. (2021). Single-cell RNA sequencing reveals the sustained immune cell dysfunction in the pathogenesis of sepsis secondary to bacterial pneumonia. Genomics *113*, 1219–1233. https://doi.org/10.1016/j.ygeno.2021.01.026.

Wauters, E., Van Mol, P., Garg, A.D., Jansen, S., Van Herck, Y., Vanderbeke, L., Bassez, A., Boeckx, B., Malengier-Devlies, B., Timmerman, A., et al. (2021). Discriminating mild from critical COVID-19 by innate and adaptive immune single-cell profiling of bronchoalveolar lavages. Cell Res. *31*, 272–290. https://doi.org/10.1038/s41422-020-00455-9.

Wu, D., Wu, C., Zhang, S., and Zhong, Y. (2019). Risk factors of ventilator-associated pneumonia in critically III patients. Front. Pharmacol. *10*, 482. https://doi.org/10.3389/fphar.2019.00482.

Wu, M., Chen, Y., Xia, H., Wang, C., Tan, C.Y., Cai, X., Liu, Y., Ji, F., Xiong, P., Liu, R., et al. (2020). Transcriptional and proteomic insights into the host response in fatal COVID-19 cases. Proc. Natl. Acad. Sci. USA *117*, 28336–28343. https://doi.org/10.1073/pnas.2018030117.

Xu, G., Qi, F., Li, H., Yang, Q., Wang, H., Wang, X., Liu, X., Zhao, J., Liao, X., Liu, Y., et al. (2020). The differential immune responses to COVID-19 in peripheral and lung revealed by single-cell RNA sequencing. Cell Discov. *6*, 73. https://doi.org/10.1038/s41421-020-00225-2.

Yang, Y.H., Huang, Y.H., Chuang, Y.H., Peng, C.M., Wang, L.C., Lin, Y.T., and Chiang, B.L. (2005). Autoantibodies against human epithelial cells and endothelial cells after severe acute respiratory syndrome (SARS)-associated coronavirus infection. J. Med. Virol. *77*, 1–7. https://doi.org/10.1002/jmv.20407.

Yu, J., Yuan, X., Chen, H., Chaturvedi, S., Braunstein, E.M., and Brodsky, R.A. (2020). Direct activation of the alternative complement pathway by SARS-CoV-2 spike proteins is blocked by factor D inhibition. Blood *136*, 2080–2089. https://doi.org/10.1182/blood.2020008248.

Zurl, C., Hoenigl, M., Schulz, E., Hatzl, S., Gorkiewicz, G., Krause, R., Eller, P., and Prattes, J. (2021). Autopsy proven pulmonary mucormycosis due to Rhizopus microsporus in a critically ill COVID-19 patient with underlying hematological malignancy. J. Fungi *7*, 88. https://doi.org/10.3390/jof7020088.

STAR★METHODS

KEY RESOURCES TABLE

REAGENT or RESOURCE	SOURCE	IDENTIFIER
Antibodies		
Anti-SARS-CoV-2 nucleoprotein monoclonal rabbit antibody	Sino Biological	Cat# 40143-R019; clone: 019; RRID:AB_2827973
Anti-CD68 monoclonal mouse antibody	Ventana Medical Systems	Cat# 790-2931; clone: KP-1; RRID:AB_2335972
Anti-CD163 monoclonal mouse antibody	Ventana Medical Systems	Cat# 760-4437; clone: MRQ-26; RRID:AB_2335969
Anti-TTF1 monoclonal mouse antibody	Cell Marque	Cat# 343M-96; clone: 8G7G3/1; RRID:AB_1158937
Anti-TGFß1 polyclonal rabbit antibody	Santa Cruz Biotechnology	Cat# SC-146; RRID:AB_632486
Anti-TGFß polyclonal rabbit antibody	Cell Signaling Technology	Cat# 3711; RRID:AB_2063354
Anti-LAG3 polyclonal rabbit antibody	Abcam	Cat# ab180187; clone: EPR4392(2); RRID:AB_2888645
Anti-C1q polyclonal rabbit antibody	Agilent	Cat# A0136; RRID:AB_2335698
Anti-GAPDH monoclonal rabbit antibody	Cell Signaling Technology	Cat# 2118; clone: 14C10; RRID:AB_561053
HRP-linked ECL Anti-Rabbit IgG	GE Healthcare	Cat# NA934; RRID:AB_772206
Dako REAL TM EnVision TM HRP rabbit/mouse detection-system	Agilent	Cat# K5007; RRID:AB_2888627
ultraView DAB detection-system	Roche	Cat# 760-500; RRID:AB_2753116
Bacterial and virus strains		
SARS-CoV-2 strains from study	This study	N/A
Bacterial and fungal strains from study	This study	N/A
Biological samples		
Autopsy tissue and body fluid samples	This study	N/A
Respiratory tract swabs	This study	N/A
Chemicals, peptides, and recombinant proteins		
Thioglycollate broth	Oxoid	Cat# CM0173
OptiPro SFM medium	Gibco	Cat# 12309019
L-Glutamine	Gibco	Cat# 11539876
Penicillin-Streptomycin (10.000 U/ml)	Gibco	Cat# 11548876
TRIzol®	Invitrogen	Cat# 15596026
RIPA buffer	Sigma	Cat# R0278
Pefabloc	Roche	Cat# 11429868001
cOmplete™ Mini	Merck	Cat# 11836153001
PhosSTOP™	Roche	Cat# 4906845001
Laemmli buffer	Bio-Rad	Cat# 1610737EDU
Critical commercial assays		
MagNA Lyser green beads tubes	Roche	Cat# 03358941001
Maxwell 16 LEV simplyRNA blood kit	Promega	Cat# AS1310
QIAamp Viral RNA Mini Kit	Qiagen	Cat# 221413
High-Capacity cDNA Reverse Transcription Kit with RNase inhibitor	Applied Biosystems	Cat# 4374966

(*Continued on next page*)

Continued

REAGENT or RESOURCE	SOURCE	IDENTIFIER
SuperScript III One-Step RT-PCR System with Platinum Taq High Fidelity DNA Polymerase mastermix	ThermoFisher	Cat# 12574018
SYBR Green PCR Mastermix	Applied Biosystems	Cat# 4309155
Ampure XP beads	Beckman Coulter	Cat# A63881
NEBNext Fast DNA Fragmentation & Library Prep Set for Ion Torren kit	New England Biolabs	Cat# E6285L
KAPA RNA HyperPrep Kit with RiboErase (HMR) for Illumina® platforms	KAPABIOSYSTEMS	Cat# KR1351
16s Complete PCR Mastermix kit	Molzym	Cat# S-020-0250
QiaQick gel extraction kit	Qiagen	Cat# 28706X4
Ponceau S solution	Sigma	Cat# P7170
ECL Select Western Blot Reagent	Amersham	Cat# 12644055
RNAlater	ThermoFisher	Cat# AM7024
Deposited data		
16S rRNA gene-, ITS- and RNAseq data	European nucleotide archive (ENA)	Acc. no. PRJEB45873
Experimental models: Cell lines		
Vero CCL-81 cells	European Collection of Authenticated Cell Cultures	ECACC 84113001
Oligonucleotides		
RdRp_SARSr-F GTGARATGGTCATGTGTGGCGG	(Corman et al., 2020)	N/A
RdRp_SARSr-P2 FAM-CAGGTGGAACCTCATCAGGAGATGC-BBQ	(Corman et al., 2020)	N/A
RdRp_SARSr-R CARATGTTAAASACACTATTAGCATA	(Corman et al., 2020)	N/A
N_Sarbeco_F CACATTGGCACCCGCAATC	(Corman et al., 2020)	N/A
N_Sarbeco_P FAM-ACTTCCTCAAGGAACAACATTGCCA-BBQ	(Corman et al., 2020)	N/A
N_Sarbeco_R GAGGAACGAGAAGAGGCTTG	(Corman et al., 2020)	N/A
2019-nCoV_N1-F GACCCCAAAATCAGCGAAAT	https://www.cdc.gov/coronavirus/2019-ncov/lab/rt-pcr-panel-primer-probes.html	N/A
2019-nCoV_N1-R TCTGGTTACTGCCAGTTGAATCTG	https://www.cdc.gov/coronavirus/2019-ncov/lab/rt-pcr-panel-primer-probes.html	N/A
2019-nCoV_N2-F TTACAAACATTGGCCGCAAA	https://www.cdc.gov/coronavirus/2019-ncov/lab/rt-pcr-panel-primer-probes.html	N/A
2019-nCoV_N2-R GCGCGACATTCCGAAGAA	https://www.cdc.gov/coronavirus/2019-ncov/lab/rt-pcr-panel-primer-probes.html	N/A
2019-nCoV_N3-F GGGAGCCTTGAATACACCAAAA	https://www.cdc.gov/coronavirus/2019-ncov/lab/rt-pcr-panel-primer-probes.html	N/A
2019-nCoV_N3-R TGTAGCACGATTGCAGCATTG	https://www.cdc.gov/coronavirus/2019-ncov/lab/rt-pcr-panel-primer-probes.html	N/A
RP-F AGATTTGGACCTGCGAGCG	https://www.cdc.gov/coronavirus/2019-ncov/lab/rt-pcr-panel-primer-probes.html	N/A
RP-R GAGCGGCTGTCTCCACAAGT	https://www.cdc.gov/coronavirus/2019-ncov/lab/rt-pcr-panel-primer-probes.html	N/A

(*Continued on next page*)

Continued

REAGENT or RESOURCE	SOURCE	IDENTIFIER
GAPDH_f CCTCCACCTTTGACGCT	https://www.cdc.gov/coronavirus/2019-ncov/lab/rt-pcr-panel-primer-probes.html	N/A
GAPDH_r TTGCTGTAGCCAAATTCGTT	https://www.cdc.gov/coronavirus/2019-ncov/lab/rt-pcr-panel-primer-probes.html	N/A
CoV_gen_f1 TAAAGGTTTATACCTTCCCAGG	This study	N/A
CoV_gen_r1 CAGATGTGAACATCATAGCATC	This study	N/A
CoV_gen_f2 AAAGAGCTATGAATTGCAGACACC	This study	N/A
CoV_gen_r2 GGAGGGTAGAAAGAACAATACA	This study	N/A
CoV_gen_f3 GATGCTATGATGTTCACATCTG	This study	N/A
CoV_gen_r3 CAGAATCTGGATGAAGATTGCCAT	This study	N/A
CoV_gen_f4 TGTATTGTTCTTTCTACCCTCC	This study	N/A
CoV_gen_r4 CTCCATCCAAATAAGTTGGACCAA	This study	N/A
CoV_gen_f5 ATGGCAATCTTCATCCAGATTCTG	This study	N/A
CoV_gen_r5 CACATCACCATTTAAGTCAGGGAA	This study	N/A
CoV_gen_f6 TTGGTCCAACTTATTTGGATGGAG	This study	N/A
CoV_gen_r6 CACTCTGCAACTAAGCCAAA	This study	N/A
CoV_gen_f7 TTCCCTGACTTAAATGGTGATGTG	This study	N/A
CoV_gen_r7 GCCAGTAACTTCTATGTCAGATTG	This study	N/A
CoV_gen_f8 TTTGGCTTAGTTGCAGAGTG	This study	N/A
CoV_gen_r8 CACTAGTAGATACACAAACACCAG	This study	N/A
CoV_gen_f9 CAATCTGACATAGAAGTTACTGGC	This study	N/A
CoV_gen_r9 CCAGCCTGTACCAAGAAATTA	This study	N/A
CoV_gen_f10 CTGGTGTTTGTGTATCTACTAGTG	This study	N/A
CoV_gen_r10 CCAACCATGTCATAATACGCAT	This study	N/A
CoV_gen_f11 TAATTTCTTGGTACAGGCTGG	This study	N/A
CoV_gen_r11 CCAACTTACGTTGCATGGCTG	This study	N/A
CoV_gen_f12 ATGCGTATTATGACATGGTTGG	This study	N/A
CoV_gen_r12 GGATGATCTATGTGGCAACGG	This study	N/A
CoV_gen_f13 CAGCCATGCAACGTAAGTTGG	This study	N/A
CoV_gen_r13 GGTGGTATGTCTGATCCCAATATT	This study	N/A

(*Continued on next page*)

Continued

REAGENT or RESOURCE	SOURCE	IDENTIFIER
CoV_gen_f14 CCGTTGCCACATAGATCATCC	This study	N/A
CoV_gen_r14 GCATGTTAGGCATGGCTCTATCA	This study	N/A
CoV_gen_f15 AATATTGGGATCAGACATACCACC	This study	N/A
CoV_gen_r15 GGTCGTAACAGCATTTACAA	This study	N/A
CoV_gen_f16 TGATAGAGCCATGCCTAACATGC	This study	N/A
CoV_gen_r16 GTCTCAGGCAATGCATTTAC	This study	N/A
CoV_gen_f17 TTGTAAATGCTGTTACGACC	This study	N/A
CoV_gen_r17 GCTTCTCTAGTAGCATGACACCC	This study	N/A
CoV_gen_f18 GTAAATGCATTGCCTGAGAC	This study	N/A
CoV_gen_r18 CACATGGACTGTCAGAGTAATAGA	This study	N/A
CoV_gen_f19 GGGTGTCATGCTACTAGAGAAGC	This study	N/A
CoV_gen_r19 CACTTAGATGAACCTGTTTGCGC	This study	N/A
CoV_gen_f20 TCTATTACTCTGACAGTCCATGTG	This study	N/A
CoV_gen_r20 GACTAGAGACTAGTGGCAATAA	This study	N/A
CoV_gen_f21 GCGCAAACAGGTTCATCTAAGTG	This study	N/A
CoV_gen_r21 GCAAATCTGGTGGCGTTAAA	This study	N/A
CoV_gen_f22 TTATTGCCACTAGTCTCTAGTC	This study	N/A
CoV_gen_r22 GAGGAGAATTAGTCTGAGTCT	This study	N/A
CoV_gen_f23 TTTAACGCCACCAGATTTGC	This study	N/A
CoV_gen_r23 GCTCTGATTTCTGCAGCTCTAATT	This study	N/A
CoV_gen_f24 AGACTCAGACTAATTCTCCTC	This study	N/A
CoV_gen_r24 CCTTGGAGAGTGCTAGTTGCC	This study	N/A
CoV_gen_f25 AATTAGAGCTGCAGAAATCAGAGC	This study	N/A
CoV_gen_r25 GGCATAGGCAAATTGTAGAAGACA	This study	N/A
CoV_gen_f26 GGCAACTAGCACTCTCCAAGG	This study	N/A
CoV_gen_r26 GTGAAACTGATCTGGCACGTAACT	This study	N/A
CoV_gen_f27 TGTCTTCTACAATTTGCCTATGCC	This study	N/A
CoV_gen_r27 CCATAGGGAAGTCCAGCTTCTG	This study	N/A
CoV_gen_f28 AGTTACGTGCCAGATCAGTTTCAC	This study	N/A

(*Continued on next page*)

Continued

REAGENT or RESOURCE	SOURCE	IDENTIFIER
CoV_gen_r28 GTCCTCCCTAATGTTACACA	This study	N/A
CoV_gen_f29 CAGAAGCTGGACTTCCCTATGG	This study	N/A
CoV_gen_r29 TTTGTATGCGTCAATATGCTT	This study	N/A
CoV_gen_f30 TGTGTAACATTAGGGAGGAC	This study	N/A
CoV_gen_r30 TTTGTCATTCTCCTAAGAAGC	This study	N/A
16S_515_f TGCCAGCAGCCGCGGTAA	(Maiwald 2011)	
16S_806_r GGACTACCAGGGTATCTAAT	(Maiwald 2011)	
ITS1 TCCGTAGGTGAACCTGCGG	(Halwachs et al., 2017)	
ITS2 GCTGCGTTCTTCATCGATGC	(Halwachs et al., 2017)	
Software and algorithms		
R (v4.1)	https://www.R-project.org/	N/A
GISAID SARS-CoV-2 (hCoV-19) database	GISAID	https://www.gisaid.org
clustalw (v2.1)	(Larkin et al., 2007)	ftp://ftp.ebi.ac.uk/pub/software/clustalw2/
figtree (v1.4.4)		http://tree.bio.ed.ac.uk/software/figtree/
STAR	(Dobin et al., 2013)	https://github.com/alexdobin/STAR
bowtie2-2.4.1	(Langmead and Salzberg 2012)	http://bowtie-bio.sourceforge.net/bowtie2/index.shtml
HTSeq (v0.12.4)	G Putri, S Anders, PT Pyl, JE Pimanda, F Zanini Analysing high-throughput sequencing data in Python with HTSeq 2.0 https://doi.org/10.1093/bioinformatics/btac166(2022)	https://htseq.readthedocs.io/en/master/
xCell	(Aran et al., 2017)	https://github.com/dviraran/xCell
edgeR	(Robinson et al., 2010)	https://bioconductor.org/packages/release/bioc/html/edgeR.html
Gene set enrichment analysis online tool	(Subramanian et al., 2005)	https://www.gsea-msigdb.org/gsea/msigdb/annotate.jsp
Single-cell atlas database SCovid	(Qi et al., 2022)	http://bio-annotation.cn/scovid/
MetaPhlAn2 (v2.6.0)	(Segata et al., 2012)	https://github.com/biobakery/MetaPhlAn2
Pathseq (GATK v4.1.0.0)	(Kostic et al., 2011)	https://github.com/broadinstitute/gatk
QIIME2 (v. 2020.6)	(Bolyen et al., 2019)	https://qiime2.org/
LEfSe	(Segata et al., 2011)	https://www.bioconductor.org/packages/release/bioc/html/lefser.html
DADA2	(Callahan et al., 2016)	https://bioconductor.org/packages/release/bioc/html/dada2.html
UNITE reference database	(Nilsson et al., 2018) Nilsson RH, Larsson K-H, Taylor AFS, Bengtsson-Palme J, Jeppesen TS, Schigel D, Kennedy P, Picard K, Glöckner FO, Tedersoo L, Saar I, Kõljalg U, Abarenkov K. 2018. The UNITE database for molecular identification of fungi: handling dark taxa and parallel taxonomic classifications. Nucleic Acids Research, https://doi.org/10.1093/nar/gky1022	https://unite.ut.ee/
SILVA reference database	(Quast et al., 2013)	https://www.arb-silva.de/
bcftools (v1.3.1)		http://github.com/samtools/bcftools
Incscape (v0.92)		https://inkscape.org/de/release/inkscape-0.92/
fastx (v0.0.13)		http://hannonlab.cshl.edu/fastx_toolkit/

(*Continued on next page*)

Continued		
REAGENT or RESOURCE	SOURCE	IDENTIFIER
seqclean		https://sourceforge.net/projects/seqclean/
samtools	(Danecek et al., 2021)	http://www.htslib.org/
GraphPad Prism™		https://www.graphpad.com/scientific-software/prism/
ImageJ		https://imagej.nih.gov/ij/index.html
BioRender		https://biorender.com/
Other		
eSwab	Copan	Cat# 80490CEA
Inform EBER Epstein Barr Virus early RNA kit	Ventana	Cat# 800-2824
ISH invers blue detection-system	Ventana	Cat# 800-092
Genbox anaer	bioMérieux	Cat# 45534
Blood agar	BD Diagnostics	Cat# 256506
MacConkey agar	BD Diagnostics	Cat# 215197
Chocolate agar	BD Diagnostics	Cat# 257456

RESOURCE AVAILABILITY

Lead contact

Further information and requests for resources and reagents should be directed to and will be fulfilled by the lead contact, Gregor Gorkiewicz (gregor.gorkiewicz@medunigraz.at)

Materials availability

There are restrictions to the availability of tissue samples, viral, bacterial and fungal strains generated by the study (e.g. ethics, biosafety). Inquiries should be directed to the lead contact.

Data and code availability

The RNAseq, 16S rRNA gene and ITS amplicon sequencing data has been deposited in the European Nucleotide Archive (ENA): PRJEB45873.

This paper does not report original code.

Any additional information required to re-analyze the data reported in this paper is available from the lead contact upon request.

EXPERIMENTAL MODEL AND SUBJECT DETAILS

Twenty consecutive covid-19 patients which deceased at the first pandemic peak in our institution (23/3/2020 and 26/4/2020) were post-mortally examined. In addition, 14 age-matched non-covid-19 controls which deceased within the same time period were included for subsequent analyses. They were selected based on age and matching comorbidities. Details of subjects are given in the main text and Tables S1 and S2. The study was approved by the ethics committee of the Medical University of Graz (EK-number: 32–362 ex 19/20).

METHOD DETAILS

Autopsy procedure & specimen collection

Autopsies were performed according to CDC guidelines (https://www.cdc.gov/coronavirus/2019-ncov/hcp/guidance-postmortem-specimens.html) and the epidemic response plan of the county of Styria in a BSL-3 facility that has been specifically designed for post-mortem examinations and sample collection (Loibner et al., 2021). Full autopsies were performed and swabs (eSwab, Copan), tissue and body fluid samples were taken. To omit cross-contaminations between the respiratory tract and the GI tract, the autopsy was sequentially performed. First, the thorax was opened with sterile instruments and lungs and the upper respiratory tract were dissected and sampled. Subsequently, the remaining organs were sectioned with

new sterile instruments and sampled. Tissues were immediately fixed in 10% buffered formalin (for histology) or 2,5% buffered (sodium cacodylate; pH 6.5; Sigma) glutaraldehyde (for electron microscopy), snap frozen in liquid nitrogen or preserved in RNAlater (ThermoFisher) and stored at -80°C until further processing.

Histopathology and immunohistochemistry

Formalin-fixed paraffin-embedded (FFPE) tissue specimens were processed and stained according to standard procedures. Stains consisted of hematoxylin & eosin (H&E), periodic acid–Schiff (PAS), chromotrope aniline blue (CAB), sirius red, Gomori, Prussian blue, Giemsa and toluidine blue. Chronic renal changes involving the individual renal compartments were scored according to Sethi et al. (Sethi et al. (2017). Liver fibrosis was scored according to Ishak et al. (Ishak et al. (1995). The following antibodies were used: Anti-SARS-CoV-2 nucleoprotein (NP) antibody (dilution 1:100; detection-system: Dako REAL TM EnVision); CD68 (dilution 1:100; detection-system: Ventana UltraView DAB); TTF1 (dilution 1:200; detection-system: Dako K5007); TGFβ1 (dilution 1:50; detection-system: Ventana UltraView DAB); LAG3 (dilution 1:5000; detection-system: Dako K5007); C1q (dilution 1:5000; detection-system: Dako K5007); CD163 (dilution 1:50; detection-system: Ventana UltraView DAB). RNA in-situ hybridization for EBV was performed with the Inform EBER Epstein Barr Virus early RNA kit and the detection-system ISH iView Blue Plus (Ventana).

Scoring of histological lung features

From each case multiple specimens from each lobe were taken to account for variations in disease representation (at least 2 specimens per lobe corresponding to 10 specimens per case at least, mean: 13, range: 10-21) and assessed for histopathological features. The histologic progression of DAD includes classically 3 phases (exudative, proliferative, and fibrotic) that correlate with disease duration (Castro, 2006). In our series fibrotic (late) changes were only sparsely present (see Figure 2C) and early and late features of DAD were heterogeneously distributed and often intermixed, thus, we summarized features into (a) early (exudative) and (b) late (proliferative, fibrotic) phases for simplification, as well as included (c) additional features present in DAD histopathology (Hughes and Beasley, 2017). Features consisted of: Interstitial edema/thickening of the alveolo-capillary membranes (non-fibrotic); alveolar edema; hyaline membranes; intra-alveolar (loose) fibrin; scaled of pneumocytes; intra-alveolar proliferation of pneumocytes; alveolar septal fibrosis (early stage organizing DAD); alveolar septal fibrosis (end stage organizing DAD); bronchialisation; squamous metaplasia; virus induced cellular changes in pneumocytes and/or alveolar macrophages; alveolar hemorrhage; interstitial hemorrhage; interstitial hemosidern (free); alveolar hemosiderin (siderophages); fibrin thrombi (capillaries); fibrin thrombi (larger vessels); vascular remodeling (increased density, vascular fissures); intra-alveolar macrophage accumulation; lymphocytes (within alveolo-capillary membranes); lymphocytes (within interstitial space); intra-alveolar (fibro-) cellular infiltrate; lymphocytes (alveolar); megakaryocytes (capillaries); alveolar neutrophils; bronchial neutrophils; a 4-grade scoring system was used to describe the severity of the different pathological features. Score 0 (feature absent), score 1 (feature present in $\leq$33%), score 2 (feature present in $\leq$66%), score 3 (feature present in >66%). Scores per slides were summed up and a final score (mean value) was calculated for the respective case.

Microbial culture and identification

Native lung tissues were transferred into mixing vessels (ProbeAX; AxonLab) containing 5 mL of physiological saline and were homogenized using a dispersion instrument (ULTRA-TURRAX® Tube Drive; AxonLab). The homogenates were inoculated (0.1 mL aliquots) onto aerobic blood agar, MacConkey agar, chocolate agar, and anaerobic blood agar plates (BD Diagnostics) and into thioglycollate broth (Oxoid). Plates were incubated at 35°C and 37 °C aerobically, in an atmosphere containing 5% carbon dioxide and anaerobically (Genbox anaer, bioMérieux) for up to 14 days, respectively. Cloudy thioglycollate broths were sub-cultured onto plates. Colonies were identified using matrix-assisted-laser-desorption-ionization time-of-flight mass-spectrometry (MALDI-TOF MS) using the Vitek® MS (bioMérieux) or MALDI Biotyper™ (Bruker) instruments or by 16S rRNA gene sequencing (Gorkiewicz et al., 2003).

Virus isolation

Lung tissues and swabs from lung parenchyma were used for cultivation of SARS-CoV-2 (Table S3). After mechanical disruption samples were frozen (−80 °C) and thawed (37 °C) twice to increase cell lysis and viral release. 2 mL OptiPro SFM medium (Gibco) with 4 mM L-Glutamine (Gibco) and 1% penicillin-streptomycin (10,000 U/mL; Gibco) were added to the samples. After centrifugation (10 min, 1500 rcf) the supernatants

were filtered through a 0.45 μm membrane filter (Millipore) and inoculated on Vero CCL-81 cells with OptiPro SFM medium with 4 mM L-Glutamine and 1% penicillin-streptomycin in T25 flasks (ThermoFisher). After 3–4 days incubation at 37 °C and 5% CO2, the whole cells were mechanically detached with cell scrapers and passaged including the supernatant on to new Vero CCL-81 cells growing in T75 flasks (ThermoFisher). After 1 week the cells were harvested and supernatants were stored after centrifugation (10 min, 1500 rcf) at −80 °C. Viral load was determined by qRT-PCR as described below.

RNA extraction

Samples consisted of swabs (eSwab, Copan), tissues and body fluids, the latter were collected with sterile syringes. Fresh tissues were sampled directly into Magna Lyser Green Beads tubes (Roche) pre-filled with 400μL lysis buffer. Tissues were homogenized with a MagnaLyser instrument (Roche) with 6500 rpm for 30 sec. and 3 repetitions. RNA was extracted from 200 μL eSwab solution, 200 μL liquid sample or tissue homogenate using the Maxwell 16 LEV simplyRNA Blood Kit (Promega) according to the manufacturer's instructions. RNAs from Vero cell cultures were isolated by using the QIAamp Viral RNA Mini Kit (Qiagen) without addition of carrier RNA and transcribed into cDNA with the High-Capacity cDNA Reverse Transcription Kit with RNase Inhibitor (Applied Biosystems) according to manufacturer's instructions.

SARS-CoV-2 quantitative RT-PCR

qRT-PCR for detection and quantification of SARS-CoV-2 in autopsy samples were performed as described (Corman et al., 2020). Briefly, primers, probes and 5 μL of RNA were added to 10 μL of SuperScript III One-Step RT-PCR System with Platinum Taq High Fidelity DNA Polymerase mastermix (ThermoFisher). PCR was performed on a Quantstudio 7 instrument (ThermoFisher) with the following cycling conditions: 55 °C for 15 min, 95 °C for 3 min; 45 cycles consisting of 95 °C for 15 sec and 58 °C for 30 sec. Amplification data was downloaded and processed using the qpcR package of the R project (https://www.r-project.org/). Amplification efficiency plots were visually inspected and Cp2D (cycle peak of second derivative) values were calculated for samples with valid amplification curves. Plots were generated with R using the reshape, tidyverse and ggplot packages. qRT-PCR of virus cultures employed primer sets recommended by the CDC detecting three different regions of the viral nucleocapsid and human RNAseP or GAPDH as control (https://www.cdc.gov/coronavirus/2019-ncov/lab/rt-pcr-panel-primer-probes.html). PCR was performed with the SYBR Green PCR Mastermix (Applied Biosystems) on a Quantstudio 7 instrument (ThermoFisher) with the following cycling conditions: 25 °C for 2 min, 50 °C for 15 min, 95 °C for 10 min, 45 cycles consisting of 95 °C for 3 sec and 55 °C for 30 sec.

Viral genome sequencing

PCR primers spanning the whole genome of SARS-CoV-2 were designed yielding in about 2kb amplicons (Table S9). 2.5 μL of RNA were used in three separate RT-PCR reactions as described above with oligonucleotide primers at 400 nM concentration with the following cycling conditions: 55 °C for 15 min, 95 °C for 3 min; 35 cycles consisting of 95 °C for 15 sec and 57 °C for 3 min; final extension at 72 °C for 10 min. PCR products were combined and purified by incubation with 1.8X Ampure XP beads (Beckman Coulter) followed by two washes with 75% ethanol and elution in 30 μL water. Amplicons were fragmented to 150–250 bp length and Ion Torrent barcode and sequencing adapters were ligated to the fragments using the NEBNext Fast DNA Fragmentation & Library Prep Set for Ion Torren kit (New England Biolabs) according to the manufacturer's recommendations. Libraries were sequenced on an Ion Torrent S5XL instrument using a 540 Chip Kit and the 200 bp sequencing kit (ThermoFisher). Sequences were aligned to the SARS-CoV-2 reference genome (acc. no.:NC_045512.2) using TMAP (v5.10.11) and variants were called with the Torrent Variant Caller (v5.10–12). All called variants were visually inspected and consensus sequences of the viral genomes were generated with bcftools (v1.3.1). Consensus sequences were aligned using clustalw (v2.1) (Larkin et al., 2007), guide trees were visualized in figtree (v1.4.4) and final adjustments were made with Incscape (v0.92). SARS-CoV-2 genomes from our study were uploaded and analyzed with the GISAID SARS-CoV-2 (hCoV-19) databasewhich can be accessed via https://www.gisaid.org/epiflu-applications/next-hcov-19-app/ (Hadfield et al., 2018; Sagulenko et al., 2018).

RNA sequencing

Libraries for RNA sequencing (RNA-seq) from lung tissues (19 covid-19 cases #2-#20 and 7 control cases #21, #23-#28) were prepped with the KAPA RNA HyperPrep Kit with RiboErase (HMR) for Illumina® platforms (KAPABIOSYSTEMS) according to the manufacturers protocol. Slight modifications from the

protocol consisted of a fragmentation step at 65 °C for 1min, 12 cycles of PCR, as well as an additional bead cleanup at the end of the prep. Libraries were pooled in two pools of 13 samples each by concentration measured with Qubit (ThermoFisher), followed by a bead-cleanup step and an additional QC with Qubit (ThermoFisher) and BioAnalyzer (Agilent). Sequences were resolved on a NovaSeq 6000 Sequencer (Illumina) with a standard paired-end protocol. RNA-seq data were aligned to the human reference genome using STAR (Dobin et al., 2013) (GRCh38 assembly, Ensembl V99 gene models) in 2-pass mode with the following parameters: -sjdbOverhang 100-outFilterMultimapNmax 20-outFilterMismatchNoverLmax 0.05-outFilterScoreMin 0-outFilterScoreMinOverLread 0-outSJfilterReads Unique-outSJfilterOverhangMin 20 15 15 15 15-outSJfilterCountUniqueMin 3 3 3 3-outSJfilterCountTotalMin 3 3 3 3-outSJfilterDistToOtherSJmin 0 0 0 0--outSJfilterIntronMaxVsReadN 100000-alignIntronMin 20-alignIntronMax 100000–alignMatesGapMax 100000-alignSJoverhangMin 12-alignSJstitchMismatchNmax 5–1 5 5-alignSJDBoverhangMin 7-alignSplicedMateMapLmin 0-alignSplicedMateMapLminOverLmate 0.5-limitSjdbInsertNsj 5000000-clip3pAdapterMMp 0.5-outSAMmultNmax 1-outSAMmapqUnique 60-outFilterType BySJout-outSAMunmapped Within-outWigType bedGraph-outReadsUnmapped None SortedByCoordinate-outSAMattrIHstart 1-twopassMode Basic-chimSegmentMin 8-chimOutType Junctions WithinBAM SoftClip-chimScoreMin 1-chimScoreDropMax 20-chimJunctionOverhangMin 8-chimSegmentReadGapMax 3-quantMode GeneCounts-outSAMstrandField intronMotif-outFilterIntronStrands None-chimMainSegmentMult Nmax 2-outSAMattributes NH HI AS nM NM MD jM jI XS ch. Alignment to the virus genome reference NC_045512.2 was performed using bowtie2-2.4.1 (Langmead and Salzberg, 2012) on all reads that did not map to the human genome. Read counts on plus-/minus-strand were counted using custom python scripts. Exact positioning of the reads on plus-/minus-strand was done splitting the bam files aligned to NC_045512.2 using samtools-f 0 × 10 and samtools-F 0 × 10 (v0.1.19–44428cd) and bedtools genomecov-ibam BAM NC_045512.2-d (bedtools v2.17.0).

RNA profiling

Gene counts were determined using HTSeq (v0.12.4) (Anders et al., 2015) and normalized as fragments per kilobase per million (FPKM) after TMM correction. Gene set variation analysis (GSVA) was performed against a set of immune signatures with xCell (Aran et al., 2017) and means were calculated per cell type using custom R-scripts. Graphs and analyses were generated using R (v.3.6.0). Differential gene expression was conducted using edgeR (Robinson et al., 2010). Differentially expressed genes were selected with FDR<0.05, logCPM>1, and FPKM>1 in at least 5 samples. Clustering of differentially expressed genes was performed using hclust hierachical clustering and subsequent cutting of the gene tree at R function cutree with h = 0.25. Gene set enrichment analysis for clusters was done using the online tool (https://www.gsea-msigdb.org/gsea/msigdb/annotate.jsp) (Subramanian et al., 2005) for canonical pathways and FDR<0.05.

Single cell transcriptomic metanalysis

Selected genes from single-cell transcriptomic metadata from Xu et al. (Xu et al. (2020) and Delorey et al. (Delorey et al. (2021) were analyzed with the single-cell atlas database SCovid (Qi et al., 2022).

Microbiome analysis based on RNAseq

Microbiome analysis was performed with the following steps using all reads from STAR alignment not mapping to the human reference: quality filtering using fastx-q 30-p 26-Q33 (v0.0.13) cleaning of the fasta file using seqclean-x86_64-N-M-A, realigning to the human reference using blastn against all databases and removal of all reads with 94% similarity. Remaining reads were annotated using MetaPhlAn2 (v2.6.0) (Segata et al., 2012) and Pathseq (GATK v4.1.0.0) (Kostic et al., 2011) with default settings.

Microbiome analysis based on the 16S rRNA gene and internal transcribed spacers (ITS)

Bacterial (16S rRNA gene) and fungal (ITS) microbiome analysis from lung tissue was done from FFPE samples which enabled us to preselect samples based on histology showing unambiguous pathology (i.e. DAD vs. pneumonia). DNA was extracted from FFPE tissues using the Maxwell 16 Tissue DNA Purification Kit (Promega). DNA concentration was measured by Picogreen fluorescence. The variable V4 region of the bacterial 16S rRNA gene was amplified with PCR using oligonucleotide primers 16S_515_f and 16S_806_r (Maiwald, 2011) from 50 ng DNA extracted from lung tissue. Likewise, fungal ITS sequences were amplified with primers ITS1 and ITS2 (Halwachs et al., 2017). PCR was performed using the 16S Complete PCR Mastermix Kit (Molzym). The first PCR reaction product was subjected to a second round of PCR

with primers fusing the 16S/ITS primer sequence to the A and P adapters necessary for Ion Torrent sequencing whileadditionally including a molecular barcode sequence to allow multiplexing of up to 96 samples simultaneously. PCR products were subjected to agarose gel electrophoresis and the band of the expected length (about 330 bp) was excised from the gel and purified using the QIAQick (Qiagen) gel extraction system. DNA concentration of the final PCR product was measured by Picogreen fluorescence. Amplicons from up to 60 samples were pooled equimolarly and sequencing was performed on Ion Torrent XL benchtop sequencer using the Ion 400 bp sequencing chemistry (all reagents from ThermoFisher). Sequences were split by barcode and transferred to the Torrent suite server. Raw bam-files comprised of single-end reads generated by NGS, were converted from bam files to fastq.gz files by using samtools (Danecek et al., 2021). Quality control and preprocessing of sequences was performed using FastQC (version 0.7), MultiQC (version 1.7) and trimmomatic (version 0.36.5) using following parameters: LEADING:3 TRAILING:3 SLIDINGWINDOW:4:15 MINLEN:200. Sequence processing and microbiome analysis was performed using QIIME2 (version 2020.6) (Bolyen et al., 2019). After quality filtering all samples with less than 9833 reads/sample were excluded from downstream analysis. In concordance with RNA-Seq analysis Covid-1 was excluded for sub-analysis (cause of death: myocardial infarction), resulting in 18 Covid-19 and 12 control samples for 16S analysis (average frequency: 28201.7 reads/sample). For ITS analysis only 1 sample showed more than 9833 reads/per sample (case #18: 10272 reads). All other samples showed no clear ITS signal with a sequencing depth of maximum 219 reads per sample and were therefore discarded. Denoising, dereplication and chimera filtering of single-end reads were performed using DADA2 (denoise-pyro) (Callahan et al., 2016). 16S-based analysis was performed with the latest SILVA 138 taxonomy and the Naive Bayes classifier trained on Silva 138 99% OTUs full-length sequences (Quast et al., 2013). For ITS-based analysis a classifier was trained on the UNITE reference database (ver8-99-classifier; 04.02.2020) (Nilsson et al., 2019) according to John Quensen (http://john-quensen.com/tutorials/training-the-qiime2-classifier-with-unite-its-reference-sequences/; assessed 20/08/2020). Differences in microbial composition between groups were tested with implemented QIIME2 plugins using PERMANOVA ($p < 0.05$, qiime diversity beta-group-significance: Bray-Curtis, Jaccard, Unweighted UniFrac, Weighted UniFrac) and Kruskal-Wallis ($p < 0.05$, qiime diversity alpha-group-significance: Observed features, Shannon, Evenness, Faith PD). For metagenomic biomarker discovery taxonomic feature-tables served as input for the LEfSe (linear discriminant analysis effect size) method (Galaxy version 1.0; $p < 0.05$, LDA>2, All-against-all) (Segata et al., 2011). Plots were generated with R (version 3.6.2)6 in RStudio (1.1.463)7 using following packages: tidyverse (1.3.0)8, qiime2r (0.99.6)9, ggplot2 (3.3.3)10, dplyr (1.0.6)11 and ggpubr (0.4.0.999)12 and GraphPad Prism. The graphical abstract was created with BioRender (www.BioRender.com).

Protein isolation and western blot

Proteins from lung tissues were extracted with TRIzol® (ThermoFisher) according to the supplier's protocol. Briefly, tissue homogenates were subjected to phase separation wherein the organic phase containing the protein was further processed. Four volumes of ice-cold acetone were added to the organic phase and the mixture was incubated at −20 °C overnight, followed by a centrifugation step (13000 rpm) at 4 °C for 15 min. The supernatant was discarded and the pellets were dried at 60 °C for 60 min. Subsequently, 100 µL RIPA buffer (Sigma) containing protease inhibitors and phosphatase (0.1 mM Pefabloc, 1 mM DTT, 1X cOmplete™ Mini, 1X PhosSTOP™) and 1 % SDS (Roche) were added and the mixture incubated at 65 °C for 90 min. Supernatants were transferred to a new Eppendorf tube and 100 µL 8 M urea in 0.05 M Tris (pH 8,5) and 1% SDS were added and incubated at 55 °C for 30 min. Corresponding supernatants and pellets were pooled and transferred to 2 mL MagNA Lyser tubes (Roche) with ceramic beads and homogenized 2 times at 6500 rpm for 20 sec. Samples were incubated on ice for 10 min and subsequently centrifugated with 13000rpmat 4 °C for 15 min. Supernatants were transferred to new Eppendorf tubes. For western blotting proteins were mixed with 4X Laemmli buffer (Bio-Rad) and incubated for 10minat 95 °C and then loaded onto 11% (v/v) SDS-PAGE gels (Amersham) and electrophoresed at 80 mA for 2 h and subsequently transferred onto nitrocellulose membranes (Amersham). Blotting efficiency was determined with Ponceau staining (Ponceau S solution, Sigma). Non-specific binding was blocked with 5% (w/v) non-fat dry milk (Bio-Rad) in TRIS-buffered saline and 0.1% (v/v) Tween 20 (Merck) for 1 h. Subsequently, the membranes were incubated with antibodies against C1q (Dako Denmark A/S 1:5000), TGFß1 (Cell Signaling Technology, 1:1000), and GAPDH (Cell Signaling Technology, 1:1000) overnight at 4 °C. Thereafter, membranes were washed and incubated with the appropriate HRP-conjugated secondary antibody (Amersham, ECL Anti-Rabbit IgG, 1:5000). Immunolabeling was detected using ECL Select Western Blot Reagent (Amersham) and visualized with the ImageQuant™ LAS 500 instrument (Amersham). GAPDH was used as

loading control to determine protein abundance and band density was quantified and compared by using ImageJ.

QUANTIFICATION AND STATISTICAL ANALYSIS

GraphPad Prism and R were used for data analysis and imaging. All data are represented as means ± SD if not otherwise specified. Statistical significance testing employed the Mann-Whitney and Kruskal-Wallis tests and p-values <0.05 were considered statistically significant. Correlation analyses employed Spearman and Pearson correlation. For differentially gene expression and gene enrichment analyses a False Discovery Rate (FDR) <0.05 was used. Permanova was used for statistical determination in the Principal Component Analysis (PCA). The *n* number is specific for the number of human subjects.

Surveillance of Wildlife Diseases from the National Forestry and Grassland Administration.

About the Author

Mr. Li is a graduate student at the College of Wildlife and Protected Area at Northeast Forestry University in Heilongjiang, China. His primary research interest is the epidemiology of influenza viruses.

References

1. Gu M, Liu W, Cao Y, Peng D, Wang X, Wan H, et al. Novel reassortant highly pathogenic avian influenza (H5N5) viruses in domestic ducks, China. Emerg Infect Dis. 2011;17:1060–3. https://doi.org/10.3201/eid/1706.101406
2. Wu H, Peng X, Xu L, Jin C, Cheng L, Lu X, et al. Novel reassortant influenza A(H5N8) viruses in domestic ducks, eastern China. Emerg Infect Dis. 2014;20:1315–8. https://doi.org/10.3201/eid2008.140339
3. Cui Y, Li Y, Li M, Zhao L, Wang D, Tian J, et al. Evolution and extensive reassortment of H5 influenza viruses isolated from wild birds in China over the past decade. Emerg Microbes Infect. 2020;9:1793–803. https://doi.org/10.1080/22221751.2020.1797542
4. Global Consortium for H5N8 and Related Influenza Viruses. Role for migratory wild birds in the global spread of avian influenza H5N8. Science. 2016;354:213–7. https://doi.org/10.1126/science.aaf8852
5. Li M, Liu H, Bi Y, Sun J, Wong G, Liu D, et al. Highly pathogenic avian influenza A(H5N8) virus in wild migratory birds, Qinghai Lake, China. Emerg Infect Dis. 2017;23:637–41. https://doi.org/10.3201/eid2304.161866
6. Li Y, Li M, Li Y, Tian J, Bai X, Yang C, et al. Outbreaks of highly pathogenic avian influenza (H5N6) virus subclade 2.3.4.4h in swans, Xinjiang, western China, 2020. Emerg Infect Dis. 2020;26:2956–60. https://doi.org/10.3201/eid2612.201201
7. Lewis NS, Banyard AC, Whittard E, Karibayev T, Al Kafagi T, Chvala I, et al. Emergence and spread of novel H5N8, H5N5 and H5N1 clade 2.3.4.4 highly pathogenic avian influenza in 2020. Emerg Microbes Infect. 2021;10:148–51. https://doi.org/10.1080/22221751.2021.1872355
8. Saito T, Tanikawa T, Uchida Y, Takemae N, Kanehira K, Tsunekuni R. Intracontinental and intercontinental dissemination of Asian H5 highly pathogenic avian influenza virus (clade 2.3.4.4) in the winter of 2014–2015. Rev Med Virol. 2015;25:388–405. https://doi.org/10.1002/rmv.1857
9. Sorensen MC, Dixit T, Kardynal KJ, Newton J, Hobson KA, Bensch S, et al. Migration distance does not predict blood parasitism in a migratory songbird. Ecol Evol. 2019;9:8294–304. https://doi.org/10.1002/ece3.5404
10. Li S, Meng W, Liu D, Yang Q, Chen L, Dai Q, et al. Migratory whooper swans *Cygnus cygnus* transmit H5N1 virus between China and Mongolia: combination evidence from satellite tracking and phylogenetics analysis. Sci Rep. 2018;8:7049. https://doi.org/10.1038/s41598-018-25291-1

Address for correspondence: Hongliang Chai, College of Wildlife and Protected Area, Northeast Forestry University, No. 26 Hexing Rd, Xiangfang District, Harbin 150040, Heilongjiang, China; email: hongliang_chai@hotmail.com

Rapid Antigen Test for Postmortem Evaluation of SARS-CoV-2 Carriage

Martin Zacharias, Verena Stangl, Andrea Thüringer, Martina Loibner, Philipp Wurm, Stella Wolfgruber, Kurt Zatloukal, Karl Kashofer, Gregor Gorkiewicz

Author affiliation: Medical University of Graz, Graz, Austria

DOI: https://doi.org/10.3201/eid2706.210226

Detecting severe acute respiratory syndrome coronavirus 2 in deceased patients is key when considering appropriate safety measures to prevent infection during postmortem examinations. A prospective cohort study comparing a rapid antigen test with quantitative reverse transcription PCR showed the rapid test's usability as a tool to guide autopsy practice.

Rapid detection of severe acute respiratory syndrome coronavirus 2 (SARS-CoV-2) is essential to prevent viral dissemination. Rapid antigen tests (RATs) have recently been approved and are now widely used in the current coronavirus disease (COVID-19) pandemic (1). Although the performance of RATs has been evaluated extensively in clinics (2–4), data on postmortem testing are still lacking (5).

We performed a prospective cohort study in which we evaluated the performance of the Roche/SD Biosensor SARS-CoV-2 RAT (https://www.roche.com) in 30 consecutive deceased COVID-19 patients at the University Hospital, Medical University of Graz (Graz, Austria), during November 28–December 23, 2020. We tested each corpse with nasopharyngeal swabs for RAT (using the manufacturer's kit) and eSwabs (https://www.copanusa.com) for quantitative reverse transcription PCR (qRT-PCR) targeted to the viral envelope (E) and nucleocapsid (N) genes of SARS-CoV-2. Furthermore, we used virus isolation from lung tissue swabs from an additional cohort of deceased COVID-19 patients (n = 11) to compare molecular detection and virus cultivability (Appendix, https://wwwnc.cdc.gov/EID/article/27/6/21-0226-App1.pdf).

All patients were Caucasian, median age was 78 years (range 62–93 years), and 51.2% were female. The median disease duration (interval between the first positive SARS-CoV-2 PCR and death) was 11 days (range 1–43 days). The median postmortem interval (time between death and specimen sampling) was 23 hours (range 8–124 hours; Table; Appendix).

PCR is the current standard for SARS-CoV-2 detection (*1*,*2*). In our cohort, qRT-PCR targeted to the E gene showed a higher sensitivity than qRT-PCR for

Table. Patient characteristics and postmortem data for investigation of rapid antigen test for postmortem evaluation of SARS-CoV-2 carriage, Graz, Austria*

Characteristic	RAT cohort, n = 30	Culture cohort, n = 11
Age, y, median (range)	78 (62–93)	79 (65–93)
Sex, no. (%)		
M	14 (47.7)	6 (56)
F	16 (53.3)	5 (45.4)
Disease duration,† d, median (range)	12 (1–43)	9 (3–34)
Postmortem interval‡, h, median (range)	22 (8–124)	25 (14–68)
qRT-PCR positive, no. (%)	24 (80)	11 (100)
C_t value, median (range)		
E gene	22.8 (14.1–37.3)	19.9 (13.7–36.0)
N gene	26.9 (18.0–34.6)	24.6 (17.3–33.7)
Cultivation positive, no. (%)	NA	7 (63.6)
RAT positive, no. (%)	17 (56.7%)	NA
Total RAT specificity (95% CI§), n = 30	100% (61%–100%)	NA
RAT sensitivity (95% CI§), n = 30	70.8% (50.8%–85.1%)	NA
Total, n = 30		
C_t ≤35,¶ n = 23	73.9% (53.5%–87.5%)	NA
C_t ≤30,¶ n = 18	94.4% (74.2%–99.7%)	NA
C_t ≤25,¶ n = 16	100% (80.6%–100%)	NA

*C_t, cycle threshold; E, envelope; N, nucleocapsid; NA, not applicable; qRT-PCR, quantitative reverse transcription PCR: RAT, rapid antigen test; SARS-CoV-2, severe acute respiratory syndrome coronavirus 2.
†Interval from first positive (antemortem) SARS-CoV-2 PCR to death.
‡Interval from death to specimen sampling.
§Determined via the hybrid Wilson/Brown method (*10*).
¶Determined via E gene qRT-PCR.

the N gene (Appendix Figure 1). Consequently, we used E gene qRT-PCR as the reference in subsequent evaluations. Results showed that 80% (24/30) of cases were qRT-PCR positive, whereas 56.7% (17/30) were RAT positive (Figure, panel A). RAT had an overall specificity of 100% (95% CI 61%–100%) and an overall sensitivity of 70.8% (95% CI 50.8%–85.1%) when using E gene qRT-PCR as the reference. RAT negative cases showed significantly higher C_t values in qRT-PCR compared with RAT positive cases (mean 38.24 [SD 7.01] vs 20.74 [SD 3.46]; Figure, panel B). Correspondingly, RAT sensitivity increased when cases were stratified according to C_t values (C_t ≤35, sensitivity 73.9% [95% CI 53.5%–87.5%]; C_t ≤30, sensitivity 94.4% [95% CI 74.2%–99.7%]; C_t ≤25, sensitivity 100% [95% CI 80.6%–100%]; (Table; Appendix Table 1). Furthermore, when we compared qRT-PCR results from nasopharyngeal swabs of patients in which viral culture was performed (from corresponding lung tissue swabs of an additional cohort), cultivability was restricted to cases with C_t values ≤23.7, which is below the threshold of false-negative RAT cases (C_t values ≥25.8; Figure, panels B, C). These results are in line with most clinical RAT studies that also used virus culture (*2*–*4*,*6*), in which cultivability is exceedingly rare in cases with low viral loads determined with qRT-PCR. We used cultivation from lung tissue swab specimens for this analysis because the lung often shows increased SARS-CoV-2 loads in deceased patients (*7*; Appendix Table 2) and therefore represents a major infection source during autopsy.

Furthermore, we determined parameters that influenced test performance. We noted a significant positive correlation between disease duration and C_t values (Figure, panel D). Such correlation was also evident in RATs; all cases with disease courses >17 days were RAT negative (Figure, panel E). Postmortem intervals did not correlate with C_t values or RAT results (Figure, panels G, H). Thus, a long disease duration rather than a long postmortem interval seems to be the main factor for increased C_t values and negative RATs. RAT and cultivation results closely mirrored each other with respect to viral load (Figure, panels B, C), disease duration (Figure, panels E, F), and postmortem interval (Figure, panels H, I).

Although RAT had an overall lower sensitivity than qRT-PCR in this study, our data suggest that viral loads of false-negative RAT cases are probably below the threshold of cultivability. Because culture is regarded as a measure of virus viability and infectivity (*8*), these cases likely pose only minimal risks of SARS-CoV-2 transmission during postmortem examinations. However, each corpse having a postmortem evaluation must be treated as potentially infectious. Even a PCR-negative nasopharyngeal swab specimen does not exclude the presence of viable virus in other body sites, as shown in COVID-19 (*7*), thus emphasizing the general application of appropriate autopsy safety measures.

In conclusion, RAT should not be seen as a potential replacement for but rather as an addition to of current postmortem testing strategies. Especially

when qRT-PCR is not readily available, RAT might be useful in selecting the most hazardous corpses that should be examined under special conditions (e.g., Biosafety Level 3 [9]). RAT could therefore be a valuable adjunct tool in guiding autopsy practice.

About the Author

Dr. Zacharias is a physician-scientist at the Diagnostic and Research Institute of Pathology, Medical University of Graz, Graz, Austria. His main research interests include pulmonary and infectious disease pathology.

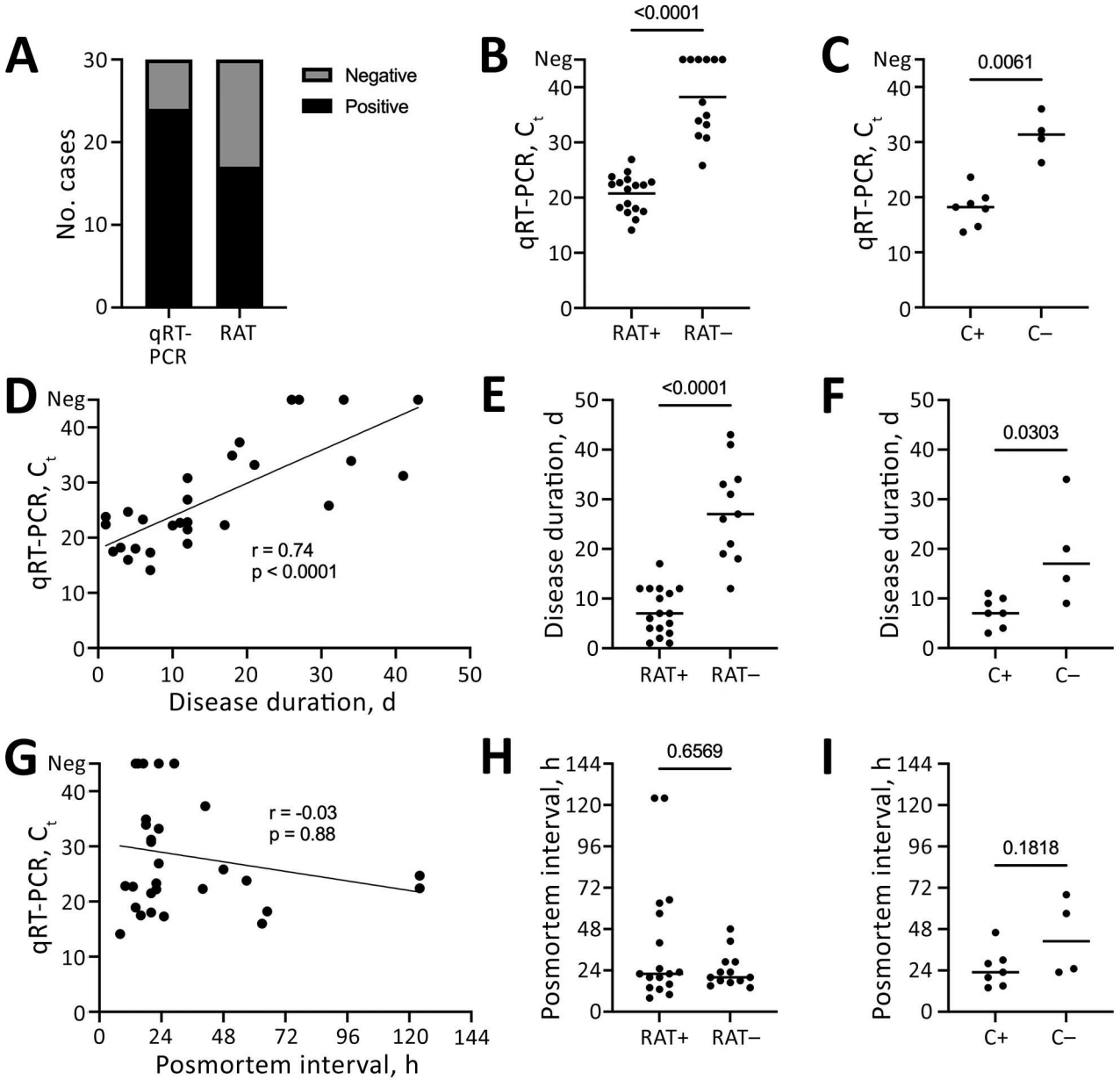

Figure. Postmortem detection and cultivation of SARS-CoV-2 for investigation of RAT for postmortem evaluation of SARS-CoV-2 carriage, Graz, Austria. A) Among 30 deceased SARS-CoV-2 patients, RAT detected fewer positive cases than did qRT-PCR. B) RAT-negative cases show significantly higher C_t values in qRT-PCR compared with RAT-positive cases (Mann-Whitney test). C) Cultivation negative and positive cases mirror C_t values of RAT results (Mann-Whitney test). D–F) Longer disease durations are significantly correlated with higher C_t values (Spearman correlation test; D), negative RAT results (Mann-Whitney test; E), and negative cultivation results (Mann-Whitney test; F). G–I) No significant correlation was found between postmortem intervals and C_t values (Spearman correlation test; G), RAT results (Mann-Whitney test; H), or cultivation results (Mann-Whitney test; I). C, cultivation; C_t, cycle threshold; neg, negative; qRT-PCR, quantitative reverse transcription PCR; RAT, rapid antigen test; SARS-CoV-2, severe acute respiratory syndrome coronavirus 2; +, positive; –, negative.

References

1. Centers for Disease Control and Prevention. Interim guidance for antigen testing for SARS-CoV-2 [cited 2021 Mar 27]. https://www.cdc.gov/coronavirus/2019-ncov/lab/resources/antigen-tests-guidelines.html
2. Dinnes J, Deeks JJ, Berhane S, Taylor M, Adriano A, Davenport C, et al.; Cochrane COVID-19 Diagnostic Test Accuracy Group. Rapid, point-of-care antigen and molecular-based tests for diagnosis of SARS-CoV-2 infection. Cochrane Database Syst Rev. 2021;3:CD013705.
3. Albert E, Torres I, Bueno F, Huntley D, Molla E, Fernández-Fuentes MÁ, et al. Field evaluation of a rapid antigen test (Panbio™ COVID-19 Ag Rapid Test Device) for COVID-19 diagnosis in primary healthcare centres. Clin Microbiol Infect. 2021;27:472.e7–10. https://doi.org/10.1016/j.cmi.2020.11.004
4. Iglòi Z, Velzing J, van Beek J, van de Vijver D, Aron G, Ensing R, et al. Clinical evaluation of Roche SD Biosensor rapid antigen test for SARS-CoV-2 in municipal health service testing site, the Netherlands. Emerg Infect Dis. 2021 Mar 16 [Epub ahead of print]. https://doi.org/10.3201/eid2705.204688
5. Centers for Disease Control and Prevention. Collection and submission of postmortem specimens from deceased persons with confirmed or suspected COVID-19: postmortem guidance [cited 2021 Mar 27]. https://www.cdc.gov/coronavirus/2019-ncov/hcp/guidance-postmortem-specimens.html
6. Singanayagam A, Patel M, Charlett A, Lopez Bernal J, Saliba V, Ellis J, et al. Duration of infectiousness and correlation with RT-PCR cycle threshold values in cases of COVID-19, England, January to May 2020. Euro Surveill. 2020;25:2001483. https://doi.org/10.2807/1560-7917.ES.2020.25.32.2001483
7. Puelles VG, Lütgehetmann M, Lindenmeyer MT, Sperhake JP, Wong MN, Allweiss L, et al. Multiorgan and renal tropism of SARS-CoV-2. N Engl J Med. 2020;383:590–2. https://doi.org/10.1056/NEJMc2011400
8. Jefferson T, Spencer EA, Brassey J, Heneghan C. Viral cultures for COVID-19 infectious potential assessment—a systematic review. Clin Infect Dis. 2020 Dec 20 [Epub ahead of print]. https://doi.org/10.1093/cid/ciaa1764
9. Loibner M, Langner C, Regitnig P, Gorkiewicz G, Zatloukal K. Biosafety requirements for autopsies of patients with COVID-19: example of a BSL-3 autopsy facility designed for highly pathogenic agents. Pathobiology. 2021;88:37–45. https://doi.org/10.1159/000513438
10. Brown LD, Cai TT, DasGupta A. Interval estimation for a binomial proportion. Stat Sci. 2001;16:101–33. https://doi.org/10.1214/ss/1009213286

Address for correspondence: Martin Zacharias, Diagnostic and Research Institute of Pathology, Medical University of Graz, Neue Stiftingtalstraße 6, 8010 Graz, Austria; email: martin.zacharias@medunigraz.at

Respiratory Viral Shedding in Healthcare Workers Reinfected with SARS-CoV-2, Brazil, 2020

Mariene R. Amorim,[1] William M. Souza,[1] Antonio C.G. Barros Jr., Daniel A. Toledo-Teixeira, Karina Bispo-dos-Santos, Camila L. Simeoni, Pierina L. Parise, Aline Vieira, Julia Forato, Ingra M. Claro, Luciana S. Mofatto, Priscila P. Barbosa, Natalia S. Brunetti, Emerson S.S. França, Gisele A. Pedroso, Barbara F.N. Carvalho, Tania R. Zaccariotto, Kamila C.S. Krywacz, André S. Vieira, Marcelo A. Mori, Alessandro S. Farias, Maria H.P. Pavan, Luís Felipe Bachur, Luís G.O. Cardoso, Fernando R. Spilki, Ester C. Sabino, Nuno R. Faria, Magnun N.N. Santos, Rodrigo Angerami, Patricia A.F. Leme, Angelica Schreiber, Maria L. Moretti, Fabiana Granja, José Luiz Proenca-Modena

Author affiliations: University of Campinas, Campinas, Brazil (M.R. Amorim, A.C.G. Barros Jr., D.A. Toledo-Teixeira, K. Bispo-dos-Santos, C.L. Simeoni, P.L. Parise, A. Vieira, J. Forato, L.S. Mofatto, P.P. Barbosa, N.S. Brunetti, E.S.S. França, G.A. Pedroso, B.F.N. Carvalho, T.R. Zaccariotto, K.C.S. Krywacz, A.S. Vieira, M.A. Mori, A.S. Farias, M.H.P. Pavan, L.F. Bachur, L.G.O. Cardoso, M.N.N. Santos, R. Angerami, P.A.F. Leme, A. Schreiber, M.L. Moretti, F. Granja, J.L. Proenca-Modena); University of São Paulo, São Paulo, Brazil (W.M. Souza, I.M. Claro, E.C. Sabino, N.R. Faria); Feevale University, Novo Hamburgo, Brazil (F.R. Spilki); University of Oxford, Oxford, UK (N.R. Faria); Imperial College London, London, UK (N.R. Faria); Campinas Department of Public Health Surveillance, Campinas (R. Angerami); Federal University of Roraima, Boa Vista, Brazil (F. Granja)

DOI: https://doi.org/10.3201/eid2706.210558

We documented 4 cases of severe acute respiratory syndrome coronavirus 2 reinfection by non–variant of concern strains among healthcare workers in Campinas, Brazil. We isolated infectious particles from nasopharyngeal secretions during both infection episodes. Improved and continued protection measures are necessary to mitigate the risk for reinfection among healthcare workers.

Coronavirus disease (COVID-19) is caused by severe acute respiratory syndrome coronavirus 2 (SARS-CoV-2), which emerged in Wuhan, China,

[1]These authors contributed equally to this article.

Article DOI: https://doi.org/10.3201/eid2706.210226

Rapid Antigen Test for Postmortem Evaluation of SARS-CoV-2 Carriage

Appendix

Materials and Methods

Case Description

Clinical parameters were obtained from electronic medical records and are shown in Table 1 and Appendix Tables 1 and 2. The study was approved by the institutional review board of the Medical University of Graz, Austria (32–362ex19/20).

SARS-CoV-2 Quantitative Reverse Transcription PCR (qRT-PCR)

We extracted RNA from 200 µL eSwab solution using the Maxwell simplyRNA Blood Kit (Promega, https://www.promega.com) eluting RNA in 50 µL distilled water. qRT-PCR detected regions of the viral envelope (E) and nucleocapsid (N) specific to SARS-CoV-2 (*1*). Primers, probes, and 5 µL of RNA solution were added to 10 µL of SuperScript III One-Step RT-PCR System withµ Platinum *Taq* High Fidelity DNA Polymerase (Thermo Fisher, https://www.thermofisher.com) master mix. PCR was performed on a Quantstudio 7 instrument (Thermo Fisher) with the following cycling conditions: 55°C 15 min, 95°C 3 min; 45 cycles (95°C 15 sec; 58°C 30 sec). We used human glyceraldehyde 3-phosphate dehydrogenase (GAPDH) mRNA as internal RNA control with the same cycling conditions. All primers and probes were from Eurofins Scientific (https://www.eurofins.com).

We downloaded and processed amplification data using the qpcR package of the R project (https://www.r-project.org). Amplification efficiency plots were visually inspected, and Cp2D (cycle peak of second derivative) values were calculated for samples with valid amplification curves. We generated plots with R using the reshape, tidyverse, and ggplot packages.

SARS-CoV-2 Cultivation

For SARS-CoV-2 cultivation, we used swabs from lung parenchyma collected during autopsy. Samples were frozen (−80°C) and thawed (37°C) twice to increase cell lysis and viral release. We added 2 mL OptiPro SFM medium (GIBCO, https://www.thermofisher.com) with 4 mM L-glutamine (GIBCO) and 1% penicillin–streptomycin (10,000 U/mL; GIBCO) were added to the samples. After centrifugation (10 min, 1,500 rcf) the supernatants were filtered through a 0.45 μm membrane filter (Millipore, https://www.sigmaaldrich.com) and inoculated on Vero-E6 cells with OptiPro SFM medium with 4 mM L-glutamine and 1% penicillin–streptomycin in T25 flasks (Thermo Fisher). After 3–4 days incubation at 37°C and 5% CO_2, the whole cells were detached and passaged, including the supernatant, to new Vero-E6 cells growing in T75 flasks (Thermo Fisher). After 1 week, we harvested the cells and stored the supernatants after centrifugation (10 min, 1,500 rcf) at −80°C.

Reference

1. Corman VM, Landt O, Kaiser M, Molenkamp R, Meijer A, Chu DK, et al. Detection of 2019 novel coronavirus (2019-nCoV) by real-time RT-PCR. Euro Surveill. 2020;25:2000045. PubMed https://doi.org/10.2807/1560-7917.ES.2020.25.3.2000045

Appendix Table 1. Case characteristics and postmortem data of the RAT cohort*

Case no.	Age, y/sex	Disease duration, d†	Postmortem interval, h‡	RAT	qRT-PCR	C_t value E gene	C_t value N gene	C_t value GAPDH
1	79/F	5	20	Positive	Positive	18	22	21.3
2	75/F	31	48	Negative	Positive	25.8	30.3	25.9
3	72/F	1	124	Positive	Positive	22.4	27.7	26.4
4	71/F	18	18	Negative	Positive	34.9	34.6	22.9
5	89/F	12	20	Negative	Positive	30.8	33.2	19.8
6	73/F	6	22	Positive	Positive	23.3	28	22.2
7	88/M	11	13	Positive	Positive	22.7	27.4	25.4
8	87/M	NA	14	Negative	Negative	NA	NA	21.2
9	73/M	41	20	Negative	Positive	31.2	33.2	23.8
10	78/M	17	40	Positive	Positive	22.3	26.9	26
11	87/F	4	63	Positive	Positive	16	20.8	25.7
12	70/M	3	65	Positive	Positive	18.2	22.6	22.6
13	84/F	1	57	Positive	Positive	23.8	28.1	27.5
14	90/F	19	41	Negative	Positive	37.3	NA	24.2
15	76/M	27	29	Negative	Negative	NA	NA	23.5
16	78/F	7	25	Positive	Positive	17.3	22.2	21.9
17	76/M	12	14	Positive	Positive	18.9	23.5	25.1
18	62/M	34	18	Negative	Positive	33.9	NA	23.2
19	90/F	4	124	Positive	Positive	24.7	29.2	26.5
20	67/M	12	23	Positive	Positive	26.9	29.7	26.7
21	73/F	10	22	Positive	Positive	22.2	25.7	23.5
22	73/F	12	20	Positive	Positive	21.5	24.4	20.8
23	80/F	12	10	Positive	Positive	22.8	25.9	25.3
24	77/M	43	15	Negative	Negative	NA	NA	25.7
25	93/F	2	16	Positive	Positive	17.5	20.8	23.6
26	87/M	26	29	Negative	Negative	NA	NA	24.2
27	91/M	21	23	Negative	Positive	33.2	NA	23.5
28	77/F	NA	23	Negative	Negative	NA	NA	21
29	79/M	33	17	Negative	Negative	NA	NA	29.7
30	87/M	7	8	Positive	Positive	14.1	18	25.4

*C_t, cycle threshold; E, envelope; GAPDH, human glyceraldehyde 3-phosphate dehydrogenase; N, nucleocapsid; NA, not applicable; RAT, rapid antigen test.
†Interval from first positive (antemortem) SARS-CoV-2 PCR to death.
‡interval from death to specimen sampling.

Appendix Table 2. Case characteristics and postmortem data of the cultivation cohort*

Case no.	Age, y/sex	Disease duration, d†	Postmortem interval, h‡	Cultivation	qRT-PCR	C_t (E gene) nasopharynx	C_t (E gene) lung	C_t (N gene) nasopharynx	C_t (N gene) lung
1	78/M	10	28	Positive	Positive	23.7	21.3	29.7	27.7
2	82/M	7	15	Positive	Positive	18.2	17.2	25.3	NP
3	78/M	9	68	Negative	Positive	32.1	32.1	33.7	33.3
4	92/F	3	14	Positive	Positive	17.9	16.6	21.5	20
5	71/F	4	30	Positive	Positive	14.7	14.5	18.4	19.5
6	93/F	9	20	Positive	Positive	13.7	16.5	17.3	21.1
7	79/M	14	25	Negative	Positive	26.3	29.5	30	32.8
8	67/M	20	23	Negative	Positive	36	34.4	NA	NA
9	80/F	7	46	Positive	Positive	18.9	22.5	22.7	26
10	80/F	11	23	Positive	Positive	19.9	25.5	23.9	28.5
11	65/M	34	57	Negative	Positive	30.6	NA	32.4	NA

* C_t, cycle threshold; E, envelope; N, nucleocapsid; NA, not applicable; NP, not performed; RAT, rapid antigen test.
†Interval from first positive (antemortem) SARS-CoV-2 PCR to death.
‡Interval from death to specimen sampling.

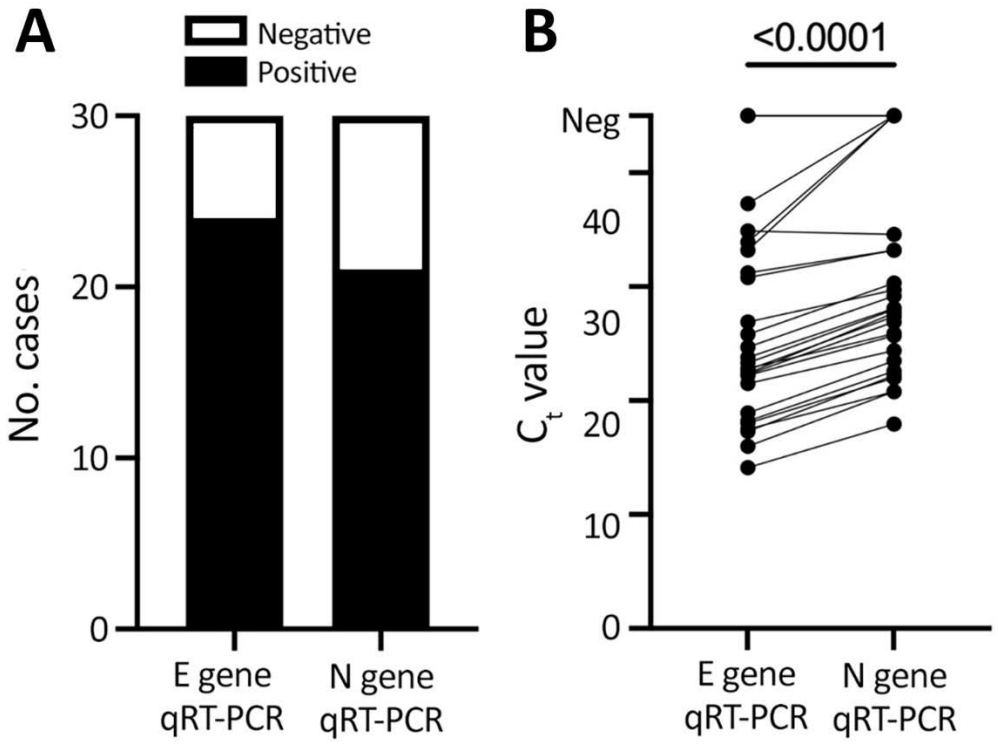

Appendix Figure 1. E gene qRT-PCR has a higher sensitivity than N gene qRT-PCR. A) More negative cases in N gene qRT-PCR compared with E gene qRT-PCR**.** B) Significantly higher C_t values in N gene qRT-PCR compared with E gene qRT-PCR (Wilcoxon matched-pairs signed rank test). C_t, cycle threshold; E, envelope; N, nucleocapsid; RAT, rapid antigen test.

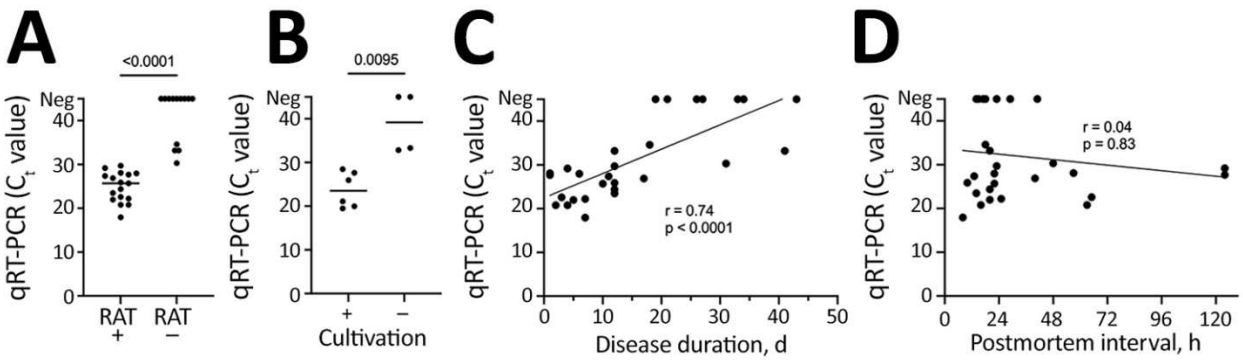

Appendix Figure 2. N gene qRT-PCR results. A) RAT negative cases show significantly higher C_t values compared with RAT positive cases (Mann-Whitney test). B) Cultivation negative and positive cases mirror C_t values of RAT results (Mann-Whitney test). C) Longer disease durations are significantly correlated with higher C_t values (Spearman correlation test). D) No significant correlation between postmortem intervals and C_t values (Mann-Whitney test). C_t, cycle threshold; E, envelope; N, nucleocapsid; RAT, rapid antigen test.

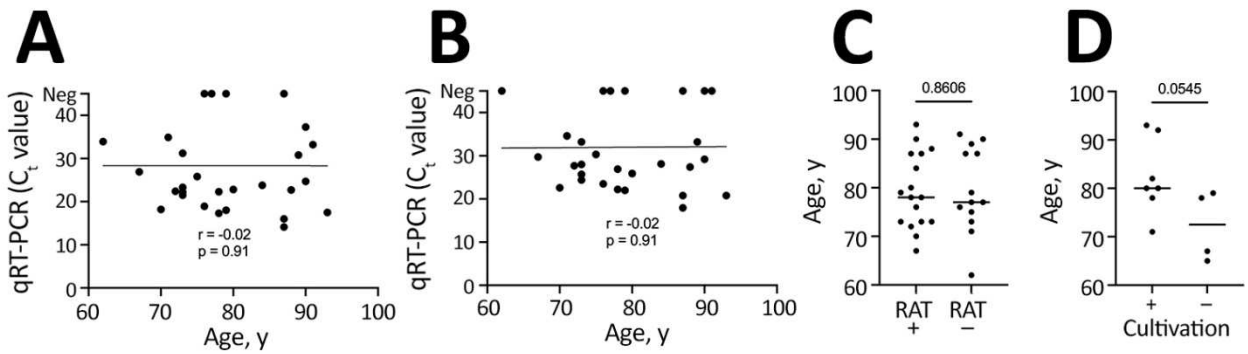

Appendix Figure 3. qRT-PCR, RAT, and cultivation results in relation to patient age. A–D) No significant correlation between age and C_t values (Spearman correlation test), RAT results (Mann-Whitney test), or cultivation results (Mann-Whitney test). C_t, cycle threshold; E, envelope; N, nucleocapsid; RAT, rapid antigen test.

Histopathology

Histopathology 2024, **84**, 702–706. DOI: 10.1111/his.15131

SHORT REPORT

The mutual value of histopathology and ITS sequencing in the diagnosis of mucormycosis

Martin Zacharias,[1] Andrea Thüringer,[1] Robert Krause,[2] Karl Kashofer[1] & Gregor Gorkiewicz[1]

[1]*Diagnostic and Research Institute of Pathology and* [2]*Division of Infectious Diseases, Medical University of Graz, Graz, Austria*

Date of submission 25 September 2023
Accepted for publication 13 December 2023

Zacharias M, Thüringer A, Krause R, Kashofer K & Gorkiewicz G (2024) *Histopathology* **84**, 702–706. https://doi.org/10.1111/his.15131

The mutual value of histopathology and ITS sequencing in the diagnosis of mucormycosis

Aims: Mucormycosis is a fast-progressing disease with a high mortality rate. The most important factor determining survival of patients is early and accurate diagnosis. Although histopathology often recognises invasive mould infections at first, histomorphology alone is insufficient in providing an accurate diagnosis. Unbiased molecular methods to detect and identify fungi are promising, yet their role in complementing routine histopathological workflows has not been studied sufficiently.

Methods and results: We performed a retrospective single-centre study examining the clinical value of complementing histopathology with internal transcribed spacer (ITS) sequencing of fungal DNA in the routine diagnosis of mucormycosis. At our academic centre, we identified 14 consecutive mucormycosis cases diagnosed by histopathology and subsequent ITS sequencing. Using histomorphological examination, fungal hyphae could be detected in all cases; however, morphological features were unreliable regarding specifying the taxa. Subsequent ITS sequencing identified a remarkable phylogenetic diversity among Mucorales: the most common species was *Rhizopus microsporus* (six of 14; 42.9%), followed by *Lichtheimia corymbifera* (three of 14, 21.4%) and single detections of *Rhizopus oryzae*, *Actinomucor elegans*, *Mucor circinelloides*, *Rhizomucor pusillus* and *Rhizomucor miehei* (one of 14; 7.1%, respectively). In one case, we additionally detected *Pneumocystis jirovecii* in the same lung tissue specimen, suggesting a clinically relevant co-infection. Fungal culture was performed in 10 cases but yielded positive results in only two of 10 (20%), revealing its limited value in the diagnosis of mucormycosis.

Conclusions: Our study demonstrates that a combination of histopathology and ITS sequencing is a practically feasible approach that outperforms fungal culture in detecting Mucorales in tissue-associated infections. Therefore, pathologists might adapt diagnostic workflows accordingly when mucormycosis is suspected.

Keywords: histopathology, ITS sequencing, molecular pathology, mucormycosis, mycology

Introduction

The rising incidence of mucormycosis during the COVID-19 pandemic has increased awareness of this rare but highly lethal fungal infection. The fast-progressing clinical course of mucormycosis leads to an overall mortality rate of up to 80%.[1,2] However,

Address for correspondence: M Zacharias and G Gorkiewicz, Diagnostic and Research Institute of Pathology, Medical University of Graz, Neue Stiftingtalstraße 6, 8010 Graz, Austria.
e-mail: martin.zacharias@medunigraz.at and gregor.gorkiewicz@medunigraz.at
K. Kashofer and G. Gorkiewicz contributed equally to this work.

individual prognosis varies, and is largely dependent upon early and accurate diagnosis.[3] In contrast to aspergillosis there are currently no routine antigen tests available for mucormycosis,[4] although promising serological tests have been described recently.[5,6] Furthermore, fungal culture has a low sensitivity in detecting Mucorales.[3,7] It is noteworthy that histopathological identification of moulds within tissue samples is often the first hint towards a diagnosis of mucormycosis.[7] However, exact specification via morphology remains error-prone; in particular, the differentiation of Mucorales from *Aspergillus* spp. (e.g. by the size of hyphae, septation features, etc.) often falls short, but is clinically highly relevant because of divergent treatment regimens.[8] Thus, the inclusion of molecular methods into existing diagnostic workflows could prove valuable. In this study, we aimed to assess the clinical value of complementing traditional diagnostic measures with internal transcribed spacer (ITS) sequencing in the routine histopathology workup of fungal infections.

Methods

We performed a retrospective single-centre study comparing the diagnostic performance of fungal culture, histopathology and ITS sequencing in detection of mucormycosis. The study was approved by the ethics committee of the Medical University of Graz (EK-number: 32–362 ex 19/20). Our cohort included all consecutive mucormycosis cases diagnosed by histopathology and subsequent ITS sequencing at our academic centre between 2015 and 2022. Clinical, pathological and microbiological metadata of these cases were collected retrospectively from electronic medical records and correlated with sequencing results.

ITS sequencing was performed as previously described.[9–11] Briefly, DNA extraction from formalin-fixed paraffin-embedded (FFPE) tissues was performed via mechanical tissue disruption (MagNA Lyser; Roche, Indianapolis, IN, USA) and via an semi-automated extraction system (Maxwell Tissue DNA Purification; Promega, Madison, WI, USA). DNA concentration was measured by Picogreen fluorescence (Promega) and fungal ITS sequences were amplified with the primers ITS1 5′-TCCGTAGGTGAACCTGCGG-3′ and ITS2 5′-GCTGCGTTCTTCATCGATGC-3′. Sequencing was performed on the Ion Torrent S5XL platform using the Ion 400 bp Sequencing Kit (Thermo Fisher Scientific, Waltham, MA, USA). All sequences were bioinformatically processed as previously described.[9–11] The phylogenetic relatedness of detected Mucorales ITS sequences was inferred by using the maximum likelihood method and the Tamura–Nei model,[12] conducted with MEGA11.[13,14]

Results

We identified 14 consecutive mucormycosis cases diagnosed by histopathology and subsequent ITS sequencing. Ten patients were male, and the median age was 53.5 years (range = 5–74 years). All 14 patients had severe comorbidities, mainly haematological malignancies (10 of 14, 71.4%). The most common specimen site of ITS-based Mucorales detection was the lung (eight of 14; 57.1%), followed by the upper respiratory tract and the myocardium (two of 14; 14.3%, respectively), as well as bone and soft tissue (one of 14, 7.1%, respectively). Clinicopathological characteristics of our cohort are summarised in supporting information, Table S1. Using histomorphological examination, fungal hyphae could be detected in all cases and always presented with angioinvasion (Figure 2), a hallmark feature of mucormycosis. This angioinvasivness often leads to vascular occlusion and subsequent infarction of the infected organ, mimicking thromboembolic events clinically. Importantly, angioinvasion is regarded as the main factor driving the fast-progressing clinical course of mucormycosis.[15] Laboratory findings are summarised in supporting information, Tables S2 and S3. Of note, all cases with available blood laboratory parameters presented with varying degrees of lymphopaenia (lymphocyte count range = 0.1–0.9 $\times$ 10^9/l, median = 0.4 $\times$ 10^9/l).

Detected Mucorales showed a remarkable phylogenetic diversity. The most common species was *Rhizopus microsporus* (six of 14; 42.9%), followed by *Lichtheimia corymbifera* (three of 14, 21.4%) and single detections of *Rhizopus oryzae*, *Actinomucor elegans*, *Mucor circinelloides*, *Rhizomucor pusillus* and *Rhizomucor miehei* (one of 14; 7.1%, respectively). Phylogenetic relatedness of detected Mucorales is shown in Figure 1.

Exact species identification enabled by ITS sequencing has important implications for epidemiology and for a clearer understanding of infection routes.[7] This is exemplified, for instance, by case 10, wherein we identified *Rhizomucor miehei*, a fungus thus far mainly described in cheese production, as the causative agent of pulmonary mucormycosis. Of note, this organism was detected in two separate samples from the same patient (BAL and lung tissue) and was also microscopically visible in tissue, excluding the possibility of mere contamination. In another patient (case 14),

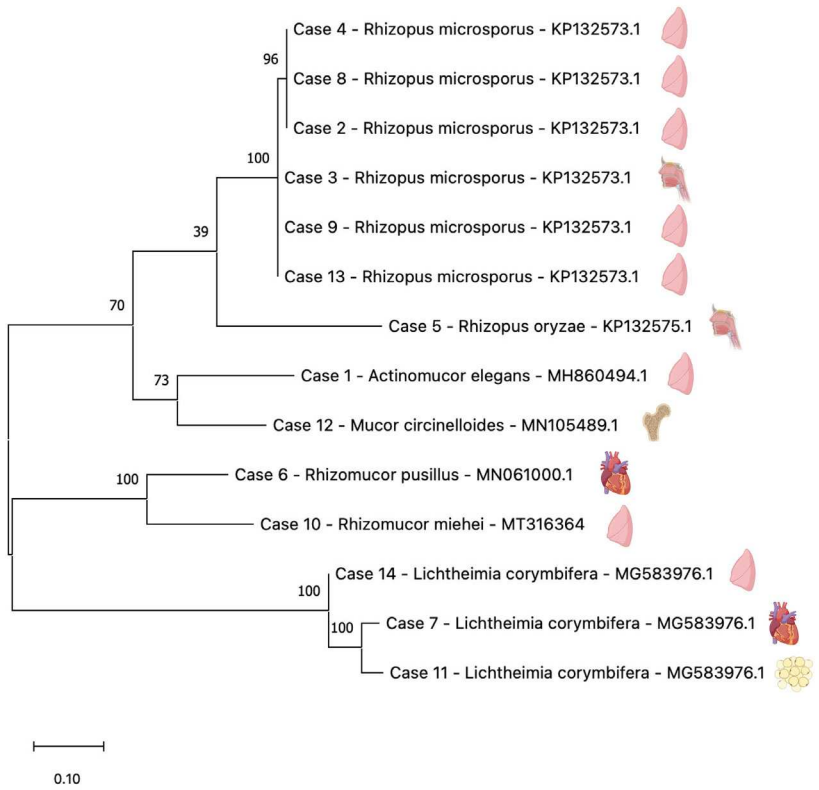

Figure 1. Phylogenetic tree of detected Mucorales. The tree is based on maximum-likelihood analysis (Tamura–Nei model[12]). Bootstrap values (expressed as percentages of 1000 replications) are shown at branch points. The scale bar indicates the number of substitutions per site of branch lengths. GenBank Accession numbers of most homologous hits and tissues of Mucorales detection are also shown. Analysis was performed with MEGA11.[13,14]

our approach enabled us to concomitantly detect *Lichtheimia corymbifera* and *Pneumocystis jirovecii* in the same lung tissue specimen, suggesting a clinically relevant co-infection. In general, species identification of Mucorales is an increasingly recognised factor that might influence treatment efficacy of antifungal agents.[16] For example, *Rhizopus* spp. have shown resistance against amphotericin B and *M. circinelloides* against posaconazole.[17] The translation of such preclinical data to patient care relies upon studies that integrate unbiased species identification which might be achieved by ITS sequencing.

Subsequently, we compared the diagnostic performance of ITS sequencing to fungal culture, currently the method of choice to detect Mucorales. Fungal culture was performed in 10 of 14 (71.4%) of our mucormycosis cases, yielding positive results in only two of 10 (20%; Figure 2A). A false-negative culture result was irrespective of the number of Mucorales reads detected by ITS sequencing (Figure 2B) and irrespective of clearly visible fungal hyphae on histology (Figure 2C,D). Low sensitivity of culture in detection of mucormycosis is in accordance with previous studies,[3,7] underscoring the value of a tissue-based molecular pathology approach.

Discussion

Our study provides evidence that ITS sequencing should be applied when mucormycosis is suspected and tissue is available. Notably, histopathology often raises the first suspicion of mucormycosis, e.g. by presence of angio-invasive moulds associated with ischaemic necrosis, which can then be confirmed immediately by ITS sequencing. In contrast to fungal culture, ITS sequencing can be performed on FFPE tissues, making additional sampling redundant and enabling a rapid and accurate diagnosis.[9] In addition, due to the universal detection of fungal DNA by ITS sequencing, mixed fungal infections can also be detected. This is especially important for patients at risk, which are typically immunocompromised and thus prone to fungal infections. Furthermore, our small series suggests that tissue-based ITS sequencing

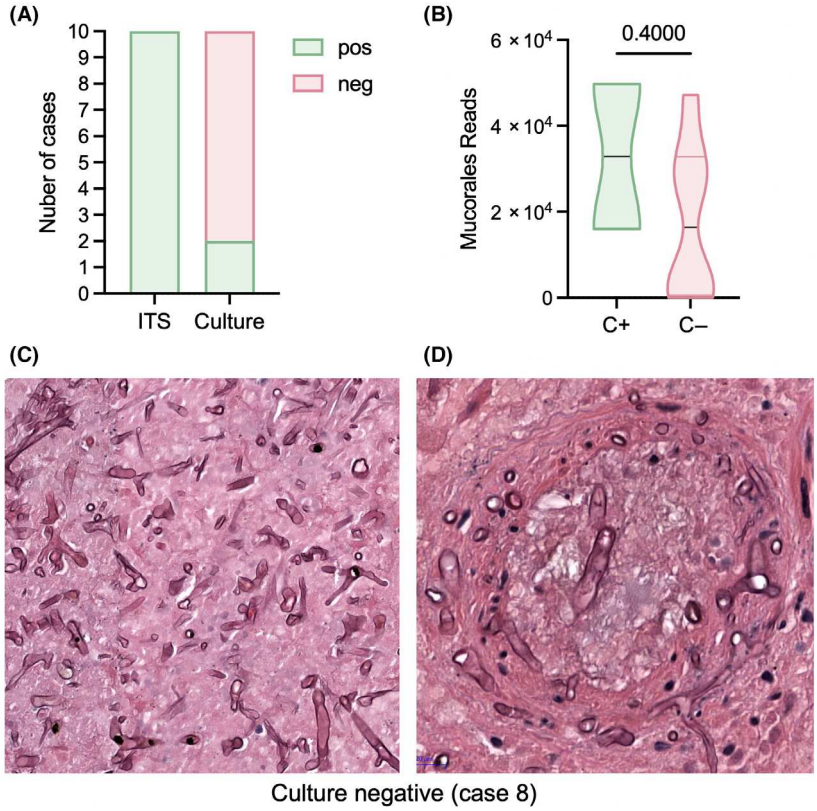

Figure 2. Fungal culture has low sensitivity in the diagnosis of mucormycosis. **A,** Fungal culture was performed in 10 cases, yielding negative results in eight cases. **B,** The number of Mucorales reads determined via ITS sequencing did not show significant differences between culture-positive (C+) and culture-negative (C–) cases (Mann–Whitney test). **C,D,** Abundant fungal hyphae are visible on haematoxylin and eosin (H&E) stain; however, fungal culture yielded negative results (case 8). **D,** Angioinvasion is a hallmark feature of mucormycosis with fungal hyphae concentrated within the wall and the lumen of blood vessels.

has a significantly higher sensitivity than fungal culture in detecting Mucorales, irrespective of the fungal load, which might also be related to the focal nature of Mucorales infection. Additionally, the remarkably high phylogenetic diversity of Mucorales found in our cohort suggests impaired sensitivity when taxon-specific polymerase chain reaction assays would be applied. The ability of ITS sequencing for the differentiation of specific Mucorales species is in line with previous experimental evidence.[18] It is noteworthy that exact species identification enabled by ITS sequencing yields important epidemiological clues for a clearer understanding of infection sources and may guide personalised treatment, even in cases where fungi cannot be cultivated.

In conclusion, we demonstrate that combining histopathology and ITS sequencing is a practically feasible approach that outperforms fungal culture in detecting Mucorales in tissue-associated infections. Therefore, pathologists might adapt diagnostic workflows accordingly when mucormycosis is suspected.

Acknowledgements

No funding was received for this study.

Conflicts of interest

The authors declare no competing interests.

Data availability statement

The data that supports the findings of this study are available in the supplementary material of this article.

References

1. Roden MM, Zaoutis TE, Buchanan WL *et al.* Epidemiology and outcome of zygomycosis: a review of 929 reported cases. *Clin. Infect. Dis.* 2005; **41**; 634–653.
2. Hoenigl M, Seidel D, Carvalho A *et al.* The emergence of COVID-19 associated Mucormycosis: a review of cases from 18 countries. *Lancet Microbe.* 2022; **3**; e543–e552.

3. Walsh TJ, Gamaletsou MN, McGinnis MR, Hayden RT, Kontoyiannis DP. Early clinical and laboratory diagnosis of invasive pulmonary, extrapulmonary, and disseminated mucormycosis (zygomycosis). *Clin. Infect. Dis.* 2012; **54**; S55–S60.
4. Thornton CR. The potential for rapid antigen testing for mucormycosis in the context of COVID-19. *Expert Rev. Mol. Diagn.* 2023; 1–7. https://doi.org/10.1080/14737159.2023.2233906.
5. Potenza L, Vallerini D, Barozzi P *et al*. Mucorales-specific T cells emerge in the course of invasive mucormycosis and may be used as a surrogate diagnostic marker in high-risk patients. *Blood* 2011; **118**; 5416–5419.
6. Burnham-Marusich AR, Hubbard B, Kvam AJ *et al*. Conservation of mannan synthesis in fungi of the zygomycota and ascomycota reveals a broad diagnostic target. *mSphere* 2018; **3**; e00094-18.
7. Cornely OA, Alastruey-Izquierdo A, Arenz D *et al*. Global guideline for the diagnosis and management of mucormycosis: an initiative of the European confederation of medical mycology in cooperation with the mycoses study group education and research consortium. *Lancet Infect. Dis.* 2019; **19**; e405–e421.
8. Sangoi AR, Rogers WM, Longacre TA, Montoya JG, Baron EJ, Banaei N. Challenges and pitfalls of morphologic identification of fungal infections in histologic and cytologic SpecimensA ten-year retrospective review at a single institution. *Am. J. Clin. Pathol.* 2009; **131**; 364–375.
9. Halwachs B, Madhusudhan N, Krause R *et al*. Critical issues in mycobiota analysis. *Front. Microbiol.* 2017; **8**; 180.
10. Zacharias M, Kashofer K, Wurm P *et al*. Host and microbiome features of secondary infections in lethal Covid-19. *Science* 2022; **25**; 104926. https://doi.org/10.1016/j.isci.2022.104926.
11. Guenter S, Gorkiewicz G, Halwachs B *et al*. Impact of ITS-based sequencing on antifungal treatment of patients with suspected invasive fungal infections. *J. Fungi* 2020; **6**; 43.
12. Tamura K, Nei M. Estimation of the number of nucleotide substitutions in the control region of mitochondrial DNA in humans and chimpanzees. *Mol. Biol. Evol.* 1993; **10**; 512–526.
13. Tamura K, Stecher G, Kumar S. MEGA11: molecular evolutionary genetics analysis version 11. *Mol. Biol. Evol.* 2021; **38**; msab120.
14. Stecher G, Tamura K, Kumar S. Molecular evolutionary genetics analysis (MEGA) for MacOS. *Mol. Biol. Evol.* 2020; **37**; 1237–1239.
15. Ibrahim AS, Spellberg B, Walsh TJ, Kontoyiannis DP. Pathogenesis of mucormycosis. *Clin. Infect. Dis.* 2012; **54**; S16–S22.
16. Skiada A, Lass-Floerl C, Klimko N, Ibrahim A, Roilides E, Petrikkos G. Challenges in the diagnosis and treatment of mucormycosis. *Med. Mycol.* 2018; **56**; S93–S101.
17. Vitale RG, de Hoog GS, Schwarz P *et al*. Antifungal susceptibility and phylogeny of opportunistic members of the order mucorales. *J. Clin. Microbiol.* 2012; **50**; 66–75.
18. Schwarz P, Bretagne S, Gantier J-C *et al*. Molecular identification of zygomycetes from culture and experimentally infected tissues. *J. Clin. Microbiol.* 2006; **44**; 340–349.

Supporting Information

Additional Supporting Information may be found in the online version of this article:

Table S1. Clinicopathological characteristics of mucormycosis cases.

Table S2. Laboratory findings of mucormycosis cases (1/2).

Table S3. Laboratory findings of mucormycosis cases (2/2).

Original Article

Reflex testing in non-small cell lung carcinoma using DNA- and RNA-based next-generation sequencing—a single-center experience

Martin Zacharias[1#], Gudrun Absenger[2#], Karl Kashofer[1], Robert Wurm[3], Jörg Lindenmann[4], Angelika Terbuch[2], Selma Konjic[1], Stefan Sauer[1], Franz Gollowitsch[1], Gregor Gorkiewicz[1], Luka Brcic[1]

[1]Diagnostic and Research Institute of Pathology, Medical University of Graz, Graz, Austria; [2]Division of Oncology, Department of Internal Medicine, Medical University of Graz, Graz, Austria; [3]Division of Pulmonology, Department of Internal Medicine, Medical University of Graz, Graz, Austria; [4]Division of Thoracic Surgery and Hyperbaric Surgery, Department of Surgery, Medical University of Graz, Graz, Austria

Contributions: (I) Conception and design: L Brcic, G Absenger; (II) Administrative support: L Brcic, S Konjic, S Sauer, G Absenger; (III) Provision of study materials or patients: G Absenger, R Wurm, J Lindenmann, A Terbuch, G Gorkiewicz, F Gollowitsch, L Brcic; (IV) Collection and assembly of data: M Zacharias, G Absenger, S Konjic, A Terbuch, K Kashofer, S Sauer, J Lindenmann, L Brcic; (V) Data analysis and interpretation: M Zacharias, G Absenger, K Kashofer, R Wurm, A Terbuch, S Konjic, S Sauer, F Gollowitsch, G Gorkiewicz, L Brcic; (VI) Manuscript writing: All authors; (VII) Final approval of manuscript: All authors.

[#]These authors contributed equally to this work.

Correspondence to: Luka Brcic. Diagnostic and Research Institute of Pathology, Medical University of Graz, Neue Stiftingtalstrasse 6, 8010 Graz, Austria. Email: luka.brcic@medunigraz.at.

Background: Targeted treatment modalities for non-small cell lung carcinoma (NSCLC) patients are expanding rapidly and demand a constant adaptation of molecular testing strategies. In this regard, broad reflex testing via next-generation sequencing (NGS) might have several advantages. However, real-world data regarding practical feasibility and clinical relevance are scarce, especially for RNA-based NGS.

Methods: We performed a retrospective study comparing NGS use in two consecutive years (2019 and 2020). In 2019, reflex testing mainly consisted of DNA-based NGS for mutations and immunohistochemistry (IHC) for *ALK*, *ROS1*, and *NTRK* fusion products. At the beginning of 2020, our approach has changed, with DNA- and RNA-based NGS panels now being simultaneously performed. This change in protocol allowed us to retrospectively evaluate if broad molecular reflex testing brings additional value to lung cancer patients.

Results: Within the whole cohort (n=432), both DNA- and RNA-based NGS yielded almost always evaluable results. Only in 6 cases, the RNA content was too little for an appropriate analysis. After integrating RNA-based NGS in the reflex testing approach, the number of detected fusions increased significantly (2.6% *vs.* 8.2%; P=0.0021), but also more patients received targeted therapies. Furthermore, exceedingly rare alterations were more likely to be detected, including the so far undescribed *EGFR-NUP160* fusion.

Conclusions: Our study demonstrates that a comprehensive approach to reflex NGS testing is practically feasible and clinically relevant. Including RNA-based panels in the reflex testing approach results in more detected fusions and more patients receiving targeted therapies. Additionally, this broad molecular profiling strategy identifies patients with emerging biomarkers, underscoring its usefulness in the rapidly evolving landscape of targeted therapies.

Keywords: Non-small cell lung carcinoma (NSCLC); reflex testing; next-generation sequencing (NGS); DNA sequencing; RNA sequencing

Submitted Jul 15, 2021. Accepted for publication Sep 16, 2021.
doi: 10.21037/tlcr-21-570
View this article at: https://dx.doi.org/10.21037/tlcr-21-570

Introduction

Lung cancer is the leading cause of cancer death worldwide (1). However, treatment modalities for non-small cell lung carcinoma (NSCLC) patients are expanding rapidly with an ever-increasing number of approved targeted therapies. Today, approximately 15 years after applying the first EGFR tyrosine kinase inhibitor (TKI) (2,3), targeted therapies are an established cornerstone in clinical practice. Since detecting the respective molecular alteration is a prerequisite for therapy initiation, pure histologic classification of lung carcinoma is insufficient. It has to be complemented by molecular analyses, providing a complete diagnosis, including predictive and prognostic information.

The increasing number of approved targeted therapies results in a constant need to adapt molecular testing strategies and include more and more genes in testing panels, often leading to insufficient molecular testing (4). The National Comprehensive Cancer Network (NCCN) Guidelines recommend using testing panels that include the following genes: *EGFR*, *ALK*, *ROS1*, *BRAF*, *KRAS*, MET, RET, and *NTRK 1/2/3*. Furthermore, high-level *MET* amplification and *ERBB2* (*HER2*) mutations are regarded as emerging biomarkers for novel therapies (5). From a practical point of view, several international guidelines are trying to answer the questions of whom, when, and which genes to test and which methods to use (6-8). All these guidelines agree that *EGFR*, *ALK*, *ROS1*, and *BRAF* should always be included in testing panels. When available, extended testing panels should also have *KRAS*, *MET*, *RET*, and *ERBB2*. Different guidelines also agree that the optimal diagnostic method is reflex testing and that all advanced stage adenocarcinomas should be tested. Of note, there has been a recent report of a positive double-blind phase 3 trial (ADAURA trial) with osimertinib as adjuvant therapy in patients with stage IB to IIIA EGFR mutation-positive NSCLC (9). This has resulted in a rapid change in NCCN Guidelines, now recommending *EGFR* molecular testing of all newly diagnosed carcinomas, regardless of the stage (5). National guidelines are in concordance with international guidelines but reflect the local situation regarding drugs and testing availability [for review, see (10,11)]. The 2020 recommendations of the Austrian working group on lung pathology and oncology for the diagnostic workup of NSCLC with a focus on predictive biomarkers recommended reflex testing of all newly diagnosed lung adenocarcinoma for *EGFR*, *ALK*, *ROS1*, *KRAS*, *BRAF*, and *NTRK 1/2/3* with a recommendation to include also *ERBB2*, *MET* and *RET*, preferably using NGS methods (12).

At our institution (Medical University of Graz, Austria), testing strategies have changed over time, especially between 2019 and 2020. Until the end of 2019, all newly diagnosed lung adenocarcinoma samples were examined via reflex testing using a DNA-based NGS panel, including *EGFR*, *KRAS*, *BRAF*, and *ERBB2* genes. ALK was tested using immunohistochemistry (IHC) without additional confirmation if clearly and strongly positive staining was present. For ROS1 and NTRK, IHC was used as a screening method with obligate confirmation via NGS. Since January 2020, we have changed our protocol to optimize tissue management and provide better molecular profiling of tested tumors. All newly diagnosed lung adenocarcinomas are since then examined via reflex testing using DNA- and RNA-based NGS panels. The DNA-based panel ("mutation panel") comprises 22 genes, among which *EGFR*, *KRAS*, *BRAF*, *ERBB2*, *ALK*, and *MET*. The RNA-based panel ("fusion panel") encompasses, among other genes, *ALK*, *ROS1*, *NTRK*, *RET*, and *MET*.

Although reflex testing might have several advantages for NSCLC patient management, real-world data regarding practical feasibility and clinical relevance are scarce for DNA-based NGS (13-15) and non-existent for RNA-based NGS. Therefore, we performed a retrospective study comparing NGS use in two consecutive years (2019 and 2020), aiming to examine if reflex broad molecular profiling, including DNA- and RNA-based NGS, brings additional value to lung cancer patients.

We present the following article in accordance with the STROBE reporting checklist (available at https://dx.doi.org/10.21037/tlcr-21-570).

Methods

Patient cohort

All lung cancer patients diagnosed at our University Hospital whose tissue specimens were tested via DNA- and/or RNA-based next-generation sequencing between 01.01.2019 and 31.12.2020 were included in the study (n=432). Clinical data were retrospectively obtained from electronic medical records. All patients signed informed consent.

This retrospective study conformed to the principles outlined in the Declaration of Helsinki (as revised in 2013). It was approved by the Ethics Committee of the of the Medical University of Graz (33-066 ex 20/21).

DNA-based NGS

For each case, 2 to 12 FFPE tissue sections (each 4 µm thick) were used for DNA extraction. DNA was extracted from macrodissected tumor areas of FFPE sections. Extraction was performed using the Maxwell 16 instrument (Promega) and the Maxwell RSC DNA FFPE Kit (Promega, CatNr: AS1450). DNA was quantified by Picogreen fluorescence, and 10ng DNA was used for library preparation. NGS libraries were prepared using the AmpliSeq library kit 2.0 (Thermo Fisher Scientific) and the Ion Ampliseq Colon and Lung Cancer Research Panel v2 primer pool covering hotspot mutations in 22 genes (*KRAS*, *EGFR*, *BRAF*, *PIK3CA*, *AKT1*, *ERBB2*, *PTEN*, *NRAS*, *STK11*, *MAP2K1*, *ALK*, *DDR2*, *CTNNB1*, *MET*, *TP53*, *SMAD4*, *FBXW7*, *FGFR3*, *NOTCH1*, *ERBB4*, *FGFR1*, *FGFR2*). Sequencing was performed on an Ion S5XL benchtop sequencer (Thermo Fisher Scientific) to a length of 200 base pairs. Initial data analysis was done using the Ion Torrent Suite Software Plug-ins (Thermo Fisher Scientific, open-source, GPL, https://github.com/iontorrent/). Briefly, this included base calling, alignment to the reference genome (HG19) using the TMAP mapper, and variant calling by a modified diBayes approach considering the flow space information. Called variants were annotated using open source software ANNOVAR (16) and SnpEff (17). All coding, nonsynonymous mutations were further evaluated and visually inspected in IGV (http://www.broadinstitute.org/igv/), and variant calls resulting from technical read errors or sequence effects were excluded from the result.

RNA-based NGS

For each case, five to eight FFPE tissue sections (each 10 µm thick) were used for RNA-based NGS. After microdissection, RNA extraction was performed via the Maxwell RSC RNA FFPE kit (Promega, Mannheim, Germany). After RNA quantification via ribogreen fluorescence on a Qubit fluorometer (Life Tech Austria, Vienna, Austria), 250 ng of total RNA were utilized for further analyses using the Archer FusionPlex Expanded Lung 18090 v1.0 primer pool (ArcherDX, Boulder, CO, USA). Sequencing was performed on the S5XL benchtop sequencer (Ion Torrent, Thermo Fischer, Waltham, MA) using the Ion S5 Sequencing 200 kit (Thermo Fischer, Waltham, MA, USA) and Ion 550 chip kit. Acquired sequencing data were analyzed via the ArcherDX Analysis software Version 5.1.3. (ArcherDX, Boulder, CO, USA). Translocations called with more than 10 individual reads by the Archer analysis software were included in the final reports.

Validation of assays for DNA and RNA-based analyzes

All analyses were performed in the diagnostic context on the Ion Torrent platform in conjunction with Ampliseq and Archer chemistry, neither is CE-IVD. However, a thorough validation of all in-house NGS assays has been performed. In detail, assays were tested for specificity, sensitivity, the limit of detection, as well as repeatability and reproducibility to ascertain concordance to the general safety and performance requirements described in Annex I of the IVDR (EU 2017/746). For the validation, we used a mix of commercial known-truth samples and patient samples previously analyzed with alternative technologies (qPCR, Pyrosequencing, or FISH) at our Institute. Furthermore, our Institute participates regularly in EQA schemes for all diagnostic analyses.

Statistical analyses

Categorical data are reported as absolute frequencies (%), numerical data as medians (range). All statistical analyses (Fisher's exact test, Mann Whitney test, Spearman rank correlation test, as appropriate) were performed with GraphPad Prism version 9.1.0 for Mac, GraphPad Software, San Diego, California, USA, www.graphpad.com. Data are expressed as box-and-whisker plots indicating a median and interquartile range (boxes) as well as minimum and maximum (whiskers) unless otherwise specified. P values ≤ 0.05 were considered statistically significant.

Results

Patient characteristics

Within the whole cohort (n=432), the median age was 66 years (range, 32–88 years), and 194 (44.9%) patients were female (*Table 1*). Most patients were smokers (n=322; 74.5%), while only 87 (20.1%) were non-smokers. In 23 (5.3%) patients, the smoking status could not be determined. The median number of pack-years was 30 (range, 0–150). Female gender was associated with lower pack-years (r=–0.318; P<0.0001; *Figure 1*). Histologically, the most common subtype was adenocarcinoma (AC)

Table 1 Patient characteristics of the study cohort

Clinical/pathological characteristics	All (n=432)	2019 (n=189)	2020 (n=243)	P value
Basic characteristics				
Age - median (range)	66 [32–88]	66 [35–88]	66 [32–87]	0.733
Female gender, n (%)	194 (44.9)	87 (46.0)	107 (44.4)	0.697
Male gender, n (%)	238 (55.1)	102 (54.0)	136 (55.6)	0.697
Smoking status, n (%)				
Smoker	322 (74.5)	145 (76.7)	177 (72.8)	0.375
Current smoker	145 (33.6)	61 (32.3)	84 (34.6)	0.681
Former smoker	177 (41.0)	84 (44.4)	93 (38.3)	0.202
Non-smoker	87 (20.1)	34 (18.0)	53 (21.8)	0.336
Smoking status not known	23 (5.3)	10 (5.3)	13 (5.3)	>0.9999
Pack-years, median (range)	30 (0–150)	35 (0–150)	30 (0–125)	0.179
Histology, n (%)				
Adenocarcinoma	368 (85.2%)	168 (88.9%)	200 (82.3%)	0.058
Squamous cell carcinoma	36 (8.3%)	11 (5.8%)	25 (10.3%)	0.115
Other	28 (6.5%)	10 (5.3%)	18 (7.4%)	0.434
Staging, n (%)				
Initial tumor	406 (94.0)	180 (95.2)	226 (93.0)	0.416
UICC 2017 stage				0.411
IA1	15 (3.5)	9 (4.8)	6 (2.5)	
IA2	46 (10.6)	24 (12.7)	22 (9.1)	
IA3	37 (8.6)	15 (7.9)	22 (9.1)	
IB	28 (6.5)	12 (6.3)	16 (6.6)	
IIA	13 (3.0)	6 (3.2)	7 (2.9)	
IIB	26 (6.0)	10 (5.3)	16 (6.6)	
IIIA	42 (9.7)	23 (12.2)	19 (7.8)	
IIIB	21 (4.9)	6 (3.2)	15 (6.2)	
IIIC	4 (0.9)	2 (1.1)	2 (0.8)	
IVA	57 (13.2)	19 (10.1)	38 (15.6)	
IVB	117 (27.1)	54 (28.6)	63 (25.9)	
Recurrent tumor	26 (6.0)	9 (4.8)	17 (7.0)	0.416
Local recurrence	11 (2.5)	4 (2.1)	7 (2.9)	0.762
Distant recurrence	15 (3.5)	5 (2.6)	10 (4.1)	0.443

(n=368; 85.2%), followed by squamous cell carcinoma (SCC) (n=36; 8.3%). The high amount of adenocarcinoma in this population is explained by the fact that reflex testing in SCC is not officially recommended. Only certain patients are tested (e.g., younger patients). SCC histology was associated with higher numbers of pack-years (r=0.181; P=0.001) and

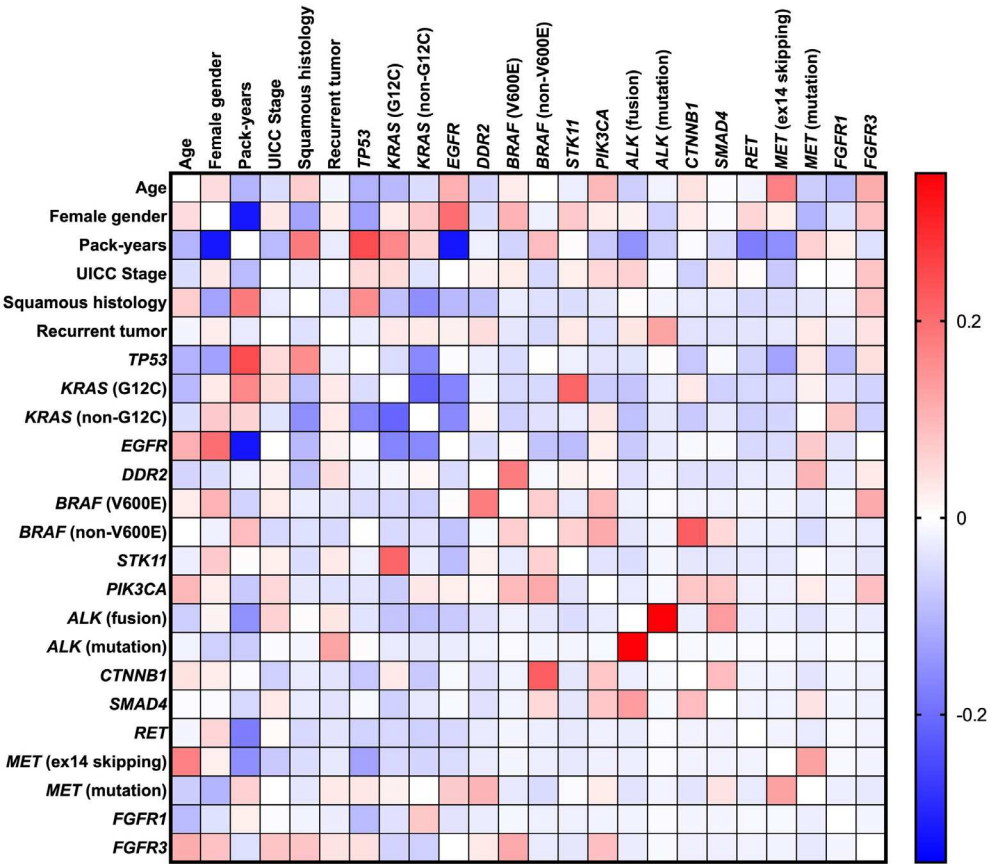

Figure 1 Correlation matrix of patient characteristics and corresponding NGS data. Positive correlation coefficients are marked red, and negative correlation coefficients are observed blue (Spearman rank correlation test). NGS, next-generation sequencing.

was less common in women (r=–0.128; P=0.010). In most cases (n=406; 94%), molecular testing was performed on the primary tumor at the time of initial diagnosis, while in 26 (6%) cases, molecular testing was performed on tumors that recurred, both locally (n=11; 2.5%) and distantly (n=15; 3.5%). It is important to note that there were no significant differences in these characteristics between 2019 (n=189) and 2020 (n=243).

DNA-based NGS

In all cases where DNA-based NGS was performed (n=407; 94.2%), also evaluable results could be obtained, although in 4 (0.9%) cases, the tumor cell content was <10%. Analyzed sample types in 2019 and 2020 included resection specimens (31.1% and 34.4%, respectively), biopsies (61.2% and 60.3%, respectively) and cytologic samples (7.7% and 5.4%, respectively). Most of the samples originated from the primary tumor in the lung (79.8% and 75.4%, in 2019 and 2020, respectively) (Table S1). A genetic alteration could be detected in 348 (80.6%) cases (Table S1). The presence of a detectable mutation was significantly associated with higher numbers of pack-years (*Figure 2*). The distribution of detected alterations in our cohort is depicted in *Figure 2*. The most frequent mutations occurred within the *TP53* gene (n=194; 44.9%), followed by *KRAS* mutations (n=142; 32.9%). The targetable G12C mutation accounted for almost half of all *KRAS* mutations (n=62; 14.4%). *EGFR* mutations occurred in 55 (12.7%) cases, with exon 19 deletions (n=22; 5.1%) and L858R mutations (n=21; 4.9%) being by far the most common ones. A T790M mutation was detected in 1 (0.2%) patient with recurrence of a tumor initially treated with afatinib due to the presence of the exon 19 deletion. As depicted in *Figure 1*, *EGFR* mutations occurred more commonly in women (r=0.199; P<0.0001) and were associated with lower numbers of pack-years (r=0.321; P<0.0001), while TP53 mutations occurred less commonly in women (r=–0.129; P=0.009) and were

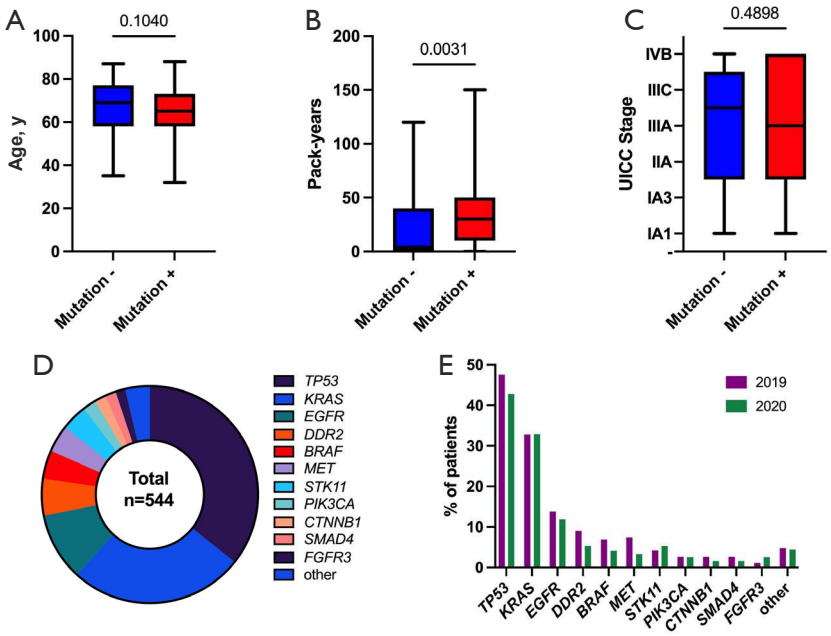

Figure 2 DNA-based NGS results. (A-C) In contrast to age and UICC stage, the number of pack-years is significantly positively correlated with the detection of at least one mutation (Mann-Whitney test); (D) Overall distribution of detected mutations; (E) Comparison of detected mutations between both subgroups (patients from 2019 and 2020). NGS, next-generation sequencing.

associated with higher numbers of pack-years (r=0.246; P<0.0001). Furthermore, there was a significant negative correlation between *EGFR* and *KRAS* mutations (r=-0.253; P<0.0001), both being well-known driver mutations and therefore most often exclusively present. In 23 (5.3%) cases, mutations within the *BRAF* gene could be detected, with almost a third of them being V600E mutations (n=7; 1.6%). In 2 (0.5%) patients with a recurrent tumor, a point mutation within the *ALK* gene was detected, both of them concurrently harbored an *EML4-ALK* fusion, which had been treated with a TKI before. In 15 (3.5%) cases with SCC histology, DNA-based NGS was performed, and in 14 (3.2%) cases, a genetic alteration could be detected. Almost all tested SCC cases harbored a *TP53* mutation (n=13; 3%), followed by mutations within *FGFR3* (n=2; 0.5%), *PTEN* (n=1; 0.2%), *MET* (n=1; 0.2%), and *EGFR* (n=1; 0.2%).

The distribution of described mutations according to different years (2019 *vs.* 2020) is presented in Table S1.

There is a discrepancy between the total number of patients tested (189 in 2019 and 243 in 2020) and the number of patients with DNA-based NGS performed (183 in 2019 and 224 in 2020). The reason is that some samples were only tested with an RNA-based panel based on clinicians' wishes or in search of eventual mutation in samples already tested for DNA (in previous years).

RNA-based NGS

RNA-based NGS was performed in 269 (62.3%) cases and almost always yielded evaluable results (Table S2). Only in 6 (1.4%) cases, the RNA content within the sample was too low or of poor quality for an appropriate analysis. Analyzed sample types in 2019 and 2020 included resection specimens (34.2% and 35.9%, respectively), biopsies (60.5% and 59.3%, respectively) and cytologic samples (5.3% and 4.8%, respectively). Out of 6 "failed" samples, two were resection specimens and 4 biopsies. All cytologic samples were satisfactory for analysis. Most of the samples originated from the primary tumor in the lung (76.3% and 77.9%, in 2019 and 2020, respectively) (Table S2). A genetic alteration could be detected in 25 (5.8%) cases. Contrary to DNA-based NGS, the presence of a detectable alteration in RNA-based NGS was significantly associated with lower numbers of pack years (*Figure 3*). The introduction of reflex testing in 2020 resulted in a significantly higher number of detected alterations (Table S2). The distribution of detected alterations in our cohort is depicted in *Figure 3*. Overall, the most frequent alterations detected via RNA-

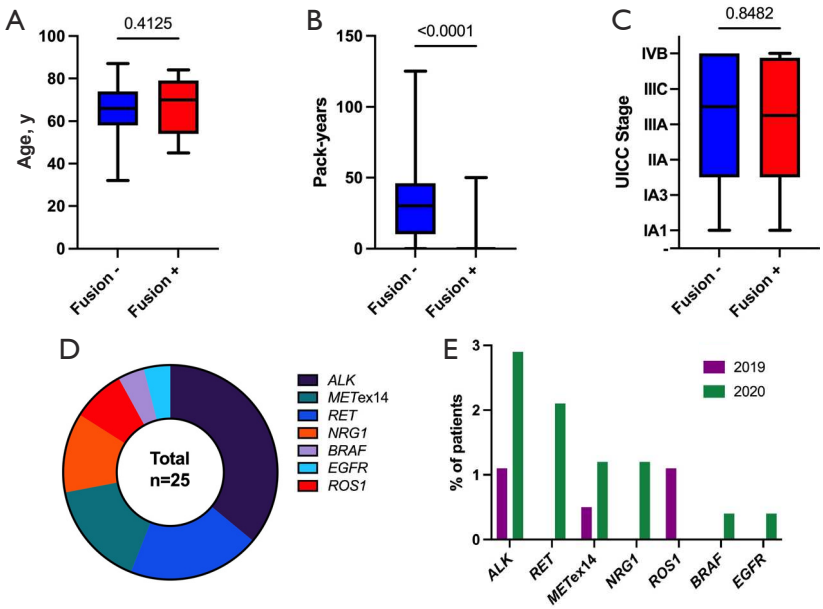

Figure 3 RNA-based NGS results. (A-C) In contrast to age and UICC stage, the number of pack-years is significantly negatively correlated with the detection of a fusion (Mann-Whitney test); (D) Overall distribution of detected fusions; (E) Comparison of detected fusions between both subgroups (patients from 2019 and 2020). NGS, next-generation sequencing.

based NGS were *ALK* fusions (n=9; 2.1%), with *EML4-ALK* fusions being by far the most common ones (n=8; 1.9%). Rearrangements involving the *RET* proto-oncogene could be detected in 5 (1.2%) cases and its fusion partners were *CCDC6* (n=3; 0.7%) or *KIF5B* (n=2; 0.5%). *MET* exon 14 (*MET*ex14) skipping was detectable in 4 (0.9%) cases and was more common in the elderly (r=0.173; P=0.005). Fusions involving *NRG1* or *ROS1* were seen in 3 (0.7%) and 2 (0.5%) cases, respectively. Furthermore, exceedingly rare rearrangements involving otherwise commonly mutated genes (*BRAF*, *EGFR*) were also observed. *RET* fusions, *NRG1* fusions, *BRAF* fusions, and *EGFR* fusions could only be detected in the year 2020 (*Figure 3*), demonstrating the importance of reflex testing in detecting rare but increasingly targetable gene rearrangements. In 30 (6.9%) cases with SCC histology, RNA-based NGS was performed, and in 2 (0.5%) cases, a genetic alteration could be detected, one harboring an *ALK-KRT6A*, the other an *EGFR-NUP160* fusion.

The distribution of detected fusions according to different years (2019 *vs.* 2020) is presented in Table S2.

There is also a discrepancy between the total number of patients tested in 2020 [243] and the number of patients with RNA-based NGS performed [231]. The reason is that only adenocarcinomas were always tested with both panels, while non-adenocarcinoma samples were sometimes not tested with RNA-based panel.

Detection of targetable genetic alterations

There are several targeted therapies approved for NSCLC patients harboring specific genetic alterations. These currently targetable alterations include *EGFR* mutations, *ALK* fusions, the *BRAF* V600E mutation, *RET* fusions, the *MET*ex14 skipping mutation, *ROS1* fusions, and *NTRK* fusions. At least one of these alterations could be detected in 82 (19%) patients (*Table 2*). In 51 (11.8%) of those cases, an additional synchronous genetic alteration was observed, with 7 (1.6%) of them harboring a second targetable alteration. Interestingly, detecting a targetable alteration was significantly more likely in patients with lower numbers of pack-years but did not significantly correlate with UICC tumor stage or age (*Figure 4*). Two SCC cases (0.5%) harbored a targetable genetic alteration, one with an *EGFR* mutation, the other with an *ALK-KRT6A* fusion.

In addition to well-established biomarkers for already approved targeted therapies, many further genetic alterations are on the horizon for implementation in clinical practice. In a recent comprehensive overview about the evolving landscape of biomarker testing in Europe,

Table 2 Clinical relevance of detected genetic alterations

Patients with genetic alterations	All, n=432 (%)	2019, n=189 (%)	2020, n=243 (%)	P value
Alteration detected (all)	364 (84.3)	163 (86.2)	201 (82.7)	0.353
Targetable alteration detected	82 (19.0)	35 (18.5)	47 (19.3)	0.902
In early stage (I–IIIA)	36 (8.3)	17 (9)	19 (7.8)	0.727
In late stage (IIIB–IV)	40 (9.3)	16 (8.5)	24 (9.9)	0.738
In recurrent tumor	6 (1.4)	2 (1.1)	4 (1.6)	0.7
With co-alteration (all)	51 (11.8)	26 (13.8)	25 (10.3)	0.294
With targetable co-alteration	7 (1.6)	3 (1.6)	4 (1.6)	>0.9999
Targeted therapy received (all)	38 (8.8)	14 (7.4)	24 (9.9)	0.397
In early stage (I–IIIA)	3 (0.7)	2 (1.1)	1 (0.4)	0.584
In late stage (IIIB–IV)	29 (6.7)	10 (5.3)	19 (7.8)	0.337
In recurrent tumor	6 (1.4)	2 (1.1)	4 (1.6)	0.7
Therapy based on detected mutation[1]	27 (6.3)	12 (6.3)	15 (6.2)	>0.9999
Osimertinib	19 (4.4)	9 (4.8)	10 (4.1)	0.815
Afatinib	11 (2.5)	5 (2.6)	6 (2.5)	>0.9999
Trametinib/Dabrafenib	4 (0.9)	2 (1.1)	2 (0.8)	>0.9999
Gefitinib	2 (0.5)	2 (1.1)	0 (0)	0.191
Mobocertinib	1 (0.2)	0 (0)	1 (0.4)	>0.9999
Therapy based on detected fusion/skipping[1]	11 (2.5)	2 (1.1)	9 (3.7)	0.123
Alectinib	6 (1.4)	0 (0)	6 (2.5)	0.038
Brigatinib	4 (0.9)	0 (0)	4 (1.6)	0.135
Selpercatinib	3 (0.7)	0 (0)	3 (1.2)	0.26
Capmatinib	1 (0.2)	1 (0.5)	0 (0)	0.438
Lorlatinib	1 (0.2)	1 (0.5)	0 (0)	0.438
Emerging biomarker[2] detected	72 (16.7)	30 (15.9)	42 (17.3)	0.795
In early stage (I–IIIA)	29 (6.7)	15 (7.9)	14 (5.8)	0.439
In late stage (IIIB–IV)	38 (8.8)	13 (6.9)	25 (10.3)	0.235
In recurrent tumor	5 (1.2)	2 (1.1)	3 (1.2)	>0.9999

Results of both subgroups (patients from 2019 and 2020, respectively) were compared using Fisher's exact test. [1], some patients received more than one substance; [2], NRG1 fusion, KRAS G12C, ERBB2, FGFR1 [according to (10)].

Kerr and colleagues regarded *ERBB2* mutations, *KRAS* G12C mutations, *NRG1* fusions, and *FGFR1* mutations as emerging biomarkers (10). At least one of these alterations could be detected in 72 (16.7%) patients in our cohort, laying the groundwork for future targeted therapy in this subgroup (*Table 2*). However, no SCC cases harbored such an alteration.

Of note, both established and emerging biomarkers were more frequently detected in 2020 (*Table 2* and *Figure 4*).

Therapeutic consequences

The detection of a targetable genetic alteration via NGS resulted in the application of targeted therapy in 38 (8.8%) patients, 14 (7.4%) in 2019, and 24 (9.9%) in 2020. Almost all of these patients (n=35; 8.1%) were in late-stage (IIIB-

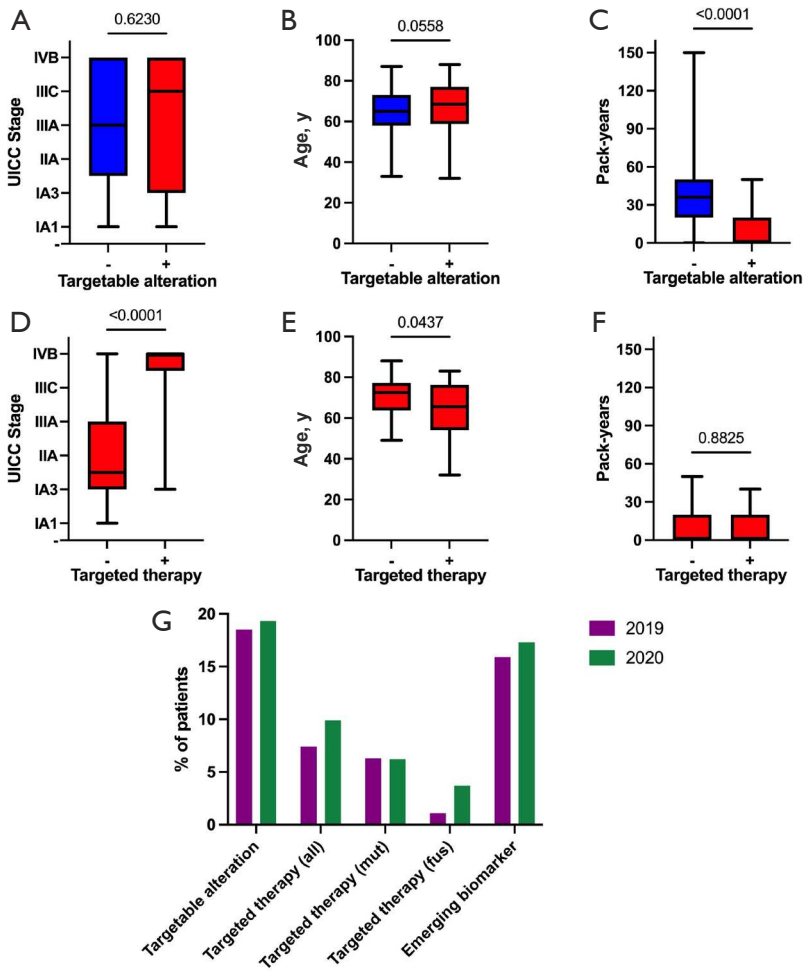

Figure 4 Clinical relevance of detected genetic alterations. (A,D) UICC stage significantly correlates with the application of targeted therapy, but not with the presence of a targetable alteration (Mann-Whitney test); (B,E) Age significantly negatively correlates with the application of targeted therapy, but not with the presence of a targetable alteration (Mann-Whitney test); (C,F) The number of pack-years significantly negatively correlates with the presence of a targetable alteration, but not with the application of targeted therapy (Mann-Whitney test); (G) Comparison of detected targetable alterations, applied targeted therapy (mutation and fusion specific), and detected emerging biomarkers between both subgroups (patients from 2019 and 2020).

IV) or in recurrence (*Table 2*). In addition to patients with AC, also one SCC patient harboring an ALK-fusion received targeted therapy. Overall, in patients with a targetable alteration, consecutive administration of targeted therapy was highly associated with an advanced tumor stage (*Figure 4*), reflecting current therapy guidelines. Younger patients with a targetable alteration were more likely to receive targeted therapy than older patients (*Figure 4*). Furthermore, patients with lower numbers of pack-years were significantly more likely to harbor a targetable alteration, mainly caused by the presence of *EGFR* mutations that are far more common in non-smokers (*Figure 1*). Importantly, the higher frequency of targeted therapies in 2020 can be clearly attributed to much higher fusion detection rates, as shown in *Figure 4*. The most commonly applied substances were Osimertinib (n=19; 4.4%), Afatinib (n=11; 2.5%), Alectinib (n=6; 1.4%), Brigatinib (n=4; 0.9%), and Trametinib/Dabrafenib (n=4; 0.9%). Especially substances targeting a genetic rearrangement were more frequently applied in 2020, mirroring the higher fusion detection rates after introducing reflex testing via RNA-based NGS (for comparisons, see *Table 2* and Table S2).

Very important issue is also the turnaround time. Introducing both NGS panels in 2020 prolonged turnaround

time for 2 working days, from 8 in 2019 to 10 in 2020.

Discussion

Comparing NGS-based NSCLC testing in two consecutive years in a real-life setting, we showed that both DNA- and RNA-based analysis could be performed in a remarkably high number of patients, identifying a plethora of targetable genetic alterations, resulting in targeted therapy for many patients. More specifically, we demonstrated that RNA-based analysis, when performed in a reflex manner at the same time as DNA-based analysis, reliably identifies patients with targetable genetic rearrangements who would otherwise be missed.

However, to have such a high yield, adequate tissue management is essential. One of the most fundamental challenges in the diagnostic process of NSCLC is tissue availability, as more and more biomarkers should be examined within small histologic (18) or cytologic specimens (19). Therefore, proper tissue handling of samples from lung cancer patients is critical. Saving tissue is actually one of the major arguments for reflex testing. At our institute, we have established a workflow that guarantees the economical use of all tiny lung cancer specimens. First, a certified pulmonary pathologist evaluates if a malignant tumor is present and orders a specific tissue re-cutting program for lung cancer specimens if that is the case. This means that the paraffin block will be cut on the same microtome by the same person, preventing the additional "leveling" steps and saving tissue. The tumor sample will be cut on up to 15 blank slides. The first six have one 4 µm thick slice (primarily reserved for immunohistochemistry), and the last nine up to three 4 µm thick slices per slide (used mainly for molecular analysis). Furthermore, the usage of diagnostic immunohistochemical stains (if needed) is restricted to thyroid transcription factor 1 (TTF1) and deltaNp63 (p40) [as recommended in (20)], as well as to programmed death-ligand 1 (PD-L1) for predictive purposes [as recommended in (21)]. Since the recent introduction of the entity "NSCLC—not otherwise specified (NOS)" in biopsy/cytologic specimens, no further immunohistochemical staining are required in cases where the amount of tumor tissue is small (22), facilitating economic tissue handling even more. In other words, if there is a very small amount of NSCLC in a sample, for the patient it is more important to have an adequate molecular profile than the exact histologic diagnosis.

Our study cohorts, looking at both years separately, were well balanced concerning all clinical and histologic parameters. Interestingly, although adenocarcinoma was the most predominant histologic type, there is still a very high proportion of males and smokers. This fact reflects still the high number of smokers in the Austrian population, and the only recently introduced smoking-ban law in Austria. SCC patients have been rarely tested (5.8% and 10% in 2019 and 2020, respectively), and as previously explained, only on the request from clinicians (e.g., for younger patients). The increase of tested SCC in 2020 is due to reflex screening of all lung carcinomas with the pan-TRK antibody, with obligate confirmation of any positive reaction with NGS.

It is known that the frequency of mutations in NSCLC is dependent on multiple factors, including ethnicity. For example, *EGFR* mutations are more common in Asians (23), while the *KRAS* G12C mutation is more common in Caucasians (24). In our cohort, frequencies of detected mutations were mostly comparable with other studies examining Caucasian lung cancer patients, although slight differences could be encountered (25-28). In comparison to the study by Volckmar *et al.*, for example, we detected more mutations in *MET* (5.1% *vs.* 3%) and *DDR2* (6.9% *vs.* 2%), while mutations in *ERBB2* (0.7% *vs.* 3%), *STK11* (4.9% *vs.* 10%), *PIK3CA* (2.5% *vs.* 6%), *FGFR3* (1.9% *vs.* 4%) and *PTEN* (0.5% *vs.* 2%) were less frequent in our cohort (27). Within the SCC subgroup, our NGS results are largely consistent with other studies that included SCC cases. For example, both in our cohort and in the CRISP study, *TP53* mutations were by far the most frequent alterations in SCC (93.3% and 69.1%, respectively) (26). Furthermore, 2 (5.3%) of our SCC patients harbored a targetable alteration (*EGFR* mutation and *ALK* fusion, respectively), with the latter even receiving targeted therapy. These findings again correspond well to the CRISP study, where targetable alterations could also be detected in SCC patients, including 4.4% with an *EGFR* mutation and 0.5% with an *ALK* fusion (26).

A major argument for multiple gene testing using DNA- and RNA-based NGS is the rapidly evolving landscape of targetable alterations in NSCLC. *KRAS* mutations, for example, have long been regarded as strictly undruggable and are now in the spotlight of drug development (29). Especially drugs targeting the *KRAS* G12C mutation (e.g., Sotrasib and Adagrasib) show promising data in clinical trials (30,31). The same is true for targeted therapies against MET, RET, and Her2 (32-34). Furthermore, *STK11* and *KEAP* mutations are associated with an impaired response to anti-PD(L)1 agents, expanding the role of NGS in detecting biomarkers for immunotherapy (35). In general,

routine testing for emerging biomarkers even before drug approval has several advantages. First, characterizing clinical and pathological parameters of a patient subgroup harboring a specific molecular alteration is paramount for upcoming clinical studies and clinical decision-making after drug approval. Two recent studies have comprehensively done this in large cohorts of lung cancer patients harboring the *KRAS* G12C mutation (36,37), which would not have been possible without previous routine testing. This need for testing before drug approval also becomes evident when looking at the early years of EGFR inhibitors, where their clinical benefit in a fraction of patients was attributed to factors like gender, smoking status, or histological subtype. Only after the correlation of these factors with sequencing data, it became clear that they are confounders of *EGFR* mutation status, which subsequently influenced treatment indications (38). Another crucial argument for routine testing of emerging biomarkers before drug approval is that patients with the detected alteration can potentially be treated in early access programs and/or immediately after drug approval.

Recently, several papers have investigated the effects of reflex testing in NSCLC, most of them confirming its benefits (13-15). However, these studies were limited to DNA-based NGS, although gene rearrangements in NSCLC are increasingly recognized and targetable. In our cohort, the inclusion of RNA-based NGS into our reflex testing approach led to much higher detection rates of the respective gene alterations. The frequencies of detected *ALK* fusions and *MET*ex14 skipping increased nearly threefold (1.1% to 2.9% and 0.5% to 1.2%, respectively), resulting in a concomitant increase of patients receiving targeted therapy (0.5% to 2.5%). Furthermore, most other detected fusions could only be recognized after introducing reflex RNA-based NGS. *RET* fusions, for example, were detected in 2.1% of patients in 2020 (with 1.2% receiving targeted therapy), while none was detected in 2019. A very peculiar finding is that in both 2019 and 2020, there is an unexpectedly low number of samples with *ROS1* fusion (1.1% and 0%, respectively) compared to the published data [ranging from 1–2% (26,27) to 3–5% (25)]. One possible explanation could be that in the Austrian population, these mutations are lower than in other published data. The second possibility is that NGS might not be the ideal method for *ROS1* fusion detection.

In addition to overall higher numbers of detected fusions, the introduction of RNA-based NGS into our reflex testing approach also enabled us to recognize exceedingly rare alterations. *EGFR* fusions, for example, do only rarely occur but are potentially targetable, with several reports showing a clinical benefit for these patients when treated with a TKI (39-42). We have also detected the so far unrecognized *EGFR-NUP160* fusion in an SCC patient and could therefore expand the known spectrum of *EGFR* rearranged NSCLC with the help of our comprehensive reflex testing approach.

It is important to stress again that parallel, reflex testing with both DNA and RNA based NGS panels prolonged turnaround time for only 2 days, which is in our opinion very good, and still in the frame of international recommendations.

Another very important issue is immunotherapy, which is out of the scope of this manuscript. However, in a real-life setting, as previously mentioned, it is very important to test for PD-L1, and to have it included in a reflex protocol. Combination of these results (PD-L1 immunohistochemistry and NGS) provides better information and can help in identification patients that could potentially be treated effectively with immunotherapy.

In conclusion, our study demonstrated that a comprehensive approach to reflex NGS testing in NSCLC is practically feasible and clinically relevant. Including RNA-based panels in the reflex testing approach results in more detected fusions and more patients receiving targeted therapies. Additionally, this broad molecular profiling strategy identifies patients with emerging biomarkers, providing some of them with the possibility of early drug access. Furthermore, a pool of patients positive for different biomarkers is known, and no additional testing will be needed after the new drugs are approved. Finally, with clinical studies increasingly using targeted therapy as adjuvant/neoadjuvant treatment, our comprehensive reflex testing approach will become even more relevant in the future.

Acknowledgments

We would like to thank Iris Halbwedl from the Medical University of Graz for her technical assistance.
Funding: All financials have been obtained from the institutional budget of the Diagnostic and Research Institute of Pathology, Medical University of Graz. No external funding has been received.

Footnote

Reporting Checklist: The authors have completed the

STROBE reporting checklist. Available at https://dx.doi.org/10.21037/tlcr-21-570

Data Sharing Statement: Available at https://dx.doi.org/10.21037/tlcr-21-570

Peer Review File: Available at https://dx.doi.org/10.21037/tlcr-21-570

Conflicts of Interest: All authors have completed the ICMJE uniform disclosure form (available at https://dx.doi.org/10.21037/tlcr-21-570). GA received payment for lectures and participated in advisory boards from Lilly, AstraZeneca, Roche, MSD, Merck, BMS, Pfizer, Novartis, Takeda, Janssen, Böhringer Ingelheim, Amgen, Sanofi; KK received grants from AstraZeneca; he also received payment for lectures and participated in advisory boards from AstraZeneca, Roche, MSD, BMS, Novartis and Thermo Fisher; RW received payment for presentations and participated in advisory boards for Takeda, Roche, Astra Zeneca, BMS, MSD, Janssen, Sanofi, Amgen and Boehringer Ingelheim; AT received grants from Sanofi, AstraZeneca, BMS, Roche and MSD; she also received payment for lectures and support for attending meetings and participated in advisory boards from Eli-Lilly, AstraZeneca, Roche, MSD, Merck, BMS, Pfizer, Novartis, Janssen and LB received grants from Takeda, AstraZeneca, BMS and Roche; he also received payment for lectures and participated in advisory boards form Invitae, Eli-Lilly, AstraZeneca, Roche, MSD, Merck, BMS, Pfizer, Novartis, Takeda, Janssen; support for attending meeting from Pfizer. He is Int. Secretary-Austrian Society of Pathology; PPS Membership and Awards Committee; Member of the Mesothelioma Committee of IASLC. The other authors have no conflicts of interest to declare.

Ethical Statement: The authors are accountable for all aspects of the work in ensuring that questions related to the accuracy or integrity of any part of the work are appropriately investigated and resolved. This retrospective study conformed to the principles outlined in the Declaration of Helsinki (as revised in 2013). It was approved by the Ethics Committee of the of the Medical University of Graz (33-066 ex 20/21). All patients signed informed consent.

References

1. Sung H, Ferlay J, Siegel RL, et al. Global Cancer Statistics 2020: GLOBOCAN Estimates of Incidence and Mortality Worldwide for 36 Cancers in 185 Countries. CA Cancer J Clin 2021;71:209-49.
2. Lynch TJ, Bell DW, Sordella R, et al. Activating mutations in the epidermal growth factor receptor underlying responsiveness of non-small-cell lung cancer to gefitinib. N Engl J Med 2004;350:2129-39.
3. Paez JG, Jänne PA, Lee JC, et al. EGFR mutations in lung cancer: correlation with clinical response to gefitinib therapy. Science 2004;304:1497-500.
4. Pennell NA, Arcila ME, Gandara DR, et al. Biomarker Testing for Patients With Advanced Non-Small Cell Lung Cancer: Real-World Issues and Tough Choices. Am Soc Clin Oncol Educ Book 2019;39:531-42.
5. NCCN Clinical Practice Guidlines in Oncology- Non-Small Cell Lung Cancer. Available online: https://www.nccn.org/professionals/physician_gls/pdf/nscl.pdf. Accessed 2021 March 3, 2021.
6. Mosele F, Remon J, Mateo J, et al. Recommendations for the use of next-generation sequencing (NGS) for patients with metastatic cancers: a report from the ESMO Precision Medicine Working Group. Ann Oncol 2020;31:1491-505.
7. Metastatic non-small cell lung cancer: ESMO Clinical Practice Guidelines for diagnosis, treatment and follow-up. Available online: https://www.esmo.org/content/download/347819/6934778/1/ESMO-CPG-mNSCLC-15SEPT2020.pdf. Accessed 15 September 2020.
8. Lindeman NI, Cagle PT, Aisner DL, et al. Updated Molecular Testing Guideline for the Selection of Lung Cancer Patients for Treatment With Targeted Tyrosine Kinase Inhibitors: Guideline From the College of American Pathologists, the International Association for the Study of Lung Cancer, and the Association for Molecular Pathology. J Mol Diagn 2018;20:129-59.
9. Wu YL, Tsuboi M, He J, et al. Osimertinib in Resected EGFR-Mutated Non-Small-Cell Lung Cancer. N Engl J Med 2020;383:1711-23.

10. Kerr KM, Bibeau F, Thunnissen E, et al. The evolving landscape of biomarker testing for non-small cell lung cancer in Europe. Lung Cancer 2021;154:161-75.
11. Thunnissen E, Weynand B, Udovicic-Gagula D, et al. Lung cancer biomarker testing: perspective from Europe. Transl Lung Cancer Res 2020;9:887-97.
12. Popper HH, Gruber-Mösenbacher U, Pall G, et al. The 2020 update of the recommendations of the Austrian working group on lung pathology and oncology for the diagnostic workup of non-small cell lung cancer with focus on predictive biomarkers. Memo 2020;13:11-26.
13. Lassalle S, Hofman V, Heeke S, et al. Targeted Assessment of the EGFR Status as Reflex Testing in Treatment-Naive Non-Squamous Cell Lung Carcinoma Patients: A Single Laboratory Experience (LPCE, Nice, France). Cancers (Basel) 2020;12:955.
14. Anand K, Phung TL, Bernicker EH, et al. Clinical Utility of Reflex Ordered Testing for Molecular Biomarkers in Lung Adenocarcinoma. Clin Lung Cancer 2020;21:437-42.
15. Miller TE, Yang M, Bajor D, et al. Clinical utility of reflex testing using focused next-generation sequencing for management of patients with advanced lung adenocarcinoma. J Clin Pathol 2018;71:1108-15.
16. Wang K, Li M, Hakonarson H. ANNOVAR: functional annotation of genetic variants from high-throughput sequencing data. Nucleic Acids Res 2010;38:e164.
17. Cingolani P, Platts A, Wang le L, et al. A program for annotating and predicting the effects of single nucleotide polymorphisms, SnpEff: SNPs in the genome of Drosophila melanogaster strain w1118; iso-2; iso-3. Fly (Austin) 2012;6:80-92.
18. Hirsch FR, Wynes MW, Gandara DR, et al. The tissue is the issue: personalized medicine for non-small cell lung cancer. Clin Cancer Res 2010;16:4909-11.
19. Lozano MD, Echeveste JI, Abengozar M, et al. Cytology Smears in the Era of Molecular Biomarkers in Non-Small Cell Lung Cancer: Doing More With Less. Arch Pathol Lab Med 2018;142:291-8.
20. Yatabe Y, Dacic S, Borczuk AC, et al. Best Practices Recommendations for Diagnostic Immunohistochemistry in Lung Cancer. J Thorac Oncol 2019;14:377-407.
21. Lantuejoul S, Sound-Tsao M, Cooper WA, et al. PD-L1 Testing for Lung Cancer in 2019: Perspective From the IASLC Pathology Committee. J Thorac Oncol 2020;15:499-519.
22. Thoracic Tumours: WHO Classification of Tumours. 5 ed. World Health Organization; 2021.
23. Zhang YL, Yuan JQ, Wang KF, et al. The prevalence of EGFR mutation in patients with non-small cell lung cancer: a systematic review and meta-analysis. Oncotarget 2016;7:78985-93.
24. Nassar AH, Adib E, Kwiatkowski DJ. Distribution of KRAS G12C Somatic Mutations across Race, Sex, and Cancer Type. N Engl J Med 2021;384:185-7.
25. Trédan O, Wang Q, Pissaloux D, et al. Molecular screening program to select molecular-based recommended therapies for metastatic cancer patients: analysis from the ProfiLER trial. Ann Oncol 2019;30:757-65.
26. Griesinger F, Eberhardt W, Nusch A, et al. Biomarker testing in non-small cell lung cancer in routine care: Analysis of the first 3,717 patients in the German prospective, observational, nation-wide CRISP Registry (AIO-TRK-0315). Lung Cancer 2021;152:174-84.
27. Volckmar AL, Leichsenring J, Kirchner M, et al. Combined targeted DNA and RNA sequencing of advanced NSCLC in routine molecular diagnostics: Analysis of the first 3,000 Heidelberg cases. Int J Cancer 2019;145:649-61.
28. Cohen D, Hondelink LM, Solleveld-Westerink N, et al. Optimizing Mutation and Fusion Detection in NSCLC by Sequential DNA and RNA Sequencing. J Thorac Oncol 2020;15:1000-14.
29. Salgia R, Pharaon R, Mambetsariev I, et al. The improbable targeted therapy: KRAS as an emerging target in non-small cell lung cancer (NSCLC). Cell Rep Med 2021;2:100186.
30. Hong DS, Fakih MG, Strickler JH, et al. KRASG12C Inhibition with Sotorasib in Advanced Solid Tumors. N Engl J Med 2020;383:1207-17.
31. Jänne PA, Rybkin II, Spira AI, et al. KRYSTAL-1: Activity and Safety of Adagrasib (MRTX849) in Advanced/Metastatic Non–Small-Cell Lung Cancer (NSCLC) Harboring KRAS G12C Mutation. Eur J Cancer 2020;138:S1-S2.
32. Drilon A, Oxnard GR, Tan DSW, et al. Efficacy of Selpercatinib in RET Fusion-Positive Non-Small-Cell Lung Cancer. N Engl J Med 2020;383:813-24.
33. Wolf J, Seto T, Han JY, et al. Capmatinib in MET Exon 14-Mutated or MET-Amplified Non-Small-Cell Lung Cancer. N Engl J Med 2020;383:944-57.
34. Smit EF, Nakagawa K, Nagasaka M, et al. Trastuzumab deruxtecan (T-DXd; DS-8201) in patients with HER2-mutated metastatic non-small cell lung cancer (NSCLC): Interim results of DESTINY-Lung01. J Clin Oncol 2020;38:9504.
35. Codima A, Monteiro G, Costa I, et al. 122P STK11 and/

or KEAP1 mutations and outcomes in non-small cell lung cancer patients treated with immune checkpoint inhibitors: A systematic literature review. J Thorac Oncol 2021;16:S764.
36. Arbour KC, Rizvi H, Plodkowski AJ, et al. Treatment Outcomes and Clinical Characteristics of Patients with KRAS-G12C-Mutant Non-Small Cell Lung Cancer. Clin Cancer Res 2021;27:2209-15.
37. Sebastian M, Eberhardt WEE, Hoffknecht P, et al. KRAS G12C-mutated advanced non-small cell lung cancer: A real-world cohort from the German prospective, observational, nation-wide CRISP Registry (AIO-TRK-0315). Lung Cancer 2021;154:51-61.
38. Camidge DR, Doebele RC, Kerr KM. Comparing and contrasting predictive biomarkers for immunotherapy and targeted therapy of NSCLC. Nat Rev Clin Oncol 2019;16:341-55.
39. Konduri K, Gallant JN, Chae YK, et al. EGFR Fusions as Novel Therapeutic Targets in Lung Cancer. Cancer Discov 2016;6:601-11.
40. Raez LE, Pinto JA, Schrock AB, et al. EGFR-RAD51 Fusion: A Targetable Partnership Originated from the Tumor Evolution? J Thorac Oncol 2018;13:e33-4.
41. Xu H, Shao C. KIF5B-EGFR Fusion: A Novel EGFR Mutation in Lung Adenocarcinoma. Onco Targets Ther 2020;13:8317-21.
42. Zhu YC, Wang WX, Xu CW, et al. EGFR-RAD51 fusion variant in lung adenocarcinoma and response to erlotinib: A case report. Lung Cancer 2018;115:131-4.

Cite this article as: Zacharias M, Absenger G, Kashofer K, Wurm R, Lindenmann J, Terbuch A, Konjic S, Sauer S, Gollowitsch F, Gorkiewicz G, Brcic L. Reflex testing in non-small cell lung carcinoma using DNA- and RNA-based next-generation sequencing—a single-center experience. Transl Lung Cancer Res 2021;10(11):4221-4234. doi: 10.21037/tlcr-21-570

Supplementary

Table S1 DNA-based NGS results. Both subgroups (patients from 2019 and 2020) were compared using Fisher's exact test

	2019	2020	P value
Testing characteristics - no. (% of all cases with NGS)	n=189	n=243	
DNA-based NGS performed	183 (96.8%)	224 (92.2%)	0.06
DNA-based NGS evaluable	183 (96.8%)	224 (92.2%)	0.06
Alteration detected	161 (85.2%)	187 (77%)	0.037
Detected alterations - no (% of all cases with NGS)	n=189	n=243	
TP53 mutation (all)	90 (47.6%)	104 (42.8%)	0.331
KRAS mutation (all)	62 (32.8%)	80 (32.9%)	>0.9999
G12C	27 (14.3%)	35 (14.4%)	
G12D	8 (4.2%)	14 (5.8%)	
G12V	8 (4.2%)	14 (5.8%)	
G12A	5 (2.6%)	3 (1.2%)	
G13C	5 (2.6%)	1 (0.4%)	
Q61H	2 (1.1%)	3 (1.2%)	
G12F	1 (0.5%)	3 (1.2%)	
G12S	2 (1.1%)	1 (0.4%)	
Q61L	0 (0%)	2 (0.8%)	
other	4 (2.1%)	4 (1.6%)	
EGFR mutation (all)	26 (13.8%)	29 (11.9%)	0.663
Exon 19 del	11 (5.8%)	11 (4.5%)	
L858R	9 (4.8%)	12 (4.9%)	
L861Q	2 (1.1%)	2 (0.8%)	
T790M	0 (0%)	1 (0.4%)	
other	6 (3.2%)	6 (2.5%)	
DDR2 mutation (all)	17 (9%)	13 (5.3%)	0.181
M441I	14 (7.4%)	9 (3.7%)	
Non-M441I	4 (2.1%)	4 (1.6%)	
BRAF mutation (all)	13 (6.9%)	10 (4.1%)	0.28
V600E	4 (2.1%)	3 (1.2%)	
Non-V600E	10 (5.3%)	7 (2.9%)	
MET mutation (all)	14 (7.4%)	8 (3.3%)	0.076
T1010I	10 (5.3%)	6 (2.5%)	
Non-T1010I	4 (2.1%)	2 (0.8%)	
STK11 mutation (all)	8 (4.2%)	13 (5.3%)	0.657
PIK3CA mutation (all)	5 (2.6%)	6 (2.5%)	>0.9999
CTNNB1 mutation (all)	5 (2.6%)	4 (1.6%)	0.513

Table S1 *(continued)*

https://dx.doi.org/10.21037/tlcr-21-570

Table S1 *(continued)*

	2019	2020	P value
SMAD4 mutation (all)	5 (2.6%)	4 (1.6%)	0.513
FGFR3 mutation (all)	2 (1.1%)	6 (2.5%)	0.475
F386L	2 (1.1%)	4 (1.6%)	
Non-F386L	0 (0%)	2 (0.8%)	
FGFR1 mutation (all)	2 (1.1%)	2 (0.8%)	>0.9999
ERBB2 mutation (all)	1 (0.5%)	2 (0.8%)	>0.9999
ERBB4 mutation (all)	2 (1.1%)	1 (0.4%)	0.584
ALK mutation (all)	1 (0.5%)	1 (0.4%)	>0.9999
FGFR2 mutation (all)	2 (1.1%)	0 (0%)	0.191
NRAS mutation (all)	1 (0.5%)	1 (0.4%)	>0.9999
PTEN mutation (all)	0 (0%)	2 (0.8%)	0.507
FBXW7 mutation (all)	0 (0%)	1 (0.4%)	>0.9999
MAP2K1 mutation (all)	0 (0%)	1 (0.4%)	>0.9999
Sample type - no. (% of all cases with DNA-based NGS)	n=183	n=224	
Resection specimen	57 (31.1%)	77 (34.4%)	0.525
Biopsy	112 (61.2%)	135 (60.3%)	0.919
Cytology/Cell block	14 (7.7%)	12 (5.4%)	0.417
Sample origin - no. (% of all cases with DNA-based NGS)	n=183	n=224	
Lung	146 (79.8%)	169 (75.4%)	0.341
Pleura	4 (2.2%)	10 (4.5%)	0.278
Lymph node	22 (12%)	26 (11.6%)	>0.9999
Distant metastasis	11 (6%)	19 (8.5%)	0.446

https://dx.doi.org/10.21037/tlcr-21-570

Table S2 RNA-based NGS results. Both subgroups (patients from 2019 and 2020) were compared using Fisher's exact test

	2019	2020	P value
Testing characteristics - no. (% of all cases with NGS)	n=189	n=243	
RNA-based NGS performed	38 (20.1%)	231 (95.1%)	<0.0001
RNA-based NGS evaluable	37 (19.6%)	226 (93%)	<0.0001
Alteration detected	5 (2.6%)	20 (8.2%)	0.021
Detected alterations - no. (% of all cases with NGS)	n=189	n=243	
ALK fusion (all)	2 (1.1%)	7 (2.9%)	0.31
EML4-ALK	2 (1.1%)	6 (2.5%)	
KRT6A-ALK	0 (0%)	1 (0.4%)	
RET fusion (all)	0 (0%)	5 (2.1%)	0.071
CCDC6-RET	0 (0%)	3 (1.2%)	
KIF5B-RET	0 (0%)	2 (0.8%)	
METex14 skipping	1 (0.5%)	3 (1.2%)	0.635
NRG1 fusion (all)	0 (0%)	3 (1.2%)	0.26
CD74-NRG1	0 (0%)	2 (0.8%)	
SLC3A2-NRG1	0 (0%)	1 (0.4%)	
ROS1 fusion (all)	2 (1.1%)	0 (0%)	0.191
EZR-ROS1	1 (0.5%)	0 (0%)	
SDC4-ROS1	1 (0.5%)	0 (0%)	
BRAF fusion (all)	0 (0%)	1 (0.4%)	>0.9999
KLHL7-BRAF	0 (0%)	1 (0.4%)	
EGFR fusion (all)	0 (0%)	1 (0.4%)	>0.9999
EGFR-NUP160	0 (0%)	1 (0.4%)	
NTRK fusion (all)	0 (0%)	0 (0%)	>0.9999
Sample type - no. (% of all cases with RNA-based NGS)	n=38	n=231	
Resection specimen	13 (34.2%)	83 (35.9%)	>0.9999
Biopsy	23 (60.5%)	137 (59.3%)	>0.9999
Cytology/Cell block	2 (5.3%)	11 (4.8%)	>0.9999
Sample origin - no. (% of all cases with RNA-based NGS)	n=38	n=231	
Lung	29 (76.3%)	180 (77.9%)	0.835
Pleura	1 (2.6%)	10 (4.3%)	>0.9999
Lymph node	5 (13.2%)	22 (9.5%)	0.558
Distant metastasis	3 (7.9%)	19 (8.2%)	>0.9999

https://dx.doi.org/10.21037/tlcr-21-570

cancers

MDPI

Article

Expanding Broad Molecular Reflex Testing in Non-Small Cell Lung Cancer to Squamous Histology

Martin Zacharias [1], Selma Konjic [1], Nikolaus Kratochwill [1], Gudrun Absenger [2], Angelika Terbuch [2], Philipp J. Jost [2], Robert Wurm [3], Jörg Lindenmann [4], Karl Kashofer [1], Franz Gollowitsch [1], Gregor Gorkiewicz [1] and Luka Brcic [1,*]

[1] Diagnostic and Research Institute of Pathology, Medical University of Graz, 8010 Graz, Austria; martin.zacharias@medunigraz.at (M.Z.); selma.konjic@medunigraz.at (S.K.); nikolaus.kratochwill@medunigraz.at (N.K.); karl.kashofer@medunigraz.at (K.K.); franz.gollowitsch@medunigraz.at (F.G.); gregor.gorkiewicz@medunigraz.at (G.G.)
[2] Division of Oncology, Department of Internal Medicine, Medical University of Graz, 8010 Graz, Austria; gudrun.absenger@medunigraz.at (G.A.); angelika.terbuch@medunigraz.at (A.T.); philipp.jost@medunigraz.at (P.J.J.)
[3] Division of Pulmonology, Department of Internal Medicine, Medical University of Graz, 8010 Graz, Austria; robert.wurm@medunigraz.at
[4] Division of Thoracic and Hyperbaric Surgery, Department of Surgery, Medical University of Graz, 8010 Graz, Austria; jo.lindenmann@medunigraz.at
* Correspondence: luka.brcic@medunigraz.at

Simple Summary: Targeted therapies have revolutionized the treatment of patients with non-small cell lung cancer (NSCLC). Adenocarcinoma, the most common histological subtype of NSCLC, is the posterchild of this therapeutic approach because of its high rate of treatable targets. In our study, we provide evidence that squamous cell carcinoma (SCC), the second most common histological subtype of NSCLC, also harbors a significant number of treatable targets, although at a lower rate than adenocarcinoma. Furthermore, we show that most SCC patients harboring such an alteration were >50 years of age and current or former smokers, questioning restrictive molecular testing strategies. Based on our data, we propose that broad molecular profiling should be performed in all newly diagnosed NSCLC cases, irrespective of histological subtype, but also irrespective of age or smoking status.

Abstract: Due to the success story of biomarker-driven targeted therapy, most NSCLC guidelines agree that molecular reflex testing should be performed in all cases with non-squamous cell carcinoma (non-SCC). In contrast, testing recommendations for squamous cell carcinoma (SCC) vary considerably, specifically concerning the exclusion of patients of certain age or smoking status from molecular testing strategies. We performed a retrospective single-center study examining the value of molecular reflex testing in an unselected cohort of 316 consecutive lung SCC cases, tested by DNA- and RNA-based next-generation sequencing (NGS) at our academic institution between 2019 and 2023. Clinicopathological data from these cases were obtained from electronic medical records and correlated with sequencing results. In 21/316 (6.6%) cases, we detected an already established molecular target for an approved drug. Among these were seven cases with an *EGFR* mutation, seven with a *KRAS* G12C mutation, four with an *ALK* fusion, two with an *EGFR* fusion and one with a METex14 skipping event. All patients harboring a targetable alteration were >50 years of age and most of them had >15 pack-years, questioning restrictive molecular testing strategies. Based on our real-world data, we propose a reflex testing workflow using DNA- and RNA-based NGS that includes all newly diagnosed NSCLC cases, irrespective of histology, but also irrespective of age or smoking status.

Keywords: lung cancer; squamous cell carcinoma; molecular testing; next-generation sequencing

check for updates

Citation: Zacharias, M.; Konjic, S.; Kratochwill, N.; Absenger, G.; Terbuch, A.; Jost, P.J.; Wurm, R.; Lindenmann, J.; Kashofer, K.; Gollowitsch, F.; et al. Expanding Broad Molecular Reflex Testing in Non-Small Cell Lung Cancer to Squamous Histology. *Cancers* **2024**, *16*, 903. https://doi.org/10.3390/cancers16050903

Academic Editor: Carlos S. Moreno

Received: 3 February 2024
Revised: 19 February 2024
Accepted: 21 February 2024
Published: 23 February 2024

1. Introduction

Targeted therapies have revolutionized the treatment of non-small cell lung carcinoma (NSCLC). However, treatment efficacy is largely dependent on the upregulation of specific oncogenic pathways in tumor cells and, therefore, the detection of the respective molecular alterations is a prerequisite before treatment initiation [1]. Molecular testing approaches for NSCLC have changed dramatically within the last years. Today, next-generation sequencing (NGS) is regarded as the gold standard method for clinically relevant molecular profiling, especially as the landscape of potentially targetable genetic alterations expands rapidly [2].

The two main entities comprising NSCLC are adenocarcinoma (AC) and squamous cell carcinoma (SCC) [3]. Since the introduction of targeted therapies, AC has been in the spotlight because of its relatively high proportion of targetable genetic alterations [4,5]. International guidelines for the management of NSCLC patients strongly recommend reflex broad molecular profiling of all newly diagnosed AC cases and mostly agree that *ALK*, *BRAF*, *ERBB2*, *KRAS*, *MET*, *NTRK*, *RET*, and *ROS1* must be included in testing panels [6–8].

In contrast to AC, molecular testing recommendations for SCC are more controversial. The latest molecular testing guidelines from the College of American Pathologists (CAP), the International Association for the Study of Lung Cancer (IASLC) and the Association for Molecular Pathology (AMP) recommend testing in non-AC only in patients with minimal (1–10 packs per years) or absent tobacco exposure and in patients younger than 50 years [7]. In line with this, the recently published European Society for Medical Oncology (ESMO) Clinical Practice Guideline for oncogene-addicted NSCLC does not recommend molecular testing in patients with a confident diagnosis of SCC, except unusual cases like never/former light smokers ($\leq$15 pack-years) or young (<50 years) patients [6]. In contrast, the current National Comprehensive Cancer Network Clinical Practice Guidelines in Oncology (NCCN Guidelines) for NSCLC recommend that "molecular testing may be considered in all patients with metastatic NSCLC squamous cell carcinoma and not just those with certain characteristics, such as never smoking status and mixed histology." [8].

At our institution (Medical University of Graz, Graz, Austria), pathologist-initiated reflex molecular testing has been routinely performed for several years in all newly diagnosed NSCLCs, independent of histology. This broad molecular profiling strategy enabled us to perform a single-center study examining the value of reflex testing in a large, unselected cohort of consecutive lung SCC cases. With this study, we add real-world evidence to the above-described controversy between different international NSCLC guidelines.

2. Materials and Methods

2.1. Patient Cohort

We included all newly diagnosed NSCLC cases with squamous histology tested by DNA- and RNA-based NGS at our academic institution (Diagnostic and Research Institute of Pathology, Medical University of Graz, Austria) between 1 January 2019 and 30 September 2023 (n = 316). Exclusion criteria were incomplete molecular testing and/or incomplete NGS data. Since our study cohort comprises all consecutive cases (irrespective of age, smoking status, and tumor stage), a selection bias can be excluded. Clinical, pathological, and molecular data were retrospectively obtained from electronic medical records. The study was conducted according to the Helsinki Declaration guidelines and was approved by the Ethics Committee of the Medical University of Graz (33-066 ex 20/21).

2.2. DNA-Based Next-Generation Sequencing

DNA-based next-generation sequencing was performed as previously described [9]. Briefly, DNA extraction was performed for between 2 and 12 FFPE tissue sections for each case using the Maxwell 16 instrument (Promega, Mannheim, Germany) and the Maxwell RSC DNA FFPE Kit (Promega, Mannheim, Germany; CatNr: AS1450). After quantification of DNA via picogreen fluorescence, library preparation was performed with 10 ng of DNA. The libraries were prepared using the AmpliSeq library kit 2.0 (Thermo Fisher Scientific, Waltham, MA, USA) and the Ion Ampliseq Colon and Lung Cancer Research Panel v2

primer pool covering hotspot mutations in 22 genes (*ALK*, *AKT1*, *BRAF*, *CTNNB1*, *DDR2*, *EGFR*, *ERBB2*, *ERBB4*, *FBXW7*, *FGFR1*, *FGFR2*, *FGFR3*, *KRAS*, *MAP2K1*, *MET*, *NOTCH1*, *NRAS*, *PIK3CA*, *PTEN*, *SMAD4*, *STK11*, *TP53*). Sequencing was performed on an Ion S5XL benchtop sequencer (Thermo Fisher Scientific, Waltham, MA, USA). The initial data analysis was performed using the Ion Torrent Suite Software Plug-ins (Thermo Fisher Scientific, open source, GPL, https://github.com/iontorrent/, accessed on 20 February 2024), and was performed as described previously [9]. In short, this included base calling, alignment to the HG19 reference genome via TMAP mapper, and variant calling via a modified diBayes approach. Called variants were annotated via the open-source software ANNOVAR ([10]) and SnpEff ([11]). As a next step, all coding and nonsynonymous mutations were further evaluated and visually inspected using IGV (http://www.broadinstitute.org/igv/, accessed on 20 February 2024). Variant calls resulting from sequence effects or technical read errors were excluded.

2.3. RNA-Based Next-Generation Sequencing

RNA-based next-generation sequencing was also performed as previously described [9]. Briefly, RNA extraction was performed on from five to eight FFPE tissue sections for each case using the Maxwell RSC RNA FFPE Kit (Promega, Mannheim, Germany). After quantification of RNA via ribogreen fluorescence (Qubit fluorometer, Life Tech Austria, Vienna, Austria), 250 ng of RNA was used for further analyses with the Archer FusionPlex Expanded Lung 18090 v1.0 primer pool (ArcherDX, Boulder, CO, USA). This panel included the genes *ALK*, *BRAF*, *EGFR*, *ERBB2*, *FGFR1*, *FGFR2*, *FGFR3*, *MET*, *NRG1*, *NTRK1*, *NTRK2*, *NTRK3*, *NUTM1*, *PIK3CA*, *RET*, and *ROS1*. Sequencing was performed on an Ion S5XL benchtop sequencer (Thermo Fisher Scientific, Waltham, MA, USA) and Ion 550 chip kit. Sequencing data were analyzed with the ArcherDX Analysis software (ArcherDX, Boulder, CO, USA). Translocations called with more than 10 individual reads were included in the final results.

2.4. Validation of Assays for DNA and RNA-Based Analyzes

A thorough validation of all in-house NGS assays was performed as previously described [9]. In short, assays were tested for diagnostic performance parameters in concordance with the requirements described in the Annex I of the IVDR (EU 2017/746). A mix of commercially available known-truth samples and patient samples previously analyzed at our institute with alternative technologies, like qPCR, pyrosequencing or FISH, were used for this purpose.

2.5. Statistical Analyses

Statistical analyses have been performed as specified in the respective graphs (Mann–Whitney test or Kruskal–Wallis test, as appropriate). Numerical data are reported as medians (range), and categorical data are reported as absolute frequencies (%). p-values ≤ 0.05 were considered statistically significant. Statistical analyses were performed with GraphPad Prism, GraphPad Software, San Diego, CA, USA.

3. Results

3.1. Patient Characteristics

Between 1 January 2019 and 30 September 2023, DNA- and RNA-based NGS was performed in 316 consecutive NSCLC cases with squamous histology. The cohort included 211 (66.8%) men and 105 (33.2%) women. The median age was 68 years (range 36–85). Nearly all patients had a smoking history (97.9% being either current or former smokers) and the median number of pack-years was 40 (range 0–200). Since we performed reflex molecular testing independent of tumor progression, our study cohort included cases in stage I (n = 52, 21.1%), stage II (n = 41, 16.6%), stage III (n = 88, 35.6%) and stage IV (n = 66, 26.7%). DNA- and RNA-based NGS was performed on different types of samples, most commonly on biopsies (n = 255, 80.7%), followed by resection specimens (n = 56, 17.7%) and cytology/cell block specimens (n = 5, 1.6%). Most commonly, lung tissue was the source for molecular testing (n = 271, 85.8%). In the remaining cases, specimens from lymph nodes, distant metastases

or pleura were tested. In accordance with current guidelines, PD-L1 testing using the tumor proportion score (TPS) was performed in all cases with a median TPS of 5% (range 0–100%). The main patient characteristics of the cohort are summarized in Table 1.

Table 1. Patient characteristics of the study cohort.

Basic Characteristics	**n = 316**
Age—median (range)	68 (36–85)
Female	105 (33.2%)
Male	211 (66.8%)
Smoking status known	**n = 242**
Smoker	237 (97.9%)
Current smoker	151 (63.7%)
Former smoker	86 (36.3%)
Never smoker	5 (2.1%)
Pack-years known	**n = 201**
≤15 pack-years	15 (7.5%)
>15 pack-years	186 (92.5%)
Pack-years median (range)	40 (0–200)
Staging known	**n = 247**
Stage I	52 (21.1%)
Stage II	41 (16.6%)
Stage III	88 (35.6%)
Stage IV	66 (26.7%)
Sample type	**n = 316**
Resection specimen	56 (17.7%)
Biopsy	255 (80.7%)
Cytology/Cell block	5 (1.6%)
Sample origin	**n = 316**
Lung	271 (85.8%)
Pleura	2 (0.6%)
Lymph node	24 (7.6%)
Distant metastasis	19 (6%)

3.2. DNA-Based NGS Results

The median tumor cell content of the examined tissue area was 40% (range 10–90%). Mutations could be detected in all 22 included genes, with varying frequency in different cases (Figure 1, Tables S1 and S2). The most commonly mutated gene was *TP53* (n = 228, 72.2%), followed by *PIK3CA* (n = 37, 11.7%) and *PTEN* (n = 20, 6.3%). In 7/316 (2.2%) cases, an *EGFR* mutation could be detected (3× deletion in exon 19, 2× p.L858R in exon 21, 1× duplication in exon 20, and 1× p.R494T in exon 12). A total of 5/6 of the *BRAF*-mutated cases harbored a point mutation in exon 11, with one exception being a case with *BRAF* p.K601E mutation in exon 15. Although no *BRAF* p.V600E mutation was detected, there is evidence that cases with the described *BRAF* p.K601E mutation might also be responsive to tyrosine kinase inhibitors [12,13]. *KRAS* mutations were present in 15/316 (4.7%) cases in our cohort, with 7/316 (2.2%) showing the now targetable *KRAS* G12C mutation. *ALK* mutations were detected in 4/316 (1.3%) cases, all being point mutations, two in exon 23 and two in exon 29. Mutations in *FGFR1*, *FGFR2* or *FGFR3* were present in 17/316 (5.4%) cases. All detected mutations within clinically relevant genes and their exact locations are visualized in Figure S1 (lollipop plots).

In addition to mutations, amplification events could be suspected in 23/316 (7.3%) cases due to detected differences in gene coverage. Subsequent confirmatory tests (e.g., CNV analyses) have not been routinely performed. Of note, amplification events are increasingly recognized as clinically relevant in NSCLC and should, thus, be reported if present [14]. In our cohort, they could be observed in *EGFR*, *ERBB2*, *FGFR1*, *FGFR3*, *KRAS*, *MET* or *PIK3CA* (Figure 1 and Table S1).

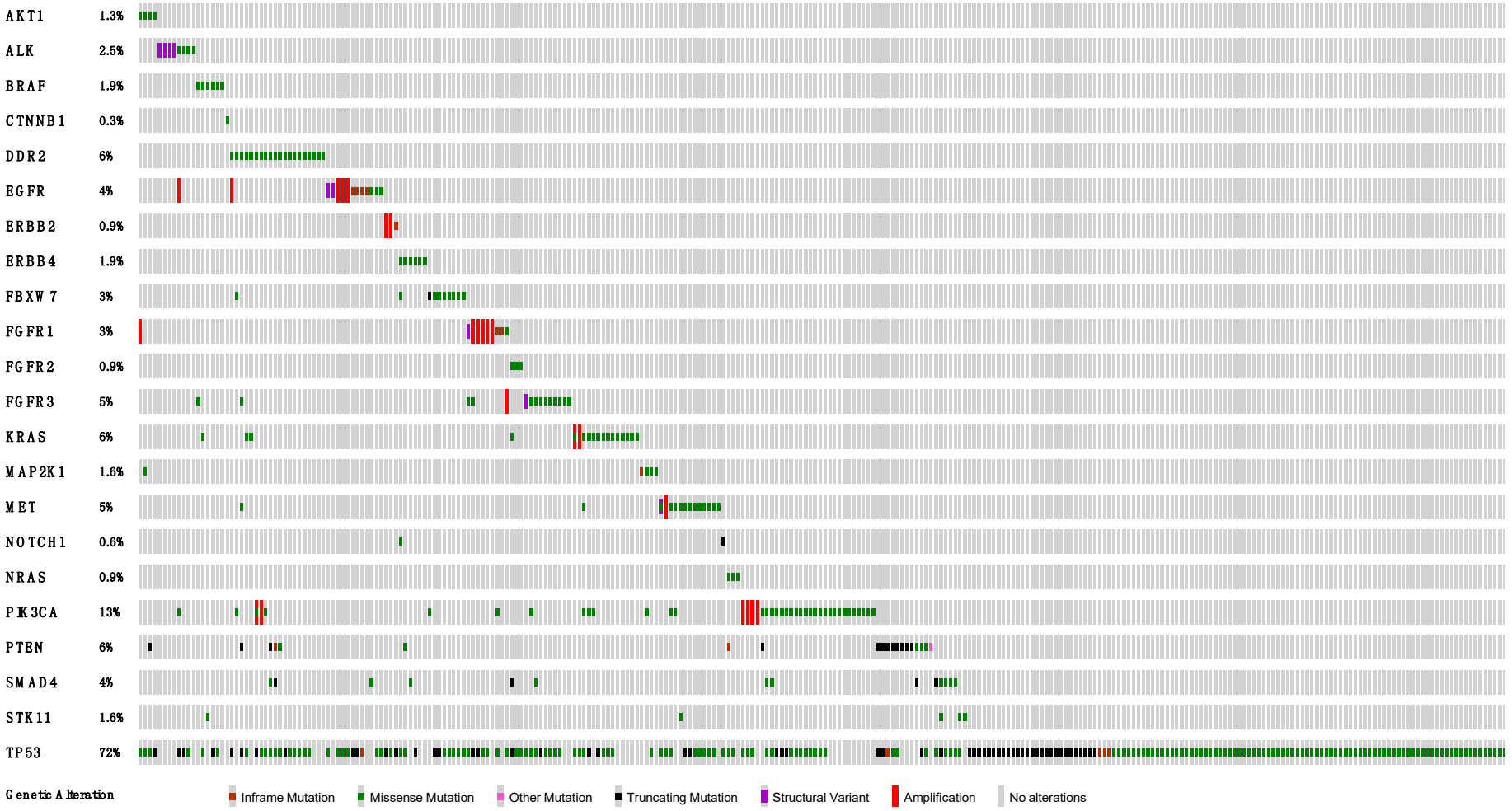

Figure 1. Oncoprint of all detected genetic alterations. Columns correspond cases and rows to genes. Percentages represent the incidence of alterations in respective genes within our cohort. Types of genetic alterations are color-coded and are shown in the legend at the bottom. Analysis and visualization were performed with Oncoprinter from cBioPortal [15,16].

3.3. RNA-Based NGS Results

Genetic rearrangements could be detected in 8/316 (2.5%) cases, with the *EML4-ALK* fusion being the most common one (n = 2, 0.6%). Furthermore, single cases harbored a *KRT6A-ALK*, *SLC24A3-ALK*, *MAD1L1-EGFR*, *EGFR-NUP160*, *ASH2L-FGFR1* or *FGFR3-TACC3* fusion, respectively. The detected translocation events of all eight cases are visualized in Figure 2. Because in the so far undescribed *SLC24A3-ALK* fusion, the 3′ partner gene maps to an intron, we additionally performed ALK immunohistochemistry, yielding a strong positive result and thus demonstrating its functional relevance. In addition to fusion events, a *MET* exon-14 skipping alteration could be detected in one case with the help of RNA-based NGS.

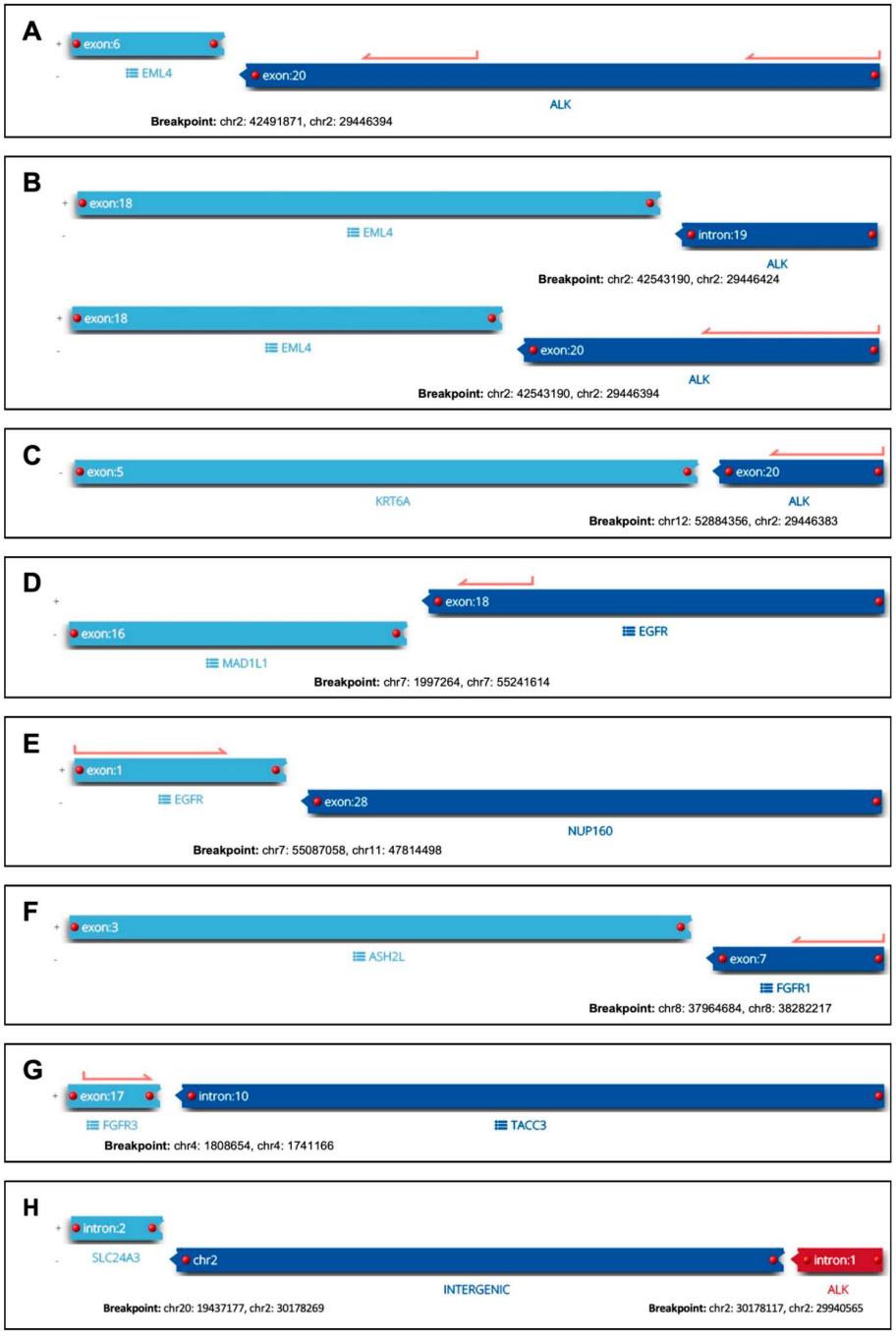

Figure 2. Visualization of detected fusions. Panels (**A**–**H**) represent the seven cases with translocation events. For each case, the involved genes, exons/introns and genomic locations are shown.

3.4. Detection of Already Established Therapeutic Targets in NSCLC

A plethora of genetic alterations are already well-established therapeutic targets for an approved drug in NSCLC, recently summarized in [14,17]. In our cohort of NSCLC with squamous histology, 21/316 (6.6%) cases harbored one of these alterations. Clinicopathological characteristics of these cases are summarized in Table 2. Among these 21 cases were seven with a *KRAS* G12C mutation, six with an *EGFR* mutation, four with an *ALK* fusion, two with an *EGFR* fusion, one with a *BRAF* p.K601E mutation, and one with a METex14 skipping event. In addition to the detected molecular drug targets, co-mutations were observed in 13 cases, most commonly within *TP53* (11/21 cases, 52.4%), and in single cases also within *CDKN2A*, *KEAP1*, *MET*, *PIK3CA*, *SMAD4*, and *STK11*. Of note, 16/21 (76.2%) patients harboring a molecular drug target were female. Table S3 summarizes the response evaluation criteria in solid tumors (RECIST) for all cases harboring an established molecular target and receiving targeted therapy.

Because most NSCLC guidelines recommend molecular testing in SCC only in never/light smokers (≤15 pack-years) or young (<50 years) patients [6,7], we correlated our molecular findings with these clinical characteristics. Of note, the majority of our patients harboring a molecular drug target had >15 pack-years (Figure 3A), and all were >50 years of age (Figure 3B), undermining restrictive molecular testing strategies. Furthermore, molecular biomarkers could be detected across all stages (Figure 3C).

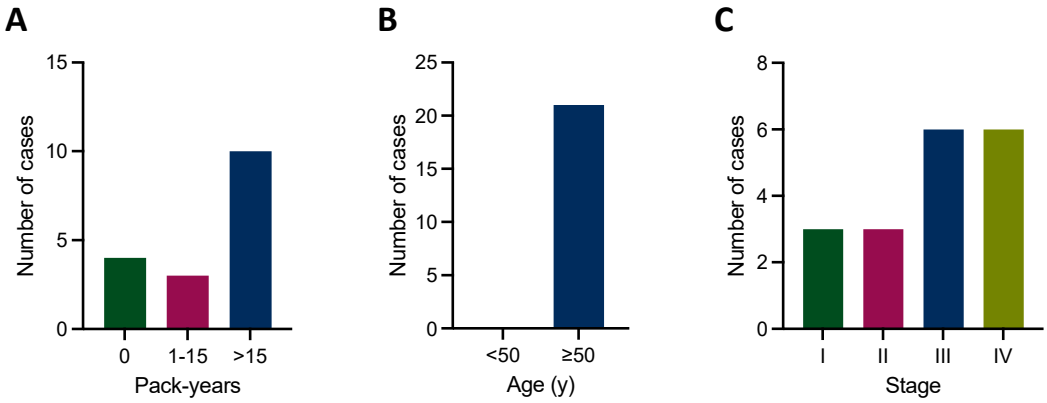

Figure 3. Established therapeutic targets and clinical characteristics. (**A**) The majority of cases harboring an established therapeutic target have >15 pack-years, and (**B**) all cases harboring an established therapeutic target are >50 years of age. (**C**) Established therapeutic targets could be detected across all tumor stages.

Recently, it has been questioned whether molecular targets typically occurring in AC can also be found in SCC or whether these target-bearing SCCs in fact represent undersampled adenosquamous carcinomas (ASC), histologically a mixture of AC and SCC components that per definition can only be diagnosed on resection specimens but not on biopsies [3,18]. To address this issue, we searched for subsequent resection specimens of these patients that harbored targetable alterations and compared the subsequent diagnosis with that of the primary sample where molecular testing had been performed. Paired biopsy and resection specimens were available in ten of these cases. In only 3/10 (30%) cases, the definite diagnosis was then ASC, while the majority of cases (7/10, 70%) represented pure SCC, proving that therapeutic targets do also occur in this histological subtype.

Table 2. Clinicopathological characteristics of cases harboring molecular targets for already approved drugs.

Case	Sex	Age	Smoker	PY	Stage	Molecular Target	Co-Mutations	PD-L1 (TPS)	Tested Specimen (Site/Type)	Subsequent Sample	Subsequent Diagnosis
1	f	72	yes (former)	40	IIB	*EML4-ALK* fusion	no	5	lung biopsy	lung resection	SCC
2	f	61	no	0	IVA	*EML4-ALK* fusion	no	0	lung biopsy	adrenal resection	ASC
3	f	74	yes (former)	30	IVA	*KRT6A-ALK* fusion	no	0	lung biopsy	no	NA
4	f	75	yes (former)	30	IIA	*SLC24A3-ALK* fusion	no	10	lung biopsy	lung resection	SCC
5	m	76	yes (current)	50	IB	*EGFR-NUP160* fusion	*TP53* p.H179R	10	lung biopsy	lung resection	SCC
6	f	69	no	0	IIA	*MAD1L1-EGFR* fusion	no	0	lung biopsy	lung resection	ASC
7	f	70	yes (former)	15	IVB	*EGFR* p.S768_D770dup	*TP53* p.E298X	10	brain resection	no	NA
8	f	70	NA	NA	IIIB	*EGFR* p.L747_P753delinsS	no	1	lung biopsy	lung resection	ASC
9	f	60	yes (former)	8	IIIA	*EGFR* p.746_750del	*TP53* p.177_182del	60	lung biopsy	no	NA
10	f	67	yes (current)	20	IVB	*EGFR* p.L747_P753delinsS	*TP53* p.M246fs	90	lung biopsy	no	NA
11	f	81	no (current)	0	IIIA	*EGFR* p.L858R	*SMAD4* p.W524X	20	lung biopsy	lung resection	SCC
12	f	69	no	0	IB	*EGFR* p.L858R *EGFR* p.S768I	*TP53* p.R213Q	2	lung biopsy	lung resection	SCC
13	m	61	NA	NA	NA	*BRAF* p.K601E	*CDKN2A* p.25_31del *STK11* p.A398V	NA	lung biopsy	no	NA
14	f	55	NA	NA	NA	*KRAS* p.G12C	TP53 p.V157F	NA	soft tissue biopsy	no	NA
15	f	67	yes (former)	10	IIIB	*KRAS* p.G12C	*PIK3CA* p.H1047R *TP53* V225fs	1	lung biopsy	no	NA
16	m	61	NA	NA	NA	*KRAS* p.G12C	*TP53* p.V274F	70	adrenal biopsy	no	NA
17	m	70	yes (current)	50	IA3	*KRAS* p.G12C	*TP53* p.R213L	100	lung biopsy	lung resection	SCC
18	f	63	yes (current)	45	IVB	*KRAS* p.G12C	no	90	soft tissue biopsy	no	NA
19	f	66	yes (current)	35	IVB	*KRAS* p.G12C	*TP53* p.P190fs *KEAP1* p.Q217X	0	lung biopsy	no	NA
20	f	63	yes (current)	30	IIIA	*KRAS* p.G12C	no	10	lung biopsy	lung resection	SCC
21	m	73	yes (current)	50	IIIA	METex14 skipping	*TP53* p.P190L *MET* p.T1010I	70	lung biopsy	no	NA

Abbreviations: PY, pack-years; TPS, tumor proportion score; NA, not applicable; SCC, squamous cell carcinoma; ASC, adenosquamous carcinoma.

3.5. Detection of Emerging Therapeutic Targets in NSCLC

In addition to already well-established therapeutic targets, there is an increasing number of genetic alterations regarded as emerging biomarkers for targeted therapy in NSCLC [14]. At least one of these emerging biomarkers recently listed by Hofman et al. was present in 87/316 (27.5%) cases of our cohort. The most common ones included genetic alterations of *PIK3CA* (44 cases) and *FGFR1-3* (26 cases). Similar to established biomarkers, most patients harboring an emerging biomarker had >15 pack-years and were >50 years of age (Figure 4A,B). Emerging molecular biomarkers could be detected across all stages (Figure 4C). Furthermore, the presence of an emerging target was significantly associated with a lower stage, while the presence of an established target was irrespective of stage (Figure S3), substantiating the importance of a stage-agnostic molecular testing workflow.

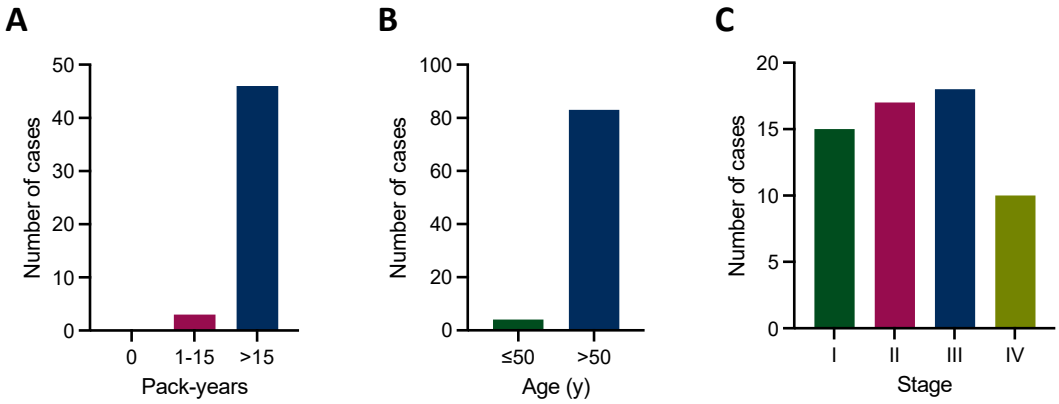

Figure 4. Emerging therapeutic targets and clinical characteristics. (**A**) The majority of cases harboring an emerging therapeutic target have >15 pack-years, and (**B**) are >50 years of age. (**C**) Emerging therapeutic targets could be detected across all tumor stages.

3.6. Correlation of PD-L1 Status with Established and Emerging Molecular Biomarkers

Apart from oncogenic mutations, personalized treatment decisions are largely influenced by PD-L1 expression and there are several clinical trials examining the benefit of combining targeted therapies with immune checkpoint inhibitors in lung SCC (NCT03735628; NCT04721223; NCT04000529). Therefore, we examined the association between PD-L1 expression and detected genetic alterations within potentially targetable oncogenes in our cohort (Figure S2). Interestingly, genetic alterations within FGFR3 were associated with a significantly lower PD-L1 TPS, possibly influencing future treatment considerations.

4. Discussion

NSCLC is a success story of biomarker-driven targeted therapy approaches. Today, most guidelines agree that broad molecular reflex testing should be performed in all Acs [8]. In contrast, testing in SCCs is more controversial. While some guidelines recommend molecular profiling only in patients that meet certain clinical criteria (e.g., non-smoker, young age), others recommend it in all SCC patients, irrespective of smoking status or age [6–8]. To add real-world evidence to this controversy, we performed a single-center study examining the value of broad molecular reflex testing in an unselected cohort of 316 consecutive lung SCC cases.

From a technical point of view, molecular testing in NSCLC becomes increasingly challenging, with ever more genetic alterations to be covered and the most common testing material being small biopsies with often low numbers of tumor cells. Thus, adequate tissue management that guarantees an economical use of biopsy specimens is key. One of the most important measures in this regard is to avoid additional leveling steps in the tissue block because this would unnecessarily use up much of the tissue. Thus, unstained slides might be cut as soon as histomorphology points towards a diagnosis of NSCLC. These slides can then be stored until molecular testing is ordered by the clinician (clinician-initiated molecular testing)

or immediately further processed by the molecular pathology laboratory (pathologist-initiated molecular testing, "reflex testing"). Of note, pathologist-initiated reflex testing in NSCLC has decidedly been recommended by a recent expert consensus paper [17].

Importantly, our NGS-based reflex testing approach for NSCLC is irrespective of clinical parameters, including tumor stage and smoking status. Hence, our cohort included a wide range of tumor stages and is therefore relevant both for palliative and neoadjuvant/adjuvant treatment considerations. The importance of this stage-agnostic molecular profiling approach is reflected by the recently published results of the ADAURA trial that led to the approval of osimertinib in the adjuvant setting of resectable stage IB-IIIA NSCLCs harboring specific EGFR mutations [19]. Substantiating this, in our cohort, both established and emerging targets could be detected across all stages, with emerging targets even being significantly associated with lower stages. Furthermore, our cohort consisted of an exceedingly high proportion of current or former smokers, reflecting the generally high smoking rate in Austria and other European countries [20]. Thus, the often-proclaimed recommendation to perform molecular profiling in SCC only in non-/light smokers would have deprived many of our patients of the chance to potentially receive biomarker-driven targeted therapy. Furthermore, the recommended pathologist-initiated reflex testing workflow is hardly feasible when the (often unreliable) smoking status has to be waited out, with the consequence of unnecessarily losing precious tissue and time.

Due to the high molecular complexity of lung SCC, combination therapies might be essential for better treatment efficacy. Combining targeted therapy with immunotherapy seems particularly promising [21]. Therefore, the relationship between specific tumor mutations and immune-related biomarkers might be of interest for future treatment considerations. We have observed that genetic alterations in FGFR3 are associated with a significantly lower PD-L1 TPS. This is in line with a recent study that identified the E3 ubiquitin ligase NEDD4 as a key factor for PD-L1 degradation in FGFR3-activated cancer, providing a mechanistic link for potential drug combinations in the future [22].

Although our study is one of the first real-world studies specifically dedicated to lung SCC, there are other NSCLC studies that have also included SCC cases. For example, Griesinger et al. reported on biomarker testing in 3717 advanced NSCLC cases, 796 of them being of squamous histology. Within the latter subgroup, 4.4% harbored a genetic alteration in EGFR, 1.4% in BRAF, 1.2% in ROS1, and 0.5% in ALK, testing results that are comparable with our experience [23]. The cohort by Adib et al. included 337/3115 (10.8%) SCC cases, showing that 5% of them harbor targetable alterations [24], again being largely consistent with our findings. In a study using DNA-based NGS in a cohort of 172 lung SCCs, Sands et al. identified potentially targetable mutations in 38% of cases, the most common being PIK3CA mutations [25]. In a recent paper from the nNGM network in Germany examining MET aberrations in NSCLC, Kron et al. reported four cases with MET ex 14 skipping mutations in stage IIIB/IV SCC, further arguing in favor of testing all NSCLC cases, irrespective of histological subtype [26].

The limitations of our study are its retrospective nature and the lack of long-term clinical outcomes, e.g., survival data. However, we were able to include the response evaluation criteria in solid tumors (RECIST) for all cases harboring an established molecular target and receiving targeted therapy. In addition, by including all consecutive SCC cases tested by DNA- and RNA-based NGS within a specified timeframe, we could exclude a selection bias. Furthermore, real-world studies like ours have the advantage of reflecting the routine setting, thus being easily applicable in future clinical practice.

In accordance with other real-world molecular testing studies that included lung SCC cases, the frequency of detected therapeutic targets in SCC is lower than in AC [9,23,24]. Although SCC patients harboring a targetable mutation have a better outcome when treated with a TKI, this effect might not be as pronounced as in AC [27]. These aspects might raise financial considerations because the reimbursement of molecular testing costs is different across countries and sometimes a challenge even for AC [28]. A mixture of AC and SCC components, with each component comprising $\geq$10% of the tumor, is defined as

adenosquamous carcinoma. These tumors might have a mutation profile similar to AC and are therefore promising candidates for targeted therapy. Importantly, the definitive diagnosis of adenosquamous carcinoma requires a resection specimen. However, the most common specimen for primary histopathological evaluation is a small biopsy that often includes only one of the components, either AC or SCC [3]. Underscoring this problem, adenosquamous carcinomas masquerading as pure SCC have been reported [29], further substantiating the need to not exclude NSCLC cases with squamous histology from reflex molecular testing approaches.

By including RNA-based NGS in our reflex testing approach, we were able to detect gene rearrangements in eight cases. Intriguingly, five of these fusion events have never been described in the literature so far: *KRT6A-ALK*, *SLC24A3-ALK MAD1L1-EGFR*, *EGFR-NUP160* and *ASH2L-FGFR1*. Although our assay for RNA-based NGS has been thoroughly validated (see Section 2), these rare fusion events and their clinical relevance need to be confirmed in future studies. In recent years, *EGFR* fusions in particular have been in the spotlight with several case reports/series being reported in lung AC. Although there is currently no approved drug specifically for *EGFR* fusions, many of these cases have been treated with EGFR TKIs and antitumor responses have been documented, both in vitro and in clinics [30–33]. Due to prevailing testing strategies that are often restricted to lung AC, data about fusion events in lung SCC are exceedingly rare [34]. However, based on our findings of potentially relevant fusion events, this might be a promising field for future clinical studies.

5. Conclusions

In conclusion, we provide real-world evidence that DNA- and RNA-based reflex testing in NSCLC with squamous histology is of clinical relevance. More specifically, we demonstrate that the majority of cases harboring already established or emerging therapeutic targets were >50 years of age and had >15 pack-years, patient groups that have so far often been excluded from molecular testing strategies. Therefore, we propose a reflex testing workflow using DNA- and RNA-based NGS for all patients with NSCLC, irrespective of histology, but also irrespective of age or smoking status (Figure 5). So far, molecular testing in NSCLC with squamous histology is only rarely implemented in centers across Europe [35]; however, we are convinced that the success story of biomarker-driven personalized medicine in NSCLC can only be further continued with a non-selective broad molecular profiling approach.

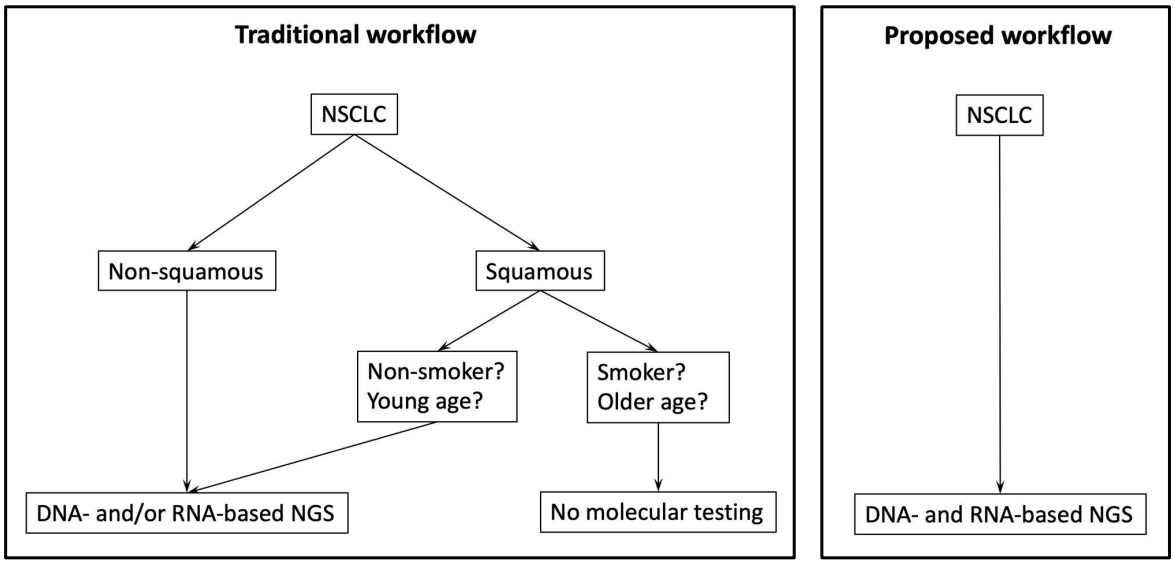

Figure 5. Comparison of routine molecular workflows for NSCLC. The currently most often used workflow is shown on the left, the proposed workflow based on data presented in this article is shown on the right.

Supplementary Materials: The following supporting information can be downloaded at: https://www.mdpi.com/article/10.3390/cancers16050903/s1, Figure S1: Visualization of detected mutations in potentially targetable oncogenes. All detected mutations and their locations within the respective genes (*ALK*, *BRAF*, *EGFR*, *ERBB4*, *FGFR1*, *FGFR2*, *FGFR3*, *KRAS*, *MET* and *PIK3CA*) are shown. Analysis and visualization were performed with MutationMapper from cBioPortal [15,16]; Figure S2: Correlation between genetic alterations in potentially targetable oncogenes and PD-L1 expression. In contrast to *ALK*, *BRAF*, *EGFR*, *FGFR1*, *FGFR2*, *KRAS* and *MET*, genetic alterations in *FGFR3* are associated with a significantly lower PD-L1 TPS (Mann–Whitney test); Figure S3: Correlation between tumor stage and the presence of an established or emerging molecular target (Kruskal–Wallis test); Table S1: DNA- and RNA-based NGS results; Table S2: Comprehensive clinicopathological and molecular metadata of the whole study cohort; Table S3: Targeted therapy and treatment response of patients harboring an established molecular biomarker.

Author Contributions: Conceptualization, M.Z. and L.B.; methodology, N.K. and K.K.; investigation, M.Z., G.A., A.T., P.J.J., R.W., J.L., F.G., G.G. and L.B.; data curation, M.Z., S.K., N.K. and A.T.; writing—original draft preparation, M.Z.; writing—review and editing, all authors; visualization, M.Z.; supervision, L.B. All authors have read and agreed to the published version of the manuscript.

Funding: This research received no external funding.

Institutional Review Board Statement: The study was conducted in accordance with the Declaration of Helsinki and approved by the Ethics Committee of the Medical University of Graz (33-066 ex 20/21).

Informed Consent Statement: Not applicable.

Data Availability Statement: The authors declare that all the data supporting the findings of this study are available from the corresponding author upon reasonable request.

Conflicts of Interest: The authors declare no conflicts of interest.

References

1. Camidge, D.R.; Doebele, R.C.; Kerr, K.M. Comparing and Contrasting Predictive Biomarkers for Immunotherapy and Targeted Therapy of NSCLC. *Nat. Rev. Clin. Oncol.* **2019**, *16*, 341–355. [CrossRef] [PubMed]
2. Kerr, K.M.; Bibeau, F.; Thunnissen, E.; Botling, J.; Ryška, A.; Wolf, J.; Öhrling, K.; Burdon, P.; Malapelle, U.; Büttner, R. The Evolving Landscape of Biomarker Testing for Non-Small Cell Lung Cancer in Europe. *Lung Cancer* **2021**, *154*, 161–175. [CrossRef] [PubMed]
3. Nicholson, A.G.; Tsao, M.S.; Beasley, M.B.; Borczuk, A.C.; Brambilla, E.; Cooper, W.A.; Dacic, S.; Jain, D.; Kerr, K.M.; Lantuejoul, S.; et al. The 2021 WHO Classification of Lung Tumors: Impact of Advances Since 2015. *J. Thorac. Oncol.* **2022**, *17*, 362–387. [CrossRef]
4. Weir, B.A.; Woo, M.S.; Getz, G.; Perner, S.; Ding, L.; Beroukhim, R.; Lin, W.M.; Province, M.A.; Kraja, A.; Johnson, L.A.; et al. Characterizing the Cancer Genome in Lung Adenocarcinoma. *Nature* **2007**, *450*, 893–898. [CrossRef] [PubMed]
5. Devarakonda, S.; Morgensztern, D.; Govindan, R. Genomic Alterations in Lung Adenocarcinoma. *Lancet Oncol.* **2015**, *16*, e342–e351. [CrossRef] [PubMed]
6. Hendriks, L.E.; Kerr, K.; Menis, J.; Mok, T.S.; Nestle, U.; Passaro, A.; Peters, S.; Planchard, D.; Smit, E.F.; Solomon, B.J.; et al. Oncogene-Addicted Metastatic Non-Small-Cell Lung Cancer: ESMO Clinical Practice Guideline for Diagnosis, Treatment and Follow-up. *Ann. Oncol.* **2023**, *34*, 339–357. [CrossRef] [PubMed]
7. Lindeman, N.I.; Cagle, P.T.; Aisner, D.L.; Arcila, M.E.; Beasley, M.B.; Bernicker, E.H.; Colasacco, C.; Dacic, S.; Hirsch, F.R.; Kerr, K.; et al. Updated Molecular Testing Guideline for the Selection of Lung Cancer Patients for Treatment with Targeted Tyrosine Kinase Inhibitors Guideline from the College of American Pathologists, the International Association for the Study of Lung Cancer, and the Association for Molecular Pathology. *J. Thorac. Oncol.* **2018**, *13*, 323–358. [CrossRef]
8. Ettinger, D.S.; Wood, D.E.; Aisner, D.L.; Akerley, W.; Bauman, J.R.; Bharat, A.; Bruno, D.S.; Chang, J.Y.; Chirieac, L.R.; D'Amico, T.A.; et al. Non–Small Cell Lung Cancer, Version 3.2022, NCCN Clinical Practice Guidelines in Oncology. *J. Natl. Compr. Cancer Netw.* **2022**, *20*, 497–530. [CrossRef]
9. Zacharias, M.; Absenger, G.; Kashofer, K.; Wurm, R.; Lindenmann, J.; Terbuch, A.; Konjic, S.; Sauer, S.; Gollowitsch, F.; Gorkiewicz, G.; et al. Reflex Testing in Non-Small Cell Lung Carcinoma Using DNA- and RNA-Based next-Generation Sequencing—A Single-Center Experience. *Transl. Lung Cancer Res.* **2021**, *10*, 4221–4234. [CrossRef]
10. Wang, K.; Li, M.; Hakonarson, H. ANNOVAR: Functional Annotation of Genetic Variants from High-Throughput Sequencing Data. *Nucleic Acids Res.* **2010**, *38*, e164. [CrossRef]
11. Cingolani, P.; Platts, A.; Wang, L.L.; Coon, M.; Nguyen, T.; Wang, L.; Land, S.J.; Lu, X.; Ruden, D.M. A Program for Annotating and Predicting the Effects of Single Nucleotide Polymorphisms, SnpEff. *Fly* **2012**, *6*, 80–92. [CrossRef]

12. Saalfeld, F.C.; Wenzel, C.; Aust, D.E.; Wermke, M. Targeted Therapy in BRAF p.K601E-Driven NSCLC: Case Report and Literature Review. *JCO Precis. Oncol.* **2020**, *4*, 1163–1166. [CrossRef] [PubMed]
13. Su, P.-L.; Lin, C.-Y.; Chen, Y.-L.; Chen, W.-L.; Lin, C.-C.; Su, W.-C. Durable Response to Combined Dabrafenib and Trametinib in a Patient with BRAF K601E Mutation-Positive Lung Adenocarcinoma: A Case Report. *JTO Clin. Res. Rep.* **2021**, *2*, 100202. [CrossRef] [PubMed]
14. Hofman, P.; Berezowska, S.; Kazdal, D.; Mograbi, B.; Ilié, M.; Stenzinger, A.; Hofman, V. Current Challenges and Practical Aspects of Molecular Pathology for Non-Small Cell Lung Cancers. *Virchows Arch.* **2023**, 1–14. [CrossRef]
15. Gao, J.; Aksoy, B.A.; Dogrusoz, U.; Dresdner, G.; Gross, B.; Sumer, S.O.; Sun, Y.; Jacobsen, A.; Sinha, R.; Larsson, E.; et al. Integrative Analysis of Complex Cancer Genomics and Clinical Profiles Using the CBioPortal. *Sci. Signal* **2013**, *6*, pl1. [CrossRef] [PubMed]
16. Cerami, E.; Gao, J.; Dogrusoz, U.; Gross, B.E.; Sumer, S.O.; Aksoy, B.A.; Jacobsen, A.; Byrne, C.J.; Heuer, M.L.; Larsson, E.; et al. The CBio Cancer Genomics Portal: An Open Platform for Exploring Multidimensional Cancer Genomics Data. *Cancer Discov.* **2012**, *2*, 401–404. [CrossRef] [PubMed]
17. Gosney, J.R.; Paz-Ares, L.; Jänne, P.; Kerr, K.M.; Leighl, N.B.; Lozano, M.D.; Malapelle, U.; Mok, T.; Sheffield, B.S.; Tufman, A.; et al. Pathologist-Initiated Reflex Testing for Biomarkers in Non-Small-Cell Lung Cancer: Expert Consensus on the Rationale and Considerations for Implementation. *ESMO Open* **2023**, *8*, 101587. [CrossRef] [PubMed]
18. Paik, P.K.; Varghese, A.M.; Sima, C.S.; Moreira, A.L.; Ladanyi, M.; Kris, M.G.; Rekhtman, N. Response to Erlotinib in Patients with EGFR Mutant Advanced Non–Small Cell Lung Cancers with a Squamous or Squamous-like Component. *Mol. Cancer Ther.* **2012**, *11*, 2535–2540. [CrossRef]
19. Wu, Y.-L.; Tsuboi, M.; He, J.; John, T.; Grohe, C.; Majem, M.; Goldman, J.W.; Laktionov, K.; Kim, S.-W.; Kato, T.; et al. Osimertinib in Resected EGFR-Mutated Non–Small-Cell Lung Cancer. *N. Engl. J. Med.* **2020**, *383*, 1711–1723. [CrossRef]
20. Pirker, R.; Prosch, H.; Popper, H.; Klepetko, W.; Dieckmann, K.; Burghuber, O.C.; Klikovits, T.; Hoda, M.A.; Zöchbauer-Müller, S.; Filipits, M. Lung Cancer in Austria. *J. Thorac. Oncol.* **2021**, *16*, 725–733. [CrossRef]
21. Lau, S.C.M.; Pan, Y.; Velcheti, V.; Wong, K.K. Squamous Cell Lung Cancer: Current Landscape and Future Therapeutic Options. *Cancer Cell* **2022**, *40*, 1279–1293. [CrossRef] [PubMed]
22. Jing, W.; Wang, G.; Cui, Z.; Xiong, G.; Jiang, X.; Li, Y.; Li, W.; Han, B.; Chen, S.; Shi, B. FGFR3 Destabilizes PD-L1 Via NEDD4 to Control T Cell-Mediated Bladder Cancer Immune Surveillance. *Cancer Res.* **2021**, *82*, 114–129. [CrossRef] [PubMed]
23. Griesinger, F.; Eberhardt, W.; Nusch, A.; Reiser, M.; Zahn, M.-O.; Maintz, C.; Bernhardt, C.; Losem, C.; Stenzinger, A.; Heukamp, L.C.; et al. Biomarker Testing in Non-Small Cell Lung Cancer in Routine Care: Analysis of the First 3,717 Patients in the German Prospective, Observational, Nation-Wide CRISP Registry (AIO-TRK-0315). *Lung Cancer* **2021**, *152*, 174–184. [CrossRef] [PubMed]
24. Adib, E.; Nassar, A.H.; Alaiwi, S.A.; Groha, S.; Akl, E.W.; Sholl, L.M.; Michael, K.S.; Awad, M.M.; Jänne, P.A.; Gusev, A.; et al. Variation in Targetable Genomic Alterations in Non-Small Cell Lung Cancer by Genetic Ancestry, Sex, Smoking History, and Histology. *Genome Med.* **2022**, *14*, 39. [CrossRef] [PubMed]
25. Sands, J.M.; Nguyen, T.; Shivdasani, P.; Sacher, A.G.; Cheng, M.L.; Alden, R.S.; Jänne, P.A.; Kuo, F.C.; Oxnard, G.R.; Sholl, L.M. Next-Generation Sequencing Informs Diagnosis and Identifies Unexpected Therapeutic Targets in Lung Squamous Cell Carcinomas. *Lung Cancer* **2020**, *140*, 35–41. [CrossRef] [PubMed]
26. Kron, A.; Scheffler, M.; Heydt, C.; Ruge, L.; Schaepers, C.; Eisert, A.-K.; Merkelbach-Bruse, S.; Riedel, R.; Nogova, L.; Fischer, R.N.; et al. Genetic Heterogeneity of MET-Aberrant NSCLC and Its Impact on the Outcome of Immunotherapy. *J. Thorac. Oncol.* **2021**, *16*, 572–582. [CrossRef] [PubMed]
27. Joshi, A.; Zanwar, S.; Noronha, V.; Patil, V.M.; Chougule, A.; Kumar, R.; Janu, A.; Mahajan, A.; Kapoor, A.; Prabhash, K. EGFR Mutation in Squamous Cell Carcinoma of the Lung: Does It Carry the Same Connotation as in Adenocarcinomas? *OncoTargets Ther.* **2017**, *10*, 1859–1863. [CrossRef] [PubMed]
28. Thunnissen, E.; Weynand, B.; Udovicic-Gagula, D.; Brcic, L.; Szolkowska, M.; Hofman, P.; Smojver-Ježek, S.; Anttila, S.; Calabrese, F.; Kern, I.; et al. Lung Cancer Biomarker Testing: Perspective from Europe. *Transl. Lung Cancer Res.* **2020**, *9*, 887–897. [CrossRef]
29. Chaft, J.E.; Rekhtman, N.; Ladanyi, M.; Riely, G.J. ALK-Rearranged Lung Cancer: Adenosquamous Lung Cancer Masquerading as Pure Squamous Carcinoma. *J. Thorac. Oncol.* **2012**, *7*, 768–769. [CrossRef]
30. Pan, Y.; Zhang, Y.; Ye, T.; Zhao, Y.; Gao, Z.; Yuan, H.; Zheng, D.; Zheng, S.; Li, H.; Li, Y.; et al. Detection of Novel NRG1, EGFR, and MET Fusions in Lung Adenocarcinomas in the Chinese Population. *J. Thorac. Oncol.* **2019**, *14*, 2003–2008. [CrossRef]
31. Konduri, K.; Gallant, J.-N.; Chae, Y.K.; Giles, F.J.; Gitlitz, B.J.; Gowen, K.; Ichihara, E.; Owonikoko, T.K.; Peddareddigari, V.; Ramalingam, S.S.; et al. EGFR Fusions as Novel Therapeutic Targets in Lung Cancer. *Cancer Discov.* **2016**, *6*, 601–611. [CrossRef]
32. Sperandio, R.C.; Tostes, F.L.T.; Campregher, P.V.; Paes, V.R.; Moura, F.; Schvartsman, G. EGFR-RAD51 Fusion in Lung Adenocarcinoma with Systemic and Intracranial Response to Osimertinib: A Case Report and Review of the Literature. *Lung Cancer* **2022**, *166*, 94–97. [CrossRef]
33. Zhu, Y.; Wang, W.; Xu, C.; Song, Z.; Du, K.; Chen, G.; Lv, T.; Song, Y. EGFR-RAD51 Fusion Variant in Lung Adenocarcinoma and Response to Erlotinib: A Case Report. *Lung Cancer* **2018**, *115*, 131–134. [CrossRef]

34. Kazdal, D.; Hofman, V.; Christopoulos, P.; Ilié, M.; Stenzinger, A.; Hofman, P. Fusion-positive Non-small Cell Lung Carcinoma: Biological Principles, Clinical Practice, and Diagnostic Implications. *Genes Chromosom. Cancer* **2022**, *61*, 244–260. [CrossRef] [PubMed]
35. Hofman, P.; Calabrese, F.; Kern, I.; Adam, J.; Alarcão, A.; Alborelli, I.; Anton, N.T.; Arndt, A.; Avdalyan, A.; Barberis, M.; et al. Real-World EGFR Testing Practices for Non-Small-Cell Lung Cancer by Thoracic Pathology Laboratories across Europe. *ESMO Open* **2023**, *8*, 101628. [CrossRef] [PubMed]